



Universidad de Oviedo
Universidá d'Uviéu
University of Oviedo

Programa de Doctorado en Materiales

PHENOMENOLOGICAL APPROACH TO FITTING AND INTERCONVERSION
OF VISCOELASTIC AND LIFETIME PROCESSES USING STATISTICAL
FUNCTIONS

MODELIZACIÓN FENOMENOLÓGICA, MEDIANTE FUNCIONES
ESTADÍSTICAS, EN EL AJUSTE E INTERCONVERSIÓN DE PROCESOS
VISCOELÁSTICOS Y DE DURACIÓN DE VIDA

TESIS DOCTORAL

Adrián Álvarez Vázquez

Julio 2020



Universidad de Oviedo
Universidá d'Uviéu
University of Oviedo

Programa de Doctorado en Materiales

PHENOMENOLOGICAL APPROACH TO FITTING AND INTERCONVERSION
OF VISCOELASTIC AND LIFETIME PROCESSES USING STATISTICAL
FUNCTIONS

MODELIZACIÓN FENOMENOLÓGICA, MEDIANTE FUNCIONES
ESTADÍSTICAS, EN EL AJUSTE E INTERCONVERSIÓN DE PROCESOS
VISCOELÁSTICOS Y DE DURACIÓN DE VIDA

TESIS DOCTORAL

Directores de tesis

Dr. D. Alfonso Fernández Canteli

Dra. Dña. María Jesús Lamela Rey



RESUMEN DEL CONTENIDO DE TESIS DOCTORAL

1.- Título de la Tesis	
Español: Modelización Fenomenológica, mediante Funciones Estadísticas, en el Ajuste e Interconversion de Procesos Viscoelásticos y de Duración de Vida.	Inglés: Phenomenological Approach to Fitting and Interconversion of Viscoelastic and Lifetime Processes Using Statistical Functions.
2.- Autor	
Nombre: Adrián Alvarez Vázquez	DNI: .
Programa de Doctorado: Materiales	
Órgano responsable: Comisión Académica Programa Doctorado en Materiales	

RESUMEN (en español)

Los materiales viscoelásticos comprenden una amplia variedad de materiales, tales como polímeros, materiales cuasi-frágiles, madera, tejidos, así como metales a altas temperaturas, ampliamente usados en componentes mecánicos, estructuras y biológicos en numerosas aplicaciones en ingeniería. Todos ellos se caracterizan por una combinación entre comportamiento elástico y viscoso cuando se les aplican tensiones o deformaciones. Sin embargo, su característica principal es su dependencia con respecto al tiempo y a la temperatura, bien sea bajo cargas estáticas o dinámicas, además de otros factores externos como la presión, la humedad o el envejecimiento.

El uso de este tipo de materiales viscoelásticos en el diseño de componentes mecánicos o estructurales requiere de una caracterización previa de su comportamiento mecánico, dado que la dependencia con estos factores externos influye no sólo en el diseño de componentes, sino también en la fabricación y modelización numérica.

La caracterización viscoelástica es compleja debido a la limitación de tiempo en el que se desarrolla una campaña experimental, dado su comportamiento a largo plazo, por lo que se requiere de una serie de restricciones en el proceso de caracterización. En primer lugar, la necesidad de llevar a cabo dicha caracterización a partir de una serie de curvas cortas de ensayos de relajación a distintas temperaturas. En segundo lugar, la evaluación conjunta de estos resultados experimentales para obtener la curva maestra del material, como por ejemplo en el caso del módulo de relajación, lo que requiere de modelos adecuados. En tercer lugar, la conversión de la curva maestra para una determinada temperatura de referencia a cualquier condición de tiempo y temperatura, lo cual implica la extrapolación de las curvas viscoelásticas fuera de los límites de los resultados de experimentales.

El principio de Superposición Tiempo-Temperatura (TTS) es el método más utilizado para la construcción de las curvas maestras del material a una determinada temperatura de referencia, basado en una presumible equivalencia entre las variables tiempo y temperatura por la cual las curvas cortas a distintas temperaturas pueden ser transformadas a una curva maestra común a partir de un modelo de transformación tiempo-temperatura adecuado.

Los modelos de caracterización viscoelástica actuales basados en el principio TTS presentan ciertas desventajas e inconsistencias, tales como la necesidad de que las curvas cortas se solapen durante, al menos, una década de tiempo, o el requerir la combinación de dos modelos TTS distintos para poder definir la curva maestra en todo el rango de temperaturas. Sin embargo, el inconveniente principal de estas metodologías actuales reside en no satisfacer las dos condiciones necesarias para ser modelos válidos, como son la unicidad y la compatibilidad. De esta forma, las transformaciones en tiempo y temperatura de las curvas cortas a la curva maestra dependen de la



temperatura de referencia de origen.

Por ello, los modelos fenomenológicos propuestos de caracterización viscoelástica, basados en la identificación de la evolución de las funciones viscoelásticas con las distribuciones normal y Gumbel, constituyen alternativas adecuadas para evitar estos inconvenientes de las metodologías clásicas, dado que su derivación está rigurosamente basa en condiciones físicas y estadísticas, tales como la condición de compatibilidad, justificando ser así una solución válida para la caracterización viscoelástica. La normalización del módulo de relajación con respecto a su inherente doble acotación, entre los módulos elástico y relajado, además de su condición de función monótona y estrictamente decreciente permite que sea asimilada, por definición, por una función de supervivencia, lo que permite evidencia una base estadística que subyace en el fenómeno viscoelástico en sus diferentes representaciones. Con ello, la caracterización viscoelástica puede llevarse a cabo de una forma más objetiva y directa, evitando además las inconsistencias de los modelos clásicos basados en el principio TTS. Así mismo, los parámetros de los modelos que se proponen tienen una interpretación física más directa.

La selección de las cdf de la distribución normal para la descripción de la evolución temporal del módulo de relajación está justificada por el teorema central del límite cuando se considera la elongación total de una probeta de material viscoelástico sometida a un ensayo de fluencia como la suma de una serie de elongaciones aleatorias correspondientes a los elementos primarios en los que se puede subdividir dicha probeta. Por otro lado, el comportamiento a largo plazo del fenómeno de relajación requiere de una extrapolación de los datos disponibles experimentalmente en las curvas cortas a distintas temperaturas para los casos límite $t \rightarrow 0$ y $t \rightarrow \infty$. Por ello, el uso de la familia de distribuciones de valores extremos constituye una solución natural a la caracterización viscoelástica, en particular la distribución de Gumbel por ser el dominio de atracción de la distribución normal o log-normal.

Por ello, se desarrollan en esta tesis dos aproximaciones distintas, tal que representan dos formas de analizar el efecto de la temperatura. En el primer caso, se asume que el efecto de la temperatura actúa modificando el parámetro de escala en la función de distribución acumulada de ambas distribuciones normal y Gumbel. De esta forma, la estimación de la curva maestra para una determinada temperatura de referencia se consigue a partir de las curvas cortas experimentales a distintas temperaturas, debido a la imposibilidad práctica de extender la ventana temporal del ensayo. En el segundo caso, la condición de compatibilidad estadística entre la distribución del módulo de relajación para una temperatura dada, $E(t; T)$, y la distribución del módulo de relajación para un tiempo dado, $E(T; t)$, se aplica para obtener la definición analítica del campo $T-t$. Como resultado, los datos experimentales de las curvas cortas de relajación pueden ser representados en una única curva maestra perteneciente a la distribución de Gumbel, constituyendo así la curva maestra más general posible. Así, una vez dicho campo es estimado, las curvas maestras para los dos campos correspondientes $E(t; T)$ y $E(T; t)$ pueden ser obtenidas directamente para cualquier condición de tiempo y temperatura.

Adicionalmente, dado que los fenómenos viscoelásticos y su evolución en el tiempo constituyen fenómenos estocásticos, las técnicas Bayesianas se aplican a los modelos propuestos para lograr así una definición probabilística del módulo de relajación y obtener las distribuciones estadísticas de los parámetros que intervienen en dichos modelos.

Finalmente, con el objetivo de corroborar la aplicabilidad de los modelos propuestos, se realiza una campaña experimental con ensayos de relajación a diferentes temperaturas en un material viscoelástico comercial, conocido como polyvinyl-butyril (PVB), comúnmente utilizada en aplicaciones en ingeniería.

Los modelos fenomenológicos desarrollados en esta tesis se enfocan en el estudio de la evolución de las tensiones en el caso del fenómeno de relajación, o bien de deformaciones en el caso de la fluencia. Aún a pesar de su importancia en la caracterización mecánica de materiales viscoelásticos, este enfoque resulta incompleto



cuando se consideran posibles fallos a fractura y fatiga, presentes en las condiciones de servicio de componentes reales, los cuales no pueden ser resueltos por medio de los modelos propuestos anteriormente. Por ello, esta tesis presenta una metodología para la derivación de modelos de predicción de fractura estática con consideración del efecto de la temperatura, basada en los modelos propuestos en la caracterización viscoelástica. En este sentido, los desarrollos que se proponen en fractura, con consideración no sólo del efecto del efecto de la temperatura, sino también del radio de entalla, deben de ser entendidos como un primer paso en la derivación de metodologías universales en la caracterización de materiales viscoelásticos para el diseño real.

En efecto, aún a pesar de que las condiciones de servicio reales suelen incluir la combinación de efectos externos, tales como la temperatura o el radio de entalla, las metodologías actuales de caracterización a fractura suelen estar focalizadas en uno sólo de estos efectos. Por este motivo, se propone un modelo probabilístico para considerar el efecto de entalla en la predicción de la tenacidad a fractura en componentes entallados, basada en la teoría de las distancias críticas, permitiendo así tener en cuenta la inherente dispersión de los ensayos a fractura en la predicción probabilística del fallo bajo cualquier condición geométrica de la entalla.

Como extensión, esta tesis extiende este modelo probabilístico para el análisis del efecto de entalla para incluir el debido a la temperatura, por medio de la aplicación de la compatibilidad estadística entre las distribuciones acumuladas que intervienen, permitiendo así definir las zonas inferior e intermedia de la curva de transición frágil a dúctil de una forma probabilística y con la tenacidad a fractura para componentes entallados. Mediante la aplicación de las técnicas Bayesianas se consiguen mejorar los modelos propuestos proporcionando las distribuciones estadísticas de las curvas percentiles de fallo, a modo de intervalos de confianza. Finalmente, la aplicabilidad de los modelos propuestos se corrobora por medio de una extensa campaña experimental externa en dos aceros ferríticos distintos que incluye distintas condiciones de temperatura y radios de entalla.

RESUMEN (en Inglés)

Viscoelastic materials comprise a broad variety of materials, such as polymers, quasi-brittle materials, woods, tissues and metals at high temperature, widely used as mechanical, structural and biological components in many engineering fields. They are characterized by a combination of elastic and viscous behaviour when stress or strain conditions are applied. Time and temperature are the main factors influencing the behaviour of viscoelastic materials under static load or deformation, while frequency can be added as an influencing factor when dynamic load is applied. Many other external effects such as pressure, humidity and ageing, exert an influence on their response.

The use of viscoelastic materials in mechanical and structural elements and components requires a previous characterization of their viscoelastic mechanical behaviour. This is required in the limit states analysis when the component is subject to complex stress and strain loading conditions as implied in the prototype predesign, manufacturing process and computational design.

Viscoelastic characterization is likewise complex, particularly because of the limited time interval in which the data can be recorded. The infeasibility of extending a test to an infinite time, or at least to a long-term duration, leads to a number of requirements in the characterization process. Firstly, the necessity of carrying out an experimental campaign based on short term viscoelastic curves at different temperatures. Secondly, the joint evaluation of those short-term viscoelastic curves. For instance, the evolution of the relaxation modulus can be used to estimate the master curve of this viscoelastic variable using an adequate model. Thirdly, the conversion of the master curve using the model to determine the value of the viscoelastic variable, for any time and temperature. This may imply extrapolation of the viscoelastic curves outside the range of the experimental records.



The Time-Temperature Superposition (TTS) principle is widely used for building this master curve at a certain reference temperature, based on a presumable equivalence between time and temperature. This means that an adequate time-and-temperature-dependent mathematical model allows the master curve to be derived by transforming the short-term curves at different temperatures to a common reference temperature.

Currently used models based on the application of the TTS principle evidence certain disadvantages and inconsistencies, such as a minimum required overlapping between the short-term curves and the necessity of using at least two different TTS models for the master curve to be derived. Nevertheless, the most critical drawback of such models is the fact that they do not fulfil the basic conditions for a model to be valid, namely, uniqueness and compatibility. As a result, the fitted master curve depends on the temperature initially taken as a reference.

Phenomenological viscoelastic models, based on identification of the viscoelastic evolution as statistical functions of normal and Gumbel distributions, are suitable alternatives to overcome all these drawbacks. Their derivation fulfils basic physical and statistical requirements, including the compatibility condition, proving to be a valid solution for viscoelastic characterization. The normalization of the relaxation modulus with respect to its inherent twofold bounding limits represented by the elastic and relaxed moduli, as well as the observation of its monotonically decreasing character, suggest it can be represented, by definition, as a survival function. This evidences the statistical basis underlying the viscoelastic phenomena in their different manifestations. As a result, the viscoelastic characterization can now be directly achieved more objectively, avoiding the main inconsistencies of the classic TTS methodologies. The physical interpretation of the model parameters is straightforward.

The selection of the cdf of the normal distribution to describe the time evolution of the normalized relaxation module is justified by using the central limit theorem when the total elongation of a viscoelastic sample in a creep test is supposed to be the sum of the random elongations of a large set of primary elements, in which the specimen is virtually divided. The long-term characteristics of the relaxation phenomenon requires the extrapolation of available data from the short-term curves recorded in the tests for different temperatures towards the limiting cases, $t \rightarrow 0$ and $t \rightarrow \infty$. Thus, the use of distributions from the generalized extreme value family represents the natural solutions for viscoelastic characterization. In particular, the Gumbel distribution, as the domain attraction of the normal and log-normal ones, appears as the optimal candidate to completely describe the relaxation modulus over time.

To this end, two different approaches are developed in this thesis, which represent two ways of handling the temperature effect. In the first approach, the temperature effect is supposed to act as a change of the scale parameter on the cumulative distribution function of both normal and Gumbel distributions. The estimation of a master curve for a reference temperature succeeds from the short-term curves recorded in the experimental campaign at different temperatures in an experimental window interval between two fixed times due to practical limitations of the tests. In the second approach, the statistical compatibility condition between the value of the relaxation modulus over time for a given temperature $E(t; T)$ and the value along temperature for a given time $E(T; t)$ is applied, allowing the T - t field to be analytically defined. As a result, all experimental data from the short-time relaxation curves at different temperature are pooled together into one sole Gumbel cumulative distribution function representing the most suitable equation to fit the master curve. Once this field is estimated, the master curves of both $E(t; T)$ and $E(T; t)$ fields can be derived directly.

The viscoelastic phenomena prove to be stochastic processes, in which time and temperature are the main influencing variables (in addition to the limiting values, i.e. elastic and relaxed moduli). The Bayesian technique provides the probabilistic dimension to the main viscoelastic variables, i.e. relaxation modulus and creep compliance, for both types of deterministic viscoelastic approaches, currently used and statistics-based ones, respectively, by defining the statistical distributions of the intervening parameters.

Finally, the applicability of these proposed models is confirmed using the results of an



experimental campaign consisting of a series of relaxation tests at various temperatures on a polyvinyl-butyril (PVB), as a widely used viscoelastic material.

The phenomenological models developed in this thesis address deformation progress in the relaxation case and stress evolution in the creep case. While this is an important contribution to the mechanical characterization of viscoelastic materials, it may be incomplete as static and fatigue failures would likely cause a premature interruption of the service function of the component. This cannot be solved with the models, including the probabilistic models, developed up to here. This thesis presents a way to predict static fracture and fatigue lifetime taking temperature effect into account by applying an adapted version of previous phenomenological models, based on statistical functions. The resulting fracture development, which deals with the concomitant effect of notches and temperature, should be understood as a first step towards the development of a universal concept of practical design of components made of viscoelastic materials.

In fact, though real service conditions are usually concerned with these effects acting simultaneously, currently used methodologies focused on only one of them in the prediction of fracture resistance properties. Unlike these deterministic methodologies, such as the theory of critical distances, this thesis proposes a probabilistic model to consider the notch effect in notch fracture toughness. This approach takes the inherent scatter of experimental fracture results into account in the failure prediction, under any notch geometry conditions.

The thesis extends the proposed fracture model to include the temperature effect, based on the compatibility condition between the intervening cumulative distribution functions, which allows the lower and intermediate regions of the brittle-to-ductile transition curve to be defined using the notch fracture toughness concept in a probabilistic manner. The model can be improved by applying the Bayesian technique, which provides the statistical distributions of the failure percentile as their confidence intervals. Finally, the fracture results of a large external experimental campaign on ferritic steels, involving different notch and temperature conditions, is assessed to corroborate the applicability of the proposed models.

SR. PRESIDENTE DE LA COMISIÓN ACADÉMICA DEL PROGRAMA DE DOCTORADO EN MATERIALES

Phenomenological Approach to Fitting and Interconversion of Viscoelastic and Lifetime Processes Using Statistical Functions

Adrián Álvarez Vázquez
Alfonso Fernández Canteli
María Jesús Lamela Rey

Phenomenological Approach to
Fitting and Interconversion of
Viscoelastic and Lifetime Processes
Using Statistical Functions



Universidad de Oviedo
University of Oviedo

Adrián Álvarez Vázquez: Phenomenological Approach to Fitting and Interconversion
of Viscoelastic and Lifetime Processes Using Statistical Functions

© 2020 University of Oviedo

Cover Design: Frido Steinen-Broo, eStudio Calamar

PhD Dissertation
All Rights Reserved

First Edition, July 2020

To Andrea

Acknowledgements

As well known, a Ph.D thesis is never the result of a single person, but an uncountable number of contributing people. These words are dedicated to all of them.

First and foremost, I wish to express my deep gratitude to Prof. Alfonso Fernández Canteli and Dr. María Jesús Lamela Rey, supervisors of this Ph.D. thesis, for their constant, unconditional and tireless support, dedication, patience, motivation and friendship. Thanks for giving me the opportunity to meet incredible researchers and scientists. I sincerely feel myself fortunate to have participated in their way of understanding work, research, relationships and life. Thanks for giving me the chance of being the scientist that I am today.

I would also like to thank Prof. Enrique Castillo for his dedication to this thesis as if he were another director, for his teachings and discussions, unconditional support, warmth in the treatment, for having reminded me of my passion for mathematics and serving as inspiration in work and life.

I would also like to especially acknowledge Dr. Miguel Muñiz Calvente, who was more than just a co-worker from the beginning. Thank you for your interesting discussions, unreserved support and boundless and selfless kindness. I am glad a friendship has resulted beyond this thesis.

Thanks also to Dr. Pelayo Fernández Fernández for having supported me from the beginning, your enriching discussions and for treating me as if I were your doctoral student.

Thanks also to all the doctoral students with whom, during the last four years, I shared hours of work, meals and hundreds of conversations. Thank you for receiving me so warmly from the first day.

Thank also to my parents for trusting always in me and for their constant support in everything I have entered in since my first studies, even without understanding many times what I spent so many hours on.

I cannot finish these words without especially thanking my couple, Andrea, who has shared with me the sorrows and joys of these years with patience, always supporting me, serving as a guide and putting my achievements before hers on many occasions. Without you, I wouldn't have got it.

Finally, I acknowledge the Ministry of Economy and Competitiveness for financial support of the project DPI2016-80389-C22-2-R.

Abstract

Viscoelastic materials comprise a broad variety of materials, such as polymers, quasi-brittle materials, woods, tissues and metals at high temperature, widely used as mechanical, structural and biological components in many engineering fields. They are characterized by a combination of elastic and viscous behaviour when stress or strain conditions are applied. Time and temperature are the main factors influencing the behaviour of viscoelastic materials under static load or deformation, while frequency can be added as an influencing factor when dynamic load is applied. Many other external effects such as pressure, humidity and ageing, exert an influence on their response.

The use of viscoelastic materials in mechanical and structural elements and components requires a previous characterization of their viscoelastic mechanical behaviour. This is required in the limit states analysis when the component is subject to complex stress and strain loading conditions as implied in the prototype predesign, manufacturing process and computational design.

Viscoelastic characterization is likewise complex, particularly because of the limited time interval in which the data can be recorded. The infeasibility of extending a test to an infinite time, or at least to a long-term duration leads to a number of requirements in the characterization process. Firstly, the necessity of carrying out an experimental campaign based on short term viscoelastic curves at different temperatures. Secondly, the joint evaluation of those short term viscoelastic curves. For instance, the evolution of the relaxation modulus can be used to estimate the master curve of this viscoelastic variable using an adequate model. Thirdly, the conversion of the master curve using the model to determine the value of the viscoelastic variable, for any time and temperature. This may imply extrapolation of the viscoelastic curves outside the range of the

experimental records.

The Time-Temperature Superposition (TTS) principle is widely used for building this master curve at a certain reference temperature, based on a presumable equivalence between time and temperature. This means that an adequate time-and-temperature-dependent mathematical model allows the master curve to be derived by transforming the short-term curves at different temperatures to a common reference temperature.

Currently used models based on the application of the TTS principle evidence certain disadvantages and inconsistencies, such as a minimum required overlapping between the short-term curves and the necessity of using at least two different TTS models for the master curve to be derived. Nevertheless, the most critical drawback of such models is the fact that they do not fulfil the basic conditions for a model to be valid, namely, uniqueness and compatibility. As a result, the fitted master curve depends on the temperature initially taken as a reference.

Phenomenological viscoelastic models, based on identification of the viscoelastic evolution as statistical functions of normal and Gumbel distributions, are suitable alternatives to overcome all these drawbacks. Their derivation fulfils basic physical and statistical requirements, including the compatibility condition, proving to be a valid solution for viscoelastic characterization. The normalization of the relaxation modulus with respect to its inherent twofold bounding limits represented by the elastic and relaxed moduli, as well as the observation of its monotonically decreasing character, suggest it can be represented, by definition, as a survival function. This evidences the statistical basis underlying the viscoelastic phenomena in their different manifestations. As a result, viscoelastic characterization can now be directly achieved more objectively, avoiding the main inconsistencies of the classic TTS methodologies. The physical interpretation of the model parameters is straightforward.

The selection of the cdf of the normal distribution to describe the time evolution of the normalized relaxation module is justified by using the central limit theorem when the total elongation of a viscoelastic sample in a creep test is supposed to be the sum of the random elongations of a large set of primary elements, in which the specimen is virtually divided. The long-term characteristics of the relaxation phenomenon requires the extrapolation of available data from the short-term curves recorded in the tests for different temperatures towards the limiting cases, $t \rightarrow 0$ and $t \rightarrow \infty$. Thus, the use of distributions from the generalized extreme value family represents the natural solution for viscoelastic characterization. In particular, the Gumbel distribution, as the domain attraction of the normal and log-normal ones, stands out as the optimal candidate to completely describe the relaxation modulus over time.

To this end, two different approaches are developed in this thesis, which represent two ways of handling the temperature effect. In the first approach, the temperature effect is supposed to act as a change of the scale parameter on the cumulative distribution function of both normal and Gumbel distributions. The estimation of a master curve for a reference temperature succeeds from the short-

term curves recorded in the experimental campaign at different temperatures in an experimental window interval between two fixed times due to practical limitations of the tests. In the second approach, the statistical compatibility condition between the value of the relaxation modulus over time for a given temperature $E^*(t^*; T^*)$ and the value along temperature for a given time $E^*(T^*; t^*)$ is applied, allowing the $T^* - t^*$ field to be analytically defined. As a result, all experimental data from the short-time relaxation curves at different temperature are pooled together into one sole Gumbel cumulative distribution function representing the most suitable equation to fit the master curve. Once this field is estimated, the master curves of both $E^*(t^*; T^*)$ and $E^*(T^*; t^*)$ fields can be derived directly.

The viscoelastic phenomena prove to be stochastic processes, in which time and temperature are the main influencing variables (in addition to the limiting values, i.e. elastic and relaxed moduli). The Bayesian technique provides the probabilistic dimension to the main viscoelastic variables, i.e. relaxation modulus and creep compliance, for both types of deterministic viscoelastic approaches, currently used and statistics-based ones, respectively, by defining the statistical distributions of the intervening parameters.

Finally, the applicability of these proposed models is confirmed using the results of an experimental campaign consisting of a series of relaxation tests at various temperatures on a polyvinyl-butyril (PVB), as a widely used viscoelastic material.

The phenomenological models developed in this thesis address stress evolution in the relaxation case and deformation progress in the creep case. While this is an important contribution to the mechanical characterization of viscoelastic materials, it may be incomplete as static and fatigue failures would likely cause a premature interruption of the service function of the component. This cannot be solved with the models, including the probabilistic models, developed up to here. This thesis presents a way to predict static fracture and fatigue lifetime taking temperature effect into account by applying an adapted version of previous phenomenological models, based on statistical functions. The resulting fracture development, which deals with the concomitant effect of notches and temperature, should be understood as a first step towards the development of a universal concept of practical design of components made of viscoelastic materials.

In fact, though real service conditions are usually concerned with these effects acting simultaneously, currently used methodologies focused only on one of them in the prediction of fracture resistance properties. Unlike these deterministic methodologies, such as the theory of critical distances, this thesis proposes a probabilistic model to consider the notch effect in notch fracture toughness. This approach takes the inherent scatter of experimental fracture results into account in the failure prediction, under any notch geometry conditions.

The thesis extends the proposed fracture model to include the temperature effect, based on the compatibility condition between the intervening cumulative distribution functions, allowing the lower and intermediate regions of the brittle-to-ductile transition curve to be probabilistically defined using the notch frac-

ture toughness concept. The model can be improved by applying the Bayesian technique, which provides the statistical distributions of the failure percentile as confidence intervals. Finally, the fracture results of a large external experimental campaign on ferritic steels, involving different notch and temperature conditions, is assessed to corroborate the applicability of the proposed models.

Adrián Álvarez Vázquez
Gijón, July 2020

Resumen

Los materiales viscoelásticos comprenden una amplia variedad de materiales, tales como polímeros, materiales cuasi-frágiles, madera, tejidos, así como metales a altas temperaturas, ampliamente usados en componentes mecánicos, estructuras y biológicos en numerosas aplicaciones en ingeniería. Todos ellos se caracterizan por una combinación entre comportamiento elástico y viscoso cuando se les aplican tensiones o deformaciones. Sin embargo, su característica principal es su dependencia con respecto al tiempo y a la temperatura, bien sea bajo cargas estáticas o dinámicas, además de otros factores externos como la presión, la humedad o el envejecimiento.

El uso de este tipo de materiales viscoelásticos en el diseño de componentes mecánicos o estructurales requiere de una caracterización previa de su comportamiento mecánico, dado que la dependencia con estos factores externos influye no sólo en el diseño de componentes, sino también en la fabricación y modelización numérica.

La caracterización viscoelástica es compleja debido a la limitación de tiempo en el que se desarrolla una campaña experimental, dado su comportamiento a largo plazo, por lo que se requiere de una serie de restricciones en el proceso de caracterización. En primer lugar, la necesidad de llevar a cabo dicha caracterización a partir de una serie de curvas cortas de ensayos de relajación a distintas temperaturas. En segundo lugar, la evaluación conjunta de estos resultados experimentales para obtener la curva maestra del material, como por ejemplo en el caso del módulo de relajación, lo que requiere de modelos adecuados. En tercer lugar, la conversión de la curva maestra para una determinada temperatura de referencia a cualquier condición de tiempo y temperatura, lo cual implica la extrapolación de las curvas viscoelásticas fuera de los límites de

los resultados de experimentales.

El principio de Superposición Tiempo-Temperatura (TTS) es el método más utilizado para la construcción de las curvas maestras del material a una determinada temperatura de referencia, basado en una presumible equivalencia entre las variables tiempo y temperatura por la cual las curvas cortas a distintas temperaturas pueden ser transformadas a una curva maestra común a partir de un modelo de transformación tiempo-temperatura adecuado.

Los modelos de caracterización viscoelástica actuales basados en el principio TTS presentan ciertas desventajas e inconsistencias, tales como la necesidad de que las curvas cortas se solapen durante, al menos, una década de tiempo, o el requerir la combinación de dos modelos TTS distintos para poder definir la curva maestra en todo el rango de temperaturas. Sin embargo, el inconveniente principal de estas metodologías actuales reside en no satisfacer las dos condiciones necesarias para ser modelos válidos, como son la unicidad y la compatibilidad. De esta forma, las transformaciones en tiempo y temperatura de las curvas cortas a la curva maestra dependen de la temperatura de referencia de origen.

Por ello, los modelos fenomenológicos propuestos de caracterización viscoelástica, basados en la identificación de la evolución de las funciones viscoelásticas con las distribuciones normal y Gumbel, constituyen alternativas adecuadas para evitar estos inconvenientes de las metodologías clásicas, dado que su derivación está rigurosamente basa en condiciones físicas y estadísticas, tales como la condición de compatibilidad, justificando ser así una solución válida para la caracterización viscoelástica. La normalización del módulo de relajación con respecto a su inherente doble acotación, entre los módulos elástico y relajado, además de su condición de función monótona y estrictamente decreciente permite que sea asimilada, por definición, por una función de supervivencia, lo que permite evidencia una base estadística que subyace en el fenómeno viscoelástico en sus diferentes representaciones. Con ello, la caracterización viscoelástica puede llevarse a cabo de una forma más objetiva y directa, evitando además las inconsistencias de los modelos clásicos basados en el principio TTS. Así mismo, los parámetros de los modelos que se proponen tienen una interpretación física más directa.

La selección de las cdf de la distribución normal para la descripción de la evolución temporal del módulo de relajación está justificada por el teorema central del límite cuando se considera la elongación total de una probeta de material viscoelástico sometida a un ensayo de fluencia como la suma de una serie de elongaciones aleatorias correspondientes a los elementos primarios en los que se puede subdividir dicha probeta. Por otro lado, el comportamiento a largo plazo del fenómeno de relajación requiere de una extrapolación de los datos disponibles experimentalmente en las curvas cortas a distintas temperaturas para los casos límite $t \rightarrow 0$ y $t \rightarrow \infty$. Por ello, el uso de la familia de distribuciones de valores extremos constituye una solución natural a la caracterización viscoelástica, en particular la distribución de Gumbel por ser el dominio de atracción de la distribución normal o log-normal.

Por ello, se desarrollan en esta tesis dos aproximaciones distintas, tal que representan dos formas de analizar el efecto de la temperatura. En el primer caso, se asume que el efecto de la temperatura actúa modificando el parámetro de escala en la función de distribución acumulada de ambas distribuciones normal y Gumbel. De esta forma, la estimación de la curva maestra para una determinada temperatura de referencia se consigue a partir de las curvas cortas experimentales a distintas temperaturas, debido a la imposibilidad práctica de extender la ventana temporal del ensayo. En el segundo caso, la condición de compatibilidad estadística entre la distribución del módulo de relajación para una temperatura dada, $E^*(t^*; T^*)$, y la distribución del módulo de relajación para un tiempo dado, $E^*(T^*; t^*)$, se aplica para obtener la definición analítica del campo $T^* - t^*$. Como resultado, los datos experimentales de las curvas cortas de relajación pueden ser representados en una única curva maestra perteneciente a la distribución de Gumbel, constituyendo así la curva maestra más general posible. Así, una vez dicho campo es estimado, las curvas maestras para los dos campos correspondientes $E^*(t^*; T^*)$ y $E^*(T^*; t^*)$ pueden ser obtenidas directamente para cualquier condición de tiempo y temperatura.

Adicionalmente, dado que los fenómenos viscoelásticos y su evolución en el tiempo constituyen fenómenos estocásticos, las técnicas Bayesianas se aplican a los modelos propuestos para lograr así una definición probabilística del módulo de relajación y obtener las distribuciones estadísticas de los parámetros que intervienen en dichos modelos.

Finalmente, con el objetivo de corroborar la aplicabilidad de los modelos propuestos, se realiza una campaña experimental con ensayos de relajación a diferentes temperaturas en un material viscoelástico comercial, conocido como polyvinyl-butyril (PVB), comúnmente utilizada en aplicaciones en ingeniería.

Los modelos fenomenológicos desarrollados en esta tesis se enfocan en el estudio de la evolución de las tensiones en el caso del fenómeno de relajación, o bien de deformaciones en el caso de la fluencia. Aún a pesar de su importancia en la caracterización mecánica de materiales viscoelásticos, este enfoque resulta incompleto cuando se consideran posibles fallos a fractura y fatiga, presentes en las condiciones de servicio de componentes reales, los cuales no pueden ser resueltos por medio de los modelos propuestos anteriormente. Por ello, esta tesis presenta una metodología para la derivación de modelos de predicción de fractura estática con consideración del efecto de la temperatura, basada en los modelos propuestos en la caracterización viscoelástica. En este sentido, los desarrollos que se proponen en fractura, con consideración no sólo del efecto de la temperatura, sino también del radio de entalla, deben de ser entendidos como un primer paso en la derivación de metodologías universales en la caracterización de materiales viscoelásticos para el diseño real.

En efecto, aún a pesar de que las condiciones de servicio reales suelen incluir la combinación de efectos externos, tales como la temperatura o el radio de entalla, las metodologías actuales de caracterización a fractura suelen estar focalizadas en uno sólo de estos efectos. Por este motivo, se propone un modelo probabilístico para considerar el efecto de entalla en la predicción de la tenacidad a fractura en

componentes entallados, basada en la teoría de las distancias críticas, permitiendo así tener en cuenta la inherente dispersión de los ensayos a fractura en la predicción probabilística del fallo bajo cualquier condición geométrica de la entalla.

Como extensión, esta tesis extiende este modelo probabilístico para el análisis del efecto de entalla para incluir el debido a la temperatura, por medio de la aplicación de la compatibilidad estadística entre las distribuciones acumuladas que intervienen, permitiendo así definir las zonas inferior e intermedia de la curva de transición frágil a dúctil de una forma probabilística y con la tenacidad a fractura para componentes entallados. Mediante la aplicación de las técnicas Bayesianas se consiguen mejorar los modelos propuestos proporcionando las distribuciones estadísticas de las curvas percentiles de fallo, a modo de intervalos de confianza. Finalmente, la aplicabilidad de los modelos propuestos se corrobora por medio de una extensa campaña experimental externa en dos aceros ferríticos que incluye distintas condiciones de temperatura y radios de entalla.

Adrián Álvarez Vázquez
Gijón, julio 2020

Nomenclature

The main notations used in this book are herewith listed, attempting to keep the notations consistent throughout the book as much as possible.

NOTATIONS

B	parameter of the Gumbel-Gumbel model for $T^* - t^*$ field. parameter of the Gumbel-Gumbel model for $K_c^* - T^*$ field. parameter of the Weibull-Weibull model for $K_c^* - T^*$ field. specimen thickness.
B_0	reference specimen thickness.
B_{AG}	parameter model of the Adam and Gibbs model.
B_{BC}	parameter model of the Bestul and Chang model.
B_{GS}	parameter model of the Goldstein model.
C	parameter of the Gumbel-Gumbel model for $T^* - t^*$ field. parameter of the Gumbel-Gumbel model for $K_c^* - T^*$ field.
C_1^0	parameter of the WLF model at a reference temperature T_0 .
C_2^0	parameter of the WLF model at a reference temperature T_0 .
D	creep uniaxial compliance.
E	relaxation uniaxial modulus.
E'	relaxation storage modulus.
E''	relaxation loss modulus.
E^*	normalized relaxation uniaxial modulus.
E_0	elastic or initial relaxation uniaxial modulus.

E_T	total relaxation uniaxial modulus.
E_∞	relaxed relaxation uniaxial modulus.
E_i	relaxation uniaxial modulus of the i -th sub-element.
$F(\cdot)$	cumulative distribution function.
$F^{-1}(\cdot)$	quantile function.
G	relaxation shear modulus.
G'	storage relaxation shear modulus.
G''	loss relaxation shear modulus.
$G(\lambda, \delta)$	Gumbel distribution.
G_0	elastic or initial relaxation shear modulus.
G_∞	relaxed relaxation shear modulus.
H	step or impulse function.
	enthalpy variable.
	moisture percentage.
H_T	total inverse relaxation uniaxial modulus.
H_i	inverse relaxation uniaxial modulus of the i -th sub-element.
J	creep shear compliance.
J'	storage creep shear compliance.
J''	loss creep shear compliance.
J_0	elastic or initial creep shear compliance.
J_∞	relaxed creep shear compliance.
K_0	parameter of the Wallin's model corresponding to $p = 0.632$.
K_c	critical stress intensity factor or fracture toughness.
K_c^N	notch fracture toughness.
K_{\min}	minimum experimental fracture toughness.
L	critical distance.
	length of the specimen.
$L(\cdot)$	maximum likelihood estimation function.
$N(\mu, \sigma^2)$	normal distribution.
$Q_T(\cdot)$	power or scale shift factor function.
$Q_\rho(\cdot)$	transformation function for notch radii.
R	universal gas constant.
$S(\cdot)$	survival cumulative distribution function.
S_c	entropy variable.
T	temperature.
T^*	dimensionless temperature.
T_g	glassy temperature.
T_l	threshold temperature of the Bueche model.
T_r	rubbery temperature.
V^*	normalizing variable.
$W(\lambda, \delta, \beta)$	Weibull distribution.
X	random variable.
Y	random variable.
Z	random variable.
Δg_a	parameter of the Eyring model.
$\Gamma(\cdot)$	gamma function.
$\Phi(\cdot)$	standard normal distribution.

Π	dimensionless variable.
α	extended parameter for maxima or minima operations. curing degree.
α_{extreme}	vector hyperparameter of an extreme value distribution.
α_{mean}	vector hyperparameter of the normal distribution.
β	shape Weibull parameter.
δ	scale Weibull parameter. parameter from Gumbel-Gumbel model in the $K_c^* - T^*$ field. parameter from Weibull-Weibull model in the $K_c^* - T^*$ field. parameter from Gumbel-Gumbel model in the $T^* - t^*$ field. scale Gumbel parameter.
$\delta_1(\cdot)$	scale family of parameters for the $E^* - T^*$ field.
$\delta_2(\cdot)$	scale family of parameters for the $K_c^* - T^*$ field. scale family of parameters for the $E^* - T^*$ field. scale family of parameters for the $K_c^* - T^*$ field.
δ_T	total displacement.
$\delta_{T^*}(\cdot)$	scale family of time-dependent functions.
$\delta_\rho(\cdot)$	scale parameter dependent of the notch radius.
$\delta_{t^*}(\cdot)$	scale family of temperature-dependent functions.
η	viscosity.
λ	location Weibull parameter. location Gumbel parameter.
$\lambda_1(\cdot)$	location family of parameters for the $E^* - t^*$ field. location family of parameters for the $K_c^* - T^*$ field.
$\lambda_2(\cdot)$	location family of parameters for the $E^* - t^*$ field. location family of parameters for the $K_c^* - T^*$ field.
λ_p	relaxation time of the p-chain's rotation.
$\lambda_{T^*}(\cdot)$	location family of time-dependent functions.
$\lambda_\rho(\cdot)$	location parameter dependent of the notch radius.
$\lambda_{t^*}(\cdot)$	location family of temperature-dependent functions.
$U(a, b)$	uniform distribution.
μ	mean.
ν	number of dimensionless variables.
ω	test frequency.
ρ	notch root radius.
ρ^*	dimensionless notch root radius.
ρ_{num}	concentration of segments in the molecular structure.
σ	stress. standard deviation.
σ_0	characteristic stress value.
$\tan \delta$	loss tangent.
τ	relaxation time.
θ	vector parameter of a distribution.
θ_0	parameter model for the $Q^* - T^*$ field.
θ_1	parameter model for the $Q^* - T^*$ field.
θ_{extreme}	vector parameter of an extreme value distribution.
θ_{mean}	vector parameter of the normal distribution.

\tilde{G}	predictive value of G in the Bayesian approach.
ε	strain.
ε_T	total strain.
$a_T(\cdot)$	shift factor horizontal function.
a_n	normalizing constants.
$a_{T^*}(\cdot)$	shift factor horizontal function for dimensionless temperature.
a_α	curing degree shift factor function.
a_{t_e}	ageing shift factor function.
b	parameter of the Wallin's model.
b_1	parameter of the Bueche model.
b_2	parameter of the Bueche model.
$b_T(\cdot)$	shift factor vertical function.
b_n	normalizing constants.
cdf	cumulative distribution function.
f	free volume.
f_0	free volume at a reference temperature T_0 .
i	reference integer.
j	reference integer.
k	reference integer.
k_B	Boltzmann's constant.
p	percentile value or probability of failure.
q_{\max}	distribution for maxima.
q_{\min}	distribution for minima.
r	distance around a notch tip.
s	Laplace variable.
t	time.
t^*	dimensionless time.
t_c	reference time value.
t_e	ageing time.
t_{\inf}	minimum value of the time experimental window.
t_{\sup}	maximum value of the time experimental window.

Contents

Abstract	vii
Resumen	xi
Nomenclature	xv
I Introduction and Motivation	1
1 Introduction	3
1.1 Motivation	3
1.2 Objectives	5
1.3 Thesis Outline	6
II Phenomenological Model Building	9
2 Derivation of Phenomenological Models	11
2.1 Introduction	11
2.2 Elements in Phenomenological Building Models	12
2.2.1 Physical phenomena	12
2.2.2 Model properties	13
2.2.3 Feasible conditions	14
2.2.4 Model definition	14
2.3 General Methodology	14
2.4 Concluding Remarks	17

3	Mathematical and Statistical Methods	19
3.1	Introduction	19
3.2	Dimensional Analysis	20
	3.2.1 Dimensional consistency	20
	3.2.2 Physically valid consistency	21
	3.2.3 Buckingham's Theorem	22
	3.2.4 Dimensional and dimensionless models	23
3.3	Functional Equations	24
	3.3.1 Basic concepts and definitions	24
	3.3.2 Equations for one function of one variable	25
	3.3.3 Equations with several functions in one variable	26
	3.3.4 Equations for one function of several variables	28
	3.3.5 Equations with functions of several variables	28
3.4	Probabilistic Theoretical Considerations	30
	3.4.1 Operation-stable families	30
	3.4.2 Reproductivity property	30
3.5	Extreme Value Theory	31
	3.5.1 Order statistics	32
	3.5.2 Extreme value distributions	33
	3.5.3 Limit distributions for maxima and minima	34
	3.5.4 Extended families for extreme values	37
	3.5.5 Parameter estimation	39
3.6	Conditional Specification of Statistical Models	40
	3.6.1 The Weibull-Weibull model	42
	3.6.2 The Gumbel-Gumbel model	44
	3.6.3 The Weibull-Gumbel model	44
3.7	Concluding Remarks	45
III	Viscoelastic Characterization Models	47
4	An Overview of Viscoelasticity	49
4.1	Introduction	49
4.2	Viscoelastic Characterization	50
	4.2.1 Static experiments	52
	4.2.2 Dynamic experiments	55
4.3	Mathematical Models	58
	4.3.1 Differential representation	58
	4.3.2 Integral representation	59
	4.3.3 Mechanical models	60
	4.3.4 Models based on fractional derivatives	64
	4.3.5 Prony series	65
	4.3.6 Stretched exponential model	66
	4.3.7 Viscoelastic spectrum representation	67
4.4	Interconversion among the Linear Viscoelastic Functions	68
	4.4.1 Exact interconversions	70
	4.4.2 Approximate interconversions	71

5	Statistical Approaches to Viscoelasticity	73
5.1	Introduction	73
5.2	Previous Statistical Approaches	74
5.3	The Proposed Statistical Approaches	75
5.3.1	The central limit approach	77
5.3.2	The extreme value approach	78
5.3.3	The Bayesian approach	81
5.4	Concluding Remarks	84
6	Temperature Effect	85
6.1	Introduction	85
6.2	Current Methodologies	87
6.3	Necessary Conditions for Valid Models	92
6.3.1	Dimensional analysis	92
6.3.2	Temperature-dependent normalization	93
6.3.3	Uniqueness condition	96
6.4	Proposed Models based on the Scale-Effect Property	98
6.4.1	Derivation of the model	98
6.4.2	Proposed models	99
6.4.3	Parameter estimation	102
6.5	Proposed Models based on the Compatibility Condition	103
6.5.1	Derivation of the model	103
6.5.2	Proposed models	107
6.5.3	Parameter estimation	108
6.5.4	Model validation	109
6.6	Probabilistic Models	110
6.7	Example of Application	113
6.7.1	Description of the experimental program	113
6.7.2	Proposed models based on the scale-effect property	114
6.7.3	Proposed models based on the compatibility condition	116
6.7.4	Probabilistic models	120
6.8	Concluding Remarks	126
7	Software ProVisco	129
7.1	Introduction	129
7.2	Description of the Software Program	130
7.3	Main ProVisco Applications	132
8	Extension to Related Viscoelastic Phenomena	135
8.1	Introduction	135
8.2	Moisture Effect	136
8.3	Physical Ageing	137
8.4	Curing Effect	138
8.5	Interconversion among Viscoelastic Functions	140
8.5.1	Relaxation and creep functions	140
8.5.2	Static and dynamic functions	141
8.6	Concluding Remarks	143

IV	Fracture Characterization Models	145
9	Notch and Temperature Effects in Fracture of Metals	147
9.1	Introduction	147
9.2	Current Methodologies	149
9.2.1	Influence of the notch effect	149
9.2.2	Influence of the temperature effect	152
9.3	Proposed Methodology for Modelling the Notch Effect	155
9.3.1	Minimal required conditions	155
9.3.2	Derivation of the model	157
9.3.3	Parameter estimation	159
9.4	Proposed Methodology to Model Notch and Temperature Effects	160
9.4.1	Minimal required conditions	160
9.4.2	Proposed models based on the scale-effect property	161
9.4.3	Proposed models based on the compatibility condition	166
9.4.4	Proposed Bayesian Models	170
9.5	Examples of Practical Application	171
9.5.1	Proposed methodology for the notch effect	171
9.5.2	Proposed methodology for notch and temperature effects	174
9.6	Concluding Remarks	180
V	Conclusions, Original Contributions and Future Work	183
10	Conclusions	185
10.1	Conclusions	185
10.2	Conclusiones	188
11	Original Contributions	191
11.1	Original Contributions	191
11.2	Contribuciones Originales	193
12	Future Work	195
12.1	Future Work	195
12.2	Trabajo Futuro	197
VI	Appendixes	199
A	Solution of the Weibull-Gumbel Model	201
	Bibliography	205
	Publications	221

I

Introduction and Motivation

1

Introduction

1.1 Motivation

The development of phenomenological models in science and engineering for dealing with physical phenomena is a complex task since modeling requires a subtle equilibrium between pure and applied perspectives. The former existing approaches represent too simple or excessively complex models with large sets of variables and parameters, for which the existence of a solution is not ensured. The empirical perspective of these approaches may provide inconsistent models, ignoring important feasible conditions, and leading to inconsistent or even erroneous results and conclusions. The process must consider only the physical and statistical properties of the phenomenon under study and avoid arbitrary assumptions as much as possible. Therefore, the derivation of consistent models must be systematically built according to rigorous methodologies based on stronger theoretical principles and conditions.

Special mention must be given to physical phenomena with a probabilistic nature, frequently appearing in science and engineering. As a particular enrichment of the phenomenological models, probabilistic considerations require additional theoretical background in their derivation. From a suitable identification of the random variables involved in the problem, to the characterization of their statistical distributions, the use of rigorous methodologies and guidelines is strongly recommended in the development of these models.

Viscoelastic characterization represents an example of this complex counterbalance where the derivation of phenomenological models is a compulsory requirement due to the complexity of the time-and-frequency dependent mechanical properties. Indeed, the characteristic long-term behaviour of these phenomena over several decades requires the development of extrapolation methods or model properties able to use affordable and practical experimental information in a short time interval to predict viscoelastic properties beyond these limits. To this aim, a wide variety of mathematical models have been proposed over recent decades suggesting an equivalence between time and temperature, based on the so-called Time-Temperature Superposition (TTS) principle, in an attempt the viscoelastic properties for the largest and shortest values of time to be obtained from the experimental results of specimens tested at different temperatures. Thus, the derivation of mathematical transformations between time and temperature variables is the key to building a master curve of the material, entirely covering the evolution of viscoelastic properties over time, by testing and transforming the experimental data at several temperatures.

Nevertheless, this kind of transformations must not be arbitrarily defined and rigorous conditions should be studied and imposed in establishing model. Indeed, the current methodologies show some disadvantages and contradictions in practical applications, being dependent on the experience of the user to pre-determining conditions in the fitting together with the requirement of a minimum overlapping between the short-term curves to provide a suitable estimation of the master curve. Another inconvenient is the large set of parameters required to fit the experimental data in a real application. Finally, two additional drawbacks are the absence of the most critical necessary conditions, namely, the uniqueness and the compatibility, leading to time-and-temperature transformations depending on the reference temperature taken as origin.

Furthermore, the evolution of viscoelastic properties in time are inherently stochastic processes with non-negligible scatter, being unfortunately ignored in current deterministic methodologies. For this reason, the use of the Bayesian techniques to develop probabilistic models able to define the master curves of the material as percentile curves instead of one single curve should be addressed as an important enhancement of currently-used methodologies to provide the practical design of viscoelastic components.

However, the viscoelastic characterization problem formulated as above is incomplete, since the mechanical characterization of viscoelastic materials should also consider the static and fatigue failures in real service conditions. To this aim, new phenomenological approaches must be developed to take into account the real service conditions aiming at a universal concept of practical design of components made of viscoelastic materials based on the probabilistic characterization of their deformation and creep behavior over time as well as the probabilistic prediction of fracture and fatigue lifetime of these components

Some first steps to achieve this aims are given by analyzing the influence of the notch effect on fracture resistance properties, which has been widely studied with a wide variety of proposed models and methodologies in literature. Unfor-

tunately, these current methodologies conceive fracture resistance properties as non-random variables, which is clearly unrealistic since the scatter is well-known to be non-negligible. For this reason, the development of probabilistic methodologies able to predict the failure of notched components and the influence of change in the notch radius, is of practical importance in the engineering design of structural and mechanical components.

The influence of other external effects due to the service conditions in the fracture behaviour of these components has also been studied in depth, especially the temperature effect. In this case, probabilistic approaches are well-established in the contemporary methodologies and international standards. However, their parameters are defined as fixed values, experimentally identified as valid for a certain family of materials. This reduces its applicability and ignores some important statistical considerations. To this end, an initial identification of the required feasible conditions must be performed in order to build consistent and general models to describe the temperature effect on the fracture resistance properties encompassed in a probabilistic approach.

More importantly, due to the concurrency of different effects in the real service conditions of these components, the development of phenomenological models must be focused on their combined influence on the predictions of failure, such as the case of the notch and temperature effects addressed in this thesis. Again, the derivation of these advanced methodologies require strong statistical and physical conditions in order to make use of largely heterogeneous experimental information from different testing conditions, based on a probabilistic approach able to consider the inherent scatter of the fracture process.

Finally, as an enhancement of the proposals in this work for dealing with both effects, i.e time and temperature, the application of Bayesian methods make it possible to define the statistical distribution of the percentile curves of failure probability interpreted as their confidence bands, assessing the practical design with valuable information.

1.2 Objectives

Accordingly, the general objectives of this Ph.D. thesis are herewith summarized:

1. To define a rigorous consistent general methodology for building valid phenomenological mathematical models to study viscoelastic phenomena, ensuring consistency and feasibility from different viewpoints and allowing the viscoelastic behaviour to be predicted for other conditions of time and temperature.
2. To develop phenomenological models for viscoelastic characterization involving different external effects, such as temperature, pressure and moisture, with the following specific objectives:
 - To recognize the statistical nature of viscoelastic phenomena, and de-

veloping approaches based on the use of statistical distributions to define analytically the evolution of viscoelastic functions (relaxation and creep moduli) over time.

- To identify the necessary conditions to be imposed in the derivation of any viscoelastic characterization models dealing with time- and temperature-dependent transformations, or other external effects.
 - To derive alternative transformation laws, between time and temperature to those currently implied in the TTS principle, to build the master curve of the material at any reference temperature, avoiding the inconsistencies and practical limitations of the current methodologies.
 - To include into the proposed phenomenological models additional viscoelasticity related effects, such as that due to moisture and curing.
 - To apply the Bayesian technique to the viscoelastic characterization of materials, handling the time evolution of the viscoelastic properties under study (relaxation modulus) as a stochastic process, in contrast with current deterministic approaches.
3. To derive phenomenological models to characterize fracture of steel materials under simultaneous acting of temperature and notch effects. based on the experience gained in the development of the models applied to the viscoelastic characterization in the first objective and with the following specific objectives:
- To identify the feasible conditions to be imposed in the derivation of any fracture characterization model dealing with temperature and notch effects, acting either concurrently or separately.
 - To derive regression models to consider the notch effect in fracture resistance properties, conceiving them in a probabilistic manner, that is, able to take into account their inherent scatter in the prediction of failure, in contrast with current deterministic methodologies.
 - To derive regression models to consider the concurrent effect of temperature and the notch radius based on rigorous statistical and physical conditions.
 - To apply Bayesian techniques to the fracture characterization, enhancing the proposed probabilistic models in previous specific objectives providing the statistical distributions of the percentile curves of failure probability, interpreted as their confidence intervals.

1.3 Thesis Outline

Accordingly, this thesis is organised in five main parts as follows:

Part I presents an introduction and motivation together with the main objectives and the organization of the thesis.

Part II is concerned with the twofold purpose of this thesis. As a first aim, the general methodology or guidelines to follow in the derivation of phenomenological-mathematical models for viscoelastic and fracture characterization are described in detail in Chapter 2. The second aim, presented in Chapter 3, is to explain the theoretical mathematical and statistical background to be applied in the derivation of these models.

Part III is devoted to the development of the phenomenological-mathematical models for viscoelastic characterization. To this end, some previous concepts in viscoelasticity are introduced in Chapter 4. The proposed statistical approaches for viscoelastic characterization are outlined in detail and further discussed in Chapter 5, in which three possible statistical principles are distinguished from which the proposed models will be derived, namely, the central limit, the extreme value and the Bayesian approaches. Chapter 6 describes the derivation of the different models proposed for viscoelastic characterization based on these statistical approaches and analyzes the temperature effect and their application to experimental data. The software ProVisco is developed in order to apply some of the proposed models to practical case under a user-friendly environment, presented in Chapter 7. Lastly, Chapter 8 illustrates the effect of other external variables related to the viscoelastic phenomena, such as the effect of moisture, curing and physical ageing, to which the proposed methodology can also be successfully applied.

Part IV is concerned with the extension of probabilistic methodologies to fracture characterization. The proposed models for determining the influence of the notch effect on the fracture resistance properties and failure prediction are presented in Chapter 9. The concurrency of the temperature and notch effects is included, and illustrated with practical applications to experimental data with ferritic steels.

Finally, Part V summarizes the main conclusions of this thesis in Chapter 10, detailing the original contributions in Chapter 11 and proposing future work in Chapter 12.

II

Phenomenological Model Building

2

Derivation of Phenomenological Models

2.1 Introduction

The phenomenological models play a decisive role in the modelling of physical phenomena in engineering and science allowing to describe and predict their properties. Due to their excessive complexity, the assumption of some simplifications is compulsory in their derivation. However, a subtle equilibrium between these simplifications, that make them mathematically possible, and the fidelity with real-world problems is always present in this building process (see Frigg and Hartmann (2017)), as has been mentioned in previous chapter. Namely, a mathematical model reproducing exactly a physical phenomenon may lead to intractable expressions with quite number of variables and parameters, raising the computational cost without ensuring the existence of a solution. In turn, an excessively simplified model could ignore relevant features of the phenomenon providing erroneous predictions.

Moreover, these models must be carefully built taking into account a large variety of mathematical and theoretical considerations that ensure them to be valid from multiple perspectives. Frequently, there are current existing models violating some of these considerations, which could lead to serious errors and calculations since they are daily used for predicting and describing physical phenomena. Consequently, the design of adequate methodologies to be rigorously followed for building mathematical models in a systematic manner could avoid these inconveniences.

Accordingly, though being aware of the non-existence of universal nor perfect methodologies, this chapter is devoted to suggest a general, systematic and rigorous methodology to be used as guidelines in the derivation of mathematical models as an important contribution from this thesis, as previously indicated in Chapter 1. Indeed, the proposed models in both viscoelastic and fracture characterization problems will be derived in the following chapters according to these guidelines.

To this aim, the organisation of this chapter is as follows. On the one hand, the terms and concepts to be used in the formal statement of this methodology are discussed in Section 2.2, in order to be as much exact as possible. For this reason, an abstraction from particular mathematical models is required trying to identify the common elements shared within them, being a challenging task. On the other hand, the proposed general methodology is described in detail in Section 2.3, starting with the initial definition of the problem to the final expression and further application of the mathematical model.

2.2 Elements in Phenomenological Building Models

As a matter of fact, the difficult task of trying to identify the common ingredients of a phenomenological model, as a previous step before the detailed description of the general methodology, shows two interesting advantages. Firstly, this definition facilitates drawing a general scheme of the phenomenological building process, outlining the idea of the completeness for a model as a whole. That is, a mathematical model will be completely specified if those elements are conveniently defined. Secondly, a more exact use of terms in the formal statement of the methodology is allowed if the concepts are correctly employed. In fact, it is very common to face with engineering- and scientific-related models using quite different terms such as properties and feasible conditions as synonyms, which is not correct as will be shown in this chapter. More precisely, the underlying idea is that models are always based on properties and satisfy feasible conditions, which is not equivalent.

Three main different elements can be distinguished in the derivation of any phenomenological model, being illustrated as a flowchart in Figure 2.1 and described in detail in the following subsections. As the general idea, this process begins with the definition of the model properties replicating strictly the physical features of the phenomenon under study. Then, the feasible conditions must be imposed afterwards ensuring the proposed models to be valid from different points of view, resulting as final output the model definition.

2.2.1 *Physical phenomena*

The origin of a mathematical model is always located in the study of a certain physical phenomenon, providing entirely with the information for its derivation.

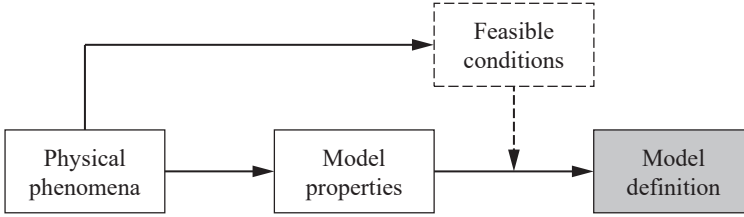


Figure 2.1: Elements in the process of derivation of a mathematical model.

A detailed description and analysis of the phenomenon must include the relevant aspects from a mathematical point of view, such as for instance a list of the involved variables with their general properties (boundless or unboundless, discrete or continuous,...), relevant external effects influencing the phenomenon, among others. Also of interest is to delimit the scope of the model to be proposed, distinguishing the features being object of study and whose not.

2.2.2 Model properties

Any mathematical model is built based on a certain set of properties, whose must be replicated from the analysis of the physical phenomenon under consideration. Indeed, only those properties derived directly from the phenomenon are justified in the mathematical model building, since any auxiliar or assumed properties not strictly based on it must be avoided as much as possible.

Afterwards, these properties must be formally translated into mathematical terms, which constitutes the most difficult part. A deep and heterogeneous knowledge about different mathematical disciplines could be required, ranging from statistics, functional equations, analysis, algebra, among others, where the functional equations theory could extraordinarily serve to this aim, as pointed out in Galambos (1982), Castillo and Ruiz-Cobo (1992) and Castillo et al. (2004b). Their formal statement usually adopt the form of equations, constraints or system of equations. Examples of model properties are the linearity or non-linearity, the additive property or the lack of memory, among others. The latter ones is used in the following example to illustrate how they can be used to specify the model and avoid arbitrary assumptions.

Example 2.1 (Lack of memory property). Consider the random lifetime of a certain system X such that it is known to show the lack of memory property. In other words, the probability of having a life greater or equal to some value x , i.e. $\Pr(X \geq x)$, is not influenced if z time has already occurred, that is, $\Pr(X \geq x + z | X \geq z)$. This property can be written in mathematical terms as follows:

$$\Pr(X \geq x + z | X \geq z) = \Pr(X \geq x), \quad (2.1)$$

such that it can be easily demonstrated that the unique solution of Eq. (2.1) is the exponential distribution $F(x) = 1 - e^{-bx}$, $x \geq 0$ for some parameter $b > 0$

(see, for example, Galambos and Kotz (1978, p. 7–8) and Galambos (1982)). Thus, a correct identification and solution of a property directly derived from the physical phenomenon, such as the lack of memory property, avoids to choose presumably a statistical distribution for the lifetime. Even worse, for any other distribution to be suggested different to the exponential, the model would be ignoring this property since it is only satisfied by the exponential distribution. \square

2.2.3 Feasible conditions

Even properly having selected the set of properties, a mathematical model could still leading to serious errors and inconveniences. Namely, a correct identification and replication of the model properties is necessary but not sufficient for defining valid mathematical models, since a set of feasible conditions must be also imposed (see Figure 2.1). There are two possible origins where the feasible conditions could come from: a) the physical phenomenon and b) the theoretical background. In the first case, the feasible conditions are related with the characteristics of the physical phenomenon to be replicated in the proposed model. In the second case, the feasible conditions result from mathematical and statistical principles and considerations, whose must be satisfied in any case, as will be illustrated in Example 2.2. In Chapter 3 different kind of conditions of this second type will be reviewed and described coming from different mathematical disciplines.

Example 2.2 (Random summation of lifetimes). Continuing with Example 2.1, suppose that the system is now divided into n parts, such that the random lifetime must be calculated by adding these individual contributions. If the resulting random variable from this summation is assumed to hold being exponential, an important error will be committed, since this distribution is not reproductive and the sum of exponentials does not belong to the exponential family of distribution. \square

2.2.4 Model definition

Once both sets of model properties and feasible conditions are conveniently defined and formally stated, the model is now justified to be derived based on the former and satisfying the latter. Usually, a mathematical model definition adopts the form of an explicit functional relating the variable of interest Y as a function of the other involved variables (X_1, X_2, \dots, X_n) , besides a vector of parameters $(\theta_1, \theta_2, \dots, \theta_m)$ for the model to be estimated and particularized to real data.

2.3 General Methodology

Despite of being a tough task trying to state a methodology in something as abstract as mathematical modelling science, some efforts were devoted to propose methodologies for deriving models systematically, such as for instance Saaty and

Joyce (1981), Berry et al. (1984), Meyer (1984), Kapur (1988) and Towers et al. (2001). Unfortunately, these methodologies were conceived from a conceptual thinking and educational points of view and a lack of applicability to real-world problem is evident. In turn, the proposal to be followed in this work is more precisely and mathematically defined for serving as guidelines in a real mathematical building process, which is suggested to be developed in six main steps:

1. *Problem definition.* An incorrect definition of the problem of the physical phenomenon under study can clearly conditioned the rest of the mathematical building process. Equally relevant is also the delimitation of the scope of the study within the features of the physical phenomenon.
2. *Identification of variables.* The initial set of involved variables must be correctly identified in the problem, indicating their basic properties (discrete or continuous, quantitative or qualitative, boundless or unboundless, deterministic or random variables, possible systems of units, etc.). This step is quite relevant in the modelling process since if a variable is ignored, then future predictions will not be able to take into account the effects due to these ignored variables. Let X_i be the i -th variable, with $1 \leq i \leq n \leq m$, such that the initial set of involved variables ν_0 can be written as follows:

$$\nu_0 \equiv \{X_1, X_2, \dots, X_n, X_{n+1}, \dots, X_m\}. \quad (2.2)$$

3. *Classification of variables.* Due to the intrinsic complexity of scientific problems, being influenced of large sets of variables, a classification should allow to identify those of them strongly affecting the physical phenomenon, namely, the first order variables ν_1 against the second order variables ν_2 , that is,

$$\nu_1 \equiv \{X_1, X_2, \dots, X_n\}, \quad \nu_2 \equiv \{X_{n+1}, \dots, X_m\}. \quad (2.3)$$

4. *Dimensional analysis.* According to the good-practices in building scientific formulas, a physical phenomena involving n first order variables can be expressed, without loss of generality, as a function of $n - k$ dimensionless variables based on the dimensional analysis, such that,

$$g(\Pi_1, \Pi_2, \dots, \Pi_{n-k}) = 0, \quad (2.4)$$

being k the number of fundamental magnitudes of the involved variables in ν_1 and Π_i a dimensionless variable. In other words, the dimensional analysis allows to identify the minimum number of variables governing the physical phenomenon, avoiding to consider an excessive number of them. Note that the problem is being greatly simplified from the original number of variables m to $n - k$, such that depending on the particular problem, the latter can be quite lower than the former. This step is of practical importance in order to avoid models violating some important feasible conditions related with the dimensional analysis, besides providing with useful information of the phenomenon, as will be shown in Chapter 3.

5. *Model properties definition.* The physical phenomenon exhibits a set of properties whose must be replicated in the mathematical model ensuring the fidelity within them. This step may adopt heterogeneous forms, such as constraints, equations, functional equations relating different variables, among others. Additionally, the distribution of one or more random variables could also be specified in this step if the variables are of random type, as occurs in the Example 2.1 with the memoryless property.
6. *Feasible conditions definition.* Once the model properties have been properly identified based on the study of the physical phenomenon, the feasible conditions must also be applied in order to avoid inconsistencies coming from two origins, that is, the physical properties of the phenomenon and theoretical considerations. Usually, these conditions adopt the form of constraints, inequalities, equations, functional equations, etc. An extensive treatment of different feasible conditions coming from theoretical considerations will be presented in Chapter 3.
7. *Model definition.* A mathematical model definition is usually stated as a function relating the variable of interest depending on the rest of the variables together with a set of constraints delimiting the acceptable region where the model is valid. This function must be conceived in a general sense, since it could be a distribution function if the variables are random. Thus, by assuming Π_j as the variable of interest in Eq. (2.4), the final formal statement of the mathematical model is as follows:

$$\Pi_j = h(\Pi_1, \Pi_2, \dots, \Pi_{n-k-1}), \quad (2.5)$$

with $h(\cdot)$ as the function of interest.

8. *Parameter estimation.* The parameters allows the mathematical model to provide particular solutions for a real-world problem. There are multiple estimation techniques and methods for any kind of model, being deterministic or probabilistic. However, these techniques are not valid whatever of model is proposed, since some conditions must be satisfied. In a general setting, the model parameter estimation can be defined as follows. Given a set of data points of the form (y_i, \mathbf{x}_i) , $y_i \in \mathbb{R}$, $\mathbf{x}_i \in \mathbb{R}^p$, $i = 1, 2, \dots, N$ and a parametric family of functions

$$F = \{f_\theta(\mathbf{x}, \theta) : \theta \in \Theta\}, \quad (2.6)$$

covering all the possible relations within the variables in Eq. (2.5), i.e. an equivalent formulation, such that for a given value of \mathbf{x} , the function $f(\mathbf{x})$ best approximates the corresponding value of y .

9. *Model validation.* Once the mathematical model is fitted to real data according to some appropriate estimation technique, a measurement of the quality of such model should also be addressed in order to assess the future predictions based on the model. There are a large variety of methods for validation, being usually divided into graphical and non-graphical methods.

Mainly, this measurement of the quality adopts the form of some confidence intervals for the parameters of the model obtained with different methods, such as for instance the hypothesis testing, the Bootstrap, Bayesian and Monte-Carlo methods, among others.

10. *Model prediction.* The common objective of any engineering- and science-related mathematical model can be undoubtedly located in the prediction or extrapolation of the physical phenomenon properties for other conditions of practical interest. In fact, this objective constitutes the genuine motivation of the mathematical model building and the most challenging one. For this reason, only models based on adequate properties and fulfilling suitable feasible conditions ensure valid extrapolations.

2.4 Concluding Remarks

The derivation of phenomenological models is conditioned to the complexity of the real-world problems to be confronted and some simplifications are always required. However, any proposed model must not be arbitrarily defined and a systematic methodology to be followed is highly recommended. To this end, a detailed and rigorous methodology is suggested in this chapter allowing to build mathematical models based on the properties taken from the physical phenomena under study and satisfying a certain set of feasible conditions. Thus, if and only if both components of the model are conveniently handled, the predictions provided by the model are valid.

3

Mathematical and Statistical Methods

3.1 Introduction

This chapter is concerned with the description of the mathematical and statistical methods being used in the following chapters for developing the viscoelastic and fracture characterization models. The pursued aim is twofold: a) to provide to the reader with the broad theoretical framework used for interpreting the research presented in this work and b) to define rigorous statistical and physical conditions to be fulfilled for any valid and consistent model from different perspectives. These conditions are general and must be applied in combination with those restrictions imposed by the physical phenomenon properties on themselves, as has been stated in previous chapter. In any case, the fulfillment of these feasible conditions allows the consistent models to be distinguished in a first glance from those whose are not, independently of the particular topic field being studied. Only those satisfying these conditions must be considered in order to avoid serious errors with predictions.

The organization of this chapter is related with different disciplines where these feasible conditions come from: dimensional analysis (Section 3.2), functional equations (Section 3.3), some considerations of probability theory (Section 3.4), extreme value theory (Section 3.5) and the conditional specification of statistical models (Section 3.6). At the end of these sections, a summary of the main feasible conditions resulting from each of them is included as general recipes.

3.2 Dimensional Analysis

The dimensional analysis constitutes a powerful tool which should be systematically used for building scientific and mathematical models. Originally treated by Buckingham (1915), several efforts were devoted to its development and mathematical formulation (see Bridgman (1922), Luce (1964), Aczél (1966, 1986, 1987), Falmagne and Narens (1983), Castillo and Ruiz-Cobo (1992) and Castillo et al. (2004b)). The most important and interesting result of a dimensional analysis is an equivalent formulation of a problem with a reduced number of variables from those initially involved, without loss of generality, being based on the idea that a physical law must not depend on the system of units arbitrarily chosen. Moreover, the dimensional analysis establishes two important feasible conditions for building mathematical models, namely, dimensional and physical consistencies, both based on the well-known Buckingham's Theorem, whose are frequently violated in current existing models, as indicated in Castillo et al. (2014a) and Castillo et al. (2014c).

In addition, the dimensional analysis also distinguishes different categories of physical variables, as the variables allowing a scale, location or scale-location changes, defining the valid transformations on them, whose are also described in this section. For further details about the dimensional analysis, a large variety of practical examples illustrating its applicability in engineering and science can be found in Sedov (1993), Barenblatt (1996, 2003), Sonin (2001), Szirtes and Rózsa (2006), Tan (2011), Simon et al. (2017) and Zohuri (2015, 2017).

3.2.1 Dimensional consistency

As the most simple expression of the dimensional analysis, the dimensional consistency of a scientific formula establishes the natural idea that both sides of an equation relating variables must share identical dimensions. Sonin (2001) suggests the following implications due to this feasible condition of dimensional consistency (see Castillo et al. (2014c)):

- a) If there are sum of quantities on the right hand side of an equation, all the terms in the sum must have the same dimensions.
- b) The arguments of special functions appearing in the equation, such as logarithm, exponential or trigonometric, must be dimensionless.

Additionally, it is imperative that the dimensions of the quantities to be non-dependent of their numerical values, as occurs with some celebrated scientific and engineering formulas, as for instance the well-known Paris' law (see Castillo and Fernández-Canteli (2009), Castillo et al. (2014b) and Castillo et al. (2014c)), where the dimensions of the parameters could not be determined before their estimation.

3.2.2 Physically valid consistency

The dimensional analysis also establishes the feasible condition related with the so-called physically valid models, since the previous dimensional homogeneity is not enough for an expression to be consistent. Accordingly to this condition, a scientific formula must be invariant with respect to changes at both sides of the equation. In other words, a change in scale or location at right hand side of an equation must imply valid scale or location changes in the left hand side, which is not always ensured since there are physical variables admitting only one of these kinds of changes (see Aczél (1987, p. 35) and Castillo et al. (2014c)):

- a) *Scale variables.* Consider a physical variable x_{n+1} that can be written in terms of other fundamental physical variables x_1, x_2, \dots, x_n such that there exists a relation of the form $x_{n+1} = u(x_1, x_2, \dots, x_n)$. If a change of scale is performed at the right hand side throughout a function $R(\cdot)$, the invariant condition can be defined as follows:

$$u(\mathbf{r}\mathbf{x}) = R(\mathbf{r})u(\mathbf{x}); \quad \mathbf{r}, \mathbf{x} \in \mathbb{R}_{++}^n \quad (3.1)$$

which is a functional equation with solution

$$u(\mathbf{x}) = a \prod_{i=1}^n x_i^{c_i}; \quad R(\mathbf{r}) = \prod_{i=1}^n r_i^{c_i}, \quad (3.2)$$

where a and c_1, c_2, \dots, c_n are non-null constants. Then, the most general possible form of relating variables being invariant with respect to changes of scale is of the form of Eq. (3.2), that is, only products of a constant and some variables raised to powers (positive or negative). In other words, those models implying scale variables are physically valid if and only if Eq. (3.2) holds.

- b) *Scale-location variables.* As a more general case, there exist variables admitting both scale and location changes by means of certain functions $R(\cdot)$ and $P(\cdot)$, respectively, such that,

$$u(\mathbf{r}\mathbf{x}) = R(\mathbf{r})u(\mathbf{x}) + P(\mathbf{r}); \quad \mathbf{r}, \mathbf{x} \in \mathbb{R}_{++}^n \quad (3.3)$$

which constitutes a functional equation with solutions

$$u(\mathbf{x}) = \sum_{i=1}^n c_i \log x_i + b; \quad R(\mathbf{r}) = 1; \quad P(\mathbf{r}) = \sum_{i=1}^n c_i \log r_i; \quad (3.4)$$

and

$$u(\mathbf{x}) = a \prod_{i=1}^n x_i^{c_i} + b; \quad R(\mathbf{r}) = \prod_{i=1}^n r_i^{c_i}; \quad P(\mathbf{r}) = b \left[1 - \prod_{i=1}^n r_i^{c_i} \right]; \quad (3.5)$$

where a, b and c_1, c_2, \dots, c_n are non-null constants. Note that the most

general possible form of relating variables being invariant with respect to changes in scale an location must be of the form of products and sums of constants with some variables in logarithmic for the first solution Eq. (3.4) and with products and sums of constants with some variables raised to powers (positive or negative) for the second solution Eq. (3.5). These results come from a theorem which can be found in Aczél (1987, p. 35–70) and Castillo et al. (2004b, p. 237–242).

Now consider these two following examples discussing the valid changes in both types of physical variables previously discussed.

Example 3.1 (Scale variables). The scale variables are the most common in Science and engineering. Physical variables such as length, time, area, volume, speed, etc. are all valid examples. Formulas implying only scale variables are usual, as for example the bending stress in a beam $\sigma_y = zM_y/W_Z$, where only products of a constant and some variables raised to powers are considered. \square

Example 3.2 (Scale-location variables). The temperature or pH constitute examples of variables admitting a location change, as for example from Celsius θ_C to Kelvin $\theta_K = \theta_C + 273.15$ and scale-location change, such as from Celsius to Fahrenheit $\theta_F = 1.8\theta_C + 32$. Consider the illustrative example due to Castillo et al. (2014a) assuming the temperature measured in Celsius θ_C to have a Log-normal distribution. The physically valid condition states that if the temperature allows a scale-location change in the transformation to Fahrenheit θ_F , then the left hand side of the equation, i.e. the Log-normal distribution, must be transformed accordingly. However, since this distribution is not stable with respect to changes in location, the resulting distribution function will be of different family if the samples are measured in Celsius or Fahrenheit, which could lead to important errors to be avoided. As a consequence, the means of the distribution are different depending on the units of the sample and any prediction based on these values will be influenced by this error. \square

3.2.3 Buckingham's Theorem

Originally formulated by Buckingham (1915), this theorem constitutes another important application of the dimensional analysis leading systematically to models ensuring both dimensional and physical consistency conditions, besides providing with quite useful information about the phenomenon under study. Thus, it should be methodically included in any general methodology for deriving mathematical models in order to avoid inconsistencies from a dimensional analysis point of view.

The Buckingham's theorem states that if a certain physical phenomenon can be described by a number of independent variables x_1, x_2, \dots, x_n throughout a functional relationship, such that,

$$f(x_1, x_2, \dots, x_n) = 0, \quad (3.6)$$

being k the fundamental magnitudes in which these variables are measured (e.g. mass M , length L , time T , etc.), an equivalent formulation of Eq. (3.6) relating only $m = n - k$ dimensionless variables Π_i can be defined, without loss of generality:

$$g(\Pi_1, \Pi_2, \dots, \Pi_m) = 0, \quad (3.7)$$

which is equivalent to say that the phenomenon being initially described by n independent dimensional variables is ultimately governed by $m = n - k$ independent dimensionless variables. In other words, a mathematical model not based on this theorem could be considering more variables than those strictly required, which is an important result to take into account. For the same reason, the theorem allows to know if the initial variables selected are adequate for describing the physical phenomenon, since if $n - k = 0$ then there is not possible model and the selected initial variables are not suitable. Finally, since the variables Π_i are dimensionless, the dimensional and physical consistencies are also ensured.

In summary, the Buckingham's theorem provides with three important results. Firstly, the minimum number m of dimensionless variables really governing the physical phenomenon. Secondly, it allows to discern whether a set of variables is valid for describing that phenomena, such that the condition $n - k > 0$ must holds. Finally, since the dimensionless variables Π_i include different combinations of the original variables, the Buckingham's theorem also provides with different valid sets of dimensionless variables to be selected by the researcher for deriving the mathematical model.

3.2.4 Dimensional and dimensionless models

Lastly, some considerations must be remarked about the dimensionality not only of a variable but also of a mathematical model as a whole. Indeed, the mathematical models can also be denoted as dimensional or dimensionless depending of the intervening variables.

Let us consider two different system of fundamental magnitudes for length (L), mass (M), time (T) and temperature (θ), denoted as ν_1 and ν_2 , such that $\nu_1 = \{L_1, T_1, M_1, \theta_1\}$ and $\nu_2 = \{L_2, T_2, M_2, \theta_2\}$. A model relating n variables with a functional form $f(x_1, \dots, x_n)$ is said to be dimensional if its functional form is sensitive to the system of units selected, that is,

$$\left. \begin{aligned} f_1(x_1, x_2, \dots, x_n) &= 0 \\ f_2(x_1, x_2, \dots, x_n) &= 0 \end{aligned} \right\} \not\Rightarrow f_1 = f_2,$$

where $f_1(\cdot)$ and $f_2(\cdot)$ represent the functional forms written in both system of units, being different because of the dimensional character of the model. In turn, for a dimensionless model both functionals satisfy the condition:

$$\left. \begin{aligned} f_1(x_1, x_2, \dots, x_n) &= 0 \\ f_2(x_1, x_2, \dots, x_n) &= 0 \end{aligned} \right\} \Rightarrow f_1 = f_2,$$

where now $f_1(\cdot)$ and $f_2(\cdot)$ are equal due to the dimensionless character of the model. As can be seen, the second choice is more robust and recommended for building scientific models, which is an additional reason to prefer working with dimensionless variables rather than dimensional ones.

Briefly, a proposed model is considered physically and dimensionally consistent if the following conditions are satisfied:

1. A mathematical model is dimensionally consistent if the constants and variables appearing in the equation share identical units at both sides.
2. A summation of physical constants and variables is only valid if they have the same dimensions.
3. Any argument of special functions (logarithms, exponentials, trigonometric, etc.) must be dimensionless.
4. Scale and location changes performed at one side of an equation must lead to valid transformations on the other side, which is only satisfied if the physical variables involved are allowed to those changes.

3.3 Functional Equations

Functional equations constitute another important and powerful tool for building mathematical models, as indicated in Aczél (1966), Galambos (1982), Castillo and Ruiz-Cobo (1992) and Castillo et al. (2004b). More precisely, the model properties and the feasible conditions can be particularly well derived from the physical phenomenon and consequently written in mathematical terms with the aid of the functional equations. By solving these functional equations, the most general solution of the functions implied in the model arise due to those properties and conditions, being avoided the arbitrary assumptions. As a result, the mathematical models are built in an objective and rigorous manner.

The aim of this section is to introduce to the reader to the functional equations theory, especially those that will be used in the development of this work. Firstly, some basic concepts and definitions are described, including a motivating example for the functional equations. Then, different types of functional equations are considered in one or several functions or in one or several variables. Further details about the demonstrations of these solutions can be found in the works by Aczél (1966), Castillo and Ruiz-Cobo (1992) and Castillo et al. (2004b) and the references therein, being especially recommended both latter ones as summaries about the possible methods for solving functional equations with illustrative examples.

3.3.1 *Basic concepts and definitions*

Despite of being a difficult task to provide a correct definition of the functional equations, as recognized by one of the founders by himself (see Aczél (1966)),

Castillo and Ruiz-Cobo (1992) and Castillo et al. (2004b) attempted it with the following definition: *In a broader sense, a functional equation can be considered as an equation which involves independent variables known functions, unknown functions and constants; but we exclude differential equations, integral equations and other kinds of equations containing infinitesimal operations. In these equations, the main operation is the substitution of known or unknown functions into known or unknown functions.* In other words, a functional equation is an equation in which the unknowns are functions, appearing as such, that is, without integrals nor derivatives.

In order to illustrate this definition, consider the following motivating example due to Legendre (1971) (see also Castillo and Ruiz-Cobo (1992) and Castillo et al. (2004b)).

Example 3.3 (A motivating example). Assume the formula providing the area of a rectangle is unknown. The experience ensures that it must be a certain function $f(b, h)$ of the base b and the height h . The question arises here is about the derivation of the formula with only identifying the properties of rectangles and the functional equations. To this end, consider a new rectangle of the same base b but with a total height of $h_1 + h_2$. The resulting area $f(b, h_1 + h_2)$ can be obtained as a sum of the area of two rectangles, that is, throughout the following functional equation

$$f(b, h_1 + h_2) = f(b, h_1) + f(b, h_2). \quad (3.8)$$

On the other hand, if the same reasoning is applied but to the base dimension, it leads to the analogous functional equation

$$f(b_1 + b_2, h) = f(b_1, h) + f(b_2, h). \quad (3.9)$$

Thus, the solution of the system of functional equations constituted by Eq. (3.8) and Eq. (3.9) provides the most general solution of the function $f(\cdot)$ for the area of a rectangle

$$f(b, h) = cbh, \quad (3.10)$$

for a certain non-negative constant c , taking into account the units of the base, height and in the calculation of the area. Note that only by taking into account the properties of the rectangle, the general solution of the function providing the area is obtained by solving functional equations, without requiring any arbitrary assumption. Moreover, the functional equations provides the interesting discover that a certain constant is always implied in the determination of an area because of being a scale variable type and the dimensions must be considered as well. \square

3.3.2 Equations for one function of one variable

One of the most celebrated and widely used functional equations involving only one function and one variable are the so-called Cauchy's equations, being originally solved by Cauchy (1821) in their four types:

a) *Type I.* If the following functional equation is satisfied

$$f(x+y) = f(x) + f(y); \quad x, y \in \mathbb{R} \quad (3.11)$$

for $f(x)$ as a) continuous-at-a-point, or b) nonnegative for small x , or c) bounded in an interval or d) integrable or e) measurable, then

$$f(x) = cx, \quad x \in \mathbb{R} \quad (3.12)$$

where c is an arbitrary constant. Note that the first type of Cauchy's equation has been already introduced when the area of the rectangle (see Example 3.3).

b) *Type II.* The most general solution of the functional equation

$$f(x+y) = f(x)f(y); \quad x, y \in \mathbb{R} \quad (3.13)$$

is defined as follows:

$$f(x) = \exp(cx), \quad f(x) = 0, \quad (3.14)$$

for an arbitrary constant c .

c) *Type III.* The most general solution of the functional equation

$$f(xy) = f(x) + f(y); \quad x, y \in \mathbb{R} \quad (3.15)$$

is given by

$$f(x) = c \log(x), \quad (3.16)$$

with c as an arbitrary constant.

d) *Type IV.* The most general solutions, which are continuous-at-a-point, of the functional equation

$$f(xy) = f(x)f(y); \quad x, y \in \mathbf{T} \quad (3.17)$$

are the following:

$$f(x) = \begin{cases} c \log(x) & \text{if } \mathbf{T} = \mathbb{R}_{++}, \\ c \log(|x|) & \text{if } \mathbf{T} = \mathbb{R} - \{0\}, \\ 0 & \text{if } \mathbf{T} = \mathbb{R}, \end{cases}$$

for c an arbitrary real number.

3.3.3 Equations with several functions in one variable

The Cauchy's functional equations previously introduced are defined for one function, limiting their practical applications. For this reason, the Pexider's equations

are their natural generalization including several functions, whose can also be of four different types:

1. *Type I.* The most general system of solutions of the functional equation

$$f(x + y) = g(x) + h(y); \quad x, y \in \mathbb{R} \quad (3.18)$$

with $f(\cdot)$ a) continuous-at-a-point, or b) non-negative for small x , or c) bounded in an interval, is

$$f(x) = Ax + B + C; \quad g(x) = Ax + B; \quad h(x) = Ax + C, \quad (3.19)$$

where A, B and C are arbitrary constants.

2. *Type II.* The most general system of solutions of the following functional equation

$$f(x + y) = g(x)h(y); \quad x, y \in \mathbb{R} \quad (3.20)$$

with $f(\cdot)$ defined as continuous-at-a-point is given by

$$f(x) = AB \exp(Cx); \quad g(x) = A \exp(Cx); \quad h(x) = B \exp(Cx), \quad (3.21)$$

for some arbitrary non-zero constants A, B and C .

3. *Type III.* The most general system of solution of the functional equation

$$f(xy) = g(x) + h(y); \quad x, y \in \mathbf{T} \quad (3.22)$$

with $f(\cdot)$ continuous-at-a-point is given by

$$\left. \begin{aligned} f(x) &= A \log(BCx) \\ g(x) &= A \log(Bx) \\ h(x) &= A \log(Cx) \end{aligned} \right\} \text{if } \mathbf{T} = \mathbb{R}_{++}, \quad (3.23)$$

$$\left. \begin{aligned} f(x) &= A \log(BC|x|) \\ g(x) &= A \log(B|x|) \\ h(x) &= A \log(C|x|) \end{aligned} \right\} \text{if } \mathbf{T} = \mathbb{R} - \{0\}, \quad (3.24)$$

$$f(x) = A + B; \quad g(x) = A; \quad h(x) = B \text{ if } \mathbf{T} = \mathbb{R} \text{ or } \mathbb{R} - \{0\} \text{ or } \mathbb{R}_{++} \quad (3.25)$$

for some arbitrary constants A, B and C .

4. *Type IV.* The most general system of solutions of the functional equation

$$f(xy) = g(x)h(y); \quad x, y \in \mathbb{R} \quad (3.26)$$

with $f(\cdot)$ continuous-at-a-point is

$$\left. \begin{aligned} f(x) &= ABx^C \\ g(x) &= Ax^C \\ h(x) &= Bx^C \end{aligned} \right\} \text{if } \mathbf{T} = \mathbb{R}_{++}, \quad (3.27)$$

$$\left. \begin{aligned} f(x) &= AB|x|^C \\ g(x) &= A|x|^C \\ h(x) &= B|x|^C \end{aligned} \right\} \text{if } \mathbf{T} = \mathbb{R} - \{0\}, \quad (3.28)$$

$$f(x) = AB; \quad g(x) = A; \quad h(x) = B \text{ if } \mathbf{T} = \mathbb{R} \text{ or } \mathbb{R} - \{0\} \text{ or } \mathbb{R}_{++} \quad (3.29)$$

3.3.4 Equations for one function of several variables

Within the functional equations defined for one function but for several variables, the Sincov functional equation is extensively applied in this work, being defined as follows:

$$f(x, y) + f(y, z) = f(x, z), \quad (3.30)$$

with solution given by

$$f(x, y) = g(y) - g(x), \quad (3.31)$$

where g is an arbitrary function. Note the importance of previous result, since a function of two variables $f(x, y)$ can be written as a function of one variable $g(x)$ according to Eq. (3.31), which is unexpected at a first glance.

3.3.5 Equations with functions of several variables

There are some remarkable functional equations with several functions and several variables to be used in this work. More precisely, the generalization of the Sincov functional equation, which is exemplified with a problem related with fatigue life of longitudinal elements, together with the generalized associativity functional equation. Particularly useful is the extended work by Aczel and Dhombres (1989) for the case of functional equations with several variables.

The original Sincov functional equation (3.30) can be generalized leading to:

$$F(x, z) = G(x, y) + H(y, z), \quad (3.32)$$

which is known as the generalized Sincov functional equation, with solution

$$F(x, z) = h(z) - f(x); \quad G(x, y) = g(y) - f(x); \quad H(y, z) = h(z) - g(y), \quad (3.33)$$

with f, g and h as arbitrary functions

Example 3.4 (Functional equation of the scale-effect). In fatigue lifetime prediction problem, Bogdanoff and Kozin (1987) proposed the following property for considering the scale-effect due to the variation of the length in longitudinal

elements:

$$F(x, z) = F(y, z)^{N(x, y)}, \quad (3.34)$$

where $F(x, z)$ and $F(y, z)$ correspond to the survival functions associated with two elements of lengths x and y , respectively, while $N(x, y)$ is an unknown positive function. In other words, the lifetime of an element with length x can be obtained from that with a length y by means of powering the latter to a function of both lengths $N(x, y)$. The solution of this functional equation is given by Castillo and Ruiz-Cobo (1992) and Castillo et al. (2004b):

$$\begin{aligned} F(x, z) &= p(z)^{q(x)}; & p(z) &= \exp\{-\exp[h(z)]\}; \\ N(x, y) &= q(x)/q(y); & q(x) &= \exp[-f(x)], \end{aligned} \quad (3.35)$$

where $q(x)$ is an arbitrary positive function and $p(x)$ is a survival function. Thus, the assumption of the property Eq. (3.34) explaining the scale-effect forces the involved functions to be not arbitrarily defined, as might be expected in a first glance. \square

Another important functional equation with several variables and functions is the generalized associativity equation:

$$G(x, y) = K[M(x, z), N(y, z)], \quad (3.36)$$

with N invertible in the first argument for any value of the second, M invertible in the both arguments, K invertible in the first argument for some fixed value of the second, and G invertible in the second for a fixed value of the first, such that the general solution continuous on a real rectangle is:

$$\begin{aligned} G(x, y) &= l^{-1}[p(x) + q(y)]; & M(x, y) &= l^{-1}[p(x) + r(y)], \\ K(x, y) &= f^{-1}[l(x) + n(y)]; & N(x, y) &= n^{-1}[q(x) - r(y)], \end{aligned} \quad (3.37)$$

where f, l, n, p, q and r are arbitrary continuous and strictly monotonic functions which are determined up to the following relations

$$\begin{aligned} f_2(x) &= cf_1(x) + a + b_1, & p_2(x) &= c_1p_1(x) + a_1, \\ q_2(x) &= c_1q_1(x) + b_1, & l_2(x) &= c_1l_1(x) + a_4, \\ n_2(x) &= c_1n_1(x) + b_1 + a_1 - a_4, & r_2(x) &= c_1r_1(x) + a_4 - a_1, \end{aligned} \quad (3.38)$$

where the a 's and b 's are arbitrary constants.

In summary, the functional equations should be systematically used in the mathematical model building for interpreting the physical properties of the phenomenon under study and translate them into mathematical terms avoiding any arbitrary assumption about their functional forms. Then, by solving these functional equations the most general possible forms are obtained and the corresponding simplifications could also be applied for deriving particular solutions for the real problem. As a matter of fact, by contrasting this general solution with the current existing models, a critical review can also be suggested since the latter

should be included in the former.

3.4 Probabilistic Theoretical Considerations

As has been mentioned in Chapter 1, random physical phenomena arise frequently in engineering and science motivating the probabilistic models, as a particular case of the mathematical ones, of extraordinary special interest. Nevertheless, the derivation of this kind of models must be in accordance with some additional considerations about probability theory to be encompassed with those from previous sections in order to avoid inconsistencies.

3.4.1 Operation-stable families

The stability condition in operations with distributions is a common and serious error when dealing with probabilistic models. A suitable definition of a family of distributions being operation-stable is due to Castillo et al. (2014a) and Castillo et al. (2014c). Given a parametric family $H(x; \mathbf{c})$ of distributions, where \mathbf{c} is a vector of parameters, it is said to be stable with respect to a given operation, such as sums, minima, maxima, translations, scale changes, etc. when a cdf of such a family subjected to the operation results in a new cdf that also belongs to the same family, that is,

$$F(x) = H(x; \mathbf{c}) \Rightarrow \hat{F}(\hat{x}) = \hat{H}(\hat{x}; \hat{\mathbf{c}}), \quad (3.39)$$

where x and \hat{x} are the initial and the transformed variables, $F(x)$ and $\hat{F}(x)$ are the initial and transformed cdf, and \mathbf{c} and $\hat{\mathbf{c}}$ are the initial and transformed vector parameters, respectively. In these cases, the parametric family of distributions $H(x; \mathbf{c})$ is said to be stable or closed with respect to the operation (see also Balakrishnan and Nevzorov (2003) and Kotz et al. (2005)). The distributions stable with respect to changes in scale and location parameters constitute a suitable example of an operation-stable family. Some continuous distributions and their properties related with the operation-stable are listed in Table 3.1, retrieved from Castillo et al. (2014a).

3.4.2 Reproductivity property

The reproductivity property constitutes another example of the operation-stable property, but it is treated separately because of its practical relevance. A family of random variables is said to be reproductive if its addition belongs to the same family of distribution. The classical example of reproductive random variables is the Normal family $N(\mu, \sigma^2)$, even for both parameters mean μ and variance σ^2 . In other words, the sum of two normal random variables $N(\mu_1, \sigma_1^2)$ and $N(\mu_2, \sigma_2^2)$ leads to the cdf $N(\mu_1 + \mu_2, \sigma_1^2 + \sigma_2^2)$. Contrarily, the Log-normal distribution does not exhibit this property, as can be seen in Table 3.1.

Table 3.1: Properties of common continuous distributions, taken from Castillo et al. (2014c).

Family	Reproductive	Stability		Extreme value	Dimensional problems
		Location	Scale		
Normal	X	X	X		
Log-normal					X
Rev. Gumbel		X	X	X	
Weibull		X	X	X	
Rev. Fréchet		X	X	X	
Gumbel		X	X	X	
Rev. Weibull		X	X	X	
Fréchet		X	X	X	

In summary, from above considerations, the concept of probability consistency condition arises in a natural manner, being originally formulated in the most general form by Castillo et al. (2014a) for the case of dealing with multivariate models. Accordingly, a model is considered probability consistent if for a given list of random variables involved in the problem, a system of relations or constraints among these variables and a joint density relating all of them, the latter is not in contradiction with the given constraints. Equivalently, the univariate formulation of this condition is straightforward: given a random variable, a set of constraints or equations and a cdf relating the probability and the random variable, the model is said to be probability consistent if the cdf does not violate the given constraints. In other words, any probabilistic model must be in accordance with the elementary theoretical considerations described in this section.

3.5 Extreme Value Theory

In the context of engineering problems, the design is constantly confronted with a compromise between capacities and loads, such as for instance the strength of a structural component under an applied load or the production capacities of supplying a changing demand of a certain product. All of these examples require to focus not (or not only) on the mean values of those both parts of the problem, but on the extremal events (see, for example, Galambos (1978), Castillo (1988) and Castillo et al. (2004a)). In other words, the critical situation to be faced is due to the minimum value of the strength and the maximum value of the load in the structural component example. Thus, the Extreme Value Theory is intimately related with the engineering problems providing a more interesting analysis than those based on the central or most probable values commonly assuming a Normal distribution.

This section is dedicated to introduce to the reader to the basic concepts of the

Extreme Value Theory in order to build valid models for dealing with extremal events. The material presented draws heavily from a large variety of reference works in literature related with this topic, from the first due to Gnedenko (1943) and Gumbel (1958) to the deeper treatments by Galambos (1978), Leadbetter et al. (1983), de Oliveria (1984), Castillo (1988), Coles (2001), Castillo et al. (2004a) and de Haan and Ferreira (2010) among others.

To this end, this section is organized in four parts. Firstly, an introduction of the order statistics is presented, in particular the minimum and maximum ones. Secondly, the family of extreme value distributions are described, namely, Weibull, Gumbel and Fréchet, including their main properties and characteristics. Thirdly, these statistical distributions are shown to exhibit the property of being the limit distribution for extreme events in maxima or minima of any other parent distribution to be considered. Finally, the probability paper is described as a suitable estimation technique.

3.5.1 Order statistics

Let X_1, X_2, \dots, X_n be a sample from a certain population with a common parent distribution $F(x)$. If this sample is ordered increasingly, then the element occupying the r -th position from the ordered sample $X_{1:n}, X_{2:n}, \dots, X_{n:n}$ is called order statistic $X_{r:n}$, with $r = 1, 2, \dots, n$. Thus, the distribution of the maximum order statistic $X_{n:n} = \max(X_1, X_2, \dots, X_n)$ and the minimum order statistic $X_{1:n} = \min(X_1, X_2, \dots, X_n)$ of the sample can be defined as follows (see, for example, Castillo (1988, p. 98–99) and Castillo et al. (2004a, p. 153–157)):

$$\Pr(X_{n:n} \leq x) = F(x)^n, \quad (3.40)$$

$$\Pr(X_{1:n} \leq x) = 1 - [1 - F(x)]^n, \quad (3.41)$$

with F as the cdf of the parent population. These particular order statistics for extremes ($r = 1, n$) result from general expressions allowing the pdf and cdf of any r -th order statistic to be obtained, even the joint densities within any combination of them.

Nevertheless, the Extreme Value Theory is focused on these special order statistics representing the extremal events and the possible distributions as candidates for $F(x)$ satisfying Eq. (3.40) and Eq. (3.41), which is equivalent to the following functional equation proposed by Gnedenko (1943), known as the origin of the Extreme Value Theory:

$$F^n(a_n + b_n x) = F(x), \quad (3.42)$$

with F as the unknown function and a_n and b_n as some normalizing constants, in order to avoid degenerate distributions. The solution of this functional equation provides the unique valid distributions $F(x)$ for dealing with extremal events. For further details about the properties and applications of the order statistics, see the extensive works by Balakrishnan and Rao (1998a,b), Castillo (1988), Castillo et al. (2004a), Arnold et al. (2008) and David and Nagaraja (2010) among others.

3.5.2 Extreme value distributions

The extreme value distributions have been found to be the most general solution of the functional equation (3.42), distinguishing three types:

- a) *Weibull distribution.* As one of the three extreme value distributions, the Weibull distribution has been widely applied in a large variety of fields in engineering and science (see Castillo (1988, p. 198–207)). More precisely, this distribution frequently arises when minima values are observed. The cdf of a Weibull random variable for minima values is given by

$$F(x) = 1 - \exp \left[- \left(\frac{x - \lambda}{\delta} \right)^\beta \right], \quad x \geq \lambda, \quad (3.43)$$

where λ, δ and β are the location, scale and shape parameters respectively, being limited on the left. The mean value and variance are defined as

$$\mu = \lambda + \delta \Gamma \left(1 + \frac{1}{\beta} \right) \quad \text{and} \quad \sigma^2 = \delta^2 \left[\Gamma \left(1 + \frac{2}{\beta} \right) - \Gamma^2 \left(1 + \frac{1}{\beta} \right) \right], \quad (3.44)$$

with Γ representing the well-known Gamma function. Alternatively, if the maximum values are of interest, then the Weibull cdf for maxima must be considered

$$F(x) = \exp \left[- \left(\frac{\lambda - x}{\delta} \right)^\beta \right], \quad \lambda \leq x, \quad (3.45)$$

where now the limit comes from the right, with mean and variances are defined as follows

$$\mu = \lambda - \delta \Gamma \left(1 + \frac{1}{\beta} \right) \quad \text{and} \quad \sigma^2 = \delta^2 \left[\Gamma \left(1 + \frac{2}{\beta} \right) - \Gamma^2 \left(1 + \frac{1}{\beta} \right) \right]. \quad (3.46)$$

A detailed taxonomy of different versions of the Weibull distribution with practical applications can be found in Murthy et al. (2004).

- b) *Gumbel distribution.* The Gumbel distribution emerges when maxima values are of interest. The cdf of a Gumbel distribution for maxima values is

$$F(x) = \exp \left[- \exp \left(\frac{\lambda - x}{\delta} \right) \right], \quad -\infty < x < \infty, \quad (3.47)$$

where λ and δ are the location and scale parameters, respectively, with mean and variance defined as

$$\mu = \lambda + 0.57772\delta \quad \text{and} \quad \sigma^2 = \frac{\pi^2 \delta^2}{6}. \quad (3.48)$$

In contrast, when minima values the Gumbel distribution for minima must

be considered,

$$F(x) = 1 - \exp \left[-\exp \left(\frac{x - \lambda}{\delta} \right) \right], \quad -\infty < x < \infty, \quad (3.49)$$

where the mean and variance are

$$\mu = \lambda - 0.57772\delta \quad \text{and} \quad \sigma^2 = \frac{\pi^2 \delta^2}{6}. \quad (3.50)$$

- c) *Fréchet distribution.* As the last of the extreme value family of distributions, the Fréchet distribution appears frequently with dealing with maxima values. Then, the cdf for a random variable belonging to the maxima Fréchet distribution is

$$F(x) = 1 - \exp \left[-\left(\frac{\delta}{\lambda - x} \right)^\beta \right], \quad x < \lambda, \quad (3.51)$$

where λ , δ and β are the location, scale and shape parameters, respectively, and with limit on the right. The mean value is given by

$$\mu = \lambda + \delta \Gamma \left(1 - \frac{1}{\beta} \right), \quad (3.52)$$

while variance is

$$\sigma^2 = \delta^2 \left[\Gamma \left(1 - \frac{2}{\beta} \right) - \Gamma^2 \left(1 - \frac{1}{\beta} \right) \right]. \quad (3.53)$$

Also the Fréchet distribution for maxima may be of interest

$$F(x) = \exp \left[-\left(\frac{\delta}{x - \lambda} \right)^\beta \right], \quad x > \lambda, \quad (3.54)$$

where the mean is given by

$$\mu = \lambda - \delta \Gamma \left(1 - \frac{1}{\beta} \right), \quad (3.55)$$

while variance is

$$\sigma^2 = \delta^2 \left[\Gamma \left(1 - \frac{2}{\beta} \right) - \Gamma^2 \left(1 - \frac{1}{\beta} \right) \right]. \quad (3.56)$$

3.5.3 Limit distributions for maxima and minima

The definition of the extremes of an ordered sequence implies that the resulting distribution by applying Eq. (3.40) for the maximum or Eq. (3.41) for the minimum must belong to the same family of the original parent $F(x)$, as stated in the

functional equation (3.42). In other words, it implies the distribution $F(x)$ to be stable with respect to power operation, being usually referred to as stability in the formation of the maximum or minimum, respectively, a property which is only satisfied by the extreme value distributions previously described, as can be seen in Table 3.1. However, under certain conditions, the maximum or minimum of any other parent distribution $F(x)$ can be conveniently approximated by the maximal or minimal expressions of these distributions, respectively, that is, the extreme value distributions also constitute the limit distributions for maxima and minima (see Figure 3.1), which is an important conclusion due to Gnedenko (1943). Moreover, the extreme value distributions appear more frequently as limiting distributions of any other parent distribution modelling physical phenomena than being the parent distribution, as indicated by Galambos (1978) and Castillo (1988).

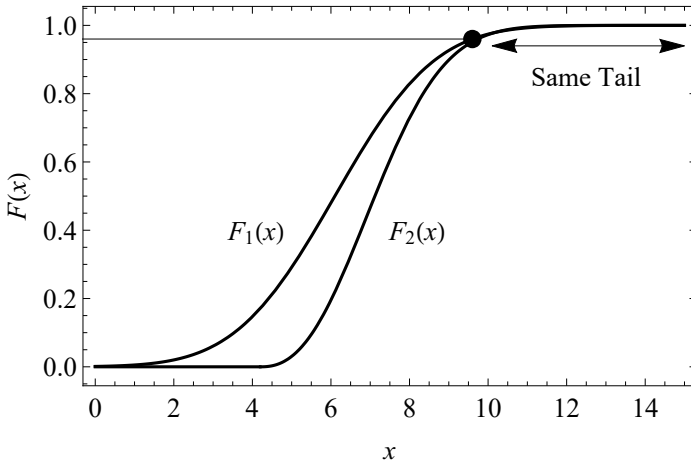


Figure 3.1: Schematic illustration of the two distinct functions with the same right tail, i.e. the same domain of attraction for maxima (see Castillo (1988) and Castillo et al. (2004a)).

Closely related with this lasting property, the concept of domain of attraction allows to distinguish whether a certain parent cdf belongs to one of these three extreme value distributions, since they constitute the only three possible domains of attraction which any continuous distribution must belong to. Thus, a given cdf, $F(x)$, is said to belong to the domain of attraction for maxima of a given cdf $H(x)$, when it satisfies, for given sequences a_n and $b_n > 0$ in order to avoid degeneration,

$$\lim_{n \rightarrow \infty} [F(a_n + b_n x)]^n = H(x), \quad \forall x, \tag{3.57}$$

and for minimal case

$$\lim_{n \rightarrow \infty} 1 - [1 - F(a_n + b_n x)]^n = L(x), \quad \forall x \tag{3.58}$$

where the function $H(x)$ can only be the Weibull, Gumbel or Fréchet families for maxima and $L(x)$ the Weibull, Gumbel or Fréchet families for minima. Table 3.2 summarises the domains of attraction of some distributions to be used in this work. There exist different methods for identifying the domain of attraction of a given distribution (see Galambos (1978), Castillo (1988), Castillo et al. (2004a) and de Haan and Ferreira (2010)), being one of the most interesting that based on the curvatures in distributions plotted in a Gumbel probability paper. The family of extreme value distributions is illustrated in Figure 3.2, where it can be seen that Gumbel distribution separates both Weibull and Fréchet families, that is, the former can be approximated for the two latter distributions.

Table 3.2: Domains of attraction of the most common distributions, from Castillo et al. (2004a).

Distribution	Domain of attraction	
	Maximal	Minimal
Normal	Gumbel	Gumbel
Exponential	Gumbel	Weibull
Gumbel _M	Gumbel	Gumbel
Gumbel _m	Gumbel	Gumbel
Weibull _M	Weibull	Gumbel
Weibull _m	Gumbel	Weibull
Fréchet _M	Fréchet	Gumbel
Fréchet _m	Gumbel	Fréchet

M =maxima m =minima

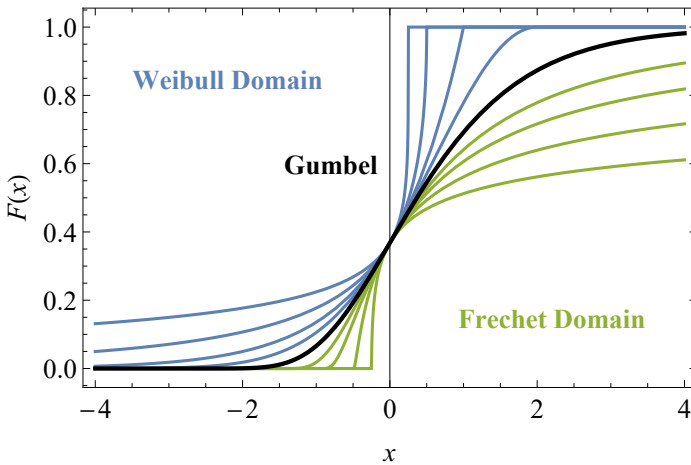


Figure 3.2: Weibull, Gumbel and Fréchet distributions indicating Gumbel as the limit between the Weibull and Fréchet regions, from Castillo et al. (2004a).

In order to illustrate the important property of being stable with respect to the formation of maximum and minimum in the extreme value distributions, and since these derivations will be used further in this work, consider the following two examples (see Castillo et al. (2004a, p. 203)).

Example 3.5 (Minimum stability of the minimal Weibull family). Consider the cdf of the minimum of an iid sample drawn from a Weibull distribution for minima $W_m(\lambda, \delta, \beta)(x)$, such that, according to (3.41) it results:

$$F_{\min}(x) = 1 - [1 - F_{W(\lambda, \delta, \beta)}(x)]^n = 1 - \exp \left[- \left(\frac{x - \lambda}{\delta} \right)^\beta \right]^n \quad (3.59)$$

$$= 1 - \exp \left[-n \left(\frac{x - \lambda}{\delta} \right)^\beta \right] = 1 - \exp \left[- \left(\frac{x - \lambda}{\delta n^{-1/\beta}} \right)^\beta \right] \quad (3.60)$$

$$= F_{W(\lambda, \delta n^{-1/\beta}, \beta)}(x), \quad (3.61)$$

which means that it is a Weibull $W(\lambda, \delta n^{-1/\beta}, \beta)$ distribution. As a remarkable result, it must be noted that only the scale parameter is changed. Figure 3.3 illustrates how the pdf and cdf of the minimum of a Weibull distribution changes as long as the sample size n is increased. \square

Example 3.6 (Minimum stability of the minimal Gumbel family). Consider the cdf of the minimum of an iid sample drawn from a Gumbel distribution for minima $G_m(\lambda, \delta)(x)$, such that, according to (3.41) it results:

$$F_{\min}(x) = 1 - [1 - F_{G(\lambda, \delta)}(x)]^n = 1 - \exp \left[- \exp \left(\frac{x - \lambda}{\delta} \right) \right]^n \quad (3.62)$$

$$= 1 - \exp \left[-n \exp \left(\frac{x - \lambda}{\delta} \right) \right] \quad (3.63)$$

$$= 1 - \exp \left[- \exp \left(\frac{x - (\lambda - \delta \log n)}{\delta} \right) \right] \quad (3.64)$$

$$= F_{G(\lambda - \delta \log n, \delta)}(x), \quad (3.65)$$

which means that it is a Gumbel $G(\lambda - \delta \log n, \delta)$ distribution. In this case, only the location parameter is changed, contrarily to the Weibull previous example. Figure 3.3 illustrates how the pdf and cdf of the minimum of a Gumbel distribution changes for different values of the sample size n . \square

3.5.4 Extended families for extreme values

Care must be taken when dealing with extreme values with other distribution than the extreme value family of distributions. Indeed, the stability with respect to the formation of the minimum or maximum is not satisfied by any other distributions and it may lead to incorrect models from an extreme value point of view. Indeed, only the Weibull, Gumbel and Fréchet distributions are stable

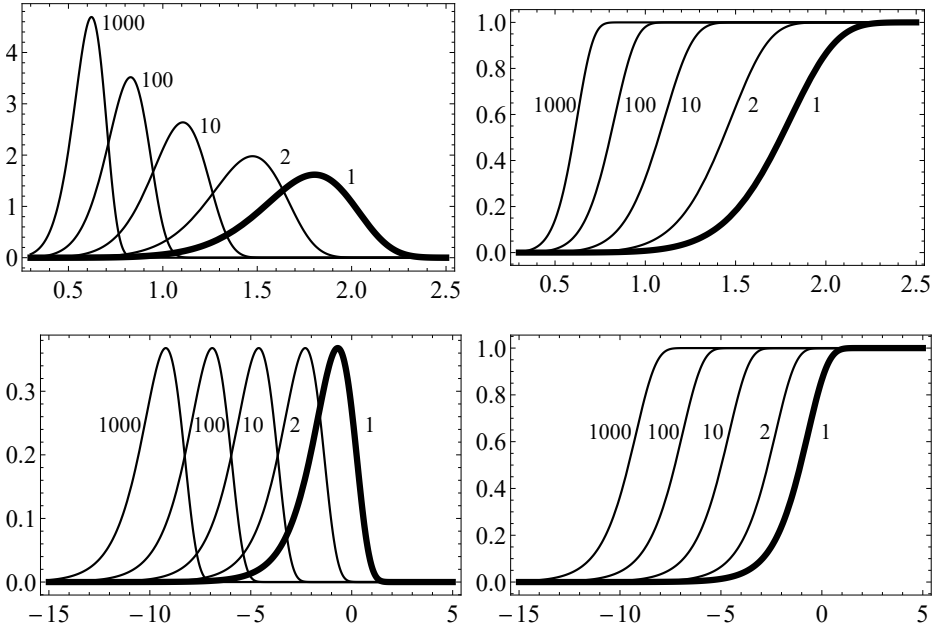


Figure 3.3: The pdf and cdf of the minimal Weibull (top) Gumbel (bottom) distribution for sample size $n = 2, 10, 100, 1000, 10000$, from Castillo et al. (2004a).

with respect to power operation. Thus, similarly to the operation-stable in the location-stable families, if a family of parametric cdf $F(x; \mathbf{c})$ is not stable with respect to formation of maximum or minimum, this family must be conveniently extended for dealing with maxima or minima operations:

- a) *Extended family for maxima.* Let X_1, X_2, \dots, X_n be a sequence of iid random variables with common non-degenerate cdf $F(x; \mathbf{c})$. If it is not stable with respect to maxima operations, the family with cdf $F(x; \mathbf{c})^n$ is the extended family stable for maxima operations, with n as a new parameter.
- b) *Extended family for minima.* Let X_1, X_2, \dots, X_n be a sequence of iid random variables with common non-degenerate cdf $F(x; \mathbf{c})$, being not stable with respect to the formation of minima, then $1 - [1 - F(x; \mathbf{c})]^n$ is the extended family stable for minima operations, for a parameter n .

To exemplify how the extended families to extreme values can be used in practice, consider the following example with the Normal distribution, which is erroneously used for modelling extremal events in some mathematical models (see, for example, Castillo et al. (1988)).

Example 3.7 (Extended normal distribution for minima). Consider the

cdf of a Normal distribution $N(\mu, \sigma^2)$

$$f(x; \mu, \sigma) = \frac{1}{\sigma\sqrt{2\pi}} \exp\left[-\frac{1}{2}\left(\frac{x-\mu}{\sigma}\right)^2\right], \quad -\infty < x < \infty, \quad (3.66)$$

such that the stability condition with respect to formation of the minimum is not satisfied (Table 3.1). Thus, according to the extended family definition for minima, if a new parameter n is considered, then,

$$F_{\min}(x) = [F_{N(\mu, \sigma^2)}(x)]^n = N_{(\mu - \sigma \log n, \sigma^2)}(x), \quad (3.67)$$

where now powers of the extended normal distribution remain being extended normal. Otherwise the normal distribution is not stable in formation of minima. As occurred with the Gumbel distribution and the formation of the minimum, the extended Normal distribution only is changed in the location parameter according to $\sigma \log n$. \square

3.5.5 Parameter estimation

Finally, some considerations about the parameter estimation of the extreme value distributions are also addressed. Within the large variety of estimation methods that can be used, (see, for example, Castillo (1988, Chapter 5) and Castillo et al. (2004a, Chapter 5)), the probability paper will be preferred in this work. The aim of this technique is looking for a transformation of the distribution function to convert it in a linear form, being more easily estimated than the original ones.

Hence, if the probability p is given by a parametric family $F(x; a, b)$, that is,

$$p = F(x; a, b), \quad (3.68)$$

then, the formula sought is a linear form throughout a certain function g ,

$$g(p) = g[F(x; a, b)] = ah(x) + b, \quad (3.69)$$

where if $u = h(x)$ and $v = g(p)$, then Eq. (3.69) can be rewritten as a linear form:

$$v = au + b. \quad (3.70)$$

The required transformations for building probabilistic papers of some common distributions are listed in Table 3.3.

In summary, attending to the description of the extreme value distributions, some important notes must be considered for their selection when dealing with extremal events (see Castillo (1988, p. 102)):

1. A parent distribution unlimited in the tail of interest cannot lie in a Weibull type domain of attraction.
2. A parent distribution limited in the tail of interest cannot lie in a Frechet

Table 3.3: Required transformations for probabilistic papers of common distributions, from Castillo et al. (2004a).

Probability paper	Reference equation	Random variable scale u	Probability scale v
Normal	(3.66)	x	$\Phi^{-1}(p)$
Weibull $_m$	(3.43)	$\log(x - \lambda)$	$\log(-\log(1 - p))$
Gumbel $_m$	(3.49)	x	$\log(-\log(1 - p))$
Fréchet $_m$	(3.51)	$-\log(\lambda - x)$	$\log(-\log(1 - p))$
Weibull $_M$	(3.45)	$-\log(\lambda - x)$	$-\log(-\log p)$
Gumbel $_M$	(3.47)	x	$-\log(-\log p)$
Fréchet $_M$	(3.54)	$\log(x - \lambda)$	$-\log(-\log p)$

type domain of attraction.

3. The maximum of a parent distribution can be approximated with the maximal family of Weibull, Gumbel and Fréchet distributions.
4. The minimum of a parent distribution can be approximated with the minimal family of Weibull, Gumbel and Fréchet distributions.
5. The Gumbel distribution can be approximated by Weibull or Fréchet distribution
6. Any distribution to be used for minima or maxima operations must be conveniently extended to these operations.

3.6 Conditional Specification of Statistical Models

This section is aimed at an important topic of recent development with the novel works by Castillo and Galambos (1987b, 1989), Castillo and Galambos (1990), Arnold et al. (1993), Arnold et al. (1994) and Arnold et al. (1998), finally culminated in the book by Arnold et al. (1999), coined the conditional specification of statistical models, arising frequently in modelling physical phenomena (see, for example, Freudenthal and Gumbel (1956) and Castillo and Fernández-Canteli (2009)). When dealing with various random variables, the joint density function plays a decisive role containing all the information about the physical phenomenon under study, as indicated by Castillo et al. (2014c). However, the specification of this joint density throughout assumptions deduced from the analysis of the physical phenomenon are not straightforward. In contrast, the conditional distributions for each random variable could facilitate the assumptions about suitable statistical distributions. In fact, the conditional specification of statistical models deals with this strategy, namely, what can be said for the joint density function if the conditional distributions are specified based on the properties of the physical phenomena?

Closely related with the conditionally specified models results the so-called compatibility condition. In this sense, the existence of the joint density is not guaranteed whatever of conditional distributions are specified, since these must be compatible. Consider the following motivating example due to Arnold et al. (1999, p. 18–19).

Example 3.8 (A motivating example). Consider a human population in which the random variables height X and weight Y are of interest, being evidently related each other. The distribution function of the height for a given weight $F_{X|Y}(x|y) = \Pr(X \leq x|Y = y)$ can be reasonably assumed to be unimodal and monotonically varying with weight, that is, as long as an individual is getting higher, the weight is also increased. Equivalently, the distribution of the weight for a given height $F_{Y|X}(y|x) = \Pr(Y \leq y|X = x)$ can also be supposed unimodal and monotonically increasing with height. Thus, instead of specifying the joint density function $f_{X,Y}(x, y)$ of both variables, the conditional specification approach allows to use previous considerations, resulting from the analysis of the variables, on the conditionals. For example, if both conditionals are assumed to have reasonably a Normal distribution, the resulting joint density has been demonstrated in Castillo and Galambos (1987a, 1989) to be bivariate Normal. Nevertheless, depending on the assumptions for mean and variance of these Normal conditionals, the joint density could not be Normal. \square

In this work, the conditional specification paradigm is used in a different sense since the problems are not oriented to specify the joint density. This quite alternative interpretation of the more general paradigm previously described is due to the study of the fatigue problem by Castillo et al. (1985) and subsequently solved by Castillo and Galambos (1987b). Consider a problem in which a variable Y depends on another regressor variable X , both intimately related with a probabilistic physical meaning. Assume that there exists also an implicit function $p = P(X, Y)$ relating both variables, being defined in such a way that $0 \leq p \leq 1$. In other words, p is considered as random with some distribution. Consequently, a family of percentile curves results as follows:

$$\Pr(Y(x) \leq y) = p, \quad 0 \leq p \leq 1, \quad (3.71)$$

$$\Pr(X(y) \leq x) = p, \quad 0 \leq p \leq 1, \quad (3.72)$$

being now defined as distribution functions because of the randomness of p , that is, there are as many curves p_i as much as percentiles (see Figure 3.4). Thus, a proposed regression model describing the problem is completely established if the distribution of X is known for any given value of $Y = y$, that is, $\Pr(X(y) \leq x)$, as indicated in Castillo et al. (2004b, p. 242–244).

The so-called compatibility condition between these distributions allows to characterize and define the regression model for the variable Y as a function of the regressor X . To this end, both distribution functions, when the other variable

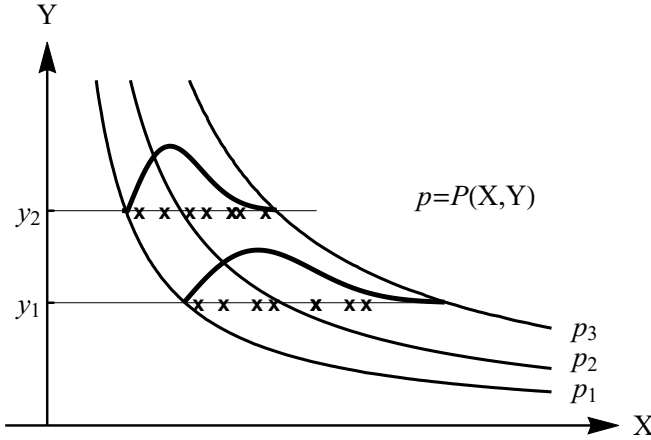


Figure 3.4: Schematic representation of the regression model, from Castillo et al. (2004b).

is given, are forced to coincide:

$$\Pr(Y(x) \leq y) = \Pr(X(y) \leq x), \tag{3.73}$$

or equivalently

$$F_X(x; y) = F_Y(y; x). \tag{3.74}$$

This formulation of the conditional specification paradigm does not deal with conditional distributions, since there is no random variable X nor any random variable Y , being only considered as two stochastically related process (see Arnold et al. (1999)). Thus, by analysing the physical phenomenon under study, both densities $X(y)$ and $Y(x)$ may be assumed to have a certain distribution and the compatibility condition in Eq. (3.74) to be applied for specifying the regression model.

In the following sections the Weibull-Weibull and Gumbel-Gumbel models are introduced as suitable distributions for the random variables $X(y)$ and $Y(x)$ in many practical applications related with extremal events, being of special interest for the purposes of this thesis, particularly the Gumbel-Gumbel model. In addition, the novel Weibull-Gumbel model was also derived and solved in this thesis for the first time.

3.6.1 The Weibull-Weibull model

Assume that for each given $y > 0$, $X(y)$ belongs to a Weibull distribution and for a given $x > 0$, $Y(x)$ belong to a Weibull distribution. From Eq. (3.74), it

leads to the following functional equation (see Arnold (2004)):

$$1 - \exp \left\{ -[a(x)y + b(x)]^{c(x)} \right\} = 1 - \exp \left\{ -[d(y)x + e(y)]^{f(y)} \right\},$$

$$y \geq -\frac{b(x)}{a(x)}, \quad x \geq -\frac{e(y)}{d(y)}, \quad (3.75)$$

with $a(x), b(x), c(x), d(y), e(y)$ and $f(y)$ as the unknown positive functions. Castillo and Galambos (1987b) obtained the following three families of solutions as the general solutions of the functional equation (3.75):

$$F(x; y) = F(y; x)$$

$$= 1 - \exp \left\{ -[E(x - A)^C (y - B)^D \exp [M \log (x - A) \log (y - B)]] \right\}$$

$$x > A, y > B, \quad (3.76)$$

$$F(x; y) = F(y; x)$$

$$= 1 - \exp \left\{ -[C(x - A)(y - B) + D]^E \right\}, \quad x > A, y > B, \quad (3.77)$$

$$F(x; y) = F(y; x)$$

$$= 1 - \exp \left\{ -[E(x - A)^C (y - B)^D]^E \right\}, \quad x > A, y > B. \quad (3.78)$$

Unfortunately, there is not integrable joint density $f_{X,Y}(x, y)$ with the conditionals given by Eqs. (3.76), (3.77) or (3.78) (see Arnold et al. (1999, p.136–140)). Figure (3.5) illustrates the iso-probability curves for the resultant Weibull-Weibull model.

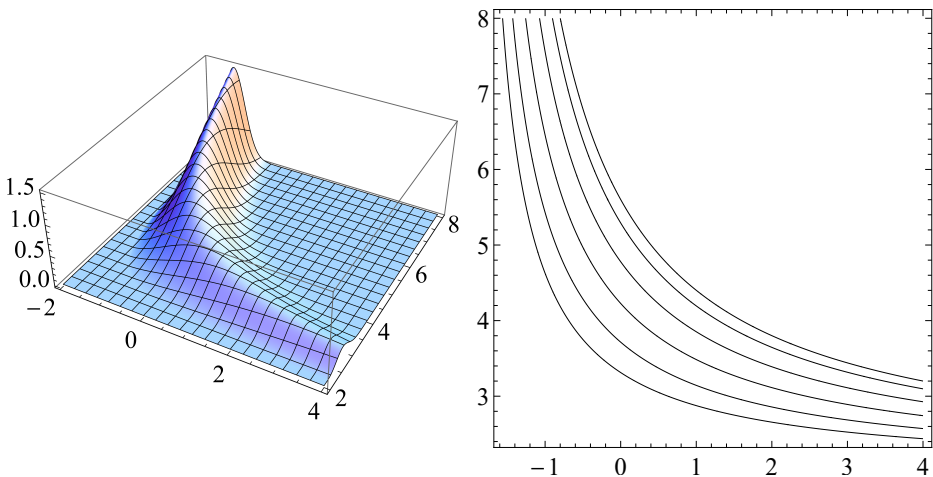


Figure 3.5: Example of a Weibull conditionals distribution showing (left) the conditional density function, and (right) the contour plot.

Moreover, different versions of the the Weibull-Weibull model result depending whether the interest is located on minima-minima or maxima-maxima values and the possible combinations between them. For instance, the S-N field in fatigue lifetime prediction constitutes an example of the Weibull-Weibull model for minima-minima values, while the crack growth curves ($a - N$ field) is for maxima-minima values, respectively, both treated in Castillo and Fernández-Canteli (2009). Due to the limiting distribution behaviour for extreme values, if the random variables $X(y)$ and $Y(x)$ were assumed to belong to a distribution pertaining to the domain of attraction of the Weibull distribution (see Table 3.2), the Weibull-Weibull model can be considered as a natural extension, without loss of generality.

3.6.2 The Gumbel-Gumbel model

Equivalently to the Weibull-Weibull model, if both random variables $X(y)$, $-\infty < y < \infty$ and $Y(x)$, $-\infty < x < \infty$ are assumed to belong to Gumbel distributions. According to Eq. (3.74), it follows that

$$1 - \exp \left[- \exp \left(\frac{x - a(y)}{b(y)} \right) \right] = 1 - \exp \left[- \exp \left(\frac{y - c(x)}{d(x)} \right) \right], \quad (3.79)$$

for the unknown functions $a(y), b(y), c(x)$ and $d(x)$, such that $b(y) > 0$ and $d(x) > 0$. The most general solution of the functional equation (3.79) is given by (see Castillo (1988), Arnold et al. (1998) and Arnold et al. (1999))

$$\begin{aligned} a(y) &= \frac{Cy - D}{Ay - B}, & b(y) &= \frac{1}{Ay - B}, \\ c(x) &= \frac{Bx - D}{Ax - C}, & d(x) &= \frac{1}{Ax - C}, \end{aligned} \quad (3.80)$$

for some arbitrary constants A, B, C and D , leading to:

$$F(x; y) = F(y; x) = 1 - \exp \{ - \exp [Axy + Bx + Cy + D] \}. \quad (3.81)$$

As in the case of the Weibull-Weibull model, there is not integrable joint density $f_{X,Y}(x, y)$ with conditionals given as in Eq. (3.80).

3.6.3 The Weibull-Gumbel model

In this work, the Weibull-Gumbel model has been originally proposed and solved as an additional interesting conditionally specified model. Hence, if $X(y)$, $y > 0$ is assumed to have a Weibull distribution while $Y(x)$, $-\infty < x < \infty$ has a Gumbel distribution, then from Eq. (3.74), it follows that

$$1 - \exp \left\{ - [a(x)y + b(x)]^{c(x)} \right\} = 1 - \exp \{ - \exp [d(y)x + e(y)] \}, \quad (3.82)$$

for the unknown positive functions $a(x), b(x), c(x), d(y)$ and $e(y)$. The most general solution of this functional equation is solved at the final of this book (see Appendix A):

$$\begin{aligned} a(x) &= Ak^x, & b(x) &= Bk^x, & e(y) &= \beta \log k, \\ c(x) &= \beta, & d(y) &= \beta \log(A + By), \end{aligned} \quad (3.83)$$

for some arbitrary constants A, B and β . and

$$F(x; y) = F(y; x) = 1 - \exp \left\{ - \left[\frac{k^x (y - G)}{\delta} \right]^\beta \right\}; \quad x \geq 0; \quad y \geq G, \quad (3.84)$$

where

$$G = -A/B, \lambda = -\log B \text{ and } \delta = 1/\beta. \quad (3.85)$$

Once again, the lack of integrability to obtain the joint density $f_{X,Y}(x, y)$ with conditionals given by Eq. (3.84) is the major problem.

As in previous sections, some feasible conditions can also be derived when dealing with conditionally specified statistical models, being herewith summarised:

- a) For multivariate models, the specification of the joint density function based on assuming some properties of the conditionals must be consistent with the compatibility condition.
- b) If the conditional specification paradigm is formulated in the sense of Eqs. (3.71) and (3.72), then the assumed distributions for densities of both random variables must be in accordance with the physical properties of the phenomenon under study.

3.7 Concluding Remarks

An extensive treatment of the mathematical and statistical methods to be used in the application of the derivation of models is presented in this chapter. Both properties and feasible conditions of any model can be conveniently defined by virtue of these methods, ensuring valid models according to different perspectives. Most of these sections must serve predominantly as feasible conditions coming from theoretical principles and considerations. By contrast, the functional equations can assist to the replication in mathematical terms for both properties and feasible conditions.

III

Viscoelastic Characterization Models

4

An Overview of Viscoelasticity

4.1 Introduction

The presence of viscoelastic materials in countless industry fields is beyond doubt: aerospace, rubber, oil, automotive, electronics, construction, piping, health and a large variety of industrial systems, throughout a vast diversity of materials such as biological, cementitious, woods, glass elements, polymer composites, among others. Nonetheless, the complex nature of viscoelasticity requires a broad and multidisciplinary knowledge to be faced, including quite different fields such as thermodynamics, continuum mechanics, advanced mathematical methods, all over imbricated under different theoretical perspectives from physics and chemistry (see Gutierrez-Lemini (2014) and Cho (2016)). As the most relevant characteristic, their time- and frequency-dependent properties imply an increasing degree of difficulty in the mathematical treatment and experimental procedures to perform the material characterization. Indeed, this fact is present as a limiting condition within the dimensions of the engineering practice, ranging from the manufacturing and production process (see Astrom (1997) and Advani and Sozer (2010)) to the design (see Jones (2001) and Rivin (2010)), passing through their computational modelling (see Marques and Creus (2012)).

From an engineering point of view, viscoelastic materials are placed in the intermediate region between purely elastic and purely viscous materials. In the former case, which is known to be subject of study of Elasticity, the energy of deformation caused by an excitation is completely stored and can be recovered

entirely upon removal of the excitation, under infinitesimal strain conditions. In turn, purely viscous materials, being subject of study of Fluid Mechanics, dissipate instantaneously and completely the energy of deformation, which is irrecoverable, under infinitesimal rates of strain. In this sense, these two concepts are ideal and truly theoretical since those instantaneous exchanges of energy are not feasible from a physical point of view. Instead, part of the total work in a viscoelastic material is dissipated as heat, while the remainder energy deformation is elastically stored.

Since the viscoelasticity field is indeed unfamiliar to many engineers and scientists, this chapter is devoted to introduce the fundamentals of the viscoelastic behaviour to the reader in order to enhance the comprehension of the following chapters where different methodologies are proposed to perform the viscoelastic characterization. To this aim, this chapter is structured as follows. Section 4.2 presents a brief survey of the viscoelastic characterization methods while Section 4.3 describes the most relevant mathematical models and approaches proposed in literature for describing the viscoelastic properties. Finally, the practical importance of the interconversion among the linear viscoelastic functions is also highlighted in Section 4.4.

4.2 Viscoelastic Characterization

The viscoelastic characterization consists in the determination of the time- and frequency-dependent properties along time or frequency, which was traditionally performed using two experimental strategies, either a strain is applied and the evolution of stress is recorded, which is known as relaxation phenomenon, or by virtue of applying a stress and to measure the evolution of strain in time, called creep phenomenon. From an experimental point of view, these procedures exhibit multiple aspects in common with standard characterization methods for other materials (see Lakes (2009)), where the applied mechanical tests may be of uniaxial, shear and bending types. For the sake of brevity and without loss of generality, in what follows the viscoelastic behavior will be described in terms of shear stress or deformation, being the extension to the uniaxial and bending type tests straightforward. It must be also emphasized that this work is only devoted to the study of linear viscoelasticity so that non-linear effects are disregarded.

Accordingly, since the viscoelastic materials are time-dependent, the classic constitutive equations relating stress σ and strain ε must be now defined in terms of material functions instead of material constants for describing their relation in a solid body (see Volterra (1959), Rabotnov (1980) and Marques and Creus (2012)). In this sense, let us consider an arbitrary, time-dependent stress history $\sigma(t)$, such that $\tau_0 \leq t < \infty$, being applied to a specimen where the corresponding strain $\varepsilon(t)$ is measured. The strain at time t will be, in general, dependent of the

stress values from τ_0 to t , and can be written as follows:

$$\varepsilon(t) = \mathbf{J} \left\{ \sigma(t) \right\}_{\tau=\tau_0}^{\tau=t}, \quad (4.1)$$

where \mathbf{J} denotes a functional¹, such that $\mathbf{J} : C(\tau_0, t) \Rightarrow \mathbb{R}$, that is, mapping the set of continuous functions $C(\tau_0, t)$ defined in the interval $[\tau_0, t]$ to real scalar values. Thus, Eq. (4.1) indicates that the value of the strain ε at time t depends not only on the single value of stress σ at t , but on the function $\sigma(\tau)$, so that $\tau_0 \leq \tau \leq t$, where τ_0 is an arbitrary initial time. Similarly, if an arbitrary strain history, $\varepsilon(t)$, is alternatively considered in the context of infinitesimal strains, then Eq. (4.1) can be rewritten as:

$$\sigma(t) = \mathbf{G} \left\{ \varepsilon(t) \right\}_{\tau=\tau_0}^{\tau=t}. \quad (4.2)$$

Hence, since this work is only focused on linear viscoelasticity, the functionals \mathbf{J} and \mathbf{G} can be simplified by limiting all continuous functions defined in $C(\tau_0, t)$ to just the linear ones. Consequently, Eqs. (4.1) and (4.2) can be simplified as:

$$\varepsilon(t) = J \sigma(t)_{\tau=\tau_0}^{\tau=t}, \quad (4.3)$$

$$\sigma(t) = G \varepsilon(t)_{\tau=\tau_0}^{\tau=t}, \quad (4.4)$$

where J and G are known as creep compliance and relaxation modulus, respectively. Note that in linear elastic materials there is no dependency with the past history, so that the lack of memory property, and Eqs. (4.3) and (4.4) provide the well-known constitutive equations for linear-elastic materials.

Due to the mathematical complexity of these constitutive equations, implying time-dependent functions in input and output, that is, $\sigma(t)$ in creep and $\varepsilon(t)$ in relaxation, the researchers propose to simplify them in the experimental procedures by considering constant inputs assuming the viscoelastic modulus and compliance to be functions of time instead, i.e. $G(t)$ and $J(t)$ respectively. In this way, the resulting constitutive equations for linear viscoelastic materials are defined as follows:

$$\varepsilon(t) = J(t)\sigma_0, \quad (4.5)$$

$$\sigma(t) = G(t)\varepsilon_0, \quad (4.6)$$

for any constant stress and strain inputs σ_0 and ε_0 , respectively, where now the compliance $J(t)$ and the modulus $G(t)$ become the objective functions to be experimentally measured.

¹A functional represents a real-valued function that maps another functions with real scalar values.

In the following sections, the relaxation and creep responses are illustrated in case of static and dynamic experiments. There exists a variety of different inputs to be considered in the characterization of these materials (see Tschoegl (1989) and Tschoegl (1997)), such as for instance, step, slope, among others, the former being the most widely used in the experimental campaigns.

4.2.1 Static experiments

On the one hand, the relaxation phenomenon occurs when a viscoelastic material is subjected to a constant strain ε_0 and the resulting stress σ decreases in time, such that from Eq. (4.6) results the ratio

$$G(t) = \frac{\sigma(t)}{\varepsilon_0}, \quad (4.7)$$

which is known as relaxation modulus under shear deformation. This viscoelastic function is known to be a non-negative, differentiable and decreasing function with time, such that,

$$\frac{dG(t)}{dt} < 0 \Rightarrow 0 \leq G(t) \leq \infty, \quad t \in \mathbb{R}, \quad (4.8)$$

where the limiting values $G(0)$ and $G(\infty)$ are characteristics of the material, called glass or instantaneous modulus and equilibrium or relaxed modulus, respectively. Figure 4.1 illustrates the step deformation input and the resulting evolution of stress along the time for a typical relaxation test. Care must be taken when consulting viscoelasticity literature since there no preferable scale is suggested for the representation, being linear-log and log-log the common representations, as indicates Shaw and MacKnight (2018).

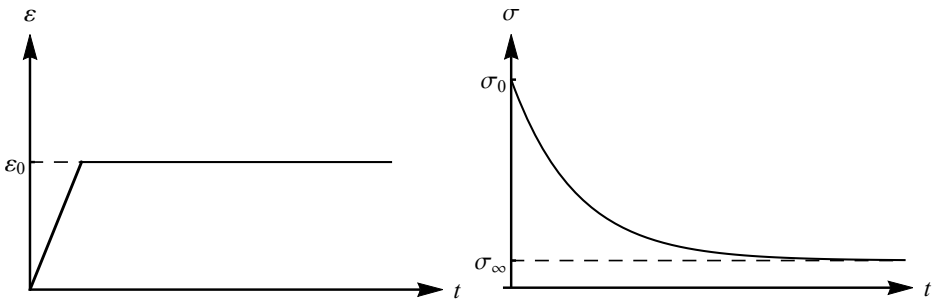


Figure 4.1: Strain step input and stress response of a viscoelastic material in a relaxation test both in a linear representation.

On the other hand, the viscoelastic nature of the material can also be described by the creep test, consisting in the application of a constant stress σ_0 and the

record of the evolution of the deformation ε along time. The quotient:

$$J(t) = \frac{\varepsilon(t)}{\sigma_0}, \quad (4.9)$$

is called creep compliance under shear stress. Similarly to the relaxation modulus $G(t)$, the creep compliance $J(t)$ also constitutes a non-negative, non-decreasing and differentiable function, that is,

$$\frac{dJ(t)}{dt} > 0 \Rightarrow 0 \leq J(t) \leq \infty, \quad t \in \mathbb{R}, \quad (4.10)$$

where the limiting values $J(0)$ and $J(\infty)$ are material characteristics, known as glass or instantaneous compliance and equilibrium or creep compliance, respectively. In Figure 4.2 a typical stress step input is shown with the corresponding evolution of the creep deformation in a time test both in a linear representation.

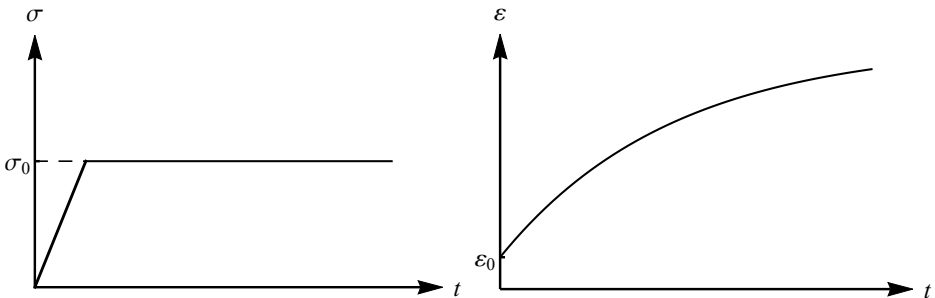


Figure 4.2: Step input and response of a viscoelastic material in a creep test in both linear representation.

Accordingly, the viscoelastic static characterization implies the determination of the relaxation modulus $G(t)$ and creep compliance $J(t)$ along the time from both different experimental procedures, which are illustrated in a log-log plot in Figures 4.3 and 4.4, respectively. At very short times, the relaxation modulus reaches its maximum value at the so-called glassy state (typically $G_0 \sim 10^9$ Pa), being independent of time, whereas at very long times it behaves as a rubber-like material (typically $G_\infty \sim 10^5$ Pa), also time independent. On the other hand, creep compliance at very short times shows its minimum value at the glassy transition (typically $J_0 \sim 10^{-9}$ Pa $^{-1}$), independently of time whereas at very long times behaves as a rubber-like with its highest value of modulus (typically $J_\infty \sim 10^{-5}$ Pa $^{-1}$), also time independent (see Ward and Sweeney (2012)).

As with other materials, viscoelastic materials can be classified into linear

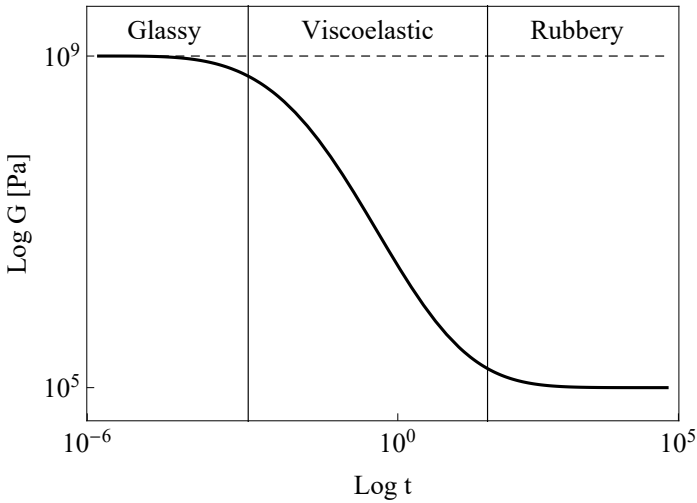


Figure 4.3: Illustration of the evolution of the relaxation modulus $G(t)$ as a function of time with its typical regions.

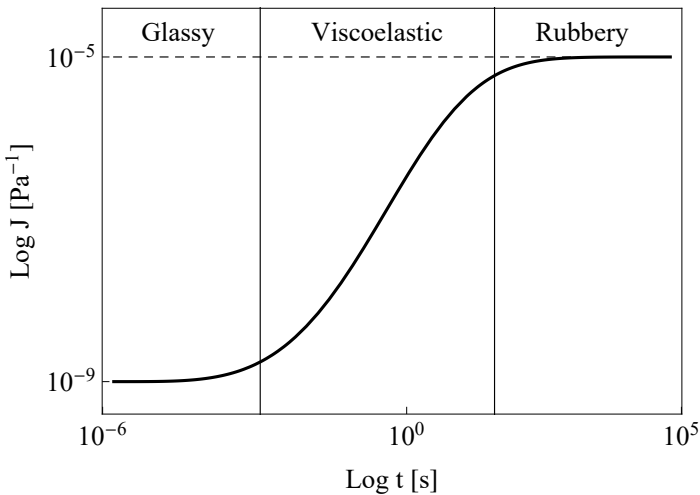


Figure 4.4: Illustration of creep compliance $J(t)$ as a function of time with its typical regions.

and non-linear depending on its behaviour, characterized by the constitutive equation relating the stress and strain in the solid. In this sense, a viscoelastic material must fulfil two conditions to be classified as a linear one (see Findley et al. (1976)). Firstly, the stress must be proportional to strain at any time and, secondly, the linear superposition principle must apply. Both conditions can be

written mathematically as follows:

$$\varepsilon[c\sigma(t)] = c\varepsilon[\sigma(t)], \quad (4.11)$$

$$\varepsilon[\sigma_1(t) + \sigma_2(t - t_1)] = \varepsilon[\sigma_1(t)] + \varepsilon[\sigma_2(t - t_1)], \quad (4.12)$$

where c is a constant. The first equation states that the strain response $\varepsilon(t)$ for a stress input of value $c\sigma(t)$ is c times the strain response to a stress input of value $\sigma(t)$. On the other hand, the second equation establishes the additive property of strains, or equivalently of stresses, such that the strain response due to a sum of stresses input applied at different times is equal to the sum of the strains arising for each of the individual stresses. This principle is firstly enunciated by Boltzmann (1878) and known as the Boltzmann superposition principle.

Figure 4.5 illustrates the typical stress-strain relations in both cases of linear and non-linear viscoelastic materials. Note the relevant difference when compared with time-independent materials, since each of these curves is now defined only for a given value of time, and as such also called isochronal. The reader is referred to Findley et al. (1976) and Wineman (2009) for an illustrative introduction to the non-linear viscoelastic behavior.

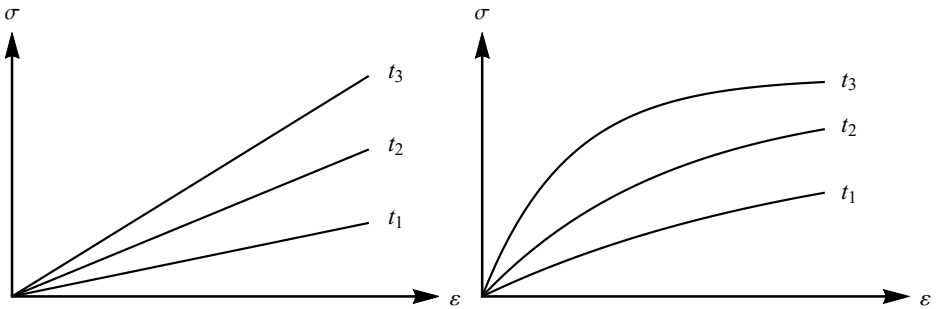


Figure 4.5: Stress versus strain at different fixed times (isochronals) for linear (left) and non-linear (right) materials.

4.2.2 Dynamic experiments

In the viscoelastic dynamic characterization, as an alternative to the static one, the specimen is subject to an alternating strain $\varepsilon(t)$ while the stress $\sigma(t)$ is registered in case of the relaxation test, and viceversa in the creep test. In the context of the linear viscoelasticity, both magnitudes vary sinusoidally once the equilibrium is reached in the steady-state with a certain offset angle between them, this being the critical difference for the time-independent materials. Therefore, if a sinusoidal strain input $\varepsilon(t)$ is applied to a viscoelastic material, the input strain

and the stress response are defined, respectively, as follows:

$$\varepsilon(t) = \varepsilon_0 \sin(\omega t), \quad (4.13)$$

$$\sigma(t) = \sigma_0 \sin(\omega t + \theta), \quad (4.14)$$

where ω represents the angular frequency and θ the offset angle (see Figure 4.6).

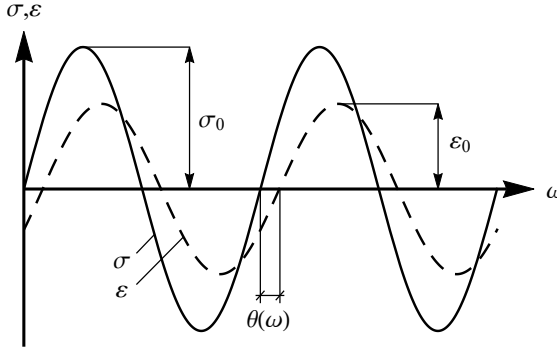


Figure 4.6: Sinusoidal stress and strain relation at the steady-state in a relaxation dynamic test.

However, since the response in the steady-state is periodic in time, the interest lies on the response as a function of the frequency ω due to periodic input, rather than the response on time. Accordingly, the functions $\sigma(t)$ and $\varepsilon(t)$ are written as $\sigma(\omega)$ and $\varepsilon(\omega)$. The relation between stress and strain in the dynamic characterization is equivalent to the static case as given by Eqs. (4.5) and (4.6), that is,

$$\sigma(\omega) = G^*(\omega)\varepsilon(\omega), \quad (4.15)$$

$$\varepsilon(\omega) = J^*(\omega)\sigma(\omega), \quad (4.16)$$

where $G^*(\omega)$ and $J^*(\omega)$ represent, the complex relaxation modulus and creep compliance in shear deformation, respectively. Thus, since $G^*(\omega)$ is defined in the complex plane, it can be decomposed into the real and complex parts:

$$G^*(\omega) = G'(\omega) + jG''(\omega), \quad (4.17)$$

where $G'(\omega)$ and $G''(\omega)$ are called the storage modulus and loss modulus, respectively, with $j = \sqrt{-1}$ as the imaginary unit. As their names indicate, the real part is concerned with the energy stored in the viscoelastic material, while the imaginary part is related to the energy as dissipated heat in the deformation, since both are directly proportional to the average of these quantities in each cycle of deformation. Note also that since $\omega = t^{-1}$, $\log G'(\omega)$ represents the reflection of $\log G(t)$. From trivial trigonometric relations, it follows that both

moduli can be defined as:

$$G'(\omega) = |G^*(\omega)| \cos \theta(\omega), \quad (4.18)$$

$$G''(\omega) = |G^*(\omega)| \sin \theta(\omega), \quad (4.19)$$

where $|G^*(\omega)|$ is the magnitude of the complex modulus $G^*(\omega)$, leading to

$$|G^*(\omega)| = \sqrt{|G'(\omega)|^2 + |G''(\omega)|^2}. \quad (4.20)$$

Particular interest has the loss tangent, which represents the phase angle $\theta(\omega)$ between the stress and strain as the dimensionless quotient between the storage and loss moduli, i.e.,

$$\tan \theta(\omega) = \frac{G''(\omega)}{G'(\omega)}. \quad (4.21)$$

Figure 4.7 illustrates the complex modulus and compliance for a typical viscoelastic material. On the one hand, at very low frequencies, the material behaviour approaches to a rubber-like one exhibiting independency with frequency respect to the frequency low storage modulus (approx. $G'(0) \approx 10^5$). In turn, at very high frequencies the material behaviour evolves to a glassy one adopting its highest value of storage modulus (approx. $G'(\infty) \approx 10^9$), proving to be also independent of frequency. In the intermediate region, the material shows viscoelastic behaviour with increasing storage modulus for increasing frequency. As mentioned above, the $\log G'(\omega)$ plot is shown to be a reflection of $\log G(t)$, as can be seen by comparing Figure 4.7 with Figure 4.3. On the other hand, the loss modulus exhibits a particular evolution with frequency, approaching to zero at both tails (very low and high frequencies) reaching its maximum value within the viscoelastic region, just at the frequency at which storage modulus has the highest derivative (Ward and Sweeney (2012)).

A summary of the different moduli and compliances in both relaxation and creep for static and dynamic experiments considering different test types is listed in Table 4.1, from Ferry (1980) (p. 30) and Fernández et al. (2011).

Table 4.1: Viscoelastic moduli and compliances for different experimental characterizations in relaxation and creep tests.

Moduli	Time		Frequency	
	Relaxation	Creep	Relaxation	Creep
Shear	$G(t)$	$J(t)$	$G'(\omega), G''(\omega)$	$J'(\omega), J''(\omega)$
Uniaxial	$E(t)$	$D(t)$	$E'(\omega), E''(\omega)$	$D'(\omega), D''(\omega)$
Bulk	$K(t)$	$B(t)$	$K'(\omega), K''(\omega)$	$B'(\omega), B''(\omega)$
Poisson	$\nu_r(t)$	$\nu_f(t)$	$\mu'_r(\omega), \mu''_r(\omega)$	$\mu'_f(\omega), \mu''_f(\omega)$

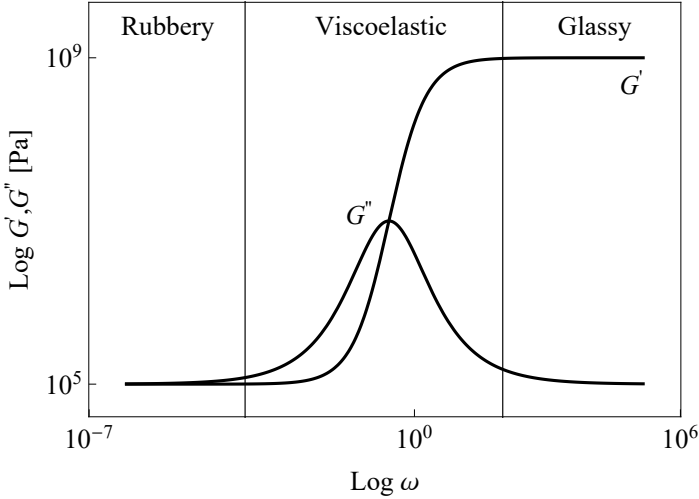


Figure 4.7: A typical example of complex relaxation moduli under shear deformation.

4.3 Mathematical Models

Once the viscoelastic characterization methods are introduced, the interest lies on the study of the most relevant mathematical models proposed in the literature for describing both relaxation and creep viscoelastic functions for either static and dynamic experiments. Further details about these models when applied to pure mathematical-related problems can be extensively found in Findley et al. (1976), Tschoegl (1989), Fabrizio and Morro (1992), Drozdov (1998) and Lakes (2009), among others.

4.3.1 Differential representation

Traditionally in science and engineering, the physical phenomena have been modelled using differential equations, also known as differential representation. In the case of the viscoelastic behaviour, linear differential equations with constant coefficients constitute a suitable mathematical framework where the linearity conditions in Eqs. (4.11) and (4.12) are inherently satisfied (see Alfrey and Doty (1945), Gross (1953)). Accordingly, the most general differential equation relating stresses and strains along the time for an isotropic viscoelastic material subject to an infinitesimally small shear deformation is defined as:

$$\left[1 + \sum_{k=1}^p a_k \frac{d^k}{dt^k} \right] \sigma(t) = \left[m + \sum_{k=1}^q b_k \frac{d^k}{dt^k} \right] \varepsilon(t), \quad (4.22)$$

where k is the degree of the differential equation and m, a_k, b_k are constants, which must be subject to some conditions in order to fulfil physical requirements in a real application (see Gutierrez-Lemini (2014)).

4.3.2 Integral representation

As an alternative to the differential representation, the physical phenomena are usually modelled using the integral representation, which seems especially useful in the viscoelastic context by considering arbitrary inputs and determining the corresponding arbitrary response. Indeed, consider an arbitrary stress $\sigma(t)$ input, which can be approximated by means of a series of step functions $H(t)$, such that,

$$\sigma(t) = \sum_{i=1}^n \sigma_i H(t - \tau_i). \quad (4.23)$$

The corresponding strain output $\varepsilon(t)$ can be defined using the Boltzmann superposition principle as the sum of the strain outputs ε_i for each of the stress input components σ_i , that is,

$$\varepsilon(t) = \sum_{i=1}^n \varepsilon_i(t - \tau_i) = \sum_{i=1}^n \sigma_i J(t - \tau_i) H(t - \tau_i), \quad (4.24)$$

where $J(t)$ represents the creep compliance. Figure 4.8 illustrates schematically the approximated strain output due to a certain stress input as the sum of step functions according to the integral representation.

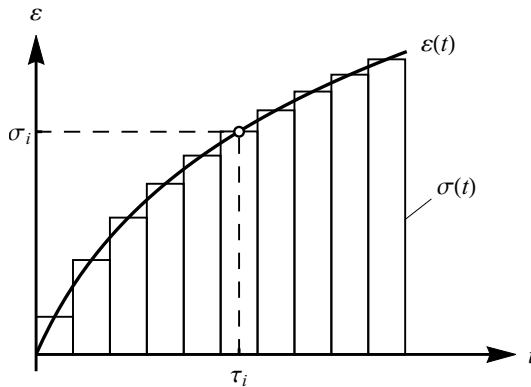


Figure 4.8: Illustration of the approximated strain output based as the sum of step functions for arbitrary stress input.

Thus, if the number of the step functions in Eq. (4.23) goes to infinity ($n \rightarrow \infty$)

the approximation closely approaches to the real strain output, such that the resulting total strain output is given by:

$$\varepsilon(t) = \int_0^t J(t - \tau) \frac{d\sigma(\tau)}{d\tau} d\tau, \quad (4.25)$$

which constitutes the integral representation of creep strain due to a general stress input. Analogously, in the case of stress relaxation due to an arbitrary strain input, its integral representation is defined as follows:

$$\sigma(t) = \int_0^t G(t - \tau) \frac{d\varepsilon(\tau)}{d\tau} d\tau, \quad (4.26)$$

with $G(t)$ as the relaxation modulus in shear deformation.

4.3.3 Mechanical models

Classical mechanical models were also proposed as a comprehensive theoretical framework providing simpler and more practical approximations of the viscoelastic behaviour. In fact, these models are currently widely used in the practical design of structural components, becoming especially popular in the computational implementation of the viscoelastic models despite, or perhaps because, their simplicity. Certainly, the complexity of the viscoelastic behavior exceeds the possibilities of the use of rigorous mathematical models, such as previous integral and differential representations. In this way, mechanical and phenomenological models represent a suitable choice to describe the viscoelastic properties of components in a suitable manner.

Accordingly, the simplest model based on spring and dashpot elements are firstly presented in what follows. Then, by means of different combinations of these two basic elements, more complex models can be derived, such as the well-known Maxwell, Kelvin and Burgers, enhancing the possibilities to describe the viscoelastic functions and the stress-strain relations in relaxation and creep cases. Finally, these models are extended to the corresponding generalized versions with n elements.

Spring and dashpot models

A linear spring is widely used in science and engineering as suitable representation of the linear stress-strain relation in the case of elastic materials becoming the first example of mechanical model. Let us consider a linear spring subject to a deformation ε with R as the elastic constant, such that the resulting stress σ is given by:

$$\sigma = R\varepsilon. \quad (4.27)$$

As the opposite limiting case, the pure viscous behaviour is usually described as a simple dashpot, in which the corresponding stress for a certain strain rate

applied is given by:

$$\sigma = \tau \frac{d\varepsilon}{dt}, \quad (4.28)$$

where τ represents the viscosity constant of the dashpot. Due to the intermediate behaviour of the linear viscoelastic materials within both limiting cases, the following mechanical models proposed in literature are based on different combinations of spring and dashpots.

The Maxwell model

The Maxwell model results as the combination of a spring with elastic constant R and a dashpot with viscosity η in a series connection type, as seen in Figure 4.9. As a result, the relaxation stress and modulus are given respectively by:

$$\sigma(t) = \sigma_0 \exp\left(-\frac{Rt}{\eta}\right), \quad (4.29)$$

$$G(t) = \exp\left(-\frac{Rt}{\eta}\right), \quad (4.30)$$

from which it follows the exponential stress decay in a typical relaxation test after removal of the strain input as shown in Figure 4.9. Particularly interesting in these mechanical models is the so-called relaxation time τ , defined as the time required for the stress to reach the particular value of σ_0/e , that is, for the decay becoming 36.7% of the initial stress value σ_0 , which in the case of the Maxwell model is given by $\tau = \eta/R$.

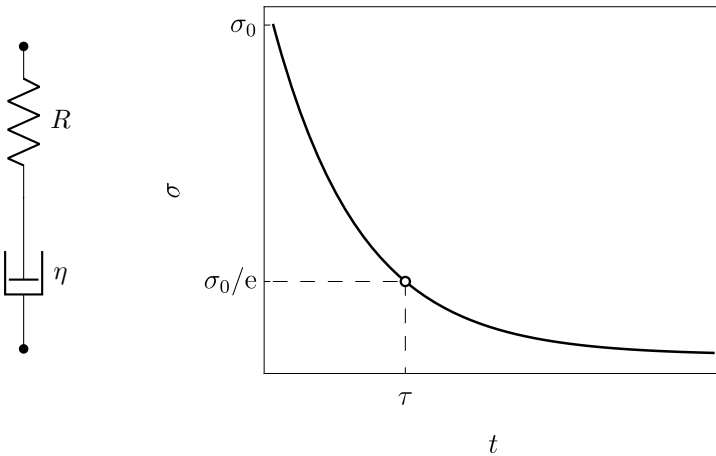


Figure 4.9: Schematic representation of the Maxwell model with spring and dashpot connected in series and of the stress relaxation along the time.

The Kelvin or Voigt model

The Kelvin or Voigt model suggests the parallel type connection between a spring and a dashpot rather than the series type from Maxwell model, as can be seen in Figure 4.10. The former Kelvin or Voigt model is the one used preferably for modelling strain under creep conditions, while the latter is generally applied for stress relaxation (see Brinson (2015)). The creep strain and compliance based on the Kelvin model are respectively given by:

$$\varepsilon(t) = \frac{\sigma_0}{R} \left[1 - \exp\left(-\frac{t}{\tau}\right) \right], \quad (4.31)$$

$$J(t) = \frac{1}{R} \left[1 - \exp\left(-\frac{t}{\tau}\right) \right]. \quad (4.32)$$

The resulting creep strain increases exponentially until the limiting value ε_∞ is reached. In this case, the characteristic time value of τ , called retardation time, corresponds with the 63% of the final value ε_∞ .

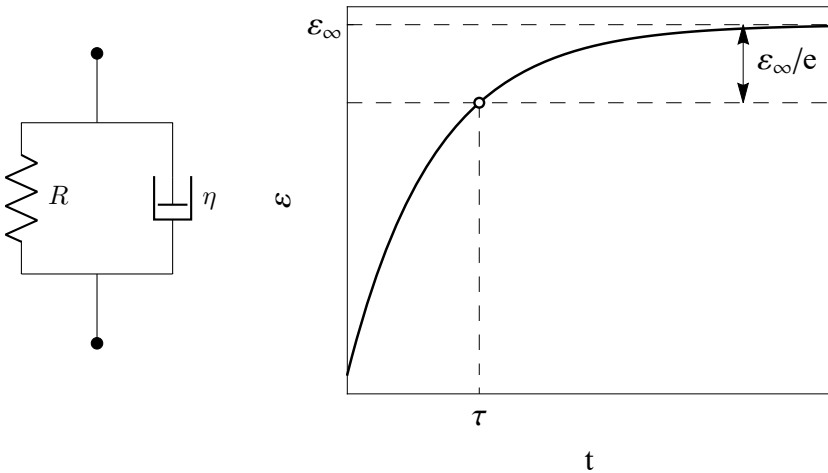


Figure 4.10: Schematic representation of the Kelvin model consisting on spring and dashpot connected in parallel and the creep deformation along the time.

The Burgers or Four-element model

The Burgers model, also known as Four-element model, represents a noticeable improvement of the previous Kelvin and Maxwell models, offering a reasonable approach to viscoelastic characterization by considering the following features: instantaneous elasticity ($1/R_1$), delayed elasticity ($1/R_2$) and flow term (t/η_1). This model consists in a combination of the Maxwell and Kelvin models in a series type connection, as shown in Figure 4.11, such that the strain evolution

with time results as:

$$\varepsilon(t) = \sigma_0 \left[\frac{1}{R_1} + \frac{t}{\eta_1} + \frac{1}{R_2} \left[1 - \exp\left(-\frac{R_2 t}{\eta_2}\right) \right] \right], \quad (4.33)$$

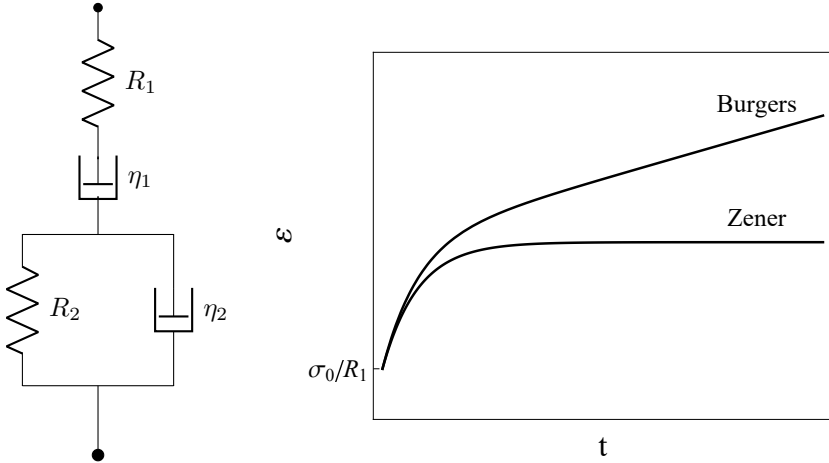


Figure 4.11: Schematic representation of the Burgers model and the resulting creep deformation along time.

As indicated by Brinson (2015), the flow term (t/η_1) in Eq. (4.33) is seen as optional in some reference textbooks, from where the well-known Zener model results (see Figure 4.11).

The Generalized models

Due to the complexity of the viscoelastic behaviour, the classic mechanical models presented above were found to be insufficient for describing the evolution in time of the relaxation and creep properties in some advanced applications. For this reason, the generalization of these mechanical models as combination of higher number of elements in series or parallel type appears as a natural improvement. In fact, current application of these models in practical design is always in terms of such generalized versions. As an example, the generalized Maxwell model consisting of n different spring-dashpot elements connected in series define the relaxation stress and modulus, respectively, as follows:

$$\sigma(t) = \varepsilon_0 \sum_{i=1}^n R_i \exp\left(-\frac{t}{\tau_i}\right), \quad (4.34)$$

$$G(t) = \sum_{i=1}^n R_i \exp\left(-\frac{t}{\tau_i}\right), \quad (4.35)$$

with R_i as the elastic constant of the i -th spring element and τ_i as the viscosity of the i -th dashpot. Equivalently, the generalization of the Voigt model implies the combination of n spring-dashpot elements in parallel, leading to the following definitions of the creep strain and compliance:

$$\varepsilon(t) = \sigma_0 \left[\frac{1}{R_0} + \sum_{i=1}^n \frac{1}{R_i} \left[1 - \exp\left(-\frac{t}{\tau_i}\right) \right] \right], \quad (4.36)$$

$$J(t) = \frac{1}{R_0} + \sum_{i=1}^n \frac{1}{R_i} \left[1 - \exp\left(-\frac{t}{\tau_i}\right) \right]. \quad (4.37)$$

Note the additional advantage of the low computational cost due to considering a high number of elements in these generalized versions implying simple exponential terms in the former expressions.

4.3.4 Models based on fractional derivatives

Fractional calculus is a branch of mathematical analysis concerned with fractional derivatives, i.e. derivatives of any arbitrary order, real or complex, allowing the application of classical differentiation and integration operators to be extended. This technique provides a novel approach to viscoelasticity characterization, alternative to the classical mechanical models and integral and differential representations. Most of its applications are focused on the linear viscoelasticity field, as pointed out by Mainardi (2010).

The more general functional definition of the stress-strain constitutive equation based on fractional derivatives is defined as follows:

$$f\left(\sigma(t), \frac{d^\nu \sigma(t)}{dt^\nu}, \varepsilon(t), \frac{d^\nu \varepsilon(t)}{dt^\nu}\right) = 0, \quad (4.38)$$

where ν is the power of the differential operator, such that $0 < \nu < 1$.

Initially, this approach was applied to provide an interesting fractional version more versatile and robust than the classical mechanical models (see Koeller (1984) and Mainardi (2010)). For instance, the stress-strain relationship for the fractional version of the Maxwell model is given by:

$$\sigma(t) + C_0 \frac{d^\nu \sigma}{dt^\nu} = C_1 \frac{d^\nu \varepsilon}{dt^\nu}, \quad (4.39)$$

for the constants C_0, C_1 . Solving Eq. (4.39), the creep compliance in shear deformation $J(t)$ is obtained:

$$J(t) = \frac{\varepsilon(t)}{\sigma(t)} = \frac{C_2}{C_1} + \frac{1}{C_3} \frac{t^\nu}{\Gamma(1 + \nu)}, \quad (4.40)$$

where $\Gamma(\cdot)$ is the well-known Gamma function, C_1, C_2 and C_3 are constants and ν represents the power of the fractional operator. Note that the fractional approach

provides an extra parameter ν to the classical models thus extending them to a parametric family of models. Figure 4.12 illustrates the resulting creep compliance for several values of this extra parameter, exhibiting a different behaviour than simple exponential form, with a much faster J growth for increasing ν (see Mainardi (2010)).

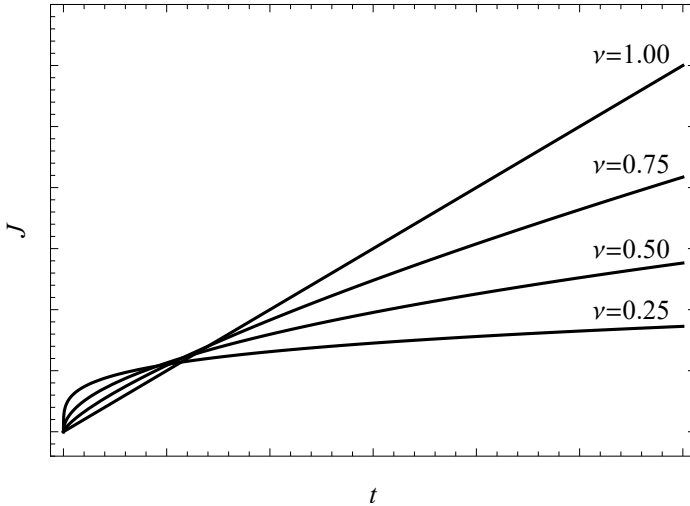


Figure 4.12: Creep compliance of the fractional Maxwell model for different values of the power of fractional operator ν .

More recently, Mainardi et al. (2019) have also achieved the generalization of the celebrated Becker model from the perspective of the fractional calculus. For further details and examples of application of the fractional derivatives in a more general context in engineering and science, the reader is referred to some textbooks of reference, such as Carpinteri and Mainardi (1997), Uchaikin (2013) and Mainardi (2018), among others.

4.3.5 Prony series

The generalized version of the Maxwell model with n spring-dashpot elements connected in series has been extensively used for describing the viscoelastic properties during the last decades (see Chen (2000)). This model was identified with another celebrated approximation method in science known as Prony series, both adopting the same functional form as a sum of exponentials thus constituting the most widely preferred mathematical model in the viscoelasticity context. In fact, most the current software packages of finite element method are based on this series for building material models in their libraries.

According to this proposal, the relaxation modulus $G(t)$ and creep compliance

$J(t)$ are defined, respectively, as follows:

$$G(t) = G_\infty + \sum_{i=1}^n G_i \exp\left(-\frac{t}{\tau_i}\right), \quad (4.41)$$

$$J(t) = \frac{1}{J_0} + \sum_{i=1}^n \frac{1}{J_i} \exp\left(-\frac{t}{\tau_i}\right), \quad (4.42)$$

where G_∞ and J_0 represent the relaxed modulus and the instantaneous compliance, respectively.

The reasons lying behind its widespread use are mainly twofold (see Brinson (2015)). Firstly, because its functional form, similar to that found in the mechanical models by combining springs and dashpots. As a result, the viscoelastic properties so defined can be straightforwardly conciliated with a comprehensive model composed by these elements. Secondly, due to the low computational cost implied by a such remarkably simple mathematical tool as represented by a series of simple exponentials with trivial derivatives and integrals.

Nevertheless, Prony series also exhibit some weaknesses. On the one side, the number of parameters for fitting the viscoelastic functions must be higher than, say, ten in order to limit the expected error, obviously excessive despite of the low computational cost. On the other side, if aiming at achieving an error minimization in the fitting process, the number of terms in the Prony series is increased, this does not imply a simple addition of new terms in the series while maintaining the values of the previous parameters. In fact, the parameter estimation of a Prony series must be carried out for the present number of terms adopted, without it being possible to use the information provided from former estimations with lower number of terms.

For a deeper mathematical discussion about the exponential-sum approximation method in engineering and science, see for example Wiscombe and Evans (1977) and Holmström and Petersson (2002).

4.3.6 Stretched exponential model

The so-called Kohlrausch function, initially developed in the context of dielectric relaxation phenomenon by Kohlrausch (1854) and Williams and Watts (1969), was found to be more appropriate than previous exponential-based solutions for modelling the relaxation process of a large variety of materials, such as polymers, bones and muscles (see Anderssen et al. (2004)).

The Kohlrausch or stretched exponential function, usually called Kohlrausch-Williams-Watts model (KWW) in the viscoelasticity context (see for example Nutting (1921), Jonscher (1977) and Palmer et al. (1984)), is generally defined as follows:

$$K_{\tau,\beta}(t) = \exp[-(t/\tau)^\beta], \quad 0 \leq t < \infty \quad (4.43)$$

with parameters τ and β . According to this model, the relaxation modulus under

shear deformation $G(t)$ is given by:

$$G(t) = (G_0 - G_\infty) \exp \left[- \left(\frac{t}{\tau} \right)^\beta \right] + G_\infty, \quad (4.44)$$

where $0 \leq \beta \leq 1$, while G_0 and G_∞ represent the limiting values of the relaxation modulus and τ the corresponding relaxation time (see Figure 4.13). In the particular case of $\beta = 1$, then Eq. (4.44) corresponds with the Debye model.

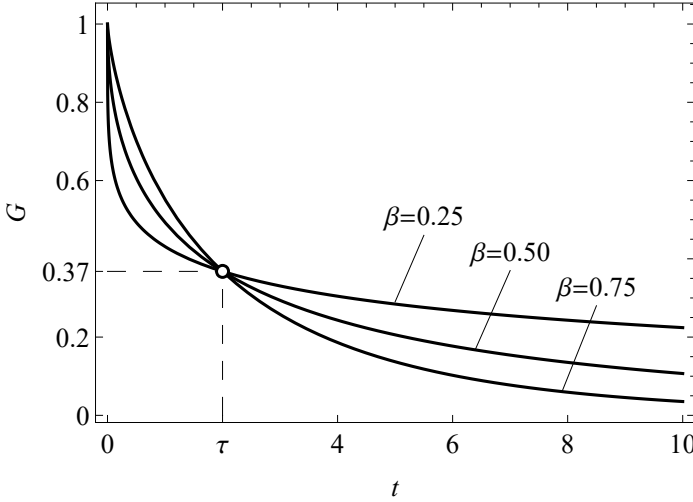


Figure 4.13: Normalized relaxation modulus $G(t)$ according to the Kohlrausch-Williams-Watts model for different values of the β parameter.

As a matter of fact, it is also worth mentioning that in viscoelastic and polymer literature, the quotient (LHS) in Eq. (4.44) is usually rewritten as follows:

$$\frac{G(t) - G_\infty}{G_0 - G_\infty} = \exp \left[- \left(\frac{t}{\tau} \right)^\beta \right], \quad (4.45)$$

which is known as the normalization representation of the viscoelastic modulus (see Nowick (1972), Riande et al. (1999) and Lakes (2009)). As will be shown in Chapter 5, Eq. (4.45) is interesting for the purposes of this thesis since its results are bounded in the interval $[0,1]$. In Chapter 6, additional arguments are provided based on the dimensional analysis to justify this normalized representation.

4.3.7 Viscoelastic spectrum representation

As mentioned previously, the generalized version of the classical mechanical models aims to extend a discrete sum of exponentials to a higher number of terms, to improve the estimation of the viscoelastic functions. Theoretically, this discrete

sum should be expanded to $n \rightarrow \infty$ in order to reproduce reliably a continuum viscoelastic solid, which is referred to as the viscoelastic spectrum approach. As a result, the number of the relaxation or retardation time values also tends to infinity, each of them being associated with each of the elements in which the solid can be divided, now being called relaxation and retardation spectra. However, the determination of these spectra was found to be an ill-posed problem, since these magnitudes can not be physically measured (see Ferry (1980), Tschoegl (1989), Emri and Tschoegl (1993), Tschoegl and Emri (1993) and Emri and Tschoegl (1994)).

To achieve a comprehensive introduction of this spectral approach, consider the relaxation modulus under shear deformation $G(t)$ due to the Maxwell model with an infinite number of elements. To this end, the limit must be taken in Eq. (4.30), leading to:

$$G(t) = \lim_{n \rightarrow \infty} \sum_{i=1}^n G_{0i} \exp\left(-\frac{t}{\tau_i}\right), \quad (4.46)$$

which, after elementary calculus, Eq. (4.46) is transformed into an equivalent expression:

$$G(t) = \int_0^{\infty} H(\tau) \exp\left(-\frac{t}{\tau}\right) d\tau, \quad (4.47)$$

where $H(\tau)$ is called the relaxation spectrum, representing the equivalent continuous distribution to the discrete distribution of the relaxation times τ_i in the Maxwell model. As noted by Gross (1953), this spectrum function $H(\tau)$ must satisfy the following condition:

$$\int_0^{\infty} H(\tau) d\tau = 1, \quad (4.48)$$

which corroborates $H(\tau)$ to be a statistical distribution function.

Note that the spectral approach avoids the non-practical situation of dealing with an high number of parameters in the mechanical models and suggest working with the distribution of the relaxation or retardation times instead. For a more comprehensive discussion of the spectral approach, the reader is referred to reference works, such as Christensen (1982), Tschoegl (1989), Ferry (1980), Emri and Tschoegl (1995) and Emri et al. (2005), among others.

4.4 Interconversion among the Linear Viscoelastic Functions

All the viscoelastic functions previously presented are mathematically interrelated, from relaxation to creep or viceversa, for both static and dynamic cases. In fact, from just an equation defining the relaxation modulus like Eq. (4.25), it is possible to derive analytically the relation to any of the remaining viscoelastic functions. Accordingly, a viscoelastic material could theoretically be

characterized from just one experiment. For this reason, great efforts have been devoted to establishing a unified and general theory of the linear viscoelasticity based on those relationships (see Gross (1953), Schwarzl and Struik (1967), Ferry (1980), Tschoegl (1989), Park and Schapery (1999a), Park and Schapery (1999b), Gross (1953), Christensen (1982), Renardy et al. (1987) and Fabrizio and Morro (1992)). There are mainly three reasons that justify the interest on the interconversion among these viscoelastic functions (see Ferry (1980) and Tschoegl (1989)):

- (a) *From the viscoelastic character.* The viscoelastic behaviour has been traditionally comprehended in a dual manner according to its two manifestations, related to relaxation and creep phenomena. As a consequence, the viscoelastic characterization comprises the definition of different viscoelastic functions depending on the selected experimental procedure, as shown in Table 4.1. Therefore, the necessity of the interrelations among all of these viscoelastic functions arise directly from the intrinsic duality of the viscoelastic behavior.
- (b) *From the experimental viewpoint.* Two arguments can be adduced in this case. Firstly, the experimental procedures in viscoelastic characterization programs are necessarily applied during limited ranges of time and frequency for practical reasons, while the study of both relaxation and creep phenomena should be extended over many decades, which is not practically affordable. For this reason, the combination of suitable measurements during short intervals allows these experimental ranges to be extended for covering the viscoelastic behavior entirely. As will be shown in Chapter 6, this experimental strategy consists basically in performing tests at different temperatures and then transforming these results by interconversion. Secondly, the interconversion is also of interest when dealing with the characterization of viscoelastic properties under a particular condition in which direct measurement is not be feasible. On the contrary, testing under some other accesible conditions permits subsequent interconversion to the desired conditions.
- (c) *From the mathematical viewpoint.* Since the dynamic relaxation and compliance moduli are defined in the complex space, the possible interrelation between real and imaginary parts, i.e. between storage and loss functions, arise in a natural manner. From a mathematical perspective, the derivation of a general theory of linear viscoelasticity is pursued according to an integrated version.

These interrelations can be classified into exact or approximate ones depending on their mathematical derivation. According to Table 4.1, there are twelve different moduli depending on the type of the applied load (axial, shear or bulk), the type of test (stress relaxation or creep) and the load character (static or dynamic). As mentioned at the beginning of this chapter, the foregoing interconversions are presented in terms of shear deformation, though they are applicable to the remaining cases (uniaxial, bulk, etc.).

4.4.1 Exact interconversions

The exact interrelations are derived analytically from pure mathematical considerations and summarized in the following sequence. Firstly, the interrelation between relaxation modulus and creep compliance within the same space, i.e. real $G(t) \leftrightarrow J(t)$ or complex $G^*(t) \leftrightarrow J^*(t)$. Secondly, the interrelation between the relaxation and retardation spectra $L(\tau) \leftrightarrow H(\tau)$ and, finally, the interconversion between the moduli within time and frequency for both relaxation $G(t) \leftrightarrow G^*(\omega)$ and creep $J(t) \leftrightarrow J^*(\omega)$ cases.

Relaxation and creep responses

The relaxation modulus and creep compliance under shear deformation $G(t)$ and $J(t)$ are not directly the inverse of each other, as it could be expected from Eqs. (4.3) and (4.4), since they are functions not equally dependent with time. Thus, the unique possible relation between them is established by the following inequality:

$$G(t)J(t) \leq 1, \quad (4.49)$$

which is converted to equalities in the two asymptotic cases, namely, for $t \rightarrow 0$ and $t \rightarrow \infty$, that is,

$$\begin{cases} G(0)J(0) = 1, \\ G(\infty)J(\infty) = 1. \end{cases}$$

On the complex plane, the relationship between the complex modulus $G^*(\omega)$ and compliance $J^*(\omega)$ under shear deformation results simpler than its equivalent in the static case in Eq. (4.49):

$$J^*(\omega) = \frac{1}{E^*(\omega)}. \quad (4.50)$$

Nonetheless, the previous direct relation does not hold for the individual components, which are interconnected by the following relations:

$$\begin{aligned} J'(\omega) &= \frac{G'(\omega)}{G'(\omega)^2 + G''(\omega)^2}, & J''(\omega) &= \frac{G''(\omega)}{G'(\omega)^2 + G''(\omega)^2}, \\ G'(\omega) &= \frac{J'(\omega)}{J'(\omega)^2 + J''(\omega)^2}, & G''(\omega) &= \frac{J''(\omega)}{J'(\omega)^2 + J''(\omega)^2}. \end{aligned} \quad (4.51)$$

Spectral functions

The spectral functions $L(\tau)$ and $H(\tau)$ are also interrelated in such a way that if one of them is known, then the other can be directly calculated, once the limiting values G_∞ , J_∞ , and η_0 are known. The relations two-by-two are defined

as follows:

$$L(\tau) = \frac{H(\tau)}{\left[G_\infty - \int_{-\infty}^{\infty} \frac{H(u)}{\tau/u - 1} d \ln u \right]^2 + \pi^2 H(\tau)^2}, \quad (4.52)$$

$$H(\tau) = \frac{L(\tau)}{\left[J_\infty - \int_{-\infty}^{\infty} \frac{L(u)}{1 - \tau/u} d \ln u - \frac{\tau}{\eta_0} \right]^2 + \pi^2 L(\tau)^2}. \quad (4.53)$$

Despite previous relations, it is well known from the literature that both spectra provide different information about the viscoelastic behavior, being recommended to deal with both spectra and avoid working with the previous interrelations (see Nowick (1972) and Ferry (1980)).

Time- and frequency-dependent response functions

The storage $G'(\omega)$ and loss modulus $G''(\omega)$ can be obtained directly from the relaxation modulus $G(t)$ using the Fourier transform:

$$G'(\omega) = G_\infty + \omega \int_0^\infty [G(t) - G_\infty] \sin \omega t dt, \quad (4.54)$$

$$G''(\omega) = \omega \int_0^\infty [G(t) - G_\infty] \cos \omega t dt. \quad (4.55)$$

Equivalently, the inverse relation from the components of the dynamic modulus $G'(\omega), G''(\omega)$ to static ones $G(t)$ is given by,

$$G(t) = G_\infty + \frac{2}{\pi} \int_0^\infty \left(\frac{G'(\omega) - G_\infty}{\omega} \right) \sin \omega t d\omega, \quad (4.56)$$

$$G(t) = \omega \int_0^\infty \left(\frac{G''(\omega)}{\omega} \right) \cos \omega t d\omega. \quad (4.57)$$

4.4.2 Approximate interconversions

As an alternative to the exact interconversion previously introduced, the approximate version is justified since the former shows different practical limitations. For example, the knowledge of the viscoelastic functions are experimentally limited to a certain range and the convergence of the integrals with infinite intervals can not be ensured, besides being a laborious task the calculations of such integrals. Nevertheless, since the interconversion approach is out of the topic of this work and for the sake of brevity, the reader is referred to reference surveys and treatises, such as Schwarzl and Struik (1967), Nowick (1972), Ferry (1980), Tschoegl (1989), Park and Schapery (1999a), Park and Schapery (1999b) and Lakes (2009) for further details about the numerical methods employed.

Statistical Approaches to Viscoelasticity

5.1 Introduction

Chapter 4 provides a comprehensive introduction of the most established models for describing the viscoelastic properties proposed during the last decades based on pure mathematical approaches, such as the classical models, differential and integral representations and their improvements. In addition, an alternative approach is also developed focused on the physical and chemical properties and structures of the viscoelastic solids from a statistical point of view (see Rouse (1953) and Zimm (1956), DeVault and McLennan (1965), Bavaud (1987), Abe et al. (2000) and Kawakatsu (2004)). Its promotion is favored by the expansion of polymer physics and chemistry in the last decades for industrial applications. Nevertheless, this set of models is found to be excessively sophisticated for describing simple relaxation and creep processes in practical applications, since they require a high number of parameters and variables, being usually applied only with research purposes.

As a possible solution to viscoelastic characterization, the proposed alternative approaches outlined and discussed in this chapter are based on a phenomenological formulation and probabilistic interpretation of the viscoelastic behaviour of materials. These models are based on solid physical and statistical conditions that result from the objective observation of the viscoelastic behavior and depend on a reduced number of parameters. In particular, the use of the normal distribution to model the creep process, and its possible extension to the re-

laxation case, is justified by the denoted central limit approach. Additionally, the experimental campaigns are subject to some limitations concerning the test duration, which can be overcome based on consideration of the statistical extreme value theory, which allows the viscoelastic properties to be registered over short-time tests and thereafter to be extrapolated up to large time periods. As an interesting extension of these approaches, the Bayesian techniques can be applied to derive probabilistic models able to consider the inherent scatter of the viscoelastic properties and their time evolution as a stochastic process.

To this aim, this chapter is devoted to broaden the discussion about the feasible statistical approaches dealing with the viscoelastic characterization problem and to present the basis of the solutions proposed in this thesis. The applicability of the phenomenological-statistical approach developed is illustrated in Chapter 6 using experimental data concerned with the temperature effect. The approach proves to be useful for dealing conveniently with relevant external effects taking advantage of the properties of the statistical distributions. In fact, due to the long-term behaviour of the viscoelastic properties along the time, the experimental procedures are usually performed, as mentioned above, based on short-term tests at different temperatures or pressures from which the master curve of the material is derived covering entirely the time range.

The chapter is organized in two main parts. Firstly, Section 8.2 presents a short description of the two main groups of viscoelastic models proposed in the literature founded on a statistical approach. Secondly, the statistical basis of the proposed methodology for viscoelastic characterization as proposed in this thesis is outlined in Section 8.3, where three different statistical approaches are considered, namely, the central limit, the extreme value and the Bayesian ones.

5.2 Previous Statistical Approaches

The models proposed in the literature for characterizing the viscoelastic behaviour of materials based on statistical approaches can be classified in two main groups:

1. *Physical or chemical models.* The simplest model is the so-called freely jointed chain, focused on the molecular level of the viscoelastic solids. It contemplates a polymer as a chain with a certain number of segments, each of them being free of to adopt any arbitrary orientation without constraints, according with a Brownian movement (see Lin et al. (2011)). Other examples of acknowledged physical and chemical models are those due to Rouse (1953) and Zimm (1956), DeVault and McLennan (1965), Bavaud (1987), Abe et al. (2000) and Kawakatsu (2004). Among them, one of the most celebrated is the Rouse model, defining the relaxation modulus G with time as follows:

$$G(t) = \frac{\rho_{\text{num}}}{N} k_B T \sum_{p=1}^{\infty} \exp\left(-\frac{t}{\lambda_p}\right), \quad (5.1)$$

where ρ_{num} represents the concentration of segments in the molecular structure, N the number of segments per molecular chain, k_B the Boltzmann's constant, T the temperature and λ_p the relaxation time related to the rotation of the p -chain. Note that this kind of models deal with an increasing number of parameters of difficult physical measurement. An extensive review of this research topic can be found in Riande et al. (1999) and Lin (2010).

2. *Phenomenological models.* Due to the complexity of the physical and chemical models, an extended version of the classic ones, as described in Chapter 4, has been developed though reformulated under a statistical approach. These models are denoted phenomenological models in contrast with previous physical and chemical ones (see Frigg and Hartmann (2017) and Cho (2016)). Some examples of these models are the enhanced Maxwell and Kelvin ones whose parameters are estimated with the so-called Bayesian Inference method (see Rappel et al. (2018) and Rappel et al. (2019)).

It is also worth mentioning that the application of these previous statistical approaches to viscoelastic modeling is not only focused on considering the viscoelastic properties as such, but also to observe the effect of relevant external variables, such as the temperature or pressure using Bayesian techniques (see Haario et al. (2014) and Hernández et al. (2017)) or applying neural networks (see Aulova et al. (2016)).

Nevertheless, care must be taken when denoting these models statistical ones, since the viscoelastic properties are defined in a deterministic form. Accordingly, any of these models is, strictly speaking, probabilistic since the probability $F(G_A) = \Pr(G(t) \leq G_A)$ is not defined, for given values of the modulus G_A . In fact, these models make use of statistical functions just to provide the analytical expression of the viscoelastic properties along the time. This is also the case for the proposed models in this work when resorting to both the central limit and the extreme value approaches. In turn, the Bayesian approach constitutes one of the major contributions of this thesis, allowing some interesting probabilistic viscoelastic models to be derived to evidence the inherent scatter of the viscoelastic properties, as will be shown in this chapter.

5.3 The Proposed Statistical Approaches

As mentioned above, current statistical approaches are usually found to be excessively complicated for describing simple viscoelastic behaviour in practical applications, thus being relegated only for research purposes. On the contrary, the proposed methodology outlined in this section provides mathematical models with a reduced number of variables and parameters, based only on rigorous statistical and physical conditions in its three different versions, namely, the central limit, the extreme value and the Bayesian approaches.

As a first step in the derivation of mathematical models for the analysis of

the viscoelastic phenomenon, two main characteristic features are considered to build the proposed methodology:

1. *Normalization.* Since the time evolution of the viscoelastic properties are twofold bounded between the limiting values G_0 and G_∞ , the quotient

$$\frac{\log G - \log G_\infty}{\log G_0 - \log G_\infty} \in [0, 1], \quad (5.2)$$

referred to as the normalization representation (see Chapter 4), is recommended. Note that this normalization arises as the natural way to follow the decreasing fraction of the viscoelastic modulus $G(t)$ with respect to the limiting values G_0 and G_∞ . Unfortunately, this notation is adopted only in few reference textbooks of viscoelasticity (see for example Tschoegl (1989) and Povolo and Hermida (1993)). In Chapter 6 an additional justification is exposed for this redefinition based on the dimensional analysis of the viscoelastic problem when the temperature effect is implied.

2. *Monotonically decreasing function.* Both relaxation moduli under uniaxial and shear deformations, denoted as E and G respectively (see Table 4.1), prove to be monotonically decreasing on time, as previously indicated in Eq. (4.8) (see Mainardi (2010, 2018)).

According with both properties in Eqs. (4.8) and (5.2), the relaxation function can be identified with the survival function $S(\cdot)$ of the cumulative distribution function (cdf) $F(x)$, satisfying the conditions $S(-\infty) = 1$ and $S(\infty) = 0$, such that $S(x) = 1 - F(x) = \Pr(X > x)$ is given as:

$$\frac{\log G - \log G_\infty}{\log G_0 - \log G_\infty} = S(\log t; \theta), \quad (5.3)$$

where θ is the vector of parameters. Note that Eq. (5.3) is not restrictive since any monotonically increasing function bounded in the interval $[0, 1]$ is by definition a cdf (see Loeve (1977), Galambos (1984), Galambos (1995) and Castillo and Pruneda (2001)). As a result, the statistical approaches proposed in this thesis to model the continuum physical phenomenon representing the time evolution of the viscoelastic behaviour are based on the analytical expression of a certain survival of a cdf. The methodology was applied by Castillo et al. (2014b) to model the crack growth rate curve $da/dN - \Delta K$. It is noteworthy that these approaches do not pursue to find suitable functions, which merely feet the sigmoidal viscoelastic behaviour over time, but rather mainly try to reproduce the probabilistic basis underlying the relaxation phenomenon, as will be shown in the following subsections.

Once the physical properties of the relaxation phenomenon are identified, a suitable cumulative distribution, fulfilling the statistical interpretation of the phenomenon, is substituted for $S(\cdot)$ in Eq. (5.3), as indicated in Section 2.3 when presenting the general methodology. The main objective is to avoid arbitrary assumptions in the selection of these statistical distributions. To this end, three

statistical-based approaches are proposed in the following sections representing different mathematical solutions for describing the relaxation modulus.

5.3.1 The central limit approach

In the first statistical approach, the phenomenological relations are derived from the analysis of a typical creep test justifying the use of the normal distribution as the suitable one to describe the time evolution of the normalized relaxation modulus. Although the model was specifically developed from the creep test due to clearness and concreteness reasons, its extension to the corresponding relaxation case is straightforward according to the theory of Viscoelasticity.

In a creep test, the viscoelastic specimen of length L , supposedly divided into n sub-elements, is subject to a constant uniaxial stress σ , as shown in Figure 5.1, so that the resulting strain is time-dependent $\varepsilon_T(t)$. According to the strain definition, the total displacement $\delta_T(t)$, also being a function of time, is defined as follows:

$$\delta_T(t) = \varepsilon_T(t)L = \frac{\sigma L}{E_T(t)}, \quad (5.4)$$

where $E_T(t)$ is the global or equivalent uniaxial relaxation modulus of the whole specimen. As a result, the total creep strain of the whole specimen is obtained as the accumulation of the random strain provided by each of the subelements into which the specimen is virtually subdivided (see Álvarez-Vázquez et al. (2020a)).

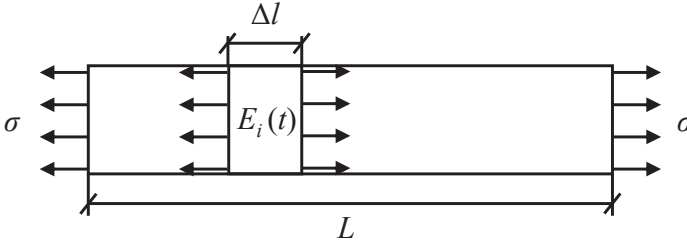


Figure 5.1: Schematic illustration of a creep test: specimen of length L subdivided in n elements of equal length Δl , all of them subjected to a constant stress σ .

Thus, the total elongation of the specimen can be calculated as the summation of the local random elongations of each of the n sub-elements, so that Eq. (5.4) can be rewritten as follows:

$$\delta(t) = \frac{\sigma L}{n} \left(\frac{1}{E_1(t)} + \frac{1}{E_2(t)} + \dots + \frac{1}{E_n(t)} \right) = \frac{\sigma L}{n} \sum_{i=1}^n \frac{1}{E_i(t)}, \quad (5.5)$$

from which the relation between the total relaxation modulus E_T and the contribution from each i -th sub-element E_i is obtained by combining Eqs. (5.4) and

(5.5), such that

$$\frac{1}{E_T(t)} = \frac{1}{E_1(t)} + \dots + \frac{1}{E_i(t)} + \dots + \frac{1}{E_n(t)} \quad (1 \leq i \leq n). \quad (5.6)$$

Then, denoting $H_i(t) = 1/E_i(t)$, Eq. (5.6) is converted into a direct summation to which the central limit theorem can be applied by considering that the inverse of the equivalent viscoelastic modulus $H_T(t) = E_T(t)^{-1}$ tends asymptotically to the normal distribution for $n \rightarrow \infty$ irrespective of the statistical distribution to which these random terms may belong. In other words, the inverse of the relaxation modulus over time of a viscoelastic specimen is assumed to follow a normal distribution in Eq. (5.3), that is,

$$\frac{\log E_0 - \log E_\infty}{\log E_T(t) - \log E_\infty} \sim 1 - N(\mu, \sigma^2), \quad (5.7)$$

with finite parameters μ and σ . This remarkable result is derived directly from the discrete viscoelastic behaviour of the n subelements without requiring any additional assumption about the statistical distribution characterizing the viscoelastic behaviour of the subelements. Note also that previous phenomenological argument establishes a novel probabilistic basis underlying the relaxation phenomenon as intrinsically related to the normal distribution according to the central limit theorem.

5.3.2 The extreme value approach

The use of the extreme value approach, complementary to the central limit approach, is based on the statistical properties of the extreme value family of distributions presented in Section 3.5. Two main considerations justify their application to the problem of viscoelastic characterization:

- *From an experimental viewpoint.* The experimental campaigns with viscoelastic materials are usually limited to the record of a certain data interval (between t_{inf} and t_{sup} in Figure 5.2), since the evolution of the viscoelastic phenomenon extends theoretically during infinite time, or at least over many decades, which is practically unaffordable. For this reason, the existence of suitable mathematical methods to extrapolate the recorded data beyond the limits of the experimental window is crucial, particularly to estimate the limiting values G_0 and G_∞ because of their practical importance. These limiting values correspond with minimal and maximal time values, so that the necessity of resort to extreme value distributions arise in a natural manner. As mentioned in Section 3.5, any statistical distribution belongs to the domain of attraction of one of the extreme value distributions, either Weibull, Gumbel or Fréchet. Therefore, whatever it is the statistical distribution selected for modelling the relaxation or creep phenomena in Eq. (5.3), the extrapolation to the asymptotic distribution tails, i.e. $t \rightarrow 0$ and $t \rightarrow \infty$ will be more reliably achieved if the corresponding extreme value

distribution is selected instead. Since the relaxation and creep phenomena are left-bounded and right unbounded in natural scale (but unbounded on both sides in logarithmic scale), only the minimum Weibull and maximum Fréchet distributions are the only ones eligible for determining the limiting value for $t \rightarrow 0$ in the first case, while the Gumbel is the only one which applies in the second case.

- *From a phenomenological viewpoint.* In the previous subsection it is demonstrated that there are phenomenological reasons to assume relaxation or creep phenomena to follow a normal distribution. Nevertheless, two questions suggest the use of the extreme value family of distributions, particularly the Gumbel one, instead of the normal distribution (see Galambos (1978), Castillo (1988) and Castillo et al. (2004a)). First, the data set of the relaxation or creep function, recorded between t_{\min} and t_{\max} must be extrapolated to define the distribution tails for both limiting cases $t \rightarrow 0$ and $t \rightarrow \infty$ (see Figure 5.2)), and second, those extrapolations can be achieved in a more reliable and advantageous way at both lower and higher tails of the cdf representing the relaxation or creep functions using the Gumbel distribution, as the domain of attraction of the normal distribution in both cases of minimum and maximum values.

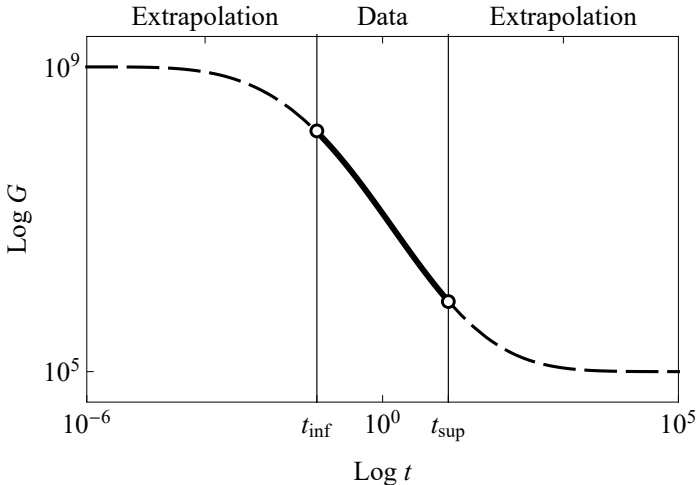


Figure 5.2: Illustration of the extrapolation of the relaxation modulus over time to the limiting values for $t \rightarrow 0$ and $t \rightarrow \infty$ from the double-bounded experimental window.

For these reasons the extreme value approach arises as the natural tool to give support in the derivation of the viscoelastic characterization. Nevertheless, the extreme value family of distributions has been systematically ignored in the development of mathematical models in the viscoelastic analysis, despite being the suitable distributions to deal events presenting maximal or minimal character.

An illustrative comparison among the extrapolation solutions for the creep compliance J_∞ is presented in Figure 5.3 involving the central limit and the extreme value approaches (GEV). Despite being quite different, the right tail is the same for all of them. Thus, the extreme value family of distributions must be used instead, being more supported theoretically with more reliable predictions (see Castillo (1988)). A similar reasoning can be applied when considering conventional models, such as Maxwell, Prony series or Kohlrausch-Williams-Watts.

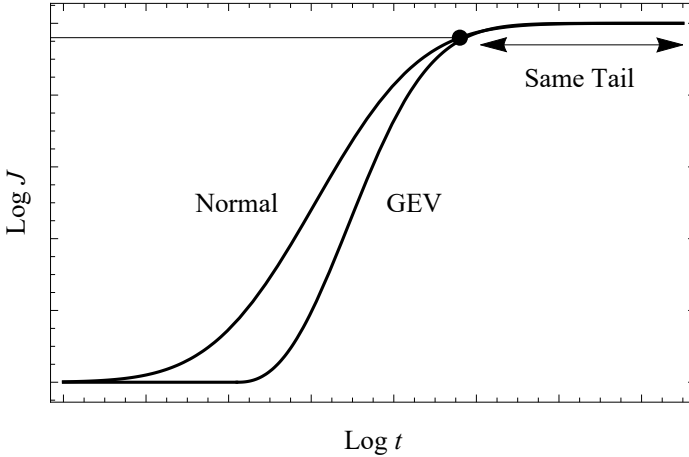


Figure 5.3: Schematic illustration of the Gumbel cdf as the domain of attraction of the normal distribution for the maxima case.

Finally, in order to illustrate the necessity of application of both limiting conditions related to practical situations in which limiting values of viscoelastic properties is critical, two different examples of typical problems in engineering design are suggested.

Example 5.1 (Ballistic impact on a viscoelastic component). A ballistic impact, as a sudden applied load case, represents an illustrative example in which the response of the viscoelastic material is related to the value of the short-term, practically instantaneous, of the compliance modulus, i.e. J_0 . Since the creep phenomenon over time is left-bounded, a Weibull distribution on a natural scale, or a Gumbel one in logarithmic scale, both for minima, are justified to determine the compliance modulus by extrapolation to $t \rightarrow 0$. Thus, the survival function $S(\cdot)$ in Eq. (5.3) must be stable with respect to the formation of the minimum value, that is,

$$[S(\log t)]^n \sim 1 - q_{\min}(\log t), \quad (5.8)$$

where $S(\cdot)$ must belong to a distribution for minimum value $1 - q_{\min}(\cdot)$. In the case of Gumbel, the following expressions result:

$$q_{\min}(\log t) = 1 - \exp[-\exp[\log t]]. \quad (5.9)$$

Note the practical implications of the previous result, since even if different designers may possibly proposed different statistical distributions for $S(\cdot)$, all of them must belong to the domain of attraction of minimum Weibull or Gumbel according on the scale selected. \square

Example 5.2 (Snow load over a glass structural component). Let us consider the structural design against creep fracture due to a snow load over a glass structural component in a roof. The response of the viscoelastic material is related to the value of the long-term, requiring the extrapolation of the cdf to the limiting value of creep compliance at the right tail, i.e. J_∞ . Then, since the creep compliance over time is right-unbounded both in natural and logarithmic scales of time, Gumbel distribution on a natural scale, or a Gumbel one in logarithmic scale, both for maxima, are justified to determine the compliance modulus by extrapolation to $t \rightarrow \infty$. Thus, the survival function $S(\cdot)$ in Eq. (5.3) must be stable with respect to the formation of the maxima, such that,

$$1 - [S(\log t)]^n \sim 1 - q_{\max}(\log t), \quad (5.10)$$

where $S(\cdot)$ must belong to a distribution for maxima value $1 - q_{\max}(\cdot)$. In the case of Gumbel, the following expressions result:

$$q_{\max}(\log t) = \exp[-\exp[-\log t]], \quad (5.11)$$

from where it follows that only previous distributions must be considered in the extrapolation to the maximal values of the time. \square

5.3.3 The Bayesian approach

As mentioned above, the approaches based on statistical functions developed in the literature, the same as those based on both central limit and extreme value ones, are not really probabilistic approaches in a strict sense, since the viscoelastic properties are based on deterministic premises. However, deterministic definitions of the properties of real materials is insufficient to guarantee safe service and failure conditions in practical design due to their inherent scatter. When one relaxation test is replicated over a certain experimental window, the resulting curves of the relaxation modulus for each test, and particularly the limiting values G_0 and G_∞ , are expected to be different (see Figure 5.4), revealing that the evolution of the viscoelastic behaviour over time represents a stochastic process. For this reason, probabilistic models must be preferred to deterministic ones, as providing more valuable information to the engineering designer.

The Bayesian theory to be applied is concerned with the mathematical definition of the multivariate probability distribution of the viscoelastic property for a given time in the form of $\Pr(\log G \leq \log G_A; \log t)$, for some value G_A . As a result, the predictions of the viscoelastic properties for a given time will be given as a distribution instead of a single value. In the previous example of design against creep fracture related to the prediction of G_∞ (see Example 5.2), the

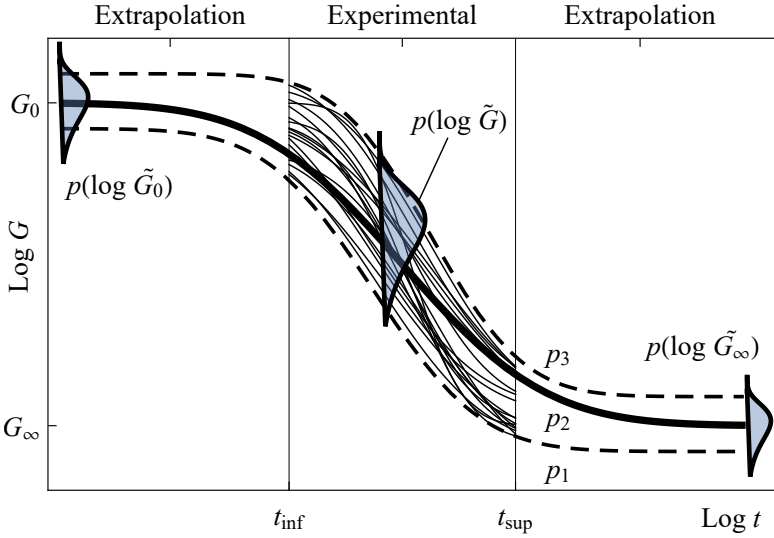


Figure 5.4: Schematic illustration of the variability field of the relaxation modulus G over time, due to the scatter of the participating model parameters.

engineering designer can now relate the design to a given probability.

To this end, the Bayesian techniques consist in assuming the parameters of a previous deterministic model as random variables as well, such that the resulting model is converted into a probabilistic one. Thus, the previous central limit and extreme value approaches may now be enhanced by the Bayesian technique. Denoting θ_{mean} and θ_{extreme} the corresponding vector parameters of the parametric family of two the former models, i.e. $S(\log t; \theta_{\text{mean}})$ and $S(\log t; \theta_{\text{extreme}})$ in Eq. (5.3) respectively, the steps implied in the Bayesian approach are the following:

1. *Prior distributions.* The prior distributions of the parameters of previous models θ_{mean} and θ_{extreme} are initially assumed based on the knowledge of the phenomenon under study, being defined as follows:

$$\theta_{\text{mean}} \sim p(\theta_{\text{mean}} | \alpha_{\text{mean}}), \quad (5.12)$$

$$\theta_{\text{extreme}} \sim p(\theta_{\text{extreme}} | \alpha_{\text{extreme}}), \quad (5.13)$$

with α_{mean} and α_{extreme} as the so-called hyperparameters for the mean and extreme value models, respectively.

2. *Prior predictive distribution.* Based on the description of the model and the prior distributions of the parameters in Eqs. (5.12) or (5.13), a first predictive value for the viscoelastic modulus \tilde{G} is defined with the prior

predictive distribution as follows:

$$p(\log \tilde{G} | \log t, \theta_j, \alpha_j) = \int_{\theta_j} p(\log G | \log t, \theta_j) p(\theta_j | \alpha_j) d\theta_j, \quad (5.14)$$

where θ_j and α_j represent the vectors of parameters and hyperparameters $\theta_{\text{mean}}, \theta_{\text{extreme}}$ and $\alpha_{\text{mean}}, \alpha_{\text{extreme}}$, respectively.

3. *Marginal likelihood.* The experimental values of viscoelastic modulus and time are now used for enhancing the knowledge about the parameters by using the maximum likelihood method,

$$p(\log G | \theta_j, \log t) \equiv L(\log G | \theta_j, \log t), \quad (5.15)$$

4. *Posterior distribution.* As the result of the combination of knowledge about the parameters from prior in Eqs. (5.12) or (5.13) and from the likelihood with the experimental data in Eq. (5.15), the prior posterior distribution of the parameters θ_j is determined by applying the Bayes theorem as follows:

$$p(\theta_j | \log G, \log t) = \frac{p(\log G | \theta_j, \log t) p(\theta_j | \log t)}{p(\log G | \log t)}. \quad (5.16)$$

5. *Posterior predictive distribution.* Finally, the posterior predictive distribution can be obtained by means of the posterior distribution in Eq. (5.16), by collecting the prior information and the experimental evidence in the posterior distribution, such that the predictions of the viscoelastic modulus \tilde{G} are given by:

$$p(\log \tilde{G} | \log G)_j = \int_{\theta_j} p(\log \tilde{G} | \theta_j) p(\theta_j | \log G, \log t) d\theta_j. \quad (5.17)$$

where j refers to the central limit or extreme value approaches. Note the probabilistic definition of the predicted viscoelastic modulus in the form of $p(\log \tilde{G})$.

Despite the demanding statistical concepts involved in the previous Bayesian formulation, the recent development of the software OpenBUGS, within the WinBUGS project due to Lunn et al. (2000), allows these calculations to be advantageously performed and they to be straightforwardly applied to more advanced and complex problems.

In summary, by applying the Bayesian theory to either the central limit or the extreme value approaches, the evolution of the viscoelastic property over time are defined statistically as a family of cdfs, in which the involved parameters, i.e. the initial and final relaxation moduli and the parameters of the assumed cumulative distribution are defined as statistical distributions and not as simple parameter estimates. In this way, the $G(t; T)$ at any time and temperature may be determined in a statistically consistent way.

5.4 Concluding Remarks

The statistical approaches developed during the last decades to define the behaviour of viscoelastic materials are relegated merely to research purposes due to their complexity and cumbersome applicability in practical design. In this chapter two novel approaches based on statistical functions, fulfilling some transcendental physical and statistical conditions, are presented and their suitability discussed providing mathematical models with a reduced number of parameters.

Initially, the central limit theorem demonstrates the theoretical suitability of the normal cdf for modelling the relaxation modulus over time in the creep test but, finally, the statistical extreme value theory justifies the adoption of the Gumbel cdf instead. This is due to the practical conditions in the experimental program, which imply censored record of data followed by unavoidable extrapolation to both limiting cases $t \rightarrow 0$ and $t \rightarrow \infty$ based on the Gumbel distribution as representing the domain of attraction of the normal distribution.

Finally, an approach based on Bayesian technique, applied to the two mentioned novel solutions is proposed, as the only one, which allows the viscoelastic characterization to be derived under a consequently probabilistic concept.

6

Temperature Effect

6.1 Introduction

The temperature effect plays a decisive role in viscoelastic characterization. It is a supplementary, influencing parameter which must be considered in the experimental planning and in the parameter assessment. In addition, an intelligent test strategy can be incorporated to collect information that allows a more robust assessment of the viscoelastic model. As mentioned in Chapter 4, theoretically the viscoelastic properties evolve indefinitely, from the initial modulus or compliance G_0 to the final value G_∞ along the master curve of the material. Accordingly, the experimental record should be extended over several decades. Nevertheless, time and cost restrictions usually limit the experimental campaign to a more pragmatic time period, while the extrapolation to the rest of the master curve must be handled with a suitable mathematical model.

One of the best-known methodologies to derive the master curve is the Time-Temperature Superposition (TTS) principle, originally developed by Leaderman (1942), Tobolsky and Andrews (1945) and Ferry (1950), in independent studies. This methodology involves testing at various temperatures in a limited time interval followed by a horizontal translation of the resulting short-term curves based on a presumable equivalency between time and temperature variables. However, this mathematical transformation of a parametric family of curves must fulfil certain requirements with respect to temperature effect if a valid model is to be achieved. This fact is unfortunately ignored in the development of most

models in the literature.

Nowadays, most of the proposed models are based on this horizontal shifting property, according to the TTS principle. However, other possible properties for establishing these mathematical transformations should also be explored to improve the current theoretical background. In addition, the current methodologies concerning the temperature effect define the viscoelastic properties in a deterministic manner, which is inappropriate, as explained in Chapter 5. Alternative methodologies based on statistical functions may be suggested allowing a straightforward improvement to be achieved by application of Bayesian techniques.

Accordingly, the objective of this chapter is fourfold:

1. *Definition of the mandatory conditions for TTS models to be valid.* The development of mathematical models for considering the temperature effect are traditionally based on the transformation from short-term curves at various temperatures to one master curve at a reference temperature. As a result, certain mandatory conditions must be met to guarantee valid mathematical transformations in these models.
2. *Improvement of the current TTS principle-based models.* The current TTS principle-based models in literature are built on what is known as the shifting property. However, this empirical principle can be understood in a different manner by means of the scale-effect property proposed in this thesis, enhancing and broadening the current TTS principle-based models.
3. *Development of the TTS non-principle-based models.* As an alternative to those models based on the TTS principle, built using the shifting property or any other property, a different approach for building the master curve of the material can be derived based on a condition instead of a property. This thesis proposes the application of the statistical compatibility condition.
4. *Development of probabilistic models.* As indicated in Chapter 5, the viscoelastic properties of current models are generally assumed to be deterministic although the variables involved are inherently random as proved when a relaxation or creep test is replicated. To solve this question, different probabilistic models related to the temperature effect are presented.

Figure 6.1 illustrates a general scheme of the proposed models dealing with the temperature effect on viscoelastic behaviour. The novel proposals of this thesis are shown in gray. The approaches proposed in this work are based on the statistical functions to model the viscoelastic behaviour outlined in Chapter 5, which are now extended to take the temperature effect into account. In other words, the mathematical models proposed in this chapter are based on different properties and conditions for dealing with time- and temperature-dependent transformations. Three different statistical approaches are considered to specify the statistical distribution to be considered in each case. Two different models, the normal and Gumbel models, are proposed to take into account the scale-effect

property. The models depend on the statistical approach, that is, based on the central limit and the extreme value ones (see Figure 6.1). Note the vital importance of a suitable distinction between the elements constituting a mathematical model, as defined in Chapter 2, such as in this case between the identification of the properties and conditions together with the characterization of the statistical distribution.

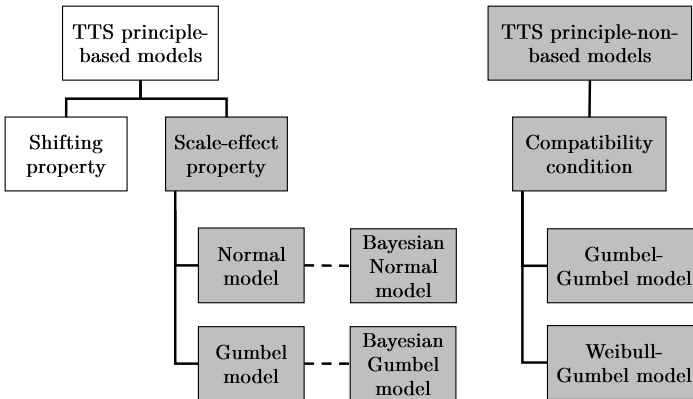


Figure 6.1: General flow chart of the current conventional and proposed models (in grey) for determining the temperature effect on the viscoelastic properties.

To this end, the organization of this chapter is as follows. Firstly, some basic concepts and considerations related to the TTS principle and the current methodologies for viscoelastic characterization concerning the temperature effect are presented in Section 6.2. Secondly, mandatory conditions to establish valid time- and temperature-dependent transformations are identified in Section 6.3. Then, different proposed models are classified in three groups: a) TTS principle-based models (Section 6.4), b) TTS non-principle-based models (Section 6.5) and c) probabilistic models (Section 6.6). Finally, a practical example to illustrate how these models can be used in practice is proposed in Section 6.7.

Before going on, it should be noted that pressure has an alternative or additional effect to that of temperature when analyzing long-term viscoelastic characterization. Some researchers prefer it as the focus of their study, although the mathematical formulation is in all aspects analogous to that of temperature.

6.2 Current Methodologies

This section presents a brief review of the current methodologies for viscoelastic characterization, based on the transformation of experimental data at different temperatures to build the master curve of the material according to the TTS principle. This material draws heavily on different reference textbooks, such as

Schwarzl and Staverman (1952), Findley et al. (1976), Ferry (1980), Christensen (1982), Tschoegl (1989), Tschoegl et al. (2002), Lakes (2009), Gutierrez-Lemini (2014), Brinson (2015), and Cho (2016), among others.

In those models, the evolution over time of the relaxation modulus in axial deformation $E(t)$ for n different temperatures T_0, \dots, T_n , is considered, that is $E(t; T_i)$ where $0 \leq i \leq n$. The aim is to obtain the master curve of the material over time at a reference temperature, T_0 , as shown in Figure 6.2. The TTS principle states that the relation between any of these functions $E(t; T_i)$ and the reference master curve, $E(t; T_0)$, is given by:

$$E(\log t; T_0) = E(\log t + \log a_T(T_0, T_i); T_i), \quad (6.1)$$

where $a_T(T_0, T_i)$ is known as the shift factor of the i -th temperature to the reference T_0 . In other words, the TTS principle assumes that the temperature effect is equivalent to a time evolution, such that the master curve can be obtained by testing at different temperatures and transforming the results after establishing a certain equivalence between the time and temperature variables. More precisely, the viscoelastic modulus corresponding to the larger time values are obtained from the test results at lower temperatures, while those corresponding to the shorter time values are obtained from the test results at higher temperatures, as shown in Figure 6.2. From a mathematical point of view, the TTS principle in Eq. (6.1) is based on a horizontal shifting from the short-term curves at different temperatures to the master curve by applying $\Delta \log t = \log a_T(T_0, T_i)$, in logarithmic scale, as a function of the origin and final points of the transformation.

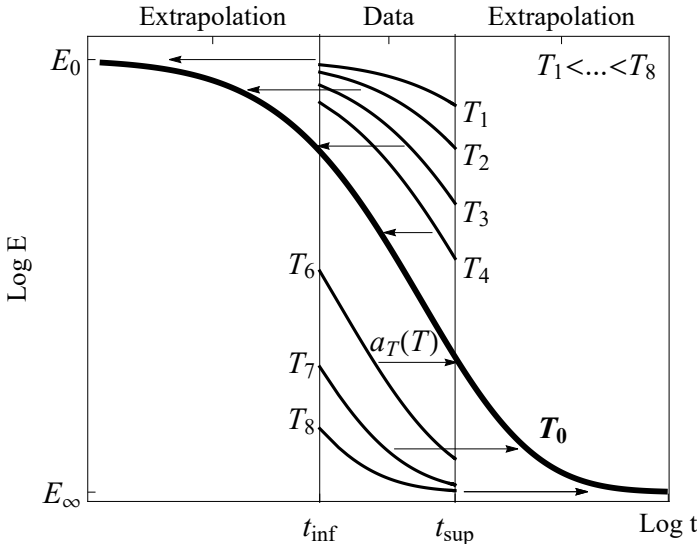


Figure 6.2: Scheme of the TTS principle for deriving the master curve at a reference temperature T_0 from short-time test records at different temperatures.

This empirical principle was due to authors such as Ferry (1950), Tobolsky and McLoughlin (1952) and Leaderman et al. (1954) and was successfully applied to a large variety of viscoelastic materials, known as thermo-rheologically simple materials. Certainly, the models proposed in recent decades differ only in the analytical definition of the shift factor $a_T(T, T_0)$, but all of them assume the horizontal shifting property according to the classic interpretation of the TTS principle. An extensive review of these definitions of the shift factor a_T is found in Tschoegl et al. (2002). The best known of these proposals, the Williams-Landel-Ferry (WLF) model, was published by Williams et al. (1955), with the following experimental definition applicable to a broad range of viscoelastic materials:

$$\log a_T(T, T_0) = -\frac{C_1^0(T - T_0)}{C_2^0 + T - T_0}, \quad (6.2)$$

where C_1^0 and C_2^0 are constants, whose numerical values are only valid for the reference temperature T_0 , as indicated in their superscripts. This analytical definition allows the experimental shift factors to be defined from the manual shifting of the short-term curves to match the master curve. This represents the greatest drawback of the current methodologies based on the TTS principle, since the user's experience plays a decisive role in determining the final estimated master curve. Furthermore, the same experimental data could lead to different master curves depending on the particular author (see Knauss (2008) and Oseli et al. (2016)).

Fortunately, new algorithms have been developed aiming at objective approaches (see Zhao et al. (2007), Knauss (2008) and Maiti (2019)), as for instances those based on minimizing the sum of square errors in horizontal distances in the overlapping (see Honerkamp and Weese (1993) and Buttlar W.G. (1998)), matching first derivatives (see Hermida and Povoio (1994) and Naya et al. (2013)), minimizing areas in the overlapping regions between two adjacent curves (see Gergesova et al. (2011) and ISO 18437-6:2017 (2017)) or minimizing the arc-length of the master curve in the complex modulus space (see Cho (2009) and Bae et al. (2011)), or based on numerical improvements due to the application of neural networks applied (see Aulova et al. (2016)), Bayesian techniques (see Hernández et al. (2017)) and uncertainty quantification with statistical bootstrap method (see Maiti (2019)). Once the experimental master curve is obtained in this way, the classic models previously described in Chapter 4 can be used to define the master curves for any other reference temperature T_i by virtue of the shift factors.

Alternatively, the original horizontal shifting property in Eq. (6.1) can be reformulated to analytically define the vertical shift factor b_T . This shift factor can be applied to the short-term curves to define the viscoelastic modulus function as a function of temperature instead of the time (see Honerkamp and Weese (1993)), that is,

$$E(\log t; T) = E(\log t; T_0) + \log b_T(T, T_0). \quad (6.3)$$

Both procedures can be combined using the expression:

$$E(\log t; T) = E(\log t + \log a_T(T, T_0); T_0) + \log b_T(T, T_0). \quad (6.4)$$

Nevertheless, some limitations of these proposed models should be commented:

- (a) *Dimensionality of the models.* The variables and parameters involved in these proposals have dimensions and their numerical values are sensitive to the system of units selected. Though the formulation of scientific laws using non-dimensional variables is not compulsory, it is recommendable in order for the derived expressions to be universal and their functional definitions insensitive to the selected system of temperatures.
- (b) *Limited applicability in the temperature range.* The experimental shift factors a_T resulting from a typical horizontal shifting method usually show two different laws depending on whether the origin of the transformation is above or below the transition temperature of the material T_g , as shown in Figure 6.3. The classic proposed definitions of these factors are not able to capture this trend change and, consequently, the short-term curves into the master curve cannot be satisfactorily transformed with a single model, such as the WLF one. Thus, at least two different models are needed. For this reason, current practical methodologies require the combination of the Arrhenius model (see Eyring (1936)) with that of Williams et al. (1955). The former is applicable in the range $T_g \leq T < T_g + 50^\circ C$ and the latter for $T \leq T_g$. Figure 6.3 illustrates the typical experimental shift factors compounding a master curve and the required combination of these two models pointing out the intermediate intersection at T_g . Some authors extend the validity of the WLF model to $T_g + 50^\circ$ but as yet there is no agreement as to this limit.
- (c) *Temperature-dependent parameters.* Most of the models proposed in the literature include parameters, which depends on the temperature to which the master curve T_0 is referred, as is the case of C_1^0 and C_2^0 from the WLF model in Eq. (6.2). As a result, the parameter values are only valid when T_0 is the reference temperature for the transformation. A new estimation of these constants must be re-evaluated if that reference is changed. Indeed, these constants must be properly identified as functions $C_1(T_0)$ and $C_2(T_0)$ dependent on the temperature. This implies that in these models some functional interdependencies are arbitrarily included in the definition of the shift factor. Such additional relations, known as symmetry condition, are defined as follows if the reference temperature is changed from T_0 to some T_1 (see Williams et al. (1955)):

$$C_2^0 - T_0 = C_2^1 - T_1, \quad (6.5)$$

$$C_1^0 C_2^0 = C_1^1 C_2^1. \quad (6.6)$$

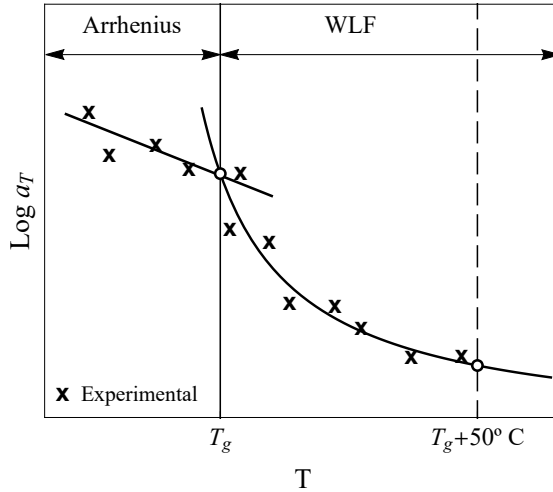


Figure 6.3: Typical experimental shift factors with theoretical validity limits according to the Arrhenius and Williams-Landel-Ferry models.

- (d) *Difficult measurement of the physical variables.* Some proposed models define the shift factor a_T as a function of certain thermodynamical variables, such as entropy in Bestul and Chang (1964) and Adam and Gibbs (1965) or enthalpy in Goldstein (1963). These variables are difficult to measure physically, as pointed out by Tschoegl et al. (2002). As a result, these models cannot be applied in practical cases, despite being based on rigorous thermodynamical and chemical principles.
- (e) *Lack of analytical definition of the vertical shift factor.* The proposed models based on the combination of both horizontal and vertical shifting factors in the form of Eq. (6.4) has improved the application of the TTS principle because more degrees of freedom are considered (see Honerkamp and Weese (1993)). In fact, the analytical definition of the vertical shift factor b_T is not compatible with that of a_T . As a result, the derivation of the master curves is limited only to those temperatures being tested.
- (f) *Overlapping requirement.* Current methodologies based on the application of the TTS principle require overlapping of the short-term curves over at least one decade in order to ensure suitable shifting of the master curve. This "rule of thumb" is applied by researchers, whatever the definition of the shift factor. This practical limitation forces the experimental campaign to be executed with care in order to ensure overlapping of the short-term curves.

For these reasons, the development of mathematical models related to the temperature effect on viscoelastic characterization problem must be based on rigorous conditions, deriving consistent models based on non-arbitrary assumptions.

6.3 Necessary Conditions for Valid Models

The identification of some mandatory conditions is necessary before the derivation of the alternative models proposed in this chapter.

6.3.1 Dimensional analysis

As indicated in Chapter 4, dimensional analysis is a powerful tool for deriving mathematical models with universal functional definitions (see Aczél (1966), Aczél (1986), Aczél (1987), Castillo et al. (2014a) and Castillo et al. (2014c)). From previous studies of viscoelastic characterization, it is known that there are eight relevant variables involved, which can be written as the following set:

$$\nu \equiv \{E, E_0, E_\infty, T, T_r, T_g, t, t_c\}, \quad (6.7)$$

where E is the viscoelastic relaxation modulus, E_0 the initial or elastic viscoelastic modulus, E_∞ the relaxed viscoelastic modulus, T the temperature, T_r the rubbery characteristic temperature, T_g the glassy characteristic temperature, t the time variable and t_c a characteristic time, usually measured in seconds. Since the viscoelastic relaxation modulus is doubly bounded, it appears simpler to consider the differences $\Delta E = E - E_\infty$ and $\Delta E_0 = E_0 - E_\infty$ between the current state E of the modulus, respectively, its initial value E_0 , and its final value E_∞ . Similarly, the variable related to temperature is defined as the difference between the temperature T and the reference temperature $\Delta T = T - T_g$ since temperature differences usually related to the heat flow provide more physical meaning than temperature alone (see Zohuri (2015, 2017) and Simon et al. (2017)).

	ΔE	ΔE_0	ΔT	ΔT_r	t	t_c
M	1	1	0	0	0	0
L	-1	-1	0	0	0	0
T	-2	-2	0	0	1	1
θ	0	0	1	1	0	0

Table 6.1: Dimensional analysis of the initial set of variables involved in the temperature-effect problem in terms of the basic magnitudes M (mass), L (length), T (time) and θ (temperature).

As a result, the initial set of the involved variables in Eq. (6.7) is transformed, with no loss of generality, into an equivalent one with the variables being yet dimensional:

$$\nu \equiv \{\Delta E, \Delta E_0, \Delta T, \Delta T_r, t, t_c\}, \quad (6.8)$$

where $\Delta E_0 = E_0 - E_\infty$ and $\Delta T_r = T_r - T_g$. The six resulting variables can be written in terms of fundamental magnitudes M (mass), L (length), T (time) and θ (temperature), as shown in Table 6.1. Based on Buckingham's Theorem

described in Chapter 3, the set, ν , of six variables in Eq. (6.8) can be now written in terms of $n - k = 6 - 3 = 3$ non-dimensional variables (with asterisks), as for example,

$$f(E^*, t^*, T^*) = 0, \quad (6.9)$$

for a certain function $f(\cdot)$, where

$$E^* = \log \Delta E / \log \Delta E_0; \quad t^* = \log(t/t_c); \quad T^* = \Delta T / \Delta T_r. \quad (6.10)$$

Indeed, Buckingham's Theorem (Buckingham (1915)) ensures that any valid physical functional form relating the eight initial variables in Eq. (6.7) is of the form of Eq. (6.9), without loss of generality. Moreover, only quotients $\Delta E / \Delta E_0$, $\Delta T / \Delta T_r$ and t/t_c , or any monotonic function of them, such as $p(\Delta E / \Delta E_0)$, $q(\Delta T / \Delta T_r)$ and $s(t/t_c)$, exert any influence on the relaxation modulus. Thus, since the interest lies in explicit functional forms of the relaxation modulus E^* , Eq. (6.9) can be transformed to:

$$E^* = g(t^*, T^*), \quad (6.11)$$

where $g(\cdot)$ is the function of interest. Note that the dimensional analysis provides the same non-dimensional variable E^* for the relaxation modulus as that given in Eq. (5.2) in terms of the normalization from previous chapter. It is now corroborated with an important additional justification. Note also the non-dimensional definition of the variables selected for the modulus and time as $\log \Delta E / \log \Delta E_0$ and $\log(t/t_c)$, respectively, instead of $\Delta E / \Delta E_0$ and (t/t_c) . This is due to the common use of logarithms in viscoelasticity.

As a result of the dimensional analysis, some of the currently used dimensional TTS models in the literature to define the shift factor a_T (see Table 6.2) can now be reformulated only in terms of non-dimensional variables. This gives functional forms insensitive to the dimensional system of the units selected (see Table 6.3).

6.3.2 Temperature-dependent normalization

In some works (see McCrum and Morris (1964) and Stouffer and Wineman (1971)), the limiting values of the relaxation modulus, E_0 and E_∞ , are thought to be non-constant, but temperature-dependent according to some monotonic functions, i.e. $E_0(T^*)$ and $E_\infty(T^*)$. Consequently, the normalized relaxation modulus is defined in a more general set as follows:

$$E^*(t^*; T^*) = \frac{\log E(t^*; T) - \log E_\infty(T^*)}{\log E_0(T^*) - \log E_\infty(T^*)} = \frac{\log(E(t^*; T^*)/E_\infty(T^*))}{\log(E_0(T^*)/E_\infty(T^*))}, \quad (6.12)$$

where $E_0(T^*) \leq E^*(t^*; T^*) \leq E_\infty(T^*)$. Although in this thesis, these asymptotic values are assumed to be constants, the proposed normalization of the relaxation modulus, as a fundamental basis of the statistical approach, can be extended

Table 6.2: Dimensional models proposed in the literature for the shift factor, a_T , in the application of the TTS principle (see Tschoegl et al. (2002)).

Model	Dimensional Form
Eyring (1936)	$\log a_T = \frac{\Delta g_a}{2.303R} \left[\frac{1}{T - T_L} - \frac{1}{T_0 - T_L} \right]$
Doolittle and Doolittle (1957)	$\log a_T = \frac{B}{2.303} \left[\frac{1}{f} - \frac{1}{f_0} \right]$
Williams et al. (1955)	$\log a_T = -\frac{c_1^g(T - T_g)}{c_2^g + T - T_g}$
Bueche (1962)	$\log a_T = b_1 \left[1 - \frac{1}{[1 + b_2(T - T_l)]^2} \right]$
Bestul and Chang (1964)	$\log a_T = \frac{B_{BC}}{2.303} \left[\frac{1}{S_c(T_g)} - \frac{1}{S_c(T)} \right]$
Goldstein (1963)	$\log a_T = \frac{B_{GS}}{2.303} \left[\frac{1}{H(T)} - \frac{1}{H(T_g)} \right]$
Adam and Gibbs (1965)	$\log a_T = \frac{B_{AG}}{2.303} \left[\frac{1}{T_r S_c(T_g)} - \frac{1}{T S_c(T)} \right]$

Table 6.3: Modified non-dimensional version of the proposed models in the literature for the shift factor, a_T , in the application of the TTS principle.

Model	Dimensionless Form
Eyring (1936)	$\log a_T = A + B \left(\frac{T_0 - T_l}{T - T_l} \right)$
Doolittle and Doolittle (1957)	$\log a_T = A + B \left(\frac{f(T_0)}{f(T)} \right)$
Williams et al. (1955)	$\log a_T = A + B \left(\frac{T_0 - T_\infty}{T - T_\infty} \right)$
Bueche (1962)	$\log a_T = A \left[1 - \left[1 + B \left(\frac{T - T_l}{T_0 - T_l} \right) \right]^{-2} \right]$
Bestul and Chang (1964)	$\log a_T = A + B \left(\frac{S_c(T_g)}{S_c(T)} \right)$
Goldstein (1963)	$\log a_T = A + B \left(\frac{H(T_g)}{H(T)} \right)$
Adam and Gibbs (1965)	$\log a_T = A + B \left(\frac{T_r S_c(T_g)}{T S_c(T)} \right)$

to include any assumed temperature-dependent limiting values. Accordingly, if these limiting values are observed experimentally to be temperature-dependent, the general expression of the normalization of the relaxation modulus in Eq. (6.12) holds and, consequently, the master curves are derived the same as in the non-temperature-dependent case.

Figure 6.4 illustrates some examples of possible cases of temperature-dependent

laws for the limiting values. In a), the initial or elastic modulus is supposed to follow the law $E_0^*(T^*) = C_0 + T^*$, so that the master curves are vertically displaced while the relaxed modulus E_∞ holds constant. On the other hand, in b), the elastic modulus E_0 is assumed to be constant whereas the relaxed modulus depends on the temperature, according with $E_\infty^*(T^*) = C_1 + T^*$. In c) both limits are considered to be temperature-dependent. Finally, in d) both elastic and relaxed moduli are supposed to be temperature independent. The absolute relaxation process is assumed to be the sum of two components, namely, a linear evolution additional to the regular sigmoidal one as represented by the Gumbel cdf, as given by

$$E_0^*(T^*) = C_2 + C_3T^* \text{ and } E_\infty^*(T^*) = C_4 + C_5T^*, \quad (6.13)$$

for some arbitrary constants C_1, C_2, C_3, C_4 and C_5 .

Despite the different possible cases to be confirmed from the experimental data, the proposed definition of the relaxation modulus in Eq. (6.12) allows the normalization with reference to the two values E_0 and E_∞ to be applied, independently of being constant or temperature-dependent, and proceed to the estimation of the model parameters as in the standard case, proving the general and robust applicability of the proposed normalization for the time evolution of the relaxation modulus.

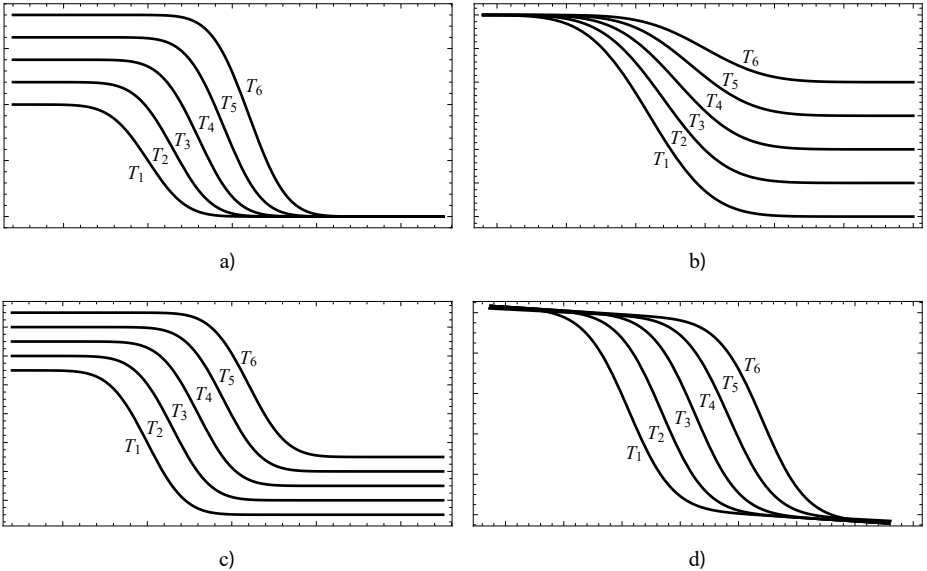


Figure 6.4: Schematic illustration of different temperature-dependent laws for the limiting values of the relaxation modulus: a) $E_0^*(T^*) = C_0 + T^*$, b) $E_\infty^*(T^*) = C_1 + T^*$, c) $E_0^*(T^*) = C_0 + T^*$ and $E_\infty^*(T^*) = C_1 + T^*$, d) $E_0^*(T^*) = C_2 + C_3T^*$ and $E_\infty^*(T^*) = C_4 + C_5T^*$.

6.3.3 Uniqueness condition

Besides the dimensional analysis and the normalization of the viscoelastic modulus, the mathematical transformation from the short-term curves to the master curve must satisfy an additional physical condition, here referred to as the uniqueness condition. The treatment transcendence of this condition has unfortunately been overlooked in the literature, considered only by Williams et al. (1955) with the symmetry conditions, but not as a general formulation to be used in the application of the TTS principle.

This uniqueness condition states that the final master curve from any transformation must be the same regardless of the origin of that transformation. In other words, the master curve at a reference temperature $E(t^*, T_2^*)$ resulting from a transformation with origin $E(t^*, T_0^*)$ or $E(t^*, T_1^*)$ must coincide, independently of the origin, as shown in Figure 6.5. Thus, let us consider this transformation based on the TTS principle in the form of Eq. (6.1), that is,

$$E^*(t^*, T_1^*) = E^*(t^* a_{T^*}(T_1^*, T_0^*); T_0^*), \quad (6.14)$$

$$E^*(t^*, T_2^*) = E^*(t^* a_{T^*}(T_2^*, T_0^*); T_0^*), \quad (6.15)$$

$$E^*(t^*, T_2^*) = E^*(t^* a_{T^*}(T_2^*, T_1^*); T_1^*), \quad (6.16)$$

from which Eqs. (6.16) and (6.15) must be equal, such that,

$$E^*(t^* a_{T^*}(T_2^*, T_1^*); T_1^*) = E^*(t^* a_{T^*}(T_2^*, T_0^*); T_0^*). \quad (6.17)$$

By substituting Eq. (6.14) into Eq. (6.17), it results

$$E^*(t^* a_{T^*}(T_2^*, T_1^*) a_{T^*}(T_1^*, T_0^*); T_0^*) = E^*(t^* a_{T^*}(T_2^*, T_0^*); T_0^*), \quad (6.18)$$

which is only fulfilled if the shift factors satisfy the following condition:

$$a_{T^*}(T_2^*, T_0^*) = a_{T^*}(T_2^*, T_1^*) a_{T^*}(T_1^*, T_0^*). \quad (6.19)$$

Taking logarithms on both sides,

$$\log a_{T^*}(T_2^*, T_0^*) = \log a_{T^*}(T_2^*, T_1^*) + \log a_{T^*}(T_1^*, T_0^*), \quad (6.20)$$

which represents the Sincov functional equation (3.30), whose solution is:

$$\log a_{T^*}(T^*, T_0^*) = m(T^*) - m(T_0^*), \quad (6.21)$$

for a certain unknown function of one variable $m(\cdot)$ to be experimentally determined. It follows that the shift factors a_T must not be defined arbitrarily since the uniqueness condition forces them to be of the form Eq. (6.21), which is the most general possible solution. Note the practical importance of this result since the shift factor function $a_{T^*}(\cdot)$ was initially conceived as a function of two variables, i.e. the origin and the end of the transformation, while the functional equations theory states that it can be defined, without loss of generality, as the difference between two values of a function of one single variable evaluated at the

temperatures implied in the transformation.

As a matter of fact, the theoretical concept of thermo-rheologically simple materials previously mentioned is in accordance with this result. Indeed, such viscoelastic materials, susceptible of being characterized by means of the TTS principle must satisfy the following relation between the shift factors and their relaxation times (see Schwarzl and Staverman (1952), Williams et al. (1955), Morland and Lee (1960), Gross (1969) and Ferry (1980)):

$$a_T(T, T_0) = \frac{\tau_i(T)}{\tau_i(T_0)}, \quad (i = 1, 2, \dots) \quad (6.22)$$

with $\tau_i(T)$ as the i -th relaxation time at a temperature T , that is, this definition supposes that all the relaxation times are equally influenced by the temperature, which is quantified by the shift factor. However, this definition also restricts the possible functional forms of the shift factors function, since it must be also expressed as a quotient of two functions of one single variable $\tau_i(T)$, such that by taking logarithms at both sides in Eq. (6.22) leads to the solution of the uniqueness condition in Eq. (6.21). In other words, the thermo-rheologically simple concept restricts by itself the possible functional forms of the shift factor function to be uniqueness.

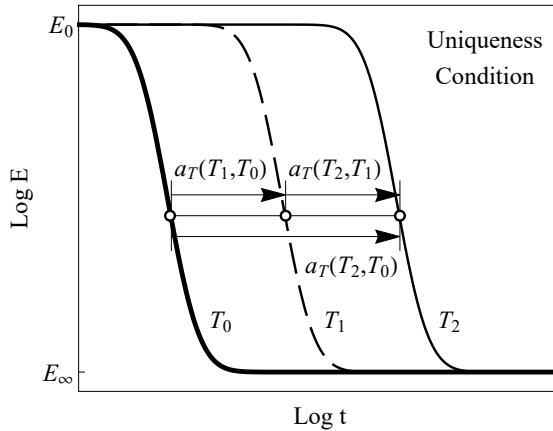


Figure 6.5: Schematic illustration of the uniqueness condition among different master curves, indicating the equivalence of the transformation law either for a direct step or in two steps.

It is also worth mentioning that this result is not only of interest because it provides the functional forms of the shift factor but, above all, because its contribution to recognize a transcendental requirement for the model to be valid. In fact, the uniqueness condition allows the most general possible model solutions to be derived, as will be shown when the uniqueness condition is applied to the proposed scale-effect property.

Example 6.1 (Uniqueness condition in WLF model). Let us consider the application of the TTS principle based on the shifting property in Eq. (6.1) to the WLF model. Direct substitution of Eq. (6.1) into the uniqueness condition, given by Eq. (6.20), leads to:

$$-\frac{C_1^0(T_2 - T_0)}{C_2^0 + (T_2 - T_0)} = -\frac{C_1^1(T_2 - T_1)}{C_2^1 + (T_2 - T_1)} - \frac{C_1^0(T_1 - T_0)}{C_2^0 + (T_1 - T_0)}, \quad (6.23)$$

which is only satisfied if the constants C_1^0, C_2^0 and C_1^1, C_2^1 are interrelated. It follows that the symmetry conditions in Eqs. (6.5) and (6.6) proposed by Williams et al. (1955) represent the only possible solution for Eq. (6.23) to be fulfilled. \square

6.4 Proposed Models based on the Scale-Effect Property

In this section, a first set of models are proposed, which comprises the temperature effect into the TTS principle but instead of being based on the classic shifting they are derived from the scale-effect property. Once this alternative property is identified, the uniqueness condition is enforced to achieve the most general solution of the shift factors (see Álvarez-Vázquez et al. (2020a)). In what follows, different models are derived from the both statistics-based approaches described in Chapter 5, i.e. the central limit and the extreme value.

6.4.1 Derivation of the model

The scale-effect property has been successfully applied in the derivation of models in other research fields, such as in fatigue lifetime prediction of longitudinal elements (see Piccioto (1970), Bogdanoff and Kozin (1987), Castillo et al. (1988) and Castillo and Fernández-Canteli (2009)). In viscoelastic terms, the scale-effect property states that the transformation of the relaxation modulus from the reference temperature T_0^* , $E^*(t^*; T_0^*)$ to any other temperature T^* , $E^*(t^*; T^*)$ is defined as follows:

$$E^*(t^*; T^*) = E^*(t^*; T_0^*) Q^*(T^*, T_0^*), \quad (6.24)$$

where the factors Q^* are the equivalent functions to the shift factors in the classic shifting property. Note that Eq. (6.24) does not represent a model definition but a condition to be satisfied by the model being searched, the same as the shifting property in Eq. (6.1), as pointed out in Chapter 2.

Previously to the application of the uniqueness condition, Eq. (6.24) can be regarded as a functional equation with unknown functions $E^*(t^*; T^*)$ and $Q^*(T^*, T_0^*)$. Accordingly, based on the functional equations theory the most general solution for the functions implied in the scale-effect property can be obtained. In this way, arbitrary assumptions about these functions are avoided and the resulting models are derived in an objective manner. Since this functional

equation is identified with the form of Eq. (3.34), its solution is given by Eq. (3.35), that is,

$$\begin{aligned} E^*(t^*; T^*) &= p(t^*)^{q(T^*)}; & p(t^*) &= \exp\{-\exp[h(t^*)]\}; \\ Q^*(T^*, T_0^*) &= q(T^*)/q(T_0^*); & q(T^*) &= \exp[-f(T^*)], \end{aligned} \quad (6.25)$$

where $q(T^*)$ is an arbitrary positive function.

On the other hand, the uniqueness condition represents a mandatory requirement whatever is the property on which the TTS principle is based. To this end, let us consider the transformation within three different temperatures T_0^* , T_1^* and T_2^* according to the alternative definition of the TTS principle based on the scale-effect property:

$$E^*(t^*; T_1^*) = E^*(t^*; T_0^*) Q^{*(T_1^*, T_0^*)}, \quad (6.26)$$

$$E^*(t^*; T_2^*) = E^*(t^*; T_0^*) Q^{*(T_2^*, T_0^*)}, \quad (6.27)$$

$$E^*(t^*; T_2^*) = E^*(t^*; T_1^*) Q^{*(T_2^*, T_1^*)}, \quad (6.28)$$

where $E^*(t^*; T_2^*)$ must be the same in Eqs. (6.28) and (6.27), so that,

$$E^*(t^*; T_1^*) Q^{*(T_2^*, T_1^*)} = E^*(t^*; T_0^*) Q^{*(T_2^*, T_0^*)}. \quad (6.29)$$

Then, substituting Eq. (6.26) into Eq. (6.29) gives:

$$E^*(t^*; T_0^*) Q^{*(T_2^*, T_1^*)} Q^{*(T_1^*, T_0^*)} = E^*(t^*; T_0^*) Q^{*(T_2^*, T_0^*)}, \quad (6.30)$$

which is satisfied only if the powers are the same, leading to the same functional equation related to the shifting property in Eq. (6.19) describing the uniqueness condition. This implies that the $Q^*(.)$ factor must display the same functional form as the shift factor a_T in the shifting property, that is,

$$\log Q^*(T^*, T_0^*) = m(T^*) - m(T_0^*), \quad (6.31)$$

for some unknown function $m(.)$ to be experimentally determined. In addition, note that the general solution for the Q^* factor resulting from the functional equation concerning the scale-effect in Eq. (6.25), is exactly the same as that obtained by applying the uniqueness condition. In other words, the most general solution of the Q^* factor function satisfies the uniqueness condition by itself.

6.4.2 Proposed models

Once the scale-effect property has been identified and formulated along with the feasible conditions, the resulting proposed models are now obtained by considering both statistics-based approaches, i.e. the central limit and extreme value models. More precisely, the normal distribution is found to represent a suitable candidate for describing the viscoelastic behaviour, particularly the relaxation

modulus in this case, being justified by physical and statistical reasons outlined in Chapter 5. Moreover, the Gumbel distribution, as a function of the extreme value family, is theoretically supported by the required asymptotic extrapolation to the limiting time values inherently implied in the viscoelastic characterization.

Normal model The normal distribution is not stable against power operations, like that represented by the scale-effect property in the application of the TTS principle, see Table 3.1. As a result, note that the final distribution $E^*(t^*; T_0^*)$ does not belong to the family of $E^*(t^*; T^*)$ after the application of the power operation using the Q^* factors in Eq. (6.24). Thus, the extended normal distribution must be considered instead, ensuring also stability against extreme operations for maxima and minima (see Example 3.7). Accordingly, the proposed normal model for describing the temperature effect on the evolution of the normalized relaxation modulus over with time is defined as follows:

$$E^*(t^*, T^*; \mu, \sigma^2, \alpha)^{-1} \sim [1 - N(\mu - \sigma \log Q^*(T^*), \sigma^2)]^\alpha, \quad (6.32)$$

for $-\infty < t^* < \infty$ and μ, σ and α being the location, scale and the extended parameter of the normal distribution, respectively. Figure 6.6 illustrates the resulting family of master curves for different temperatures from the normal model based on the scale-effect property. As can be seen, this property actually implies for the master curves a horizontal translation over time of a value $\sigma \log a_T^*(T^*)$ due to the temperature effect. In this way, the relation between the classic shift factors a_T and the proposed Q^* factors between two different temperatures T^* and T_0^* can be straightforwardly obtained from Eq. (6.32), as:

$$\log a_T(T^*, T_0^*) = \sigma [\log Q^*(T^*) - \log Q^*(T_0^*)], \quad (6.33)$$

being only function of the origin and final of the transformation.

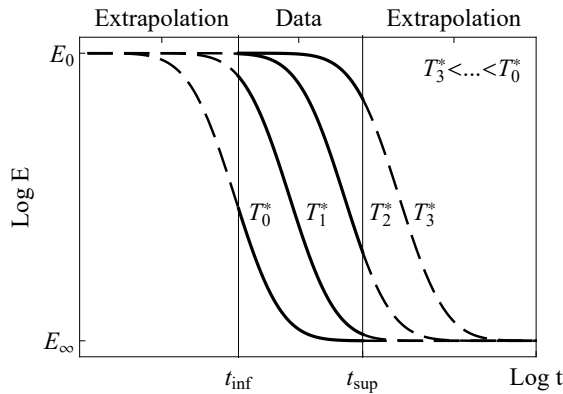


Figure 6.6: Viscoelastic moduli within the experimental window and extrapolated over time, identified as survival distribution for different values of the scale parameter associated with changes of temperature in the normal model.

Gumbel model The Gumbel distribution, as pertaining to the statistical family of extreme value, is proposed in Chapter 5 as a suitable candidate for modelling the temperature effect in viscoelasticity because: a) the normal distribution belongs to the domain of attraction of the Gumbel distribution for cases of both maximal and minimal values of interest, and b) the limiting values of the relaxation modulus, i.e. for $t = 0$ and $t = \infty$, is advantageously extrapolated by using the distributions of the extreme value family. These represent the only stable distributions against power operations (see Castillo (1988), Castillo et al. (2004a) and Castillo et al. (2014c)), without using the extended versions, as required by the normal distribution in the previous case. Thus, if the scale-effect property is applied to the Gumbel survival distribution (see Example 3.6), the resulting Gumbel model for the temperature effect on the normalized relaxation modulus is given by:

$$E^*(t^*, T^*; \lambda, \delta) = \exp \left[- \exp \left(\frac{t^* - (\lambda - \delta \log Q^*(T^*))}{\delta} \right) \right], \quad (6.34)$$

for $-\infty < t^* < \infty$ and λ and δ being the location and scale parameters of the Gumbel distribution, respectively. Similarly, as in the normal model, the relation between the classic shift factor a_T and the proposed Q^* factor for two different temperatures in the Gumbel model can be directly obtained from Eq. (6.34) as follows:

$$\log a_T(T^*, T_0^*) = \delta [\log Q^*(T^*) - \log Q^*(T_0^*)], \quad (6.35)$$

which depends only on the difference between the Q^* factors.

As will be shown in the practical example in Section 6.7, both proposed normal and Gumbel models contribute to enhancing the viscoelastic characterization, overcoming the obvious disadvantages of the current methodologies previously described. Firstly, the dimensional analysis of the viscoelastic problem allows these mathematical models to be defined in terms of non-dimensional variables. Secondly, the proposed models analytically define the parametric family of temperature-dependent curves in the $E^* - t^*$ field. Note that the classic models described in Chapter 4 are valid only for a given temperature, as evidenced by their functional form $E(t)$, and not $E(t; T)$, so that the viscoelastic characterization must be carried out in two steps: a) derivation of the experimental master curve for the reference temperature using the TTS principle and b) use of a classic model (Maxwell, Zener, etc.) to define that master curve analytically. On the contrary, the alternative proposals allow all the master curves to be estimated directly in one sole step from the experimental short-term set of curves. Thirdly, the values on the parameters in the proposed models are not dependent on the reference temperature, unlike those included in the WLF model, which require additional calculations if the reference temperature is varied. Fourthly, the Q^* factors can now be entirely applied in the temperature range of interest without requiring two different TTS models, as occurs with the WLF and Arrhenius models. Lastly, but not least important, the required minimal overlap of at least one decade for the short-term curves is avoided.

6.4.3 Parameter estimation

The parameter estimation for both normal and Gumbel models is based on the probability paper concept described in Chapter 3. The time is defined in a deterministic manner and other estimation methods, such as the Maximum Likelihood Estimator, are not justified. The steps guiding the parameter estimation are the following:

- **Step 1:** *Experimental determination of relaxation moduli.* The experimental data from a typical relaxation test at different temperatures can be written as follows:

$$\left\{ \hat{E}(t_{i,k}; T_k) \mid (i = 1, \dots, N, k = 1, \dots, M) \right\}, \quad (6.36)$$

where $\hat{E}(t_{i,k}; T_k)$ represents the experimental values of the relaxation modulus at i -th discrete time values $t_{i,k}$ tested at k -th temperature.

- **Step 2:** *Derivation of the minimization function.* Based on the probability paper concept, the statistical distributions can be transformed into linear functions, allowing the model parameters to be easily estimated. The minimization functions for normal and Gumbel models are defined as follows,

(a) *Normal model*

$$\min_{(\mu, \sigma, \alpha, E_0, E_\infty, Q_k^*)} \left\{ \sum_{k=1}^M \sum_{i=1}^N \left[\frac{\log E_0 - \log E_\infty - \log E_{ki}}{\log E_{ki} - \log E_\infty} - [1 - N(\mu - \sigma \log Q_k^*, \sigma^2)]^\alpha \right]^2 \right\}, \quad (6.37)$$

(b) *Gumbel model*

$$\min_{(\delta, \lambda, E_0, E_\infty, Q_k^*)} \left\{ \sum_{k=1}^M \sum_{i=1}^N \left[\frac{\log E_{ki} - \log E_\infty}{\log E_0 - \log E_\infty} - \left[-\exp \left(\frac{t_{ik}^* - (\lambda - \delta \log Q_k^*)}{\delta} \right) \right] \right]^2 \right\}, \quad (6.38)$$

where $Q_k^* = Q^*(T_k^*)$, so that each value of Q^* is obtained for the temperature at which the short-term curve is tested.

- **Step 3:** *Fitting the shift factor function $\log a_T^*$.* The Q^* factor function in Eq. (6.31) is derived in terms of an unknown function $m(T)^*$ to be determined experimentally. As will be shown in the practical example, the values of the experimental Q^* factors follow an exponential law, so that according to Eq. (6.31), the following linear function can be fitted:

$$\log Q^*(T^*) = \theta_0^* + \theta_1^* T^*, \quad (6.39)$$

where θ_0^* and θ_1^* are constants, such that $\theta_1^* \neq 0$. Furthermore, as the proposed models do not require the transformation of the short-term curves into the master curve, the $Q^*(T^*, T_0^*)$ factor function can be simplified as $Q^*(T^*)$, without loss of generality,

- **Step 4:** *Derivation of the final expressions.* By substituting the parameter estimations and the shift factor functions into Eqs. (6.32) and (6.34), the normal and Gumbel models are obtained. Note also that the master curves referring to temperatures different from those applied in the tests can be predicted directly by simple evaluation of the analytical expressions of these models.

The parameter estimation can be easily done with an optimization software such as GAMS (see Brooke et al. (1998)), which proves to be particularly useful when some parameters are shared. This occurs when λ and δ in the Gumbel model, or μ , σ and α in the normal model, respectively, are common to any master curve. It should be also pointed out that in the estimation process all the experimental data is included in the optimization process and the limiting values of the relaxation modulus are also defined as variables, providing these values with more robust estimations.

6.5 Proposed Models based on the Compatibility Condition

Previous normal and Gumbel models are based on the scale-effect property and the corresponding definition of the alternative TTS principle. However, the viscoelastic characterization problem including the temperature effect can also be formulated without requiring the TTS principle to become a specific condition for establishing the model, as indicated at the beginning of this chapter (see Figure 6.1). In fact, the new models proposed in this section are not based on Q^* factors being indispensable to define the master curves in the $E^* - t^*$ field (see Álvarez-Vázquez et al. (2020b)). Furthermore, these proposals are based on the statistical compatibility condition, first introduced in Chapter 3, rather than on the shifting property or the scale-effect. Once this condition is formulated and applied to the approach, the extreme value approach is used to derive the Gumbel-Gumbel model with possible extension to the Weibull-Weibull model.

6.5.1 Derivation of the model

The compatibility condition was originally developed by Castillo et al. (1985), Castillo and Fernández-Canteli (1986), Castillo and Galambos (1987b), Castillo and Fernández-Canteli (2001) and Castillo and Fernández-Canteli (2009) for modeling fatigue lifetime prediction in the S-N field. It implies a correspondence between the cdf of the number of cycles for a given stress range $p(N|\Delta\sigma)$

and the cdf of the stress range for a given number of cycles $p(\Delta\sigma|N)$. This concept can also be extended to model the viscoelastic behaviour in the $T^* - t^*$ field in an analogous way (see Schwarzl (1990) and Münstedt and Schwarzl (2014)), between the resulting distribution of the relaxation modulus over time for a given temperature, i.e. $E^*(t^*|T^*)$, and the distribution of the relaxation modulus with different temperatures for a given time, that is, $E^*(T^*|t^*)$, as illustrated in Figure 6.7.

As pointed out in previous chapters, the viscoelastic characterization involves determining the $E^* - t^*$ field through experimental campaigns, through tests at different temperatures (isothermal curves) and recording data over a limited time interval t_{inf}^* and t_{sup}^* . In this way, only experimental data of region II is available (censored data) while data about regions I and III must be determined by extrapolation. However, this type of testing strategy also gives the $E^* - T^*$ field (isochronal curves) by representing the evolution of the relaxation modulus as its value for the different temperatures at a fixed time. The extrapolation about regions I and III succeeds in the same way.

Despite being two perspectives of the same relaxation phenomenon, the $E^* - T^*$ field is traditionally ignored, considered as being not useful (see Tschoegl et al. (2002)).

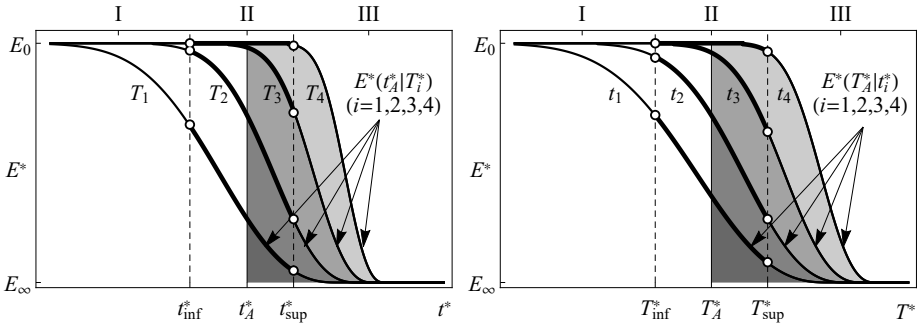


Figure 6.7: Illustration of the $E^* - t^*$ field for different temperatures (left) and the $E^* - T^*$ field for different times (right).

Consequently, following the description of the conditional specification outlined in Chapter 3, the viscoelastic characterization problem represents a typical example of a physical phenomenon obtained from experimentally censored data for any given value of an external effect, be it time, temperature or pressure.

In this sense, both E -fields can be summarized as the $T^* - t^*$ field shown in Figure 6.8, where the common $E^* - t^*$ field is represented for three different temperatures. Each experimental point in this field is of the form $(t_{i,k}^*, T_k^*)$ so that points with the same corresponding value of the normalized relaxation modulus are matched. The iso-modulus curves ($E^* = 0.10, 0.50, 0.90$) are determined in this way, being evidently comprised between the limiting values $E_0^* = 1$

and $E_\infty^* = 0$. Accordingly, the experimental result for a given temperature T^* is identified as a set of points along the t^* -axis at the corresponding temperature ordinate. Equivalently, the experimental results for a given t^* value, i.e. $E^*(T^*; t^*)$, are represented by a set of points along the T^* -axis at the corresponding x -coordinate.

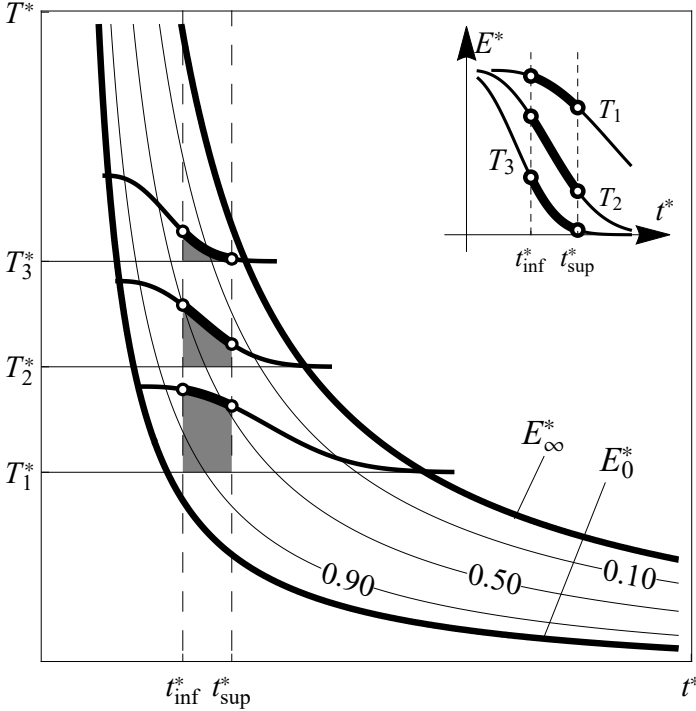


Figure 6.8: Schematic illustration of short-term curves for the relaxation modulus from experimental campaign on the $T^* - t^*$ field denoting the iso-modulus curves ($E^* = 0, 0.10, 0.50, 0.90, 1$).

Consequently, the corresponding distributions to be used in the definition of both $E^* - t^*$ and $E^* - T^*$ fields cannot be arbitrarily defined since they are dependent on each other, as indicated by Castillo and Fernández-Canteli (2009) with respect to the S-N field. For this reason, the compatibility condition between these distributions is applied to the $T^* - t^*$, that is,

$$E^*(t^* | T^*) = E^*(T^* | t^*), \tag{6.40}$$

so that their corresponding areas must be the same for a fixed time and temperature, as shown in Figure 6.9. In other words, the number of iso-modulus curves crossing the horizontal line must be the same as those exiting the vertical line.

Assuming that the evolution of the normalized viscoelastic relaxation modulus

represents a survival distribution function with location and scale parameters $\lambda_{t^*}(T^*)$, $\lambda_{T^*}(t^*)$ and $\delta_{t^*}(T^*)$, $\delta_{T^*}(t^*)$ depending, respectively, on the other variable in Eq. (6.40), the compatibility condition is expressed as:

$$1 - q_{\min} \left(\frac{t^* - \lambda_{t^*}(T^*)}{\delta_{t^*}(T^*)} \right) = 1 - q_{\min} \left(\frac{T^* - \lambda_{T^*}(t^*)}{\delta_{T^*}(t^*)} \right), \quad (6.41)$$

where $q_{\min}(x)$ represents a distribution for minima, whose survival function is defined as $S(x) = 1 - q_{\min}(x)$, with $\lambda_{t^*}(T^*)$ and $\lambda_{T^*}(t^*)$ as location parameters and $\delta_{t^*}(T^*)$ and $\delta_{T^*}(t^*)$, depending on temperature T^* and time t^* , respectively.

It is worth noting that although in this case a distribution for minima is considered for the variables $t^*|T^*$ and $T^*|t^*$, the alternative case of maxima values can also be handled based on the extreme value statistical approach described in Chapter 5. Another property of the $T^* - t^*$ field is that the iso-modulus curves allow the limits to be established between the pure elastic and the pure viscous states in which the viscoelastic behaviour occurs, as shown in Figure 6.9.

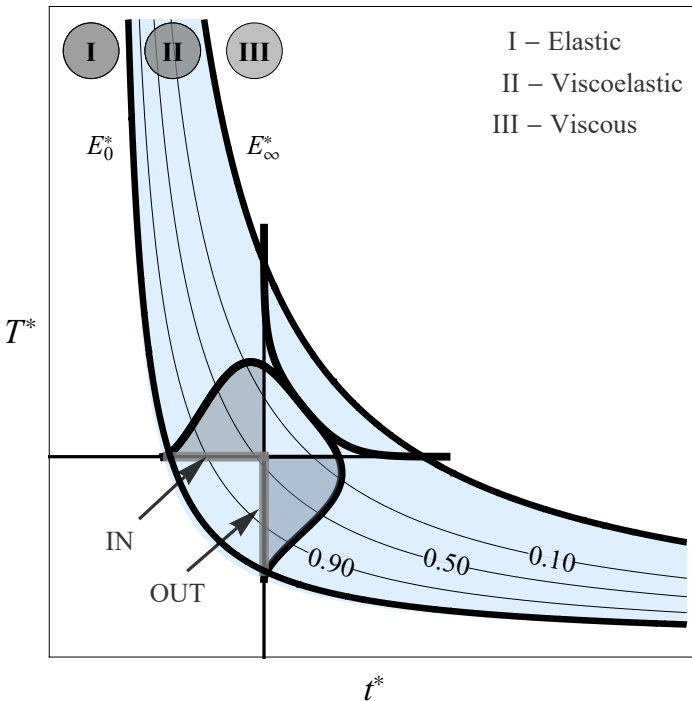


Figure 6.9: Compatibility between the distributions $E^*(t^*; T^*)$ and $E^*(T^*; t^*)$ for a given temperature and time, distinguishing the regions bounding the viscoelastic behaviour.

6.5.2 Proposed models

Gumbel-Gumbel model According to the extreme value statistical approach, the Gumbel distribution is proposed for describing the relaxation modulus analytically, by considering $q_{\min} = 1 - \exp[-\exp(x)]$ for both distributions $E^*(t^*|T^*)$ and $E^*(T^*|t^*)$ in Eq. (6.41) result as,

$$E^*(t^*|T^*) = \exp \left[-\exp \left(\frac{t^* - \lambda_{t^*}(T^*)}{\delta_{t^*}(T^*)} \right) \right]; \quad -\infty \leq t^* \leq \infty \quad (6.42)$$

$$E^*(T^*|t^*) = \exp \left[-\exp \left(\frac{T^* - \lambda_{T^*}(t^*)}{\delta_{T^*}(t^*)} \right) \right]; \quad -\infty \leq T^* \leq \infty \quad (6.43)$$

whence solving the functional equation resulting from the compatibility condition in Eq. (3.79), the Gumbel-Gumbel model is derived:

$$E^*(t^*|T^*) = E^*(T^*|t^*) = \exp \left[-\exp \left(\frac{(t^* - B)(T^* - C) - \lambda}{\delta} \right) \right] \quad (6.44)$$

where λ, δ, B and C are the parameters of the model, as illustrated in the $T^* - t^*$ field of Figure 6.10. B and C are asymptotes of the model. The first one corresponds with the time below which the material shows elastic behaviour, independently of the temperature. The second one represents the temperature below which the material exhibits linear-elastic behaviour independently of the exposure time, proving that the relaxation phenomenon does not occur below this temperature.

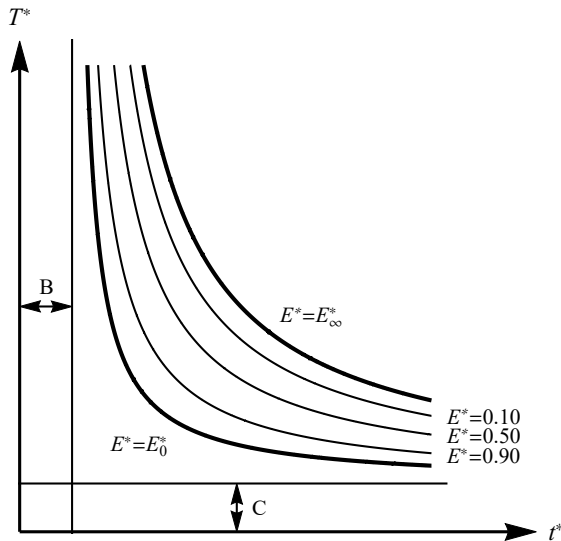


Figure 6.10: Iso-modulus curves representing the relationship between the temperature and time in the $T^* - t^*$ field for the Gumbel-Gumbel model.

The definition of the normalized variable $V^* = (t^* - B)(T^* - C)$ allows all the experimental data pertaining to the $T^* - t^*$ field to be pooled as pertaining to a single survival Gumbel distribution function with parameters λ and δ , as will be shown in the practical example in Section 6.7. Furthermore, both fields $E^* - T^*$ and $E^* - t^*$ can now be directly obtained once the $T^* - t^*$ field is estimated unlike the traditional models, which focus only on the estimation of the $E^* - t^*$ field.

So far, the normalized time variable has been considered on a logarithmic scale. If it is now measured on a natural scale and its existence field, $[0, \infty]$, is taken into account, the Gumbel distribution $E^*(t^*; T^*)$ transforms into a biparametric Weibull distribution (with zero location parameter), and consequently the Gumbel-Gumbel model becomes a Weibull-Gumbel model. Since the time in natural scale is left-bounded, the vertical asymptote coincides with the vertical axis, which is satisfied in the Weibull-Gumbel model, as shown in Eq. (3.84).

In summary, these alternative models based on the application of the compatibility condition prove to be a generalization of the normal and Gumbel models, which are grounded on the scale-effect property. However, in this case the temperature effect acting on the statistical distribution of the normalized relaxation modulus is established in a more general way, using the compatibility condition.

6.5.3 Parameter estimation

The parameter estimation of the proposed Gumbel-Gumbel model is based on that originally developed by Castillo and Fernández-Canteli (2009) (see also Castillo and Hadi (1995), Castillo et al. (1999), Arnold et al. (1999) and Castillo and Fernández-Canteli (2001)), consisting in the following steps:

- **Step 1:** *Experimental determination of the viscoelastic modulus at different temperatures.* The experimental data from the characterization campaign in testing the relaxation modulus at various temperatures can be written as in Eq. (6.36).
- **Step 2:** *Estimation of the B and C values.* According to Castillo and Fernández-Canteli (2001) and Castillo and Fernández-Canteli (2009), the minimization function to be considered for estimating the asymptotes of the Gumbel-Gumbel model is defined as,

$$Q(B, C, \mu) = \sum_{k=1}^M \sum_{i=1}^N \left(t_{ik}^* - B + \frac{\mu}{T_k^* - C} \right)^2, \quad (6.45)$$

where t_{ik}^* represents the i -th discrete time value tested at k -th temperature, with μ as the mean of time variable.

- **Step 3:** *Calculation of the V^* values.* Once the asymptotes have been estimated, the experimental data is transformed directly to values of the

normalizing variable V^* :

$$V_{ik}^* = (t_{ik}^* - B)(T_k^* - C), \quad (i = 1, \dots, N, k = 1, \dots, M) \quad (6.46)$$

- **Step 4:** *Estimation of the Gumbel parameters.* The resulting values of the normalizing variable V_{ik}^* from Eq. (6.46) are crossed one-by-one with the decreasing values of the experimental normalized relaxation modulus E_{ik}^* , pooling all of the data into a single Gumbel survival cdf representing the $E^* - V^*$ field. The estimation of the Gumbel parameters is done according to one of the standard estimation methods applicable to the distributions of the extreme value family (see Castillo (1988), Castillo and Hadi (1994) and Castillo et al. (2004a)), such as that based on the probability paper described in Chapter 3.
- **Step 5:** *Obtain the model expressions.* From the estimation of the asymptotes B and C and the resulting estimates of the parameters for the Gumbel distribution, the final expression of the Gumbel-Gumbel model is obtained. According to the compatibility condition, the $E^* - t^*$ field can now be derived from Eq. (6.44) for a constant value of temperature (isothermal curves), while the $E^* - T^*$ field is also obtained for a fixed time value (isochronal curves) from Eq. (6.44).
- **Step 6:** *Extrapolation to other testing conditions.* The prediction of the master curves in both $E^* - t^*$ and $E^* - T^*$ fields for any temperature or time condition of interest is straightforward by evaluating their corresponding Eq. (6.44).

6.5.4 Model validation

The compatibility condition in the $T^* - t^*$ field forces the location and scale families of parameters in Eqs. (6.42) and (6.43) to adopt the form of Eq. (3.80), so that the final expression of the Gumbel-Gumbel model results from Eq. (6.44) after rearranging terms. The same applies for validating the Gumbel-Gumbel model in a practical example, as will be shown in Section 6.7.

Let us assume that the families of the location and scale parameters are unknown functions, such that they can only be determined by fitting the corresponding isothermal curves in the $E^* - t^*$ field, and the isochronal curves in the $E^* - T^*$ field, to the following Gumbel distributions, respectively:

$$E^*(t^*; \lambda_1(T^*), \delta_1(T^*)) = \exp \left[- \exp \left(\frac{t^* - \lambda_1(T^*)}{\delta_1(T^*)} \right) \right], \quad (6.47)$$

$$E^*(T^*; \lambda_2(t^*), \delta_2(t^*)) = \exp \left[- \exp \left(\frac{T^* - \lambda_2(t^*)}{\delta_2(t^*)} \right) \right], \quad (6.48)$$

where the parameters are denoted $\lambda_1(T^*)$, $\delta_1(T^*)$ and $\lambda_2(t^*)$, $\delta_2(t^*)$ in order to distinguish them from those provided by the compatibility condition $\lambda_{t^*}(T^*)$, $\delta_{t^*}(T^*)$ and $\lambda_{T^*}(t^*)$, $\delta_{T^*}(t^*)$. For the $E^* - t^*$ field, each combination of $\lambda_1(T_k^*)$, $\delta_1(T_k^*)$

allows the short-term curve for the k -temperature to be estimated by minimizing the error independently of the remaining short-term curves; the same is applicable to the $E^* - T^*$ field with respect to the isochronal curves. As a result, the evolution of these parameters with time and temperature can be obtained, representing the optimal solution for each of the isothermal or isochronal curves. If the experimental values of the parameters are rearranged according to the theoretical definitions of the compatibility condition, that is,

$$\begin{aligned} \lambda_{t^*}(T^*) &= \frac{C_2 T^* - C_3}{C_0 T^* - C_1}, & \delta_{t^*}(T^*) &= \frac{1}{C_0 T^* - C_1}, \\ \lambda_{T^*}(t^*) &= \frac{C_1 t^* - C_3}{C_0 t^* - C_2}, & \delta_{T^*}(t^*) &= \frac{1}{C_0 t^* - C_2}, \end{aligned} \quad (6.49)$$

for some constants C_0, C_1, C_2 and C_3 , then the Gumbel-Gumbel model will also represent the optimal solution by minimizing the error for each of the isothermal and isochronal curves. This is also justified not only by physical and statistical conditions related to the $T^* - t^*$ field, but also as the optimal possible solution in terms of the error. In fact, as will be shown in the practical example, the resulting location and scale parameters from fitting isothermal and isochronal curves, independently of each other, conform naturally to rational functions such as those illustrated in Figure 6.11.

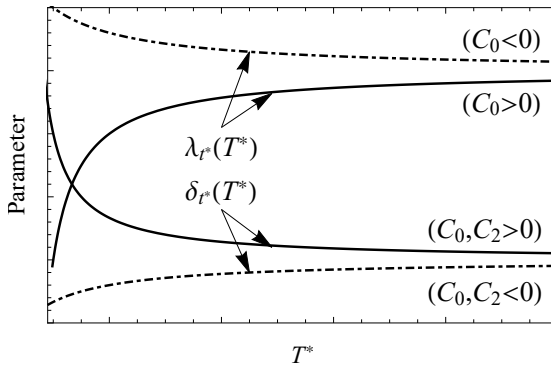


Figure 6.11: Theoretical functions of the scale and location parameters in the Gumbel-Gumbel model obtained from the compatibility condition.

6.6 Probabilistic Models

All of the models currently used, those based on the TTS principle, as well as those previously proposed, based on the scale-effect property and the compatibility condition, assume the evolution of the viscoelastic properties over time as being a deterministic process. This implies that at a given time only one value of that property is defined. However, as has been indicated at above, this

evolution of the viscoelastic properties with time constitutes a stochastic process in itself. This stochastic process should be defined as a distribution of possible values instead of as a single deterministic value (see Figure 6.12). For this reason, this section is devoted to developing novel probabilistic models which will make it possible to consider the inherent scatter in the predictions of the viscoelastic properties.

The model building requires extrapolation from a limited experimental data set (short-term curves for different temperatures recorded in a confined time interval). This has undoubtedly contributed to the scarce development of probabilistic models for the viscoelastic characterization. Fortunately, the use of the Bayesian techniques allows the statistics-based models proposed to be improved by the incorporation of probabilistic concepts, such as creep compliance and relaxation modulus, in the definition of the viscoelastic variables.

Furthermore, the proposed Bayesian technique is able to facilitate, within certain limits, a probabilistic analysis of the viscoelastic models with a moderate number of replications of the relaxation test at different temperatures.

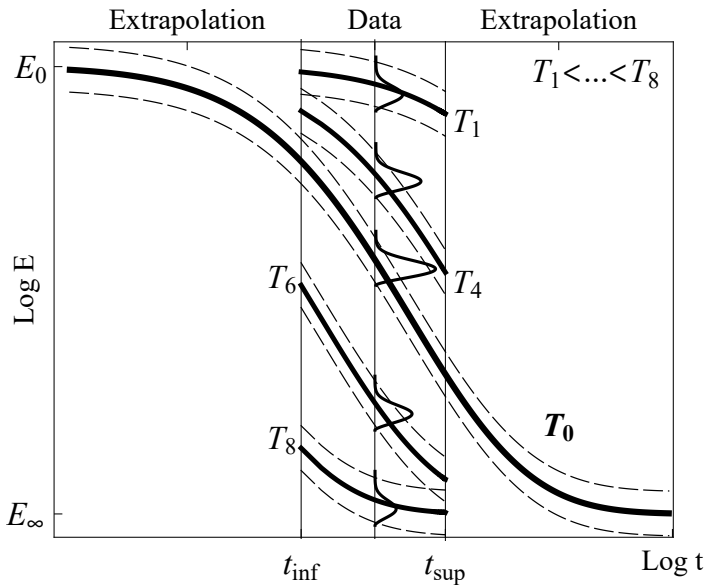


Figure 6.12: Illustration of the $E^* - t^*$ field showing the inherent scatter of the experimental data with their corresponding densities for a given time and for different temperatures.

Among the previous proposals based either on the scale-effect or on the compatibility condition, the proposed normal and Gumbel models are used in this section to illustrate how deterministic models can be further converted into probabilistic models, according to the general scheme outlined in this chapter.

The first step consists in the definition of prior distributions assumed for the parameters participating in the normal and Gumbel models. According to other works, these prior distributions are assumed to be uniform distributions bounded into an interval around the previous value obtained from the application of the deterministic model. For the normal model these distributions are defined as follows:

$$\begin{aligned}
 E_0 &\sim U(E_{0\min}, E_{0\max}), & \alpha &\sim U(\alpha_{\min}, \alpha_{\max}), & \delta &\sim U(\delta_{\min}, \delta_{\max}), \\
 E_\infty &\sim U(E_{\infty\min}, E_{\infty\max}), & \lambda &\sim U(\lambda_{\min}, \lambda_{\max}), & Q_k^* &\sim U(Q_{\min}^*, Q_{\max}^*)_k,
 \end{aligned}
 \tag{6.50}$$

where θ_{\min} and θ_{\max} are suitable confidence intervals selected by the user and θ is the generic notation for each of the parameters in the normal model. In the same way, the prior distributions of the Gumbel model are defined as:

$$\begin{aligned}
 E_0 &\sim U(E_{0\min}, E_{0\max}), & \lambda &\sim U(\lambda_{\min}, \lambda_{\max}), & Q_k^* &\sim U(Q_{\min}^*, Q_{\max}^*)_k, \\
 E_\infty &\sim U(E_{\infty\min}, E_{\infty\max}), & \delta &\sim U(\delta_{\min}, \delta_{\max}),
 \end{aligned}
 \tag{6.51}$$

Bayesian techniques for deriving probabilistic models from deterministic ones can be easily applied using the OpenBUGS software, recently developed by Lunn et al. (2000). As a result, once the deterministic normal and Gumbel models are solved for some real data, the resulting estimates of the model parameters are used to define the prior distributions according to Eqs. (6.50) and (6.51), respectively, as the input values for OpenBUGS, from which their posterior distributions are obtained. In this way, stochastic master curves are directly determined from short-term curves.

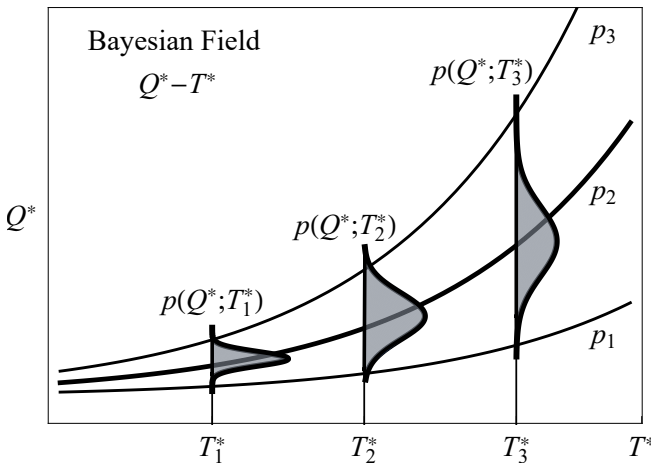


Figure 6.13: Illustration of the Bayesian $Q^* - T^*$ field showing varying density functions for different temperature values.

The probabilistic definition of the Q^* factors, as represented in Figure 6.13, allows any other master curve to be obtained together with their confidence intervals.

6.7 Example of Application

In this section, the results of the experimental campaign on a commercial polyvinylbutyral (PVB) carried out for this thesis are used to illustrate the application of the proposed models to practical viscoelastic characterization. The PVB is widely used in multiple engineering applications, such as solar panels and structural laminated glass elements (see Pelayo et al. (2017)).

6.7.1 Description of the experimental program

The experimental campaign consists on a series of relaxation tests under uniaxial deformation with a DMA RSA3 equipment by T. A. Instruments. This apparatus is equipped with a chamber controlled by temperatures over a wide range of temperatures, ranging from -60°C to 150°C . The selected material is standard polyvinyl butyral, also called PVB, in samples of 25 mm in length, 5 mm in width and 0.38 mm thick. The relaxation tests were done at eight different temperatures: $-25, -15, -5, 2, 10, 20, 30$ and 40°C for a constant strain value of $\varepsilon_0 = 1\%$. Figure 6.14 summarizes the resulting short-term curves of the relaxation modulus at various temperatures and the master curve built with the WLF model for a reference temperature of $T_0 = 20^\circ\text{C}$, with constants $C_1^{20} = 12.603$ and $C_2^{20} = 74.56$, to be compared with the results provided by the proposed models. Further details and images from the equipment and the fixtures employed can be found in a previous similar experimental campaign (see Pelayo et al. (2017)).

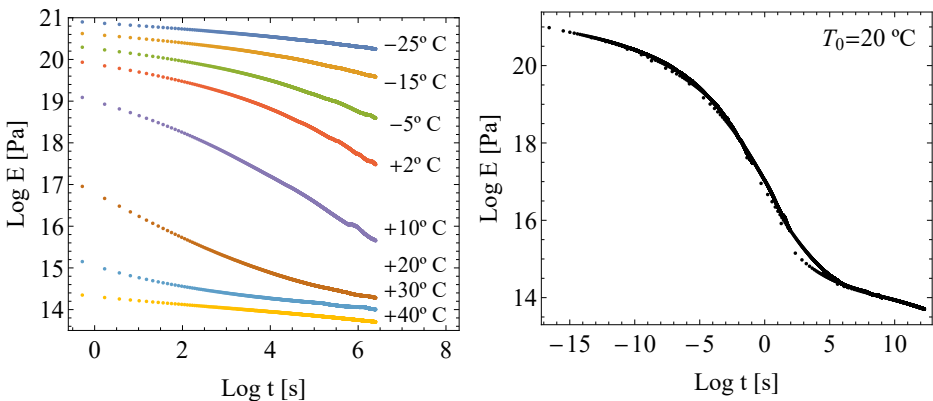


Figure 6.14: Experimental relaxation curves at different temperatures for the PVB (left) and the experimental master curve for $T_0 = 20^\circ\text{C}$ (right).

6.7.2 Proposed models based on the scale-effect property

In this subsection, both normal and Gumbel models based on the scale-effect property, as an alternative formulation of the TTS principle, are applied to the experimental data for the PVB.

According to the parameter estimation method described in subsection 6.4.3, a simple substitution of the experimental data into the minimization functions in Eqs. (6.37) and (6.38) for the normal and Gumbel models, respectively, provides the estimates of the model parameters. Table 6.4 presents the values of the model parameters, i.e. the parameters of the statistical distribution, the limiting values E_0 and E_∞ , and the different values of the Q^* factor, one per temperature, to be understood as the objective function. The experimental values for the Q^* factors are plotted against the temperature from which an exponential relationship is identified between the two sets of experimental data, as previously indicated. As a result, a simple linear function is proposed to fit the relationship $\log Q^* - T^*$ from which both constants θ_0 and θ_1 are obtained according to Eq. (6.39).

Table 6.4: Parameter estimates of the normal and Gumbel models for the PVB data.

Model	Parameters						
	$\log E_0$	$\log E_\infty$	λ	δ	α	θ_0	θ_1
Normal	20.99	13.69	-1.37	10.54	11.54	-1.86	1.52
Gumbel	21.44	13.69	-1.37	6.97	—	-0.77	2.59

Substituting the final estimates into the normal in Eq. (6.32) and Gumbel in Eq. (6.34) models gives the following analytical expressions:

$$E^*(t^*; T^*)^{-1} = \left(1 - \Phi \left[\frac{t^* + 16.02T^* - 18.23}{10.54} \right] \right)^{11.54}, \quad (6.52)$$

$$E^*(t^*; T^*) = \exp \left[- \exp \left(\frac{t^* + 18.05T^* - 3.99}{6.97} \right) \right]. \quad (6.53)$$

Figure 6.15 illustrates the resulting theoretical curves and Q^* factors (on log-scale) as a function of T^* , which prove to follow a linear function. Note that due to the physical and statistical reasons outlined in Chapter 5, the inverse of the relaxation modulus H^* is fitted instead of E^* in the case of the normal model, for which the normal distribution is justified. In both cases, an acceptable agreement between the experimental and theoretical short-term curves at different temperatures is achieved. Since the Q^* factors vary with temperature following a linear trend, with no limitation for the application of the proposed models regardless of the reference temperature selected for building the master curve. Some local discrepancies are observed at both boundary regions for $t \rightarrow 0$ and $t \rightarrow \infty$. These could be due to possible inaccuracies in recording the data of the relaxation modulus at these regions or to the influence of the temperature

on both limiting values E_0^* and E_∞^* . Once both possible detrimental effects are amended, the extrapolation to the limiting regions $t \rightarrow 0$ and $t \rightarrow \infty$ are reliably assessed with the Gumbel model as supported by the extreme value theory.

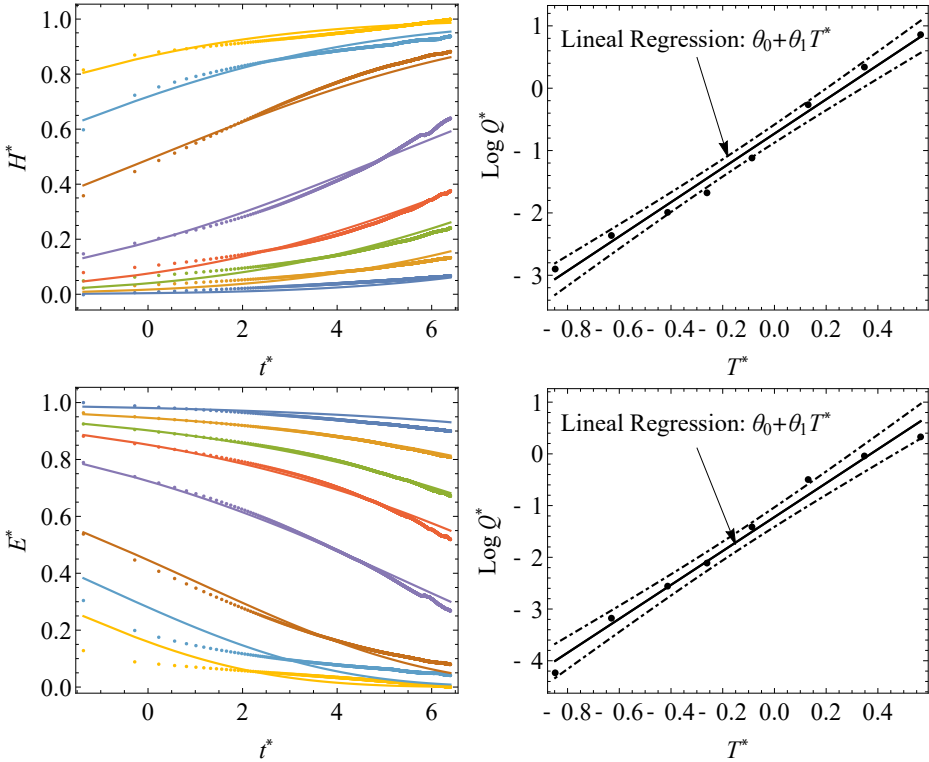


Figure 6.15: Theoretical predictions and experimental data for relaxation tests on PVB data at different temperatures (-25 to 40° C) (left) and Q^* factors with 95% confidence intervals (right) using the normal model (top) and the Gumbel model (bottom).

In addition, as the analytical definition of the $E^* - t^*$ field including the parametric family of curves for any temperature, the master curves are obtained by straightforward evaluation of both complete normal in Eq. (6.52) and Gumbel in Eq. (6.53) models over time, as shown in Figure 6.16. The master curve using the WLF model at a reference temperature of 20° C (see Figure 6.14) is also overlapped for comparison with the proposed models, being almost the same in all the cases. Note that the proposed models allow the master curve to be directly obtained from the estimation of the short-term curves without requiring the TTS principle. The analytical definition of the Q^* factors also allows the master curve for any other reference temperature to be predicted.

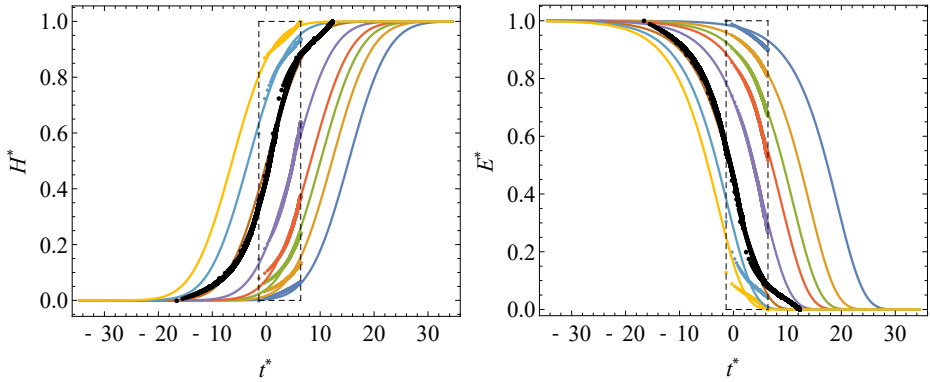


Figure 6.16: Experimental data from short-term relaxation curves for PVB data and corresponding master curves provided by the normal and Gumbel models compared with those using the WLF model (thick black line).

6.7.3 Proposed models based on the compatibility condition

After the proposed models, based on the scale-effect property, have been applied to the PVB experimental data, the experimental results are re-evaluated, this time, with the Gumbel-Gumbel model based on the compatibility condition.

As an introduction, the $E - t$ and $E - T$ fields are illustrated in Figure 6.17. The former represents the isothermal curves, as shown in Figure 6.14, while the latter, representing the isochronal curves, is shown for the first time. In this case, the experimental data for a different temperatures are now represented in vertical direction at three discrete times t_i providing the isochronal curve, as shown in Figure 6.17.

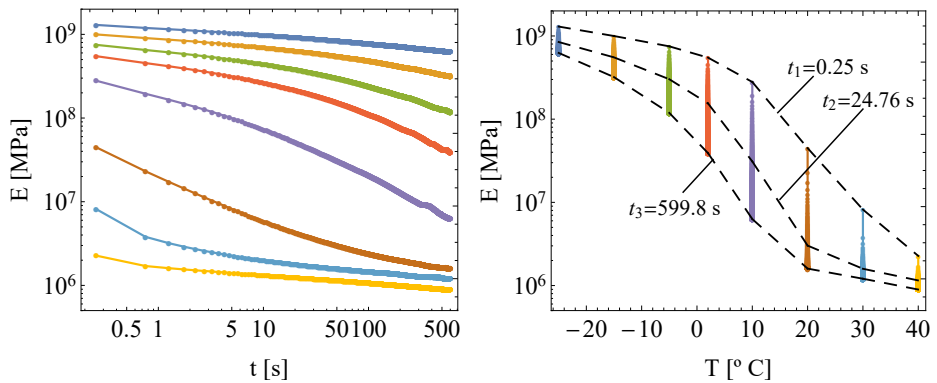


Figure 6.17: Experimental $E - t$ field (left) and $E - T$ field (right) for PVB data.

According to the parameter estimation for the Gumbel-Gumbel model, previously described in subsection 6.5.3, the following steps are required:

- **Step 1:** *Derivation of the viscoelastic modulus at different temperatures.* The experimental data recorded during the relaxation test at different temperatures are of the form of Eq. (6.36), so that two possible graphical representations can be considered providing both $E - t$ and $E - T$ fields.
- **Step 2:** *Estimation of the B and C values.* The estimation of the asymptotes B and C of the model can be easily performed by means of the minimization function in Eq. (6.45) with objective variables B, C and μ . By considering the experimental data of the PVB, the following estimates are obtained:

$$B = -16.37, \quad C = -2.90. \tag{6.54}$$

- **Step 3:** *Calculation of the V^* values.* The estimates from Eq. (6.54) used to compute the values of the normalizing variable V^* by direct substitution of the time t^* and temperatures T^* values according to Eq. (6.46). Once the vector of numerical values of the normalizing variable is assembled, a one-by-one cross with the decreasing normalized experimental values of the relaxation modulus is applied,. Thereby, E_0 and E_∞ are assigned the maximum and minimum values, respectively, achieved in the experimental campaign or, alternatively, the estimated values provided by the normal and Gumbel models from previous section. As a result, the experimental data from the $T^* - t^*$ field is rearranged as $E^* - V^*$ field, which display a typical sigmoidal shape, as shown in Figure 6.18 (right).

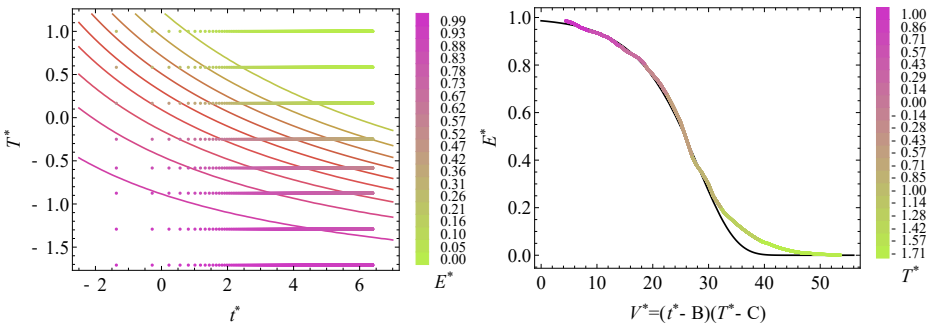


Figure 6.18: $T^* - t^*$ field with iso-modulus curves from PVB experimental data (left) and corresponding cdf for normalization variable V^* according to Gumbel-Gumbel model (right).

- **Step 4:** *Estimation of the Gumbel parameters.* It follows the estimation of the resulting $E^* - V^*$ field according to the survival Gumbel distribution in Eq. (6.44). For this doing, one of the classical estimation methods such

as the probability paper one, is applied, from which the following estimates result:

$$\lambda = 55.06, \quad \delta = 9.86. \quad (6.55)$$

The experimental data are fitted to the $E^* - V^*$ field, according to the survival cdf of Gumbel distribution, as shown in Figure 6.18 (right).

- **Step 5:** *Obtaining the model expressions.* Lastly, by substituting these parameters along with the asymptotes B and C into the Gumbel-Gumbel model, the final expression is obtained:

$$E^*(t^*; T^*) = \exp \left[- \exp \left(\frac{(t^* + 16.37)(T^* + 2.90) - 55.06}{9.86} \right) \right] \quad (6.56)$$

from which $T^* - t^*$ can now be fitted with the iso-modulus curves, as illustrated in Figure 6.18 (left). In other words, each of these iso-modulus E_i^* curves fits the experimental points of time-temperature such that the corresponding normalized relaxation modulus becomes exactly E_i^* .

In addition to estimating the $T^* - t^*$ field, the Gumbel-Gumbel model provides as well the corresponding $E^* - t^*$ and $E^* - T^*$ fields, both of interest for the viscoelastic characterization. As shown in Figure 6.19, the isothermal curves in the $E^* - t^*$ field are directly obtained by evaluating Eq. (6.56) while temperature of interest is taken a fixed value. Alternatively, the isochronal curves can also be derived from Eq. (6.56) by taking the time of interest as a fixed value.

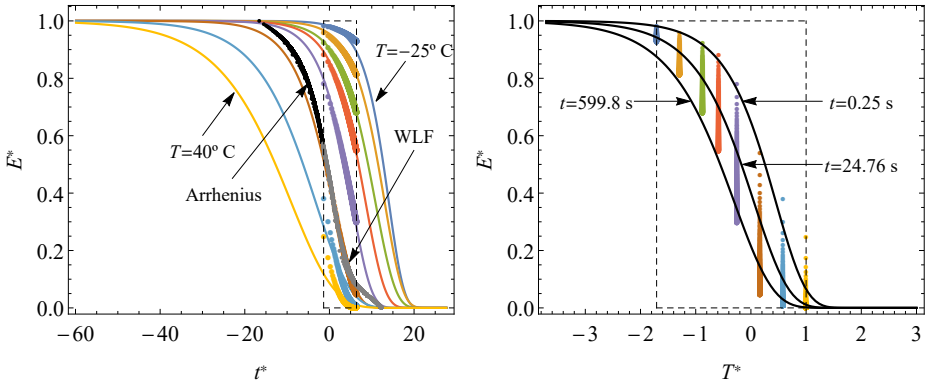


Figure 6.19: Experimental data for the $E^* - t^*$ field and master curve at a reference temperature of 20°C obtained from WLF + Arrhenius (top) and $E^* - T^*$ field (below) with the corresponding iso-thermal and isochronal curves provided by the Gumbel-Gumbel model for experimental data from PVB.

Note also that the prediction of any of those iso-curves can also be performed by simple evaluation of this Gumbel-Gumbel model fixing the time or temperature

as conditions of interest. Also the master curve at a reference temperature of 20° C obtained from the combination of both WLF (for $T > T_g$) and Arrhenius models (for $T < T_g$) is represented, so that an acceptable agreement between classical and the proposed models can be identified.

In summary, the models based on the compatibility condition shows the same advantages as those based on the scale-effect property, although they are derived under even stricter physical and statistical compatibility conditions while involving both two fields implied in the viscoelastic characterization problem. As a result, the assumption of the scale-effect due to the temperature is superfluous in this more general formulation.

Finally, the methodology, suggested in subsection 6.5.4 to validate the Gumbel-Gumbel model, is illustrated by a practical example. To this aim, the experimental values of these parameters by fitting each one of the isothermal ($n = 8$) and isochronal curve ($m = 1200$) to Gumbel survival functions are illustrated in Figure 6.20 (left).

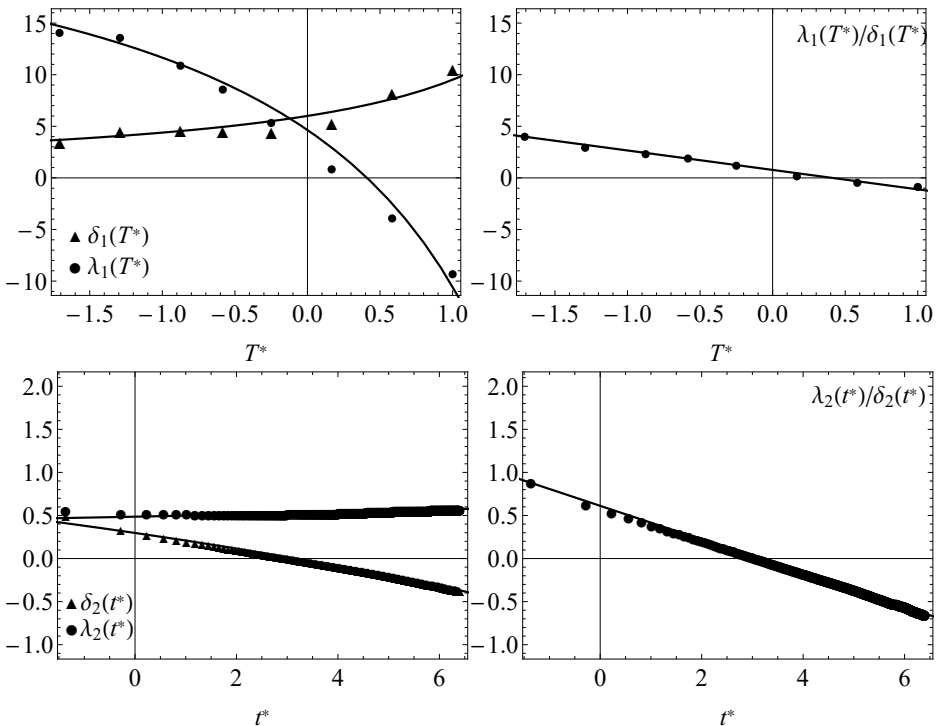


Figure 6.20: Optimal values of the location and scale parameters in the $E^*(t^*; T^*)$ field (top) and in the $E^*(T^*; t^*)$ field (bottom) from the PVB experimental data.

It is worth mentioning that only a limited coincidence among the fitted values

associated with each particular parameter is expected in the best case. In fact, since the parameters are estimated independently each other as the optimal values that minimize the error for each of the curves, it implies multiple possible solutions, so that the homogeneity among the values of the parameter sets would be questionable.

In addition, the quotients $\lambda_1(T^*)/\delta_1(T^*)$ and $\lambda_2(T^*)/\delta_2(T^*)$ prove to represent linear functions, see Figure 6.20 (right). Consequently, an acceptable agreement is noticed between the compatible solution and the theoretical definition of the parameters C_0, C_1, C_2 and C_3 according with Eq. (6.49), whose estimated values are given in Table 6.5.

Table 6.5: Parameter estimates for the normal and Gumbel models for the PVB data.

Model	Parameters			
	C_0	C_1	C_2	C_3
Gumbel-Gumbel	-0.0528	-0.1629	-1.7687	-0.6132

6.7.4 Probabilistic models

In this section, the use of the OpenBUGS software is exemplified by applying it to the derivation of the normal and Gumbel models, based on the scale-effect property, from experimental PVB data.

As described in Section 6.6, the prior distributions of the parameters in those models are bounded in intervals suggested by the user in OpenBUGS software. In this case, they are taken from the original model applied to the $E^* - t^*$ field (see Table 6.4).

The implementation of the codes to program this Bayesian evaluations is illustrated in code text in flat-format, which can also be implemented by means of the graphical interface called Doodle in OpenBUGS. In the case of the normal model, the corresponding flat code is written in Code 6.1 while the Gumbel model is in Code 6.2.

Code 6.1: OpenBUGS code for implementing the normal model.

```

1: model{
2:   for(k in 1:np) {
3:     for(i in 1:M) {
4:       Y[i, k]~dnorm(aux1[i, k], tau)
5:       aux[i, k]<-X[i, k]/delta[k]+log(Q[k])
6:       aux1[i, k]<-1-pnorm(aux[i, k], 0, 1)
7:       Q[k]~dunif(0,15)
8:       delta[k]~dunif(0.1,12)}
9:       tau~dunif(100,3000)
10:      sigma<-1/sqrt(tau)
11:      s1~dnorm(0,1)
12: }

```

After computing the initial data and the given prior distributions, the software OpenBUGS provides the posterior distributions of the model parameters, as can be seen, for example, with the δ and Q^* parameters for both normal (see Figure 6.22 and 6.23) and Gumbel models (see Figure 6.24 and 6.25) for each of the temperatures of the experimental results, respectively.

The number of simulations has to be defined for both the initial process (burn-in process) and the final sample before the model is executed. In this case, taking into account the computational time of OpenBUGS, 3,000 and 20,000 simulations are considered for the initial and final samples, respectively.

Code 6.2: OpenBUGS code for implementing the Gumbel model.

```

1: model{
2:   for(k in 1:np) {
3:     for(i in 1:M) {
4:       Y[i,k]~dnorm(aux[i,k],tau)
5:       aux[i,k]<-exp(-exp(X[i,k]/delta[k]+log(Q[k])))}
6:   Q[k]~dunif(0,10)
7:   delta[k]~dunif(0.1,10)}
8:   tau~dunif(100,3000)
9:   sigma<-1/sqrt(tau)
10: }
```

Once the corresponding codes are executed, the program performs the convergence analysis and provides the model parameters of the posterior distributions. These are introduced in Eq. (5.17) to derive the posterior predictive distribution. In this way, the percentiles of the original master curve are obtained allowing the confidence intervals for each master curve to be obtained in the original version of both normal (see Figure 6.21) and Gumbel models (Figure 6.26).

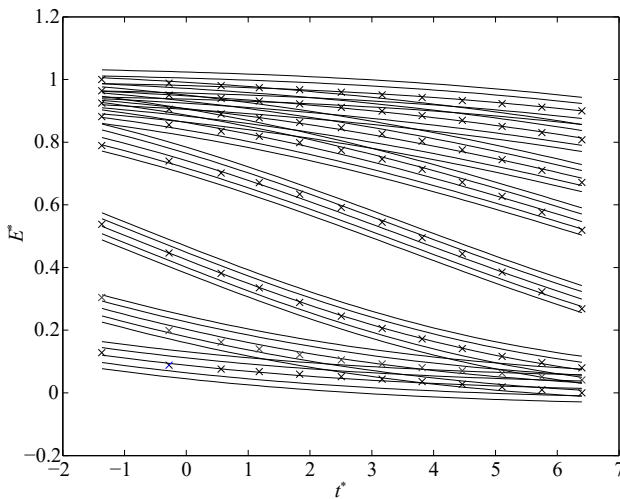


Figure 6.21: Experimental results and theoretical p -percentile curves ($p = 0.01, 0.10, 0.50, 0.90, 0.99$) for each temperature based on the normal model for PVB data.

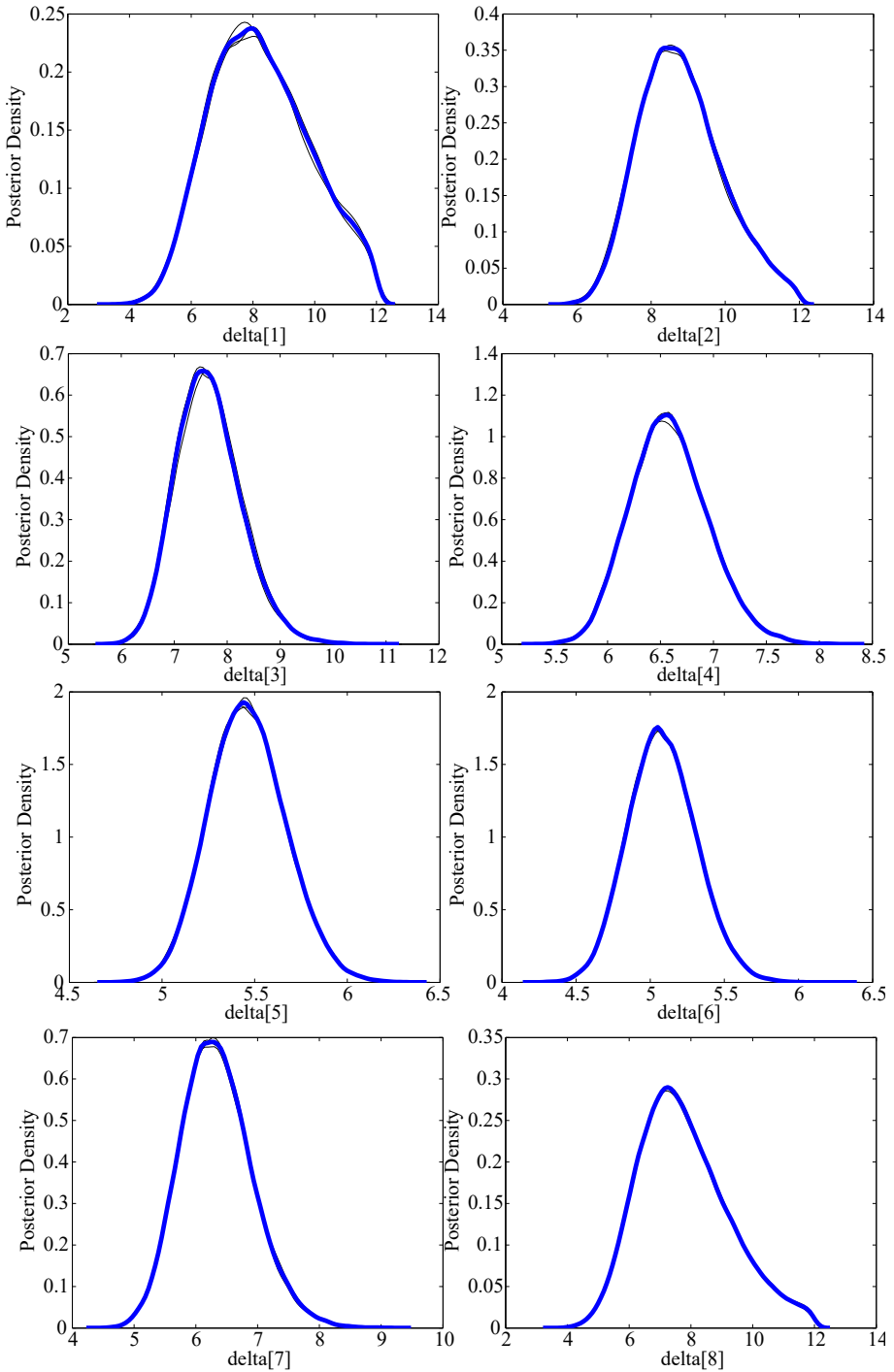


Figure 6.22: Posterior distributions of the δ parameter in the normal model for different temperatures for PVB experimental data.

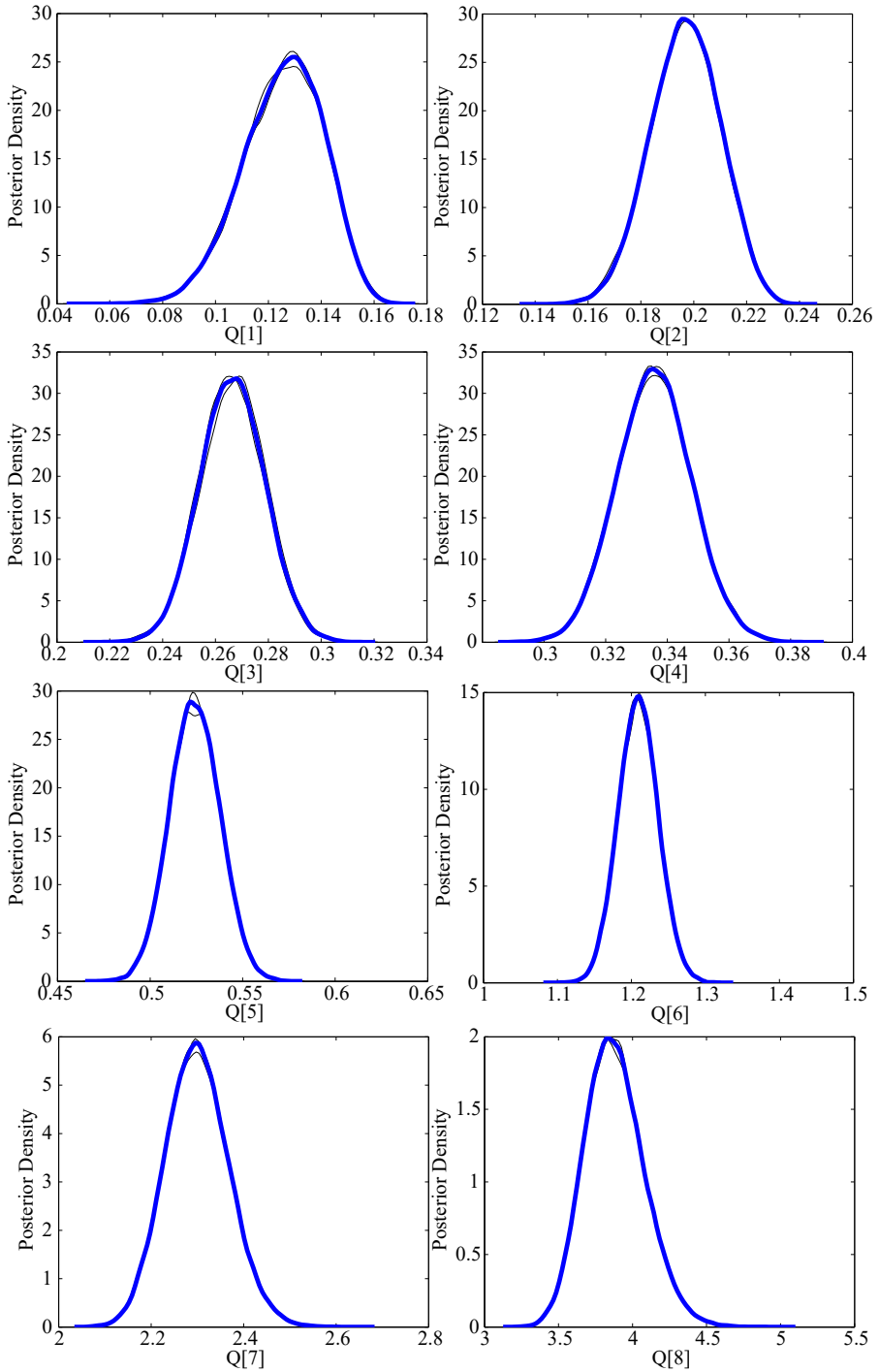


Figure 6.23: Posterior distributions of the Q^* factors in the normal model for different temperatures for PVB experimental data.

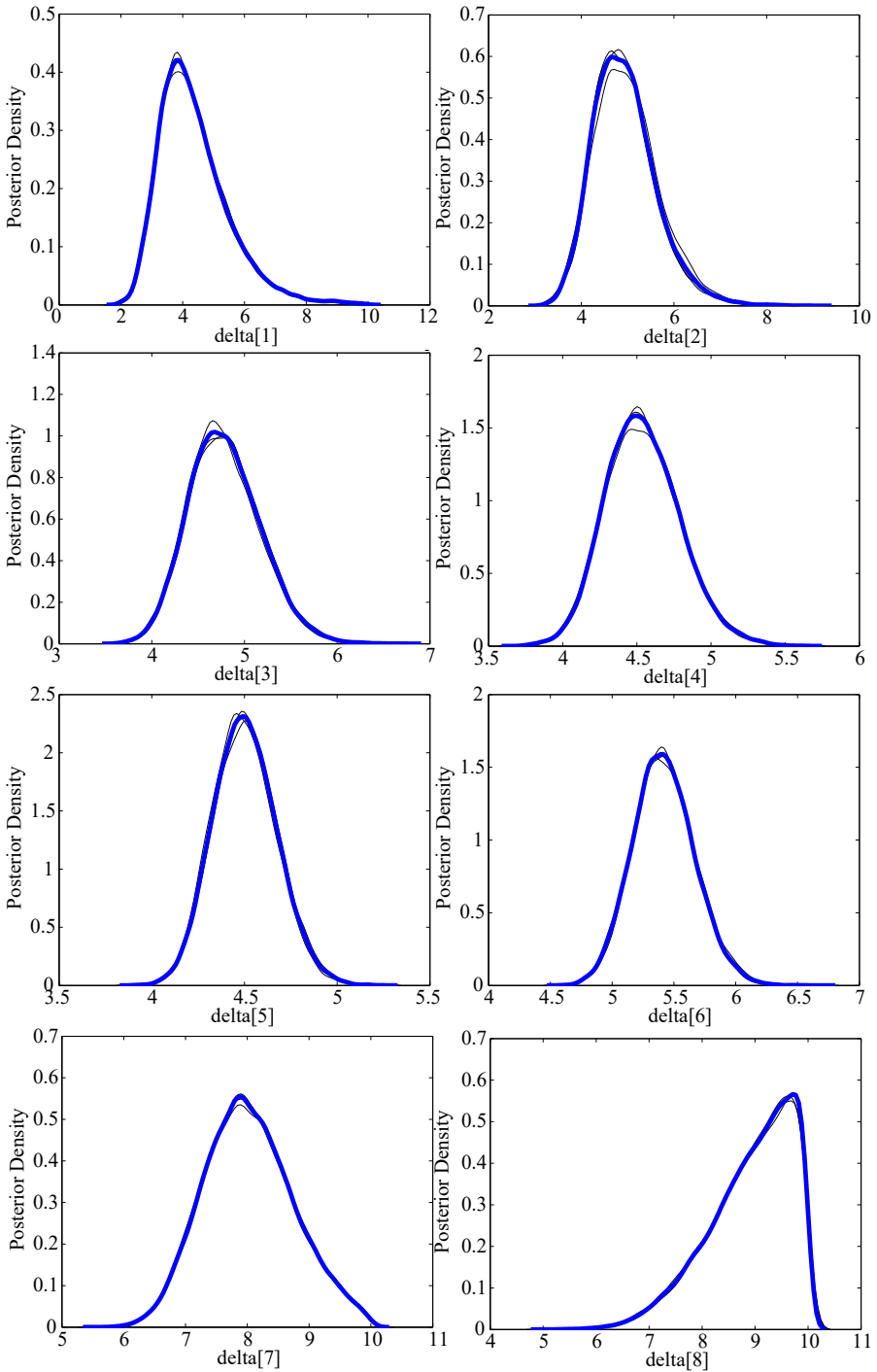


Figure 6.24: Posterior distributions of the δ parameter in the Gumbel model for different temperatures for PVB experimental data.

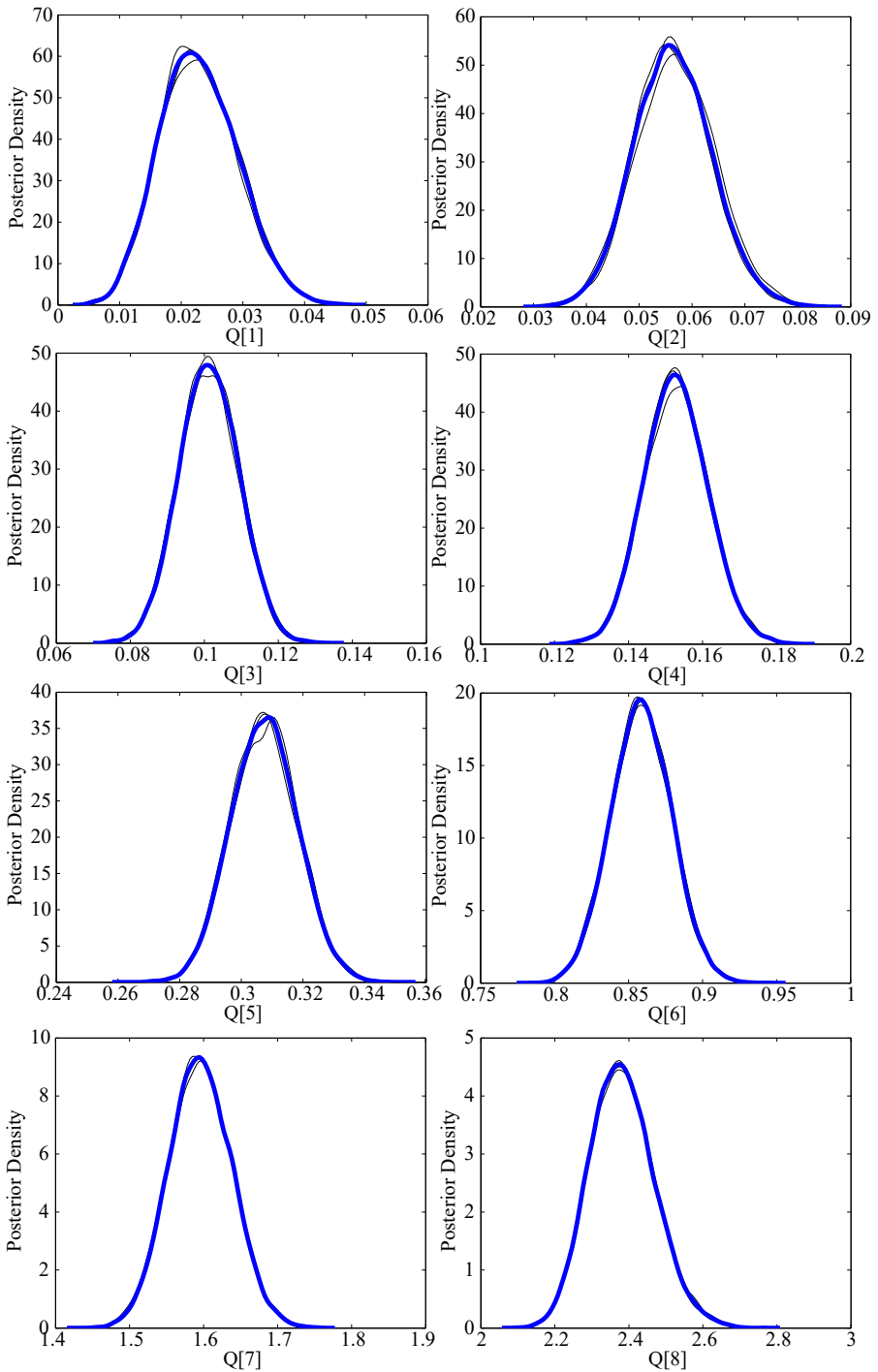


Figure 6.25: Posterior distributions of the Q^* factors in the Gumbel model for different temperature for PVB experimental data.

Note that the inherent scatter in the relaxation modulus is not negligible evidencing the urgent necessity of applying probabilistic models in the assessment of the engineering design of real viscoelastic components. In this way, the value for the viscoelastic properties for a given time are now related to a certain probability of occurrence rather than for a deterministic value. It is also worth noting that due to the large set of experimental data usually recorded in the short-term curves, the resulting Bayesian version of both normal and Gumbel models provide almost the same confidence intervals for each of the temperatures.

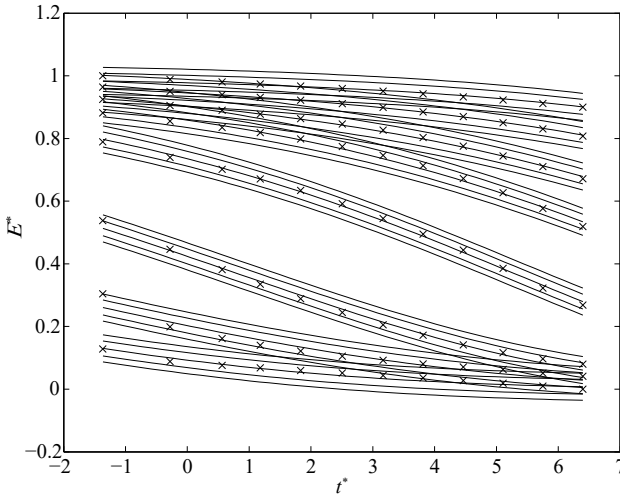


Figure 6.26: Experimental results and theoretical p -percentile curves ($p = 0.01, 0.10, 0.50, 0.90, 0.99$) for each temperature based on the Gumbel model for PVB data.

Finally, it should be noted the progressive development of viscoelastic models performed in this chapter. From the currently used models lacking analytical definition of the parametric family of curves in the $E - t$ field up to the derivation of a Bayesian model enabling the probabilistic definition of the master curve of the material and hence of any value of the $E - t$ field for specific values of time and temperature.

6.8 Concluding Remarks

In this chapter, the influence of the temperature effect on the viscoelastic properties was addressed as an indispensable experimental information to derive the master curve of the material and so to define the long-term behaviour of viscoelastic materials. Phenomenological models including both time and temperature transformations of the experimental data cannot be gratuitously defined

but based on some mandatory conditions to be fulfilled, which are strictly analyzed in this chapter. Some models are proposed based on different properties or conditions to derive the master curve of the material for a selected reference temperature. The main advantageous of those proposals based on the scale-effect property are herewith summarized:

1. *Dimensional consistency.* The dimensional analysis of the variables involved in the viscoelastic characterization problem allows phenomenological models to be derived dealing only with a reduced set of non-dimensional variables. As a result, the resulting models are more robust and insensitive with respect to the system of units selected as fundamental physical magnitudes.
2. *Non-overlapping constraint.* Current methodologies require the short-term curves at different temperatures to be overlapped at least during one decade in time, while the proposed models in this chapter avoid this practical limitation.
3. *Analytical definition of $E - t$ field.* The proposed models allow the $E - t$ field to be analytically defined without requiring to resort to the TTS principle. It implies fitting the experimental short-term curves over the time window and temperature conditions adopted in the tests and facilitating subsequently extrapolation to the limiting cases $t \rightarrow 0$ and $t \rightarrow \infty$. In this way the master curve is derived.
4. *Statistics-based approach of the viscoelastic modulus.* The different statistics-based approaches proposed in this thesis contribute to broaden the theoretical framework and to justify the relaxation phenomenon as represented by survival functions of certain statistical distributions, particularly the normal and Gumbel ones.
5. *Independence of the reference temperature.* The parametric family of the master curves are defined independently of the reference temperature implied in the first derivation.
6. *Analytical definition of Q shift factors.* The analytical definition of the Q^* factors in the proposed model function is valid over the whole range of temperature allowing the master curve for any other reference temperature in the whole range of interest to be defined. Conversely, current TTS approaches have to resort, at least, to two overlapping models to cover the entire range of temperatures.
7. *Mathematical definition of the uniqueness condition.* A rigorous analysis of the mandatory conditions required for defining valid time- and temperature-dependent transformations is made. In particular, the uniqueness condition is formulated in mathematical terms providing a general methodology allowing inconsistent models to be identified.

The proposed Gumbel-Gumbel model, based on the application of the compatibility condition to the $T^* - t^*$ field avoids the consideration of the scale effect assumption used to derive the normal and Gumbel distributions allowing both $E^* - t^*$ and $E^* - T^*$ fields to be derived simultaneously.

Finally, since the evolution of the viscoelastic properties over time constitutes inherently a stochastic process, some probabilistic models, based on the Bayesian theory, are also derived allowing the statistical distributions of the intervening parameters and the confidence intervals of the master curves to be determined.

7.1 Introduction

Some of the proposed models described in Chapter 6 concerning the temperature effect on viscoelastic characterization problem can also be applied by means of a software program developed in this thesis called ProVisco, which has been coded through the Matlab assistant for building applications. As a result, an experimental campaign consisting of a series of short-term curves at different temperatures for determining the relaxation modulus of a viscoelastic material can now be easily evaluated for providing the master curve at any reference temperature, allowing the viscoelastic characterization to be directly performed. This software is aligned with current trends to develop different packages assisting the viscoelastic characterization according to another commonly used methodologies, such as for example the Closed-Form Shift algorithm (CFS) developed by Gergesova et al. (2011), or those incorporated in machine-testing systems, for example T. A. Orchestrator, for applying the classical Williams-Landel-Ferry model (see Orchestrator (2008)).

This chapter is devoted to illustrate how ProVisco can be used in practice, being organized in two main parts. Firstly, a brief description of the main steps of the software is presented with a practical example for the experimental data of polyvinyl-butyril (PVB) used in previous chapters. Secondly, some further applications of the software are suggested based on the advantages of the proposed models related to the viscoelastic characterization.

7.2 Description of the Software Program

The current version of ProVisco software is focused only on the evaluation of the relaxation modulus under static tests, E , while another viscoelastic functions and interconversions to the dynamic functions are not still included. The basic steps for using this software program are described below:

1. *To create a new project.* The first step consists in creating a new project on the menu bar corresponding with the experimental campaign to be used (see Figure 7.1). Also a previous project can be loaded in this menu.

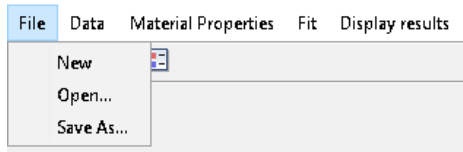


Figure 7.1: To create a new project step in the menu bar of the software ProVisco.

2. *To load the experimental data.* As the input data, the software requires the experimental short-term curves for the relaxation modulus at various temperatures, which can be loaded in the menu bar (*Partial Curves*), as can be seen in Figure 7.2. Only files denoted in the form of ' $T1.txt$ ', ' $T2.txt$ ', etc., are recognized by the software, where $T1$, $T2$ represents the numerical value of the temperature in the corresponding relaxation test in Celsius (e.g. ' $-20.txt$ ' or ' $40.txt$ '). The format data for each file is a two-column matrix, with the time values and relaxation modulus values in the first and second columns, respectively. This menu also allows the user to load a master curve defined at a certain reference value (*Master Curve*), which can be built with any other TTS models, being of interest for comparison purposes. Automatically, ProVisco displays the experimental short-term curves and the master curve side by side recently uploaded, aiming the program to be transparent for the user in each of the steps.

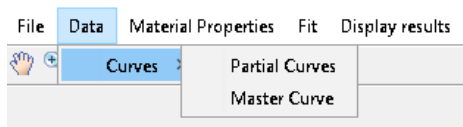


Figure 7.2: To load the experimental data step in the menu bar of the software ProVisco.

3. *To define the material properties.* As material properties, the software program only needs the reference glassy and rubbery temperatures in Celsius

degrees, T_g and T_r , respectively (*Temperatures*) for defining dimensionless variable T^* , according to the dimensional analysis in Eq. (6.9), as can be seen in Figure 7.3. Any other two reference temperatures can also be used apart from the suggested rubbery and glassy temperatures.



Figure 7.3: Definition of the material properties step in the menu bar of the software ProVisco.

4. *To fit the statistical model.* Once the experimental data and the material properties are introduced, the proposed models based on the scale-effect property can be applied, namely, Normal model in Eq. (6.32) (*Normal*) and Gumbel model in Eq. (6.34) (*Gumbel*), as can be seen in Figure 7.4. As an additional option, the software also includes the possibility of using the Weibull distribution alternatively to the Gumbel one (*Weibull*). The user must take into account that Normal model provides certainly the estimation of the short-term curves with the minimum error for the whole range of time and temperatures, while Gumbel and Weibull models must be considered as asymptotic ones, particularly recommended for estimating the limiting values in a more reliable manner.

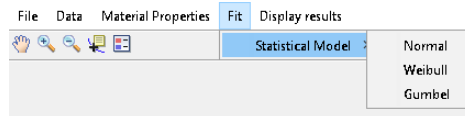


Figure 7.4: To fit the statistical model step in the menu bar of the software ProVisco.

5. *To display the results.* After the estimation of the selected model in the previous step, the software offers two display modes for showing the results (see Figure 7.5): a) to display the short-term experimental curves side-by-side with the master curve introduced by the user (*Experimental and Master*) and b) to display the experimental short-term curves superposed with the theoretical curves according to the selected model side-by-side with the resulting Q^* factors and their exponential theoretical law (*Experimental and Q Factors*), as illustrated in Figure 7.6.
6. *To predict the master curves.* As one of the most interesting contributions of the models proposed in this thesis, the master curve for any temperature over time can be straightforwardly obtained without additional calculations, since the $E^* - t^*$ field and the Q^* factor function are analytically

defined for each of the proposed models. The software also shows the corresponding Q^* factor value for the predicted master curve, according to its exponential definition (*Master Curve Prediction*), as can be seen in Figure 7.7.



Figure 7.5: Selection of the display mode in the menu bar of the software ProVisco.

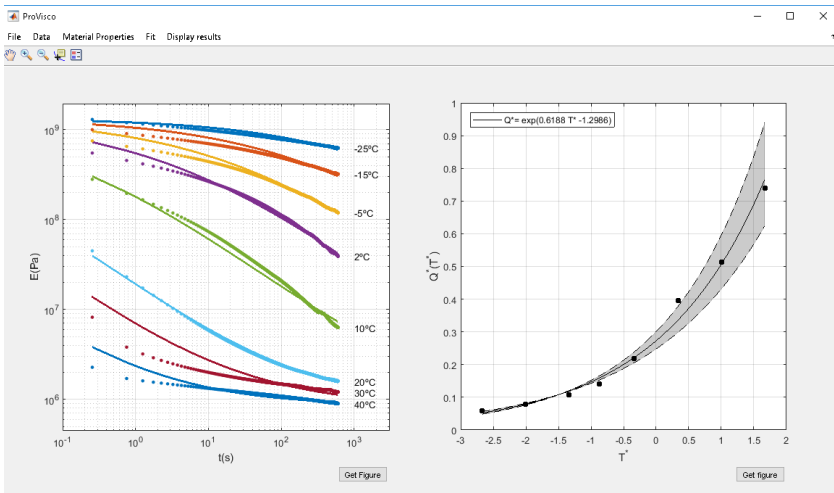


Figure 7.6: Illustration of the display mode Experimental and Q factors in software ProVisco.

7.3 Main ProVisco Applications

Finally, this section summarises some of the most interesting applications of the ProVisco software:

- a) *Viscoelastic material characterization.* This software allows the experimental data from relaxation tests at various temperatures to be introduced by the user, directly obtaining the analytical definition of the relaxation modulus for every combination of time and temperature in a unique step, without

requiring the overlapping between the short-term curves obtained by the experimental campaign.

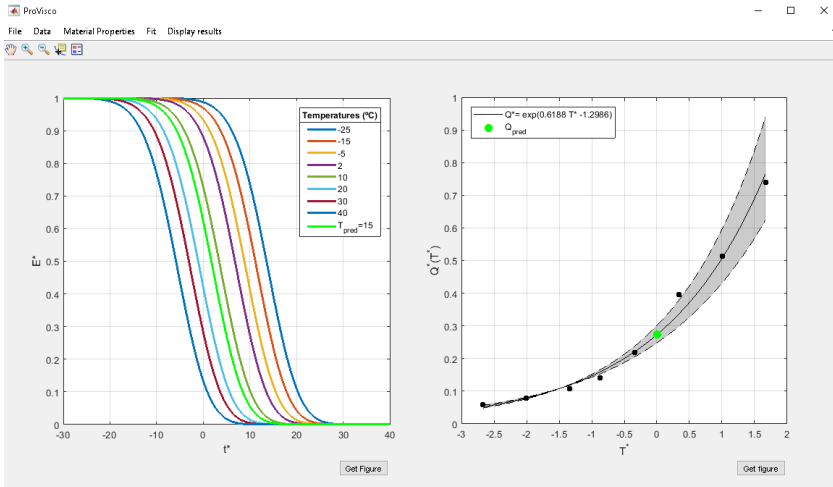


Figure 7.7: Illustration of the display mode Master Curve Prediction in the software ProVisco.

- b) *Prediction of viscoelastic properties.* Due to the analytical definition of the Q^* factors, the prediction of the master curves for any other reference temperature than those have been tested can be easily performed with this software without any additional calculations. As a result, the time evolution of the relaxation modulus can be obtained for any service condition of interest.
- c) *Determination of the limiting values.* Supported by the extreme value theory, the limiting values of the relaxation modulus can be conveniently determined by using the extreme value family of distributions in a more reliable manner than the current existing methods.
- d) *Comparison with other TTS models.* ProVisco software allows the master curve of the material at a given reference temperature, obtained with any other TTS model, to be introduced by the user, what is interesting from a practical point of view. Indeed, a critical comparison among different methodologies and the proposed one can be performed assessing the user to make decisions in the practical design.
- e) *Connection with Finite Element Method packages.* The current model libraries for viscoelastic materials in finite element programs, such as Abaqus or Ansys, are based on the Prony series and the user must introduce the parameters from an external estimation program. Alternatively, a modified material properties could be created in these libraries based on the models proposed in this thesis, since the mathematical expressions for each model

are provided by ProVisco and consequently loaded by the finite element program. As a result, the simulations with viscoelastic materials can now be performed taking advantage of the proposals and their applications.

8

Extension to Related Viscoelastic Phenomena

8.1 Introduction

The proposed models for viscoelastic characterization developed in Chapter 6 were focused and formulated on the temperature effect, being currently preferred for applying the TTS principle dealing with the long-term behaviour of the viscoelastic materials, besides pressure effect with lesser extent. However, there exists a large variety of additional external effects appearing frequently in real service conditions of viscoelastic components, such as for example the moisture, physical ageing or curing effects, among others, being also used in the viscoelastic characterization in an equivalent manner to the temperature case. For this reason, this chapter is devoted to illustrate how previous proposed models can be directly extended for dealing with other effects of practical importance.

Previous proposals were formulated in terms of the relaxation modulus among the possible viscoelastic properties mentioned in Chapter 4. Nevertheless, the interconversion from the relaxation modulus to any other viscoelastic functions are also addressed in this chapter showing that the advantages provided by the proposals in this thesis can also be used in this interconversion.

Accordingly, this chapter is organized as follows. Section 8.2 illustrates how the proposed models can be used for estimating real experimental data with the

moisture effect. Section 8.3 discusses briefly the improvement of current methodologies dealing with the physical aging based on the proposals in this thesis, while Section 8.4 is focused on the curing effect. Finally, Section 8.5 illustrates how the interconversion from the relaxation modulus of PVB experimental data from previous chapters can be performed to derive the master curves directly for other viscoelastic moduli and compliances.

8.2 Moisture Effect

Polymeric materials frequently contain certain moisture concentrations affecting significantly to the relaxation and creep processes, especially for the thermoplastic polymers (see Emri and Pavsek (1992)), as occurs for example in the practical design against creep fracture of wooden components in structures (see Tissaoui (1996)). From an experimental point of view, this effect was found to act similarly to the temperature one, as indicated by Onogi et al. (1962), Knauss and Kenner (1980), Knauss and Emri (1981), Knauss and Emri (1987) and Emri and Pavsek (1992), such that the TTS principle has been conveniently converted to Time-Humidity Superposition (THS) principle, originally coined by Onogi et al. (1962).

Hence, the dimensional analysis of the moisture effect problem involves the following variables:

$$\nu \equiv \{\Delta E, \Delta E_0, H, t, t_r\}, \quad (8.1)$$

where H represents the moisture defined as percentage¹ and t_r as some reference value of time. Then, according to the Buckingham's Theorem (Buckingham (1915)), the initial set of involved variables in (8.1) can be transformed, without loss of generality, into the equivalent set:

$$f(E^*, t^*, H^*) = 0, \quad (8.2)$$

such that if the interest lies on specifying the relaxation modulus E^* , then Eq. (8.2) must be rewritten as follows:

$$E^* = g(t^*, H^*), \quad (8.3)$$

with $t^* = \log(t/t_r)$ such that $t_r \neq 0$ and $g(\cdot)$ as the function of interest.

In order to illustrate the applicability of the proposed models based on the scale-effect property with the moisture effect, the Gumbel model based is considered to be applied to the experimental data retrieved from Onogi et al. (1962) for a polyvinyl alcohol films (PVA) in uniaxial relaxation test considering seven grades of moisture ($H(\%) = 0, 33, 43, 52, 57, 63.5, 71.2$). By applying the same steps than those described in subsection 6.4.3 for the case of the temperature effect, the estimates of the Gumbel model are listed in Table 8.1.

¹Note that H is dimensionless by itself.

Table 8.1: Estimates of the Gumbel model based on the scale-effect property applied to PVA experimental data from Onogi et al. (1962).

Model	Parameters					
	$\log E_0$	$\log E_\infty$	λ	δ	θ_0	θ_1
Gumbel	25.0727	22.896	-0.525	2.983	-4.4056	0.0567

Thus, the final expression of the Gumbel model for the moisture effect on the relaxation modulus when analyzing the experimental data of the PVA film is the following:

$$E^*(t^*; H^*) = \exp \left[- \exp \left(\frac{t^* - 0.169H^* + 12.617}{2.983} \right) \right], \quad (8.4)$$

being illustrated in Figure 8.1 the resulting theoretical short-term curves and the master curves along the time for the Gumbel model for different values of the moisture effect.

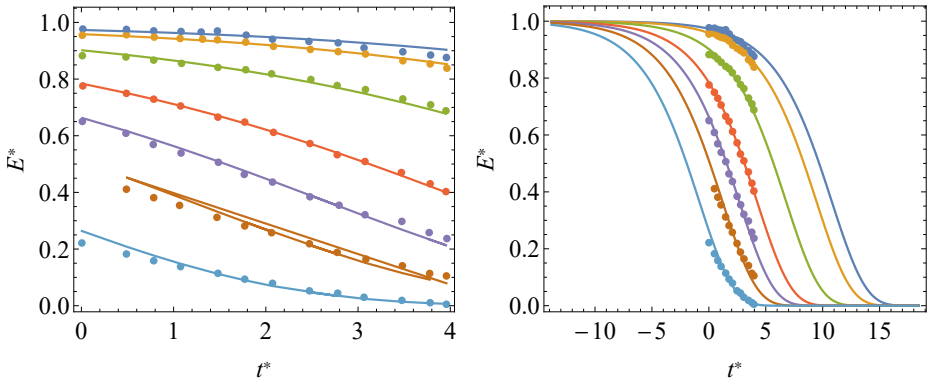


Figure 8.1: Experimental short-term curves at various moisture grades from Onogi et al. (1962) and theoretical Gumbel model (left) with the corresponding master curves for the whole range of time (right).

8.3 Physical Ageing

Initially denoted by Struik (1977), the ageing phenomena, either physically or chemically induced, has been widely studied (see for example Struik (1977), Janas and McCullough (1987), Sullivan (1990), Brinson and Gates (1995), Hutchinson (1995), Bradshaw and Brinson (1997), Martin (2012) and Hutchinson and Cortés (2018), among others). In both cases, the ageing term describes the variation of the mechanical properties of a viscoelastic material due to the time storage,

at constant temperature, at zero stress and under no influence from any other external conditions (see Hutchinson (1995)). In other words, the viscoelastic properties of a polymer will vary during time even when any forces are applied. Consequently, the mechanical response of a viscoelastic material is certainly a function of the storage time or ageing time. Examples of engineering applications in which this effect is important are the manufacturing of composite materials, permeability of materials for packaging, adhesives and glass-metal joint seals (see Riande et al. (1999)).

As in the case of the moisture effect, the TTS principle has been successfully applied to the ageing problem by Struik (1977) under the thermorheologically simple materials condition. Thus, consider an experimental campaign of physical ageing in which a viscoelastic materials is *aged* during two different times t_{e_1} and t_{e_2} . Then, if a relaxation test is performed once these times have occurred, the relation of the short-term curves of the relaxation modulus between these two different ageing times are defined as follows:

$$E(\log t; t_{e_2}) = E(\log t + \log a_{t_e}(t_{e_2}, t_{e_1}); t_{e_1}), \quad (8.5)$$

where $E(t; t_e)$ is the relaxation modulus along the time for an ageing time t_e and a_{t_e} the corresponding shift factor for physical ageing effect.

Regarding to the definition of the shift factor in this physical ageing, the Kohlrausch-Williams-Watts model is frequently used, as can be seen in Cowie et al. (1998) and Hutchinson and Cortés (2018). Nevertheless, the proposed models in this thesis may be also applied to this effect, as for example the normal or Gumbel models, equivalently to the moisture effect. In this case, the transformation within two different states of physical ageing t_{e_1} and t_{e_2} can be alternatively defined according to the scale-effect property in Eq. (6.24) as follows:

$$E^*(t^*; t_{e_2}^*) = E^*(t^*; t_{e_1}^*)^{a_{t_e}(t_{e_2}^*, t_{e_1}^*)}. \quad (8.6)$$

More recently, the effect of physical ageing has been studied with the simultaneous effect of the temperature, which shows more practical interest for being closer to the real conditions in service (see Lin et al. (2011) and Hou and Chen (2012)).

8.4 Curing Effect

The manufacturing of polymeric materials is always confronted with the curing process due to the transformation from liquid to solid states. During this process, residual stresses and warpages frequently appear modifying the mechanical properties of the resulting materials, which is known as the curing effect. Thus, the development of mathematical models allowing to predict the final mechanical properties is of great relevance (see Kim and White (1996), Sadeghinia et al. (2012), Li and Zhang (2016) and Saseendran (2017)).

Equivalently to previous moisture and physical ageing effects, the master curves for a given curing degree of reference has been conveniently constructed by means of a shift factor $a_\alpha(\alpha)$ at a given curing degree α . However, the research is focused not only in the curing effect, but also in the combination with temperature simultaneously due to the inherent interrelation within them. As a result, the current methodologies deal with two shift factors, one for temperature $a_T(T)$ and another for curing degree $a_\alpha(\alpha)$, whose are usually referred to as *dualistic shift factor* (see Lin et al. (2011)). Then, the application of the TTS principle is in two terms as follows:

$$\log E(\log t; T, \alpha) = \log E(\log t + \log a_T(T, T_0) + \log a_\alpha(\alpha, \alpha_0); T_0, \alpha_0), \quad (8.7)$$

such that if only the temperature or curing degree is changed, then one of both shift factor are null and the classical TTS principle is obtained for temperature or curing, respectively.

Nevertheless, even when only the curing effect is considered, the resulting shift factors for the curing effect are not usually arranged in a WLF-type equation and an exponential is preferred instead, as can be seen in Lin et al. (2011), that is,

$$\log a_\alpha(\alpha, \alpha_0) = C_0 + C_1 \exp(C_2 \alpha), \quad (8.8)$$

for some constants C_0, C_1 and C_2 .

Unfortunately, there is no explicit mention about the uniqueness condition in this kind of twofold transformations, that is, when both curing and temperature effects act simultaneously, which must be imposed in any case for deriving feasible definitions of the dualistic shift factor. To this end, consider the simultaneous transformations from a given temperature and curing degree (T_0, α_0) to another combination (T_1, α_1) and (T_2, α_2) , such that the functional equation obtained representing the uniqueness condition for the curing effect is:

$$\begin{cases} \log a_\alpha(\alpha_2, \alpha_0) = \log a_\alpha(\alpha_2, \alpha_1) + \log a_\alpha(\alpha_1, \alpha_0), \\ \log a_T(T_2, T_0) = \log a_T(T_2, T_1) + \log a_T(T_1, T_0), \end{cases}$$

which is the well-known Sincov functional equation. Then, the solution for the feasible condition in the dualistic shift factor is as follows:

$$\begin{cases} \log a_\alpha(\alpha, \alpha_0) = m_2(\alpha) - m_2(\alpha_0), \\ \log a_T(T, T_0) = m_1(T) - m_1(T_0), \end{cases}$$

for two arbitrary functions $m_1(\cdot)$ and $m_2(\cdot)$ whose must be experimentally determined. Once this uniqueness condition has been conveniently derived, the scale-effect property may be used alternatively of (8.7), such that:

$$E^*(t^*; T^*, a_\alpha) = E^*(t^*; T_0, \alpha_0)^{a_T(T^*, T_0)^{a_\alpha(\alpha, \alpha_0)}}, \quad (8.9)$$

where α is already dimensionless since is usually defined as a percentage.

8.5 Interconversion among Viscoelastic Functions

The interconversion between different viscoelastic functions is of great relevance in the characterization of viscoelastic materials, as has been indicated in Chapter 4. For this reason, this section illustrates how previous models can also be used with experimental data for obtaining the creep compliance $D(t)$ from the relaxation modulus $E(t)$, together with the dynamic components, that is, the storage modulus $E'(\omega)$ and the loss modulus $E''(\omega)$, despite of being the models more complex from a functional point of view in comparison with the classical ones based on simple exponentials. Moreover, all the master curves in any other viscoelastic moduli can be directly obtained or predicted by using these proposals once the relaxation modulus has been estimated, without resorting to any superposition of the short-term curves nor the Prony series. To this end, the experimental campaign of the polyvinyl butyral from previous chapters is considered once more, from which the relaxation modulus has been already estimated, and the interconversions provide the rest of the viscoelastic functions for the static and dynamic cases.

8.5.1 Relaxation and creep functions

It is well-known that the relaxation modulus $E(t)$ and creep compliance $D(t)$ are analytically related by means of the following expression (see Ferry (1980) or Lakes (2009)):

$$\int_0^t E(\tau)D(t-\tau)d\tau = t, \quad (8.10)$$

such that it is satisfied $E(t)D(t) \leq 1 \forall t$. Thus, by applying the Laplace transform, it results the relation between these two properties in terms of the Laplace variable s , that is,

$$D(s) = \frac{1}{s^2 E(s)}, \quad (8.11)$$

such that by applying this relation with the Laplace transformation of the relaxation modulus defined according to one of the proposed models, the creep compliance can be directly obtained.

In particular, the normal model in Eq. (6.52), as an example from those based on the scale-effect property, and the Gumbel-Gumbel model in Eq. (6.56), as example from those based on the compatibility condition will be used. Note that despite the lack of analytical definition for the cdf of the normal distribution, any current software of numerical or symbolic computations, such as Matlab or Mathematica, can provide suitable approximations for its Laplace transform. Care must also be taken with using expressions like Eq. (8.11) implying the relaxation modulus $E(t)$, since the proposed models use the normalized expression E^* , such that the latter must be transformed to the former by undoing the changes according to the dimensional analysis in Eq. (6.9).

Figure 8.2 illustrates the resulting master curves for the creep compliance D

at different temperatures for the case of the normal model once the numerical computations have been done according to Eq. (8.11). Note that the master curves of the creep compliance D result being horizontally displaced as expected, as occurs with the relaxation modulus E . Alternatively, the Gumbel-Gumbel model is more complete than the normal one, since now both location λ and scale δ parameters are modified with temperature according to Eq. (6.56), while in the normal model only location μ varies with temperature. As a result, the master curves are not only horizontally displaced, but also their scale parameters are changed.

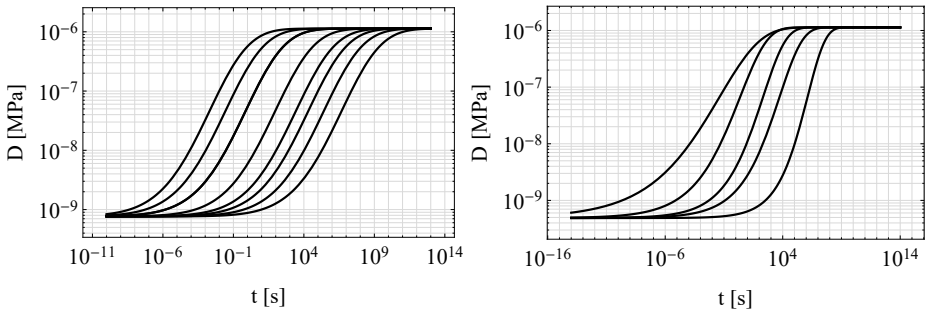


Figure 8.2: Creep compliance D at different temperatures after the interconversion based on the normal model (left) and Gumbel-Gumbel model (right) for PVB experimental data.

Nevertheless, it must be mentioned that the computational calculations of the Laplace transform of these statistical distributions result with a higher cost in comparison with a series of exponential functions, such as the case of Prony approach, due to the complexity of their functional forms. In turn, the main advantage of the proposed methodology in the interconversion among viscoelastic functions is the direct derivation of the master curves for any temperature for the creep compliance once the relaxation modulus has been estimated. In fact, the interconversion in the current methodologies can only be applied individually, that is, from one master curve in the relaxation modulus to another in the creep compliance individually.

8.5.2 *Static and dynamic functions*

As an additional interesting interconversion among viscoelastic functions, the storage $E'(\omega)$ and the loss moduli $E''(\omega)$ can also be obtained from the relaxation modulus $E(t)$ by means of the Fourier transform according to the Eqs. (4.54) and (4.55), respectively (see Findley et al. (1976, p. 102) and Ferry (1980, p. 68)), being not reproduced here for the sake of brevity. In this case, both normal and Gumbel-Gumbel models are considered again for the interconversion to the dynamic components in order to illustrate how they can be used in this

complementary interconversion.

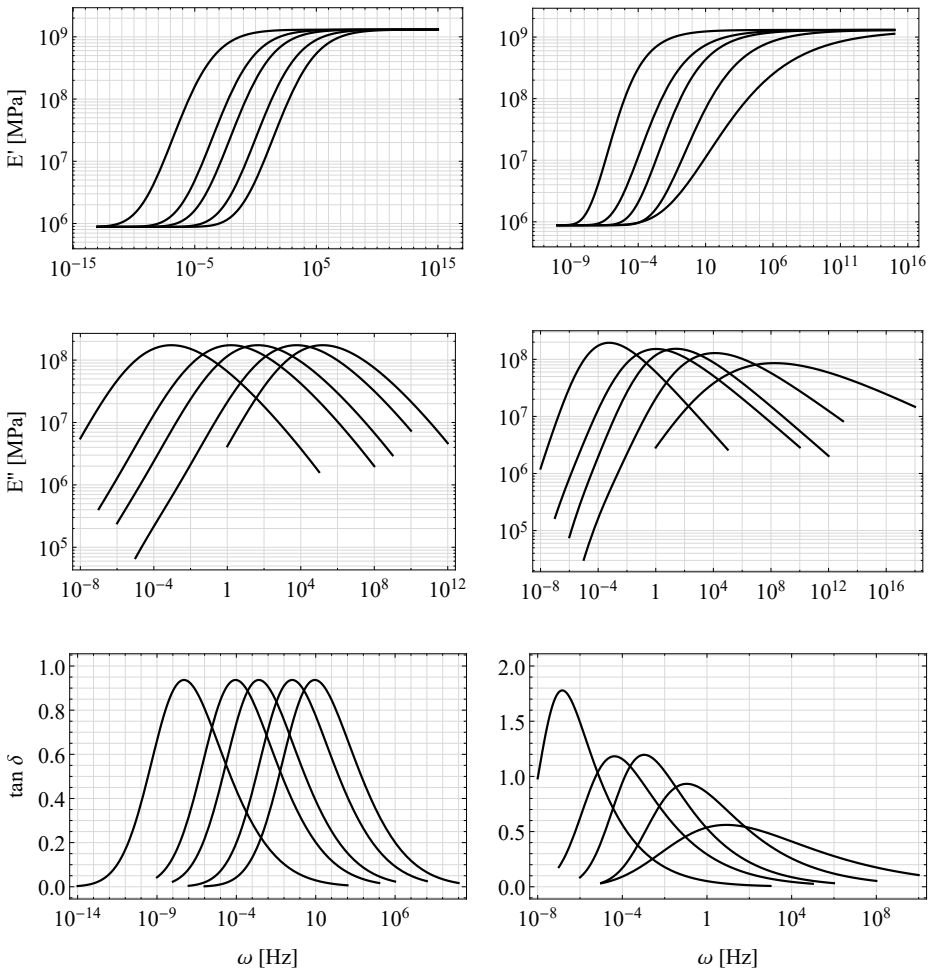


Figure 8.3: Storage modulus E' (upper), loss modulus E'' (middle) and the loss tangent $\tan \delta$ (lower) for the normal (left) and Gumbel-Gumbel (right) models with the PVB experimental data.

Figure 8.3 shows the resulting master curves of the viscoelastic functions $E'(\omega)$, $E''(\omega)$ and $\tan \delta(\omega)$ at different temperatures according to the normal and Gumbel-Gumbel models for the PVB experimental data once the Fourier transform has been obtained. In the first case, the dynamic modulus are also horizontally displaced due to the effect of the temperature, while in the second case a combination of location and scale are applied to the curves between different temperatures. This effect can be especially seen in the $\tan \delta$ plot. In any case, both models allow any master curve at any reference temperature to be directly

obtained for all of the dynamic viscoelastic functions with once the estimation of the short-term curves of the relaxation modulus has been accounted for.

8.6 Concluding Remarks

In this chapter, some of the proposals for describing the temperature effect on the viscoelastic properties are further extended to consider another external effects of practical relevance, such as the moisture, curing degree and physical ageing. Additionally, the problem of interconversion among the viscoelastic functions is also addressed, indicating that the proposed models also allow the master curve at any reference temperature to be derived for the creep compliance and the dynamic components directly from the estimation of the short-term curves of relaxation modulus at different temperatures. More precisely, the experimental data with polyvinyl-butyril from previous chapters is used for deriving all of these viscoelastic functions from the estimation of the relaxation modulus performed in Chapter 6.

IV

Fracture Characterization Models

9

Notch and Temperature Effects in Fracture of Metals

9.1 Introduction

The presence of notches, notched-type defects and their influence on the fracture and fatigue behavior of materials is widely discussed in the literature due to their practical importance in the design of structural and mechanical components, closely related to the structural integrity assessment. In a broad sense, a notch can be defined as any discontinuity in the shape or non-uniformity in a material (see Yen and Dolan (1952)) arising from manufacturing, in-service defects (e.g. corrosion pits, impact indentations or inclusions) and unavoidable geometrical features in the design of components (e.g. holes, rivets, fillets or grooves). The stress distribution in a specimen presents local concentrations around the notch tip, denoted stress risers, due to the existence of such irregularities that promote fatigue crack initiation and subsequently early failures when a cyclic loading is applied (see Glinka and Newport (1987)).

The failure of notched components is traditionally analyzed from two main perspectives (see Taylor (2007)). Firstly, some notches are found to behave similarly to the corresponding smooth specimens, in which the failure occurs when the local stress reaches the specimen critical strength. Secondly, the so-called sharp notches are usually categorized as a sharp crack of the same length. In such a

case, the failure is supposed to occur when the stress intensity factor reaches the fracture toughness of the material. Unfortunately, this failure criterion leads to overly conservative failure predictions (see Pluinage (1998), Bao and Jin (1993), Cicero et al. (2008), Cicero et al. (2011a) and Radaaj (2014)). For these reasons, the research is focused on the development of more accurate notch failure models corresponding to real cases, the design of which lies between the concept of notch stress intensity factor (NSIF) and that of notch fracture toughness. However, all of these methodologies and approaches are based on a deterministic definition of the fracture properties of the materials, being the most important limitation since their inherent randomness is not negligible, as pointed out by Wallin (1984a).

However, the real service conditions of structural and mechanical components are not only concerned with the presence of notches, but also with other concurrent significant external effects, such as for instance the temperature. In fact, the temperature is found to be one of the most influencing external factors in the fracture behaviour, particularly, in metallic materials. Despite the concurrency of different effects, the current methodologies treat them as they act independently of each other, such as those only focused in the notch effect previously mentioned.

For this reason, to achieve reliable failure predictions in engineering design, it is necessary to develop new models capable of considering the simultaneous action of different effects. There are further reasons related to the problem of materials characterization that justify this search to look for such new models. Frequently, researchers and engineers are confronted with the assessment of heterogeneous experimental results from different specimen and test conditions to characterize a certain material. This problem, related to the transferability problem, can be conveniently solved with the consistent methodology, denoted Generalized Local Model, proposed by Muñiz-Calvente (2017), allowing the results from heterogeneous test conditions to be jointly assessed.

Accordingly, this chapter aims to achieve three objectives:

1. To develop a probabilistic methodology to independently model the influence of the notch effect on the fracture resistance of metallic materials, as a function of the notch root radius. The theory of critical distances, as one of the most widely methods presently used to define the fracture resistance of materials, is improved in a probabilistic sense. In this way, the inherent randomness to the material properties is taking into account in the fracture characterization.
2. To develop a probabilistic methodology to take into account the simultaneous effect of notch and temperature on the fracture resistance of metallic materials. To this aim, two different models are proposed: The first one is an extension of the previously mentioned approach to handle the notch effect. It implies assuming the temperature to act as a scale effect on the statistical distribution of the notch fracture toughness, i.e. similarly to the temperature effect case in the viscoelastic analysis proposed in Chapter 6. The second one is based on the compatibility condition between the statis-

tical distributions of the notch fracture toughness for given the temperature and viceversa.

3. To apply Bayesian techniques to assess fracture data under notch and temperature effects, as an extension of the two above methodologies. This allows the probabilistic analysis of the fracture resistance properties of metals to be enhanced (see Anderson (2017, Chapter 5)).

As can be seen, the models previously proposed for viscoelastic characterization in Chapter 6 are now applied to a different research topic to derive probabilistic methodologies for fracture characterization. In this way, a general formulation based on sound statistical concepts is proved to be a suitable methodology for model building.

The organization of this chapter is as follows. Firstly, a brief overview of the currently used methodologies for fracture characterization is presented in Section 9.2, either focused on the influence of the notch or the temperature effects. Secondly, the proposed probabilistic methodology focused solely on the notch effect is derived in Section 9.3. Thirdly, the proposals to model simultaneously the notch and the temperature effects are derived in Section 9.4. A distinction is made between the models based on the scale-effect and those based on the compatibility condition, being the latter also extended using the Bayesian techniques. Fourthly, Section 9.5 illustrates how the proposed methodologies can be used in practice to model both the notch or temperature effects, either separately or acting simultaneously, by considering an external extensive experimental campaign of fracture tests with different notch radii and at different temperatures. Finally, Section 9.6 summarizes some concluding remarks.

9.2 Current Methodologies

9.2.1 Influence of the notch effect

In principle, three different approaches are distinguished in the literature to analyze the notch effect, namely, the global, the local and the non-local fracture criteria (see Pineau (1992)). In the first case, the entire specimen is considered to define the stress and strain fields to assess if the critical value of the NSIF is reached, in a similar manner as proposed by the linear elastic fracture mechanics or elastic-plastic fracture mechanics using the parameters K_{IC} or J_{IC} .

In contrast, the more recently developed local and non-local approaches only use the stress and strain fields in the neighbourhood of the notch tip. Between these two last methods, the non-local approach considers not only particular points, such as the local one (see, for example, Peterson (1953), Neuber (1958), Pilkey and Pilkey (2008) and Matvienko (2004)), but also additional information surrounding a certain volume, so that not always is straightforward to distinguish between them (see Justo et al. (2017)).

Among other existing methods in the literature, the theory of critical distances (TCD) is hereafter proposed thus allowing an extension from its current deterministic formulation to a new probabilistic conversion to be achieved.

The comprehensive development of the TCD, despite being inspired by the early works of Neuber (1961) and Peterson (1959), is only recently achieved by Taylor (2007) and favored by the latter improvement of the finite element stress analyses. The main advantage of adopting the TCD approach is to provide simple formulations for a large variety of applications in fracture with a diversity of materials (metals, ceramics, polymers, composites and rocks) and behaviour conditions (linear-elastic, elastoplastic).

The TCD is not really a model, but a family of models, namely the point method (PM), the line method (LM), the area method (AM) and the volume method (VM), all of them sharing the concept of the central parameter known as the critical distance L . As the simplest version of the TCD, the PM establishes that the brittle fracture will occur when the stress distribution around the notch field $\sigma(r)$ reaches a characteristic stress value σ_0 at a distance $L/2$, that is,

$$\sigma\left(\frac{L}{2}\right) = \sigma_0, \quad (9.1)$$

where the L parameter is defined as a characteristic of the material by the expression:

$$L = \frac{1}{\pi} \left(\frac{K_c}{\sigma_0} \right)^2, \quad (9.2)$$

and K_c is the critical stress intensity factor, i.e. the fracture toughness of the material. The critical stress value σ_0 must be calibrated, being usually larger than the ultimate strength of the material σ_u . It is worth noting, as suggested by Taylor (2007, Chapter 13), the possible physical interpretation of the L parameter, which governs the failure mechanism.

As a natural extension of the point method, the line method implies the evaluation of the average of the stress distribution over a certain distance d , rather than the evaluation of the stress distribution at a distance $L/2$, that is,

$$\frac{1}{d} \int_0^d \sigma(r) dr = \sigma_0. \quad (9.3)$$

In other words, the fracture will occur when the average of the stress distribution over the interval $[0, d]$ reaches the critical value σ_0 .

Particularly, the failure of notched components represents one of the most relevant practical applications in which the TCD method is successfully applied.

From a theoretical point of view, this applicability is limited to those situations in which the fracture behaviour conforms to the criteria of Linear-Elastic Fracture Mechanics (LEFM), as indicated by Taylor (2007). In these cases, the TCD approach provides simpler formulations than those from the classic models, such

as the proposed by Creager and Paris (1967):

$$\sigma(r) = \frac{K}{\sqrt{\pi}} \frac{2(r + \rho)}{(2r + \rho)^{3/2}}, \quad (9.4)$$

which approximates the stress field near the notch root, for notches of length a and root radius ρ , though only for $\rho \ll a$, being K the stress intensity factor. Thus, if the LM approach is considered, substituting Eq. (9.4) into Eq. (9.3) allows the equivalent expression of the measured notch fracture toughness K_c^N to be predicted (see Taylor (2007, chapter 7)):

$$K_c^N(\rho; L) = K_c \sqrt{1 + \frac{\rho}{4L}}, \quad (9.5)$$

using the critical distance L as the model parameter. Note that K_c in Eq. (9.5) can be understood as a certain $K_c^N(\rho_0)$ for $\rho_0 = 0$ representing the characteristic fracture toughness of the material, that is, for the smooth specimen. As a consequence, the notch fracture toughness K_c^N results as the fracture toughness of the material K_c multiplied by a factor provided by the TCD approach, which is a function of ρ and L .

Experimental data is fairly described by this expression, as corroborated by several works, such as for instance Cicero et al. (2011a), Cicero et al. (2011b) and Justo et al. (2017). Figure 9.1 shows a typical set of experimental data representing the measured fracture toughness of a ferritic steel as a function of the notch root radius, fitted according to the TCD model given by Eq. (9.5).

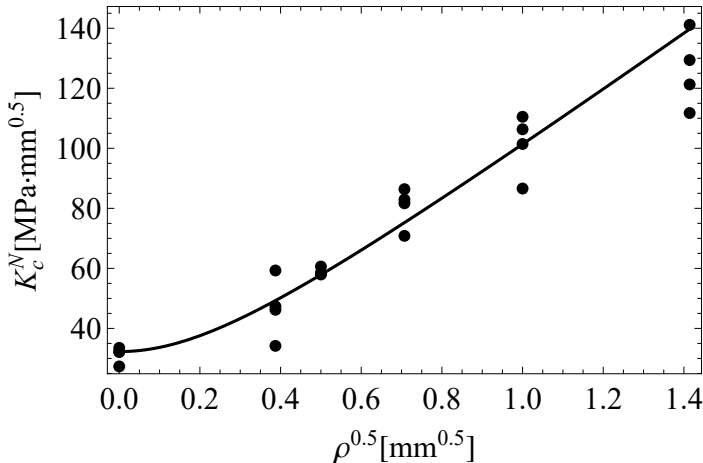


Figure 9.1: Example of application: notch fracture toughness vs. different notch radii for a ferritic steel fitted according to the TCD method ($L = 0.028$ mm and $K_c = 32.276$ MPa·mm^{0.5}).

Despite being widely accepted, the main limitation of the TCD method hap-

pens to be the same as that present in the current methodologies, namely, the deterministic concept to determine the fracture toughness for each of the notch radii considered. In this way, the random character of the results evidenced by the scatter of the failure data for a given notch radius is unjustifiably overlooked (see Figure 9.1). For this reason, the development of probabilistic approaches is mandatory to take into account the influence of the inherent scatter of these variables on the fracture characterization and subsequently in the component design.

9.2.2 Influence of the temperature effect

The effect of the temperature on the fracture resistance of materials has been widely investigated over the last decades, particularly on that of metallic materials (see Ritchie et al. (1973) and Pineau (1981)), as one of the most influencing external effects. Indeed, the type of the fracture mechanism governing the failure could even vary from a brittle to ductile depending on the service temperature conditions to which the component is subject. Traditionally, the temperature dependence with the fracture toughness is represented by the well-known ductile-to-brittle transition curve for metallic materials, in which three zones may be distinguished (see Figure 9.2):

- a) *Lower shelf.* This region corresponds the lowest temperatures, in which the fracture mode occurs by cleavage. As the temperature increases, the fracture toughness of the material grows up rapidly from a minimum value K_{\min} , showing a concave curvature.
- b) *Intermediate shelf.* Usually referred to as the ductile-to-brittle zone, it represents the region with the fastest growth of the fracture toughness, in which both cleavage and ductile or tearing instability may occur. The characteristic transition temperature T_{crit} marks the change from concave to convex denoting the transition from brittle to ductile (or viceversa) failures, a relevant issue in the design of structural components.
- c) *Upper shelf.* At high temperatures, the fracture toughness reaches its maximum value K_s while the failure is governed by ductile instability or plastic collapse.

The brittle-to-ductile transition curve is built from experimental data by recording the random fracture values. This implies that the evolution of the fracture toughness with the temperature is not a continuum process, but a discrete one. Among the three shelves observed, the researchers focus their attention on the lower and the ductile-to-brittle ones, because of the practical importance of the hazard of a failure mechanism change that may occur in that zone.

Among the models proposed in the literature, the Master Curve method is the most used one. In fact, it is regarded in the international standards as the reference methodology for fracture characterization when the temperature

effect is considered (see ASTM ASTM 1820–11 (2011)). Originally developed by Wallin (1984c), this methodology assumes the fracture toughness K_c for a specimen of thickness B to pertain to a minimal Weibull distribution, such that,

$$F(K_c) = 1 - \exp \left[-\frac{B}{B_0} \left(\frac{K_c - K_{\min}}{K_0 - K_{\min}} \right)^b \right], \quad (9.6)$$

where K_{\min} represents the minimum value of the fracture toughness observed, b is the shape parameter, $B_0 = 25 \text{ mm}$ is a reference value for thickness and K_0 is the scale parameter of the distribution that, by definition, corresponds to the 0.632 probability. For a large variety of ferritic metallic materials, K_{\min} and b can be suitably approximated as $20 \text{ MPa}\cdot\text{m}^{0.5}$ and 4.

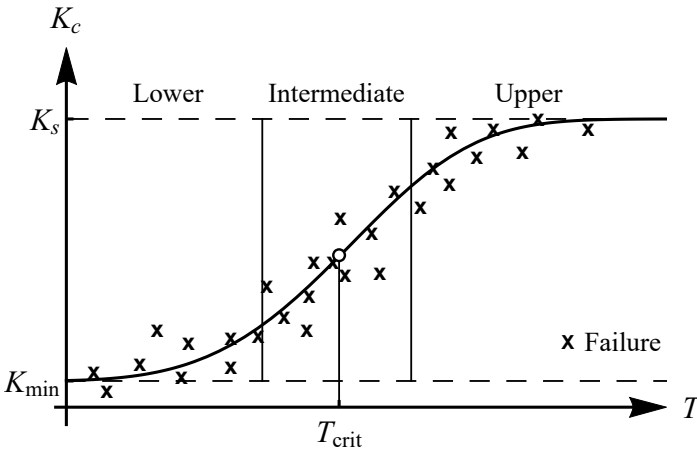


Figure 9.2: Schematic example of the brittle-to-ductile transition curve for a metallic material indicating the lower, intermediate and upper shelves.

Once the statistical distribution of the fracture toughness is identified, Wallin (1991) includes the temperature effect by assuming it acting as a change of the scale parameter K_0 in the Weibull distribution, given by

$$F(K_I; T) = 1 - \exp \left[-\frac{B}{B_0} \left(\frac{K_I - K_{\min}}{K_0(T) - K_{\min}} \right)^b \right], \quad (9.7)$$

with

$$K_0(T) = C_0 + C_1 \exp(C_2 T), \quad (9.8)$$

for the constants C_0, C_1 and C_2 (see Wallin (1984b)). The resulting parametric family of curves describes the $K_c - T$ field in both lower and intermediate zones, as illustrated in Figure 9.3, in which different density distributions of the fracture toughness may be observed for the different temperature values, according to the varying scale parameter given by to Eq. (9.8).

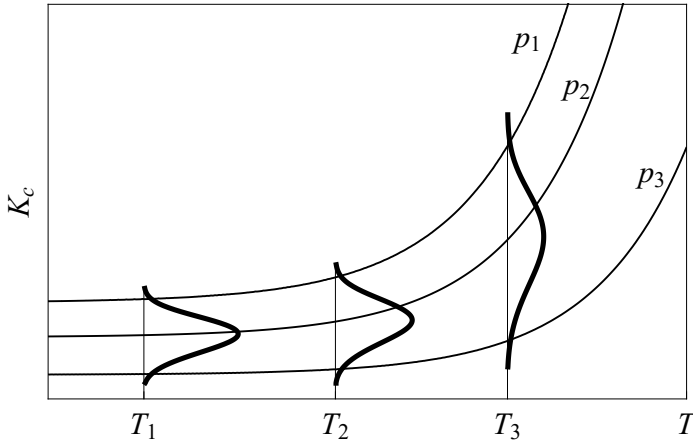


Figure 9.3: Illustration of the theoretical family of percentile curves of the $K_c - T$ field according to the master curve method, showing different density functions for some given temperature values.

The previous model is successfully applied to a large variety of ferritic steels, as reported by Wallin (1991), Wallin (1999b), Wallin (1999a) and Wallin (2002). However, the master curve method proves to show another interesting property, which justifies the designation of master curve. It was observed that the experimental $K_c - T$ field for different ferritic steels represents curves of similar shape, which match each other when these curves are simply displaced parallel to the T -axis. In this way, different experimental data may be fitted by horizontal shifting of the cdfs of the fracture toughness by redefining the initial definition of the scale parameter K_0 in Eq. (9.8), what requires to include the additional parameter T_0 :

$$K_0(T, T_0) = C_0 + C_1 \exp [C_2(T - T_0)], \quad (9.9)$$

where C_0, C_1 and C_2 are tabulated constants and T_0 is defined as a reference temperature, which varies specifically with the material. This horizontal shifting allows the results to be pooled into a unique master curve for a reference temperature. Note the similitude of this approach and that applied for the viscoelastic characterization based on the TTS principle. In the present case, the shift factors $a_T(T, T_0)$ are related to $K_0(T, T_0)$. However, the master curve for a certain material is now referred to the particular temperature value that provides a median fracture toughness of $100 \text{ MPa}\cdot\text{m}^{0.5}$ for a 25 mm thick specimen. The estimation process of the reference temperature T_0 is explained in detail in ASTM 1921-97 (2005).

Figure 9.4 illustrates the above transformations when applied to two different $K_c - T$ fields pertaining to different materials of the ferritic family, to yield one single master curve at the reference temperature T_0 , according to Eq. (9.9). As can be seen, the master curve method implies a horizontal shifting allowing the cdf of the fracture toughness to be represented as a unique master curve for all

the ferritic steels.

In summary, the practical interest of the master curve method lies on the fact that the experimental data of the fracture toughness recorded for a large variety of ferritic materials can be pooled together into a unique single master curve using one single parameter $K_0(T, T_0)$, allowing the lower and the intermediate shelves to be defined. In this way, several experimental campaigns involving different ferritic materials can now be jointly assessed for the fracture characterization.

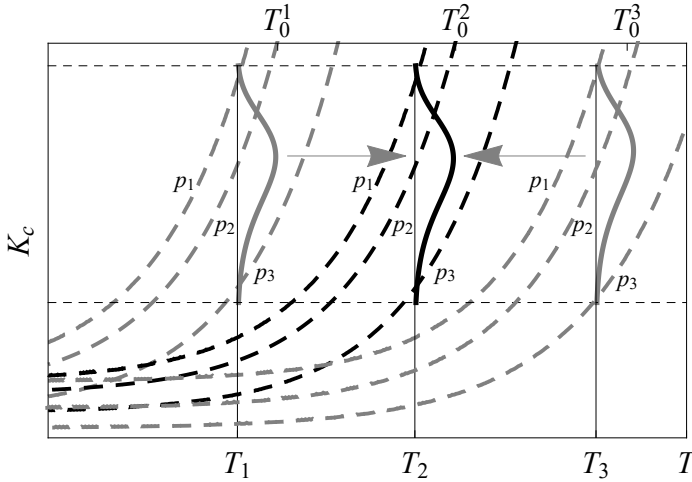


Figure 9.4: Schematic illustration of the process of master curve building process according to the master curve method for ferritic steels.

9.3 Proposed Methodology for Modelling the Notch Effect

In this section, the identification and formulation of some minimum conditions necessary to derive valid probabilistic models to deal with the notch effect are presented. They are later used to establish a statistical model based on both the Weibull distribution and the TCD method (see Muñoz-Calvente et al. (2019)). As a result, the notch fracture toughness K_c^N is calculated allowing its probabilistic distribution for a given notch radius to be determined. From an engineering point of view, this solution is more satisfactory and safe than that provided by the current deterministic models.

9.3.1 Minimal required conditions

As the first step in deriving a mathematical model to analyze the notch effect, some minimum necessary conditions must be formally defined:

1. *Physically valid formulas.* The two main variables involved in the study of the notch effect on the fracture resistance are the fracture toughness K_N and notch radii ρ . If both variables are subject to scale changes and the probabilistic model to be proposed is dimensional, the statistical functions involved must be stable with respect to scale changes in order the model to be valid. Otherwise, the model parameters will depend on the system of units selected, often leading to errors. Fortunately, most of the common continuous distributions are stable vs. scale changes (see Table 3.1).
2. *Uniqueness condition.* The transformation of the cumulative distribution function of the notch fracture toughness for a certain notch radius $K_c^N(\rho_1; L)$ into that corresponding for another notch radius $K_c^N(\rho_2; L)$ must satisfy the uniqueness condition. This implies that the distribution $K_c^N(\rho_3; L)$ obtained for a third notch radius from the transformations of both above distributions must be the same, i.e. independently of the origin considered in the transformation. To this end, let us consider the transformation according to the TCD proposal in Eq. (9.5) for two different notch radii ρ_1 and ρ_2 ,

$$\left. \begin{aligned} K_c^N(\rho_1; L) &= K_c \sqrt{1 + \frac{\rho_1}{4L}} \\ K_c^N(\rho_2; L) &= K_c \sqrt{1 + \frac{\rho_2}{4L}} \end{aligned} \right\} \Rightarrow \frac{K_c^N(\rho_2; L)}{K_c^N(\rho_1; L)} = \sqrt{\frac{4L + \rho_2}{4L + \rho_1}}, \quad (9.10)$$

from which it results that the notch effect can be written in a more general set as follows:

$$K_c^N(\rho_2; L) = K_c^N(\rho_1; L) Q_\rho(\rho_2, \rho_1), \quad (9.11)$$

where

$$Q_\rho(\rho_2, \rho_1) = \sqrt{\frac{4L + \rho_2}{4L + \rho_1}}. \quad (9.12)$$

This means that the transformation between different notch radii succeeds using a factor function only dependent of the initial and final values $Q_\rho(\rho_2, \rho_1)$. In order to derive the uniqueness condition, let us consider now the transformation implying three different notch radii ρ_1, ρ_2 and ρ_3 . According to Eq. (9.11), it follows that

$$K_c^N(\rho_2; L) = K_c^N(\rho_1; L) Q_\rho(\rho_2, \rho_1), \quad (9.13)$$

$$K_c^N(\rho_3; L) = K_c^N(\rho_1; L) Q_\rho(\rho_3, \rho_1), \quad (9.14)$$

$$K_c^N(\rho_3; L) = K_c^N(\rho_2; L) Q_\rho(\rho_3, \rho_2), \quad (9.15)$$

from which, in a similar way as in the viscoelastic case, it follows

$$\log Q_\rho(\rho_3, \rho_1) = \log Q_\rho(\rho_3, \rho_2) + \log Q_\rho(\rho_2, \rho_1), \quad (9.16)$$

which represents the well-known Sincov functional equation (3.32), the so-

lution of which is given by:

$$Q_\rho(\rho_2, \rho_1) = \exp [m(\rho_2) - m(\rho_1)], \quad (9.17)$$

where $m(\cdot)$ is an unknown function to be determined experimentally. Now the following question arises: is the uniqueness condition satisfied by the TCD proposal in Eq. (9.5)? To this aim, Eqs. (9.12) and (9.17) must be equated, leading to

$$\exp [m(\rho_2) - m(\rho_1)] = \sqrt{\frac{4L + \rho_2}{4L + \rho_1}} \Rightarrow m(\rho) = \frac{1}{2} \log \left(1 + \frac{\rho}{4L} \right), \quad (9.18)$$

which corroborates that the TCD proposal for the notch effect, being of the form of Eq. (9.17), fulfills the uniqueness condition. The uniqueness condition, despite its obligatory consideration in the derivation of any model dealing with the notch effect, has been ignored in the derivation of any model of the currently used models, though it is implicitly satisfied in the TCD proposal.

3. *Extreme value consistent models.* As the fracture is related to the condition of minima values, any suggested model not based on the generalized extreme value family of distributions must be discarded, as Frank et al. (1993, chapter 3) suggests. In fact, the fracture toughness distribution for any notch radius must be, necessarily, Weibull or Gumbel, while models based on the Fréchet distribution will be inconsistent from the extreme value point of view.

9.3.2 Derivation of the model

The characteristic fracture toughness of a material K_c can be properly transformed to predict the measured fracture toughness for different notch radii K_c^N according to the TCD proposal, as previously described. However, the inverse transformation from K_c^N to K_c , given as

$$K_c = K_c^N(\rho; L) Q_\rho(0, \rho) = K_c^N(\rho; L) \sqrt{\frac{4L}{4L + \rho}}, \quad (9.19)$$

is also of interest allowing to transform the experimental data for K_c^N into its equivalent fracture toughness in terms of K_c . In other words, the experimental data obtained for different notch radii $K_{c_1}^N, K_{c_2}^N, \dots, K_{c_n}^N$ can be conveniently transformed into a new sample data set of the fracture toughness $K_{c_1}, K_{c_2}, \dots, K_{c_n}$ with a common cdf $F(K_c)$. Thus, according to the extreme value considerations argued in the previous section, these sample values must belong to a minimal

Weibull distribution,

$$p = F(K_c; \lambda, \delta, \beta) = 1 - \exp \left[- \left(\frac{K_c - \lambda}{\delta} \right)^\beta \right], \quad (9.20)$$

with parameters λ , δ and β . Consequently, the fracture toughness of the material is now probabilistically defined using the experimental data for different notch radii conditions as if they had been obtained from a smooth specimen. Then, the $K_c^N - \rho^{0.5}$ field, as the information of practical interest, can be directly derived by combining Eqs. (9.19) and (9.20), to yield the probabilistic definition of the notch fracture toughness:

$$K_c^N(\rho; L) = F^{-1}(p) \sqrt{1 + \frac{\rho}{4L}} = \left[\lambda + \delta (-\log(1-p))^{1/\beta} \right] \sqrt{1 + \frac{\rho}{4L}}, \quad (9.21)$$

for any value of notch radii. Figure 9.5 illustrates the resulting percentile curves of the probabilistic $K_c^N - \rho^{0.5}$ field related to the density distribution of the notch fracture toughness for different notch radii. In other words, Eq. (9.21) represents the probabilistic version of the original TCD method given by Eq. (9.5). Note that the randomness character refers to the probabilistic definition of K_c , which density distribution evolves according to the notch radius.

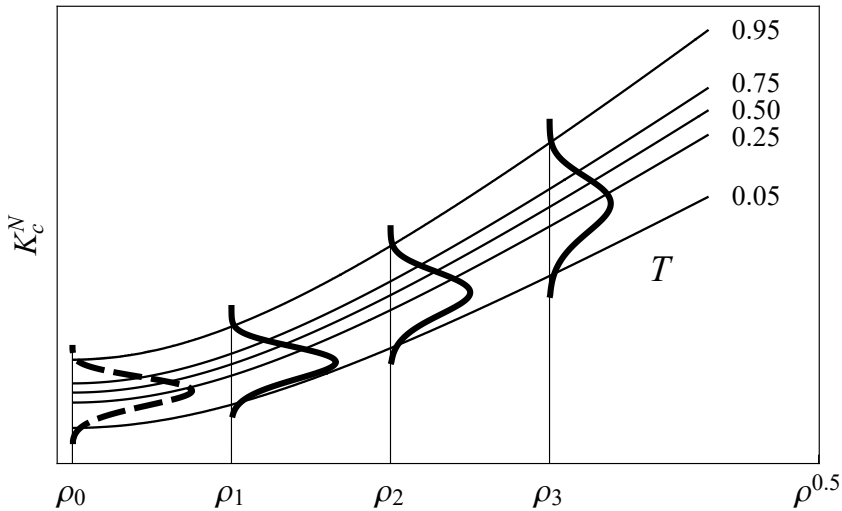


Figure 9.5: Schematic illustration of the percentile curves in the $K - \rho^{0.5}$ field for a given temperature and the corresponding pdfs of the fracture toughness for different notch radii.

Apart from the practical interest that lies in the analytical expression of the notch fracture toughness, the generalization of the cdf, initially defined for the fracture toughness $F(K_c)$, to define the notch fracture toughness $F(K_c^N)$ for any

other notch radius is also a remarkable result. Thus, by combining Eq. (9.19) into Eq. (9.20) results

$$p = 1 - \exp \left[- \left(\frac{K_c^N Q_\rho(0, \rho) - \lambda}{\delta} \right)^\beta \right] = 1 - \exp \left[- \left(\frac{K_c^N - \lambda_\rho(\rho)}{\delta_\rho(\rho)} \right)^\beta \right], \quad (9.22)$$

where now the location and scale parameters of the distribution can be assumed to be notch-dependent, according to the expressions:

$$\lambda_\rho(\rho) = \frac{\lambda}{Q_\rho(0, \rho)} = \lambda \sqrt{\frac{4L + \rho}{4L}}, \quad (9.23)$$

$$\delta_\rho(\rho) = \frac{\delta}{Q_\rho(0, \rho)} = \delta \sqrt{\frac{4L + \rho}{4L}}. \quad (9.24)$$

Figure 9.6 shows schematically the pdfs and cdfs of the notch fracture toughness for different values of notch radii according to Eq. (9.22), including the smooth specimen case for $\rho = 0$.

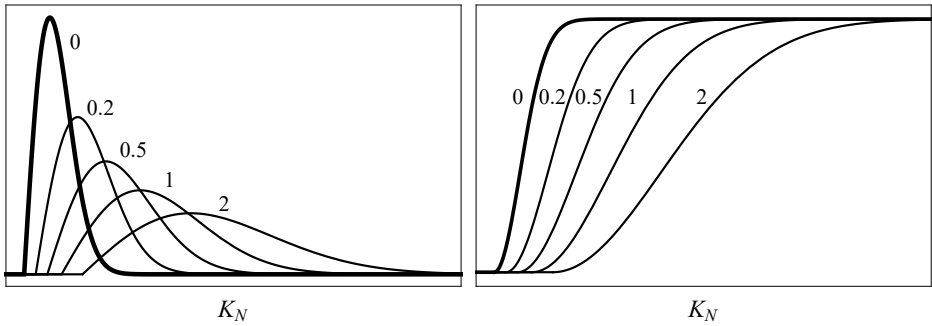


Figure 9.6: Schematic illustration of pdfs and cdfs of the notch fracture toughness for different given values of the notch radii.

9.3.3 Parameter estimation

The parameter estimation in the proposed methodology is divided in two parts: a) the estimation of the TCD method parameters L , K_{IC} , and b) the estimation of the Weibull parameters λ , δ and β . A detailed explanation of each of the required steps is given below:

- **Step 1:** *Experimental data.* The experimental data for notch fracture toughness for various notch radii $K_c^N(\rho)$ are considered as:

$$\{(\rho_i, K_{N_{ij}}) | i = 1, \dots, n; j = 1, \dots, m\}, \quad (9.25)$$

where the index i represents the set of different notch radii values and m index denotes the number of experiments for each of one notch radius.

- **Step 2:** *Estimation of K_{IC} and L .* According to the TCD method, the notch fracture toughness data are fitted using Eq. (9.5). By applying the least squares method it results:

$$S = \sum_{i=1}^n \sum_{j=1}^m \left(K_{N_{ij}} - K_{IC} \sqrt{1 + \frac{\rho_i}{4L}} \right)^2, \quad (9.26)$$

from which the estimates of K_{IC} and L are obtained, and the $K_c^N - \rho^{0.5}$ results assessed, as shown in Figure 9.1.

- **Step 3:** *Calculation of the plotting position.* The experimental values of the notch fracture toughness $K_{c_1}^N, K_{c_2}^N, \dots, K_{c_n}^N$ can be transformed into their equivalent in fracture toughness values $K_{c_1}, K_{c_2}, \dots, K_{c_n}$ according to Eq. (9.19). Thereafter, their corresponding probability values result from the application of a plotting position scheme, such as for example,

$$p_{j:m} = \frac{j - 0.3}{m + 0.4}, \quad j = 1, \dots, m. \quad (9.27)$$

- **Step 4:** *Estimation of the Weibull parameters.* The Weibull model parameters λ, δ and β in Eq. (9.20) are estimated using either the probability paper plot, according to Table 3.3, or other alternative methods, such as the the maximum likelihood and Castillo-Hadi estimators (see Castillo and Hadi (1994)).
- **Step 5:** *Prediction of the $K_c^N - \rho$ field.* Once the Weibull model is estimated, the $K_c^N - \rho$ field can be directly predicted for any value of the notch radius by their substitution in Eq. (9.21).

As will be shown in the practical example of Section 9.5, the derivation of consistent probabilistic models, opposite to the deterministic ones, to define the $K_c^N - \rho$ field is advantageous for the practical engineering design. Instead of working with one single curve as those models based on the TCD, the proposed model defines a parametric family of percentile curves providing useful and reliable information.

9.4 Proposed Methodology to Model Notch and Temperature Effects

9.4.1 Minimal required conditions

Though currently used models are based on some characteristic properties of the statistical distributions, such as that related to the scale change in the parameters

of the master curve method, there is neither explicit mention nor formal statements about them in the model derivation. For this reason, attention must be paid to the necessary conditions to model the temperature effect on the fracture resistance properties:

1. *Physically valid formulas.* The temperature is an influencing physical variable implying scale and location changes. Consequently, any mathematical model involving this variable must be consistent with change types. For example, the horizontal translation $T - T_0$ required in the master curve method is only admissible if the statistical distribution is stable with respect to scale changes (see Table 3.1). This condition is not always fulfilled, as occurs for example with the log-normal distribution as proposed in Moskovic (1993). Fortunately, since the master curve method relies on the Weibull distribution, the resulting analytical expressions are valid from a dimensional point of view.
2. *Extreme value consistent models.* Due to the minimum value condition and the existence of a lower limit of the fracture resistance, only the Weibull and Gumbel distributions are possible candidates for the model functions.

9.4.2 Proposed models based on the scale-effect property

This section illustrates how the methodology presented in Section 9.3, dealing only with the notch effect, is extended to include also the influence of the temperature. In that case, the experimental data obtained for different temperatures are evaluated independently each other, which is unnecessary since they are interrelated through the temperature. To this aim, it is assumed that the temperature-effect acts as a scale-effect onto the distribution function of the equivalent notch fracture toughness $F(K_c)$, similarly as in the case of the viscoelastic characterization in Chapter 6.

Derivation of the model

The dimensional analysis involving both notch root radius and temperature effects on the fracture resistance provides the following set of variables:

$$\nu \equiv \{\rho, \rho_0, K_c, K_{\min}, p, T, T_{\text{ref}}\}. \quad (9.28)$$

By applying the Buckingham's Theorem, the following set of dimensionless variables result:

$$K_c^* = \log\left(\frac{K_c}{K_{\min}}\right); \quad T^* = \log\left(\frac{T}{T_{\text{ref}}}\right); \quad \rho^* = \frac{\rho}{\rho_0}. \quad (9.29)$$

Note that the proposed redefinition of the temperature variable differs from that adopted in the viscoelastic characterization (see Section 6.3). In the present case, there is only one characteristic temperature T_{ref} arising naturally from the

brittle-to-ductile transition curve is used as the unique reference variable. This could be for instance the critical temperature T_{crit} , while the consideration of possible additional temperatures in the dimensional analysis would be certainly artificial. This contrasts with the viscoelastic characterization case, in which two different temperatures, that is, the rubbery and glassy ones, arise naturally.

The models based on the scale-effect contribute to an extension of those models related to the notch effect proposed in previous chapter. As a result, the statistical distribution of the equivalent fracture toughness $F(K_c)$, obtained for different notch radius, are already defined but for each temperature independently, as shown, for example, in Figure 9.12. Thus, the temperature effect on the resulting distributions can be considered additionally as a scale-effect so that their relation at two different given temperatures T_0 and T , that is, $F(K_c; T_0)$ and $F(K_c; T)$, respectively, is defined as follows:

$$F(K_c; T) = F(K_c; T_0)^{Q_T(T, T_0)}, \quad (9.30)$$

where $Q_T(T, T_0)$ represents a certain temperature-dependent function, which is the well-known functional equation of the scale-effect in Eq. (3.34), also applied for modelling the temperature effect on the viscoelastic characterization. Then, by assuming F as a minimal Weibull or Gumbel distributions functions due to the minimum value and the existence of a lower limit of the fracture resistance, as already mentioned, the temperature-dependent cdf of the equivalent fracture toughness K_c is obtained for both models:

$$F(K_c, T; \lambda, \delta, \beta) = 1 - \exp \left[- \left(\frac{K_c - \lambda}{\delta Q_T(T, T_0)^{-1/\beta}} \right)^\beta \right], \quad (9.31)$$

$$F(K_c, T; \lambda, \delta) = 1 - \exp \left[- \exp \left(\frac{K_c - \lambda + \delta \log Q_T(T, T_0)}{\delta} \right) \right], \quad (9.32)$$

where λ, δ and β are the parameters of the Weibull distribution (see Example 3.5) and λ, δ those of the Gumbel distribution (see Example 3.6). Figure 9.7 depicts the resulting parametric family of Weibull cdfs of the equivalent fracture toughness K_c for different temperatures according to the scale-effect.

Once the temperature effect is incorporated into the equivalent fracture toughness, then the transformation from the smooth specimen condition to any notch radii can be easily achieved by means of the TCD method using Eq. (9.5), which now including the effect of the temperature. This method allows the notch fracture toughness K_c^N to be obtained from the equivalent fracture toughness K_c , as already described in Section 9.3, and is even applicable to varying temperature conditions using the following expression:

$$K_c^N(\rho; T) = K_c(\rho_0; T) Q_\rho(\rho, \rho_0). \quad (9.33)$$

Accordingly, the equivalent fracture toughness $K_c(\rho_0; T)$ is calculated as a percentile of the cdf of Eq. (9.31) for the Weibull case and of Eq. (9.32) for the

Gumbel case, respectively:

$$K_c(\rho_0; T) = F^{-1}(p; T) = \lambda + (-\log(1 - p))^{1/\beta} \frac{\delta}{Q_T(T, T_0)^{1/\beta}}, \quad (9.34)$$

$$K_c(\rho_0; T) = F^{-1}(p; T) = \lambda - \delta \log Q_T(T, T_0) + \delta \log(-\log(1 - p)), \quad (9.35)$$

By substituting Eqs. (9.34) and (9.35) into Eq. (9.33), the notch fracture toughness for both Weibull and Gumbel models $K_c^N(\rho; T)$ results as:

$$K_c^N(\rho; T) = \left[\lambda + (-\log(1 - p))^{1/\beta} \frac{\delta}{Q_T(T, T_0)^{1/\beta}} \right] \sqrt{1 + \frac{\rho}{4L(T)}}, \quad (9.36)$$

$$K_c^N(\rho; T) = [\lambda - \delta \log Q_T(T, T_0) + \delta \log(-\log(1 - p))] \sqrt{1 + \frac{\rho}{4L(T)}}, \quad (9.37)$$

where the function $Q_T(T, T_0)$ being of the form of Eq. (3.35), has to be experimentally determined while L is assumed to be temperature-dependent.

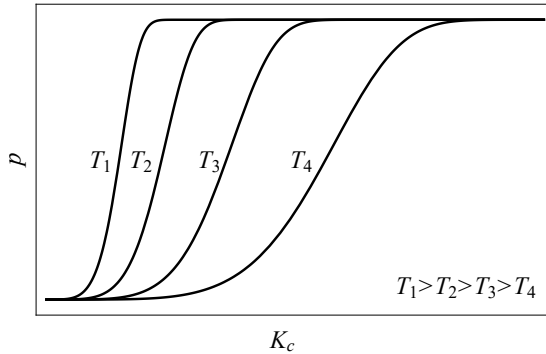


Figure 9.7: Schematic representation of the temperature effect as the scale-effect on the cdf of the notch fracture toughness.

Due to the twofold dependence of the notch fracture toughness K_c^N with both root radius and temperature effects, previous Weibull and Gumbel models allow the following fields to be derived:

- a) $K_c^N - \rho$ field. As shown in Figure 9.8, the $K_c^N - \rho$ field is obtained by considering Eqs. (9.36) and (9.37) as regression models representing the notch fracture toughness as a function of the notch radius. The statistical distribution of the equivalent fracture toughness K_c can be converted into a new one for any conditions of notch radius and temperature based on the scale-effect property. As a result, the statistical distribution for the notch fracture toughness K_c^N can be also defined for any combination of notch radius and temperature.
- b) $K_c^N - T$ field. The $K_c^N - T$ field can be alternatively derived by considering

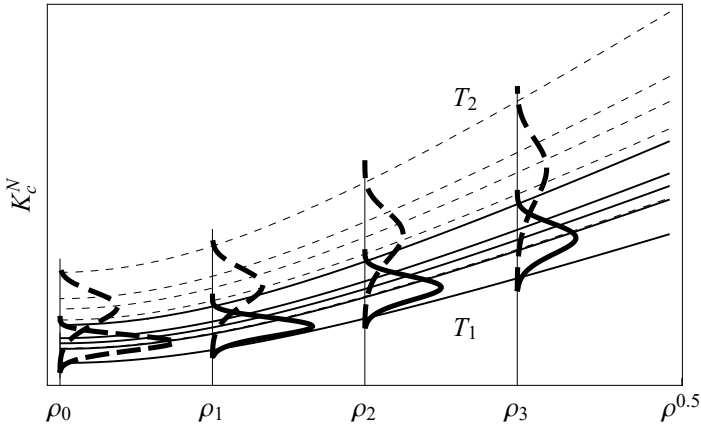


Figure 9.8: Schematic illustration of the percentile curves in the Weibull $K_c^N - \rho^{0.5}$ field for two different temperatures according to the scale-effect property in the Weibull model.

Eqs. (9.36) and (9.37) as regression models of the notch fracture toughness K_c^N as a function of temperature, providing the lower and intermediate zones in the brittle-to-ductile transition curve, as illustrated in Figure 9.9. In this case, based on the scale-effect property, the statistical distribution of the notch fracture toughness K_c^N may be converted from one temperature into another, for a given notch radius, based on the TCD method, this may be achieved from $\rho_0 = 0$ to any other notch radius for a given temperature.

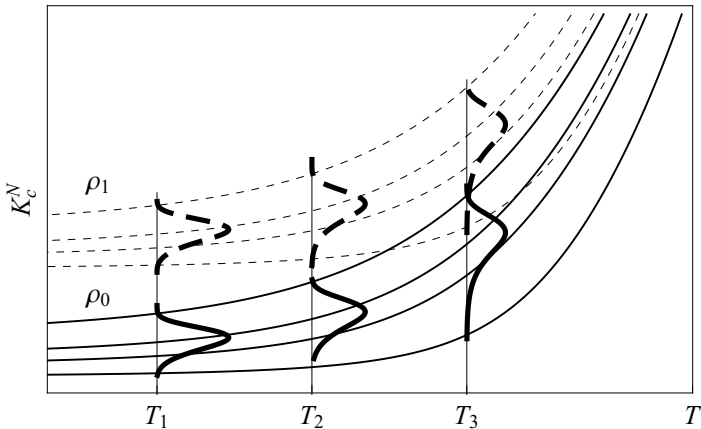


Figure 9.9: Schematic illustration of the percentile curves in the Weibull $K_c^N - T$ field for two different notch radii according to the scale-effect property in the Weibull model.

In summary, the two proposed models based on the scale-effect property represent an extension of the models developed in Section 9.3 using only the notch effect. Accordingly, the experimental fracture results from heterogeneous campaigns involving different notch radii and temperature conditions can be jointly assessed to characterize fracture of metallic materials. In these models, the random nature of the fracture results is taken into account. This is particularly interesting as providing the engineering design with useful information related to notch and temperature effects.

Parameter estimation

The parameter estimation for the above proposed models can be divided in two main parts, since it represents an extension of those models presented in subsection 9.3.3. Thus, from that first part, the experimental distributions of the equivalent fracture toughness are obtained $p - K_c$ as a result, one per each tested temperature. Then, the second part of the parameter estimation must be performed according to the following steps:

- **Step 1:** *Collecting experimental data $p - K_c$.* From the application of the TCD method, the experimental data for the equivalent fracture toughness for $\rho_0 = 0$ are obtained, as

$$\{(K_c^{ij}, p_{ij}) | i = 1, \dots, N; j = 1, \dots, M\}, \quad (9.38)$$

where K_c^{ij} represents the i -th recorded value at the j -th temperature. As a result, one experimental cdf is obtained for each temperature.

- **Step 2:** *Estimation of the Weibull parameters.* The experimental cdfs of the equivalent fracture toughness at different temperatures is estimated according to the scale-effect on both Weibull or Gumbel models by applying the probability paper estimation method (see Table 3.3). For example, the minimization function for the Weibull model is given as:

$$\sum_{j=1}^M \sum_{i=1}^N [\log(-\log(1 - p_{ij})) - \beta \log(K_c^{ij} - \lambda) - \beta \log \delta + \log Q_T(T_j)]^2, \quad (9.39)$$

from which single values of the λ and β parameters are obtained, while M different values are obtained for the Q_T factors, i.e. one for each test temperature.

- **Step 3:** *Fitting the Q_T function.* As a result of the previous step, the discrete values of the Q_T factors are now be fitted according to a certain function to be experimentally determined that can be assumed as an exponential law, pertaining to the general solution in Eq. (3.35), that is,

$$Q_T(T) = \exp[\theta_0 + \theta_1 T], \quad (9.40)$$

where θ_0 and θ_1 are constants.

- **Step 4:** *Derivation of the final expression of the notch fracture toughness.* Once the parameters and the function Q_T are fitted, the final expression of the notch fracture toughness for any combination of temperature and notch radius $K_c^N(\rho; T)$ is obtained by substituting Eq. (9.40) into the Weibull (9.36) and Gumbel (9.37) models, respectively.

9.4.3 Proposed models based on the compatibility condition

As an alternative solution to the previous models based, on the scale-effect to account for the temperature effect, the $K_c - T$ field is derived by applying the compatibility condition between the distribution of the equivalent fracture toughness for a given temperature, i.e. $K_c|T$, and that of the temperature for a given equivalent fracture toughness, that is, $T|K_c$. Both distributions depend on each other and are not allowed to be defined arbitrarily, as already shown in the derivation of the $T^* - t^*$ field for the viscoelastic characterization. Once the $K_c - T$ field is defined according to the compatibility condition, the TCD method is applied again to recover the corresponding $K_c^N - T$ field for any other notch radius.

Derivation of the model

The analysis of the brittle-to-ductile transition curve in the lower and intermediate shelves allows to identify some interesting physical properties:

1. The lower and intermediate shelves in the brittle-to-ductile transition curve are concave from above.
2. The fracture toughness K_c corresponds to the minimum value of the stress intensity factor K_I under which the fracture takes place in accordance with the weakest link principle. Consequently, only minimal Weibull and Gumbel distributions are candidates to represent the randomness of this variable.
3. The critical situation concerning the temperature influence on the fracture toughness is identified as the largest temperature value at which the transition from brittle-to-ductile behaviour takes place. It implies that the turning temperature in the $K_c - T$ field is related to a problem of maxima values, accordingly, only maximal Weibull and Gumbel distributions come into question.

Consequently, the analytical definition of the $K_c - T$ field must involve these two extremal events for both distributions, i.e. that for the equivalent fracture toughness for a given temperature $K_c^*|T^*$ and that for the temperature for a given equivalent fracture toughness $T^*|K_c^*$. In fact, both distributions depend each other and are not allowed to be defined arbitrarily, unfortunately ignored in the derivation of the current methodologies to describe the $K_c - T$ field (see

Álvarez-Vázquez et al. (2020c)). For this reason, Castillo and Fernández-Canteli (2009) originally apply the compatibility condition to derive fatigue models, such as the $\Delta\sigma - N$ field (minimum-minimum distribution case) and the crack growth curves in the $a - N$ field (maximum-minimum distribution case).

In the case of the $K_c^* - T^*$ field, the critical situation involves the minimum condition for the equivalent fracture toughness K_c^* and the maximum condition for the temperature T^* at which the material behaviour changes from brittle to ductile, as previously indicated. Thus, the compatibility condition between these distributions is defined as

$$F_{K_c^*|T^*}(K_c^*, T^*) = F_{T^*|K_c^*}(T^*, K_c^*), \quad (9.41)$$

where $F_{K_c^*|T^*}(K_c^*, T^*)$ and $F_{T^*|K_c^*}(T^*, K_c^*)$ are the cdf of K_c^* given T^* and of T^* given K_c^* , the former representing an extreme value distribution for minima and the latter one for maxima, respectively.

Thus, by considering a family of location and scale parameters, the compatibility condition in (9.41) is transformed into (see Castillo et al. (2010)):

$$1 - q_{\min} \left(\frac{K_c^* - \lambda_1(T^*)}{\delta_1(T^*)} \right) = q_{\max} \left(\frac{T^* - \lambda_2(K_c^*)}{\delta_2(K_c^*)} \right), \quad (9.42)$$

where q_{\min} and q_{\max} represent two distributions for minima and maxima, respectively, and $\lambda_1(T^*)$, $\lambda_2(K_c^*)$ and $\delta_1(T^*)$, $\delta_2(K_c^*)$ are the location and scale parameters as functions of temperature and fracture toughness, respectively.

Figure 9.10 illustrates the compatibility condition applied to the $K_c^* - T^*$ field for both distributions along with the family of percentile curves of probability of failure. Since the cumulative probability, i.e. area of each of the density functions implied at the corresponding percentile curve, must coincide, it follows that both distributions cannot be arbitrarily defined.

The solution of the functional equation represented in Eq. (9.42) comprising the functions $\lambda_1(T^*)$, $\lambda_2(K_c^*)$, $\delta_1(T^*)$ and $\delta_2(K_c^*)$ as unknowns, provides the unique possible functional form of the $K_c^* - T^*$ field that fulfills the compatibility condition comprising both minima and maxima events. Thus, by substituting the Weibull for minima and maxima, that is,

$$q_{\min}(x) = 1 - \exp[-(x)^\beta], \quad \text{and} \quad q_{\max}(x) = \exp[-(x)^\beta], \quad (9.43)$$

or, alternatively, the Gumbel distribution,

$$q_{\min}(x) = 1 - \exp\{-\exp[-(x)]\}, \quad \text{and} \quad q_{\max}(x) = \exp[-\exp(-x)], \quad (9.44)$$

into the compatibility condition of Eq. (9.42) and solving the resulting functional equations, the corresponding Weibull-Weibull and Gumbel-Gumbel models are found. In this way, the notch fracture toughness in both lower and intermediate

zones of the brittle-to-ductile transition curve, is defined as:

$$F(K_c^*, T^*; \lambda, \delta, \beta) = \exp \left[- \left(- \frac{(B - T^*)(K_c^* - C) - \lambda}{\delta} \right)^\beta \right], \quad (9.45)$$

$$F(K_c^*, T^*; \lambda, \delta) = \exp \left[- \exp \left(- \frac{(B - T^*)(K_c^* - C) - \lambda}{\delta} \right) \right], \quad (9.46)$$

where λ, δ, β and λ, δ are, respectively, the parameters of Weibull and Gumbel distributions, and B and C are the model asymptotes.

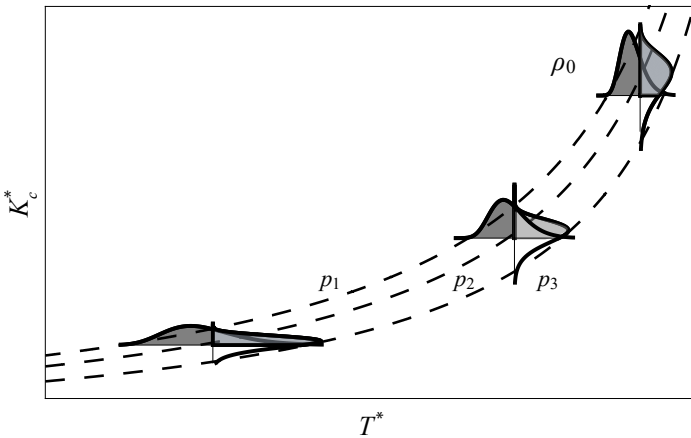


Figure 9.10: Schematic illustration of the compatibility condition in the $K_c^* - T^*$ field showing the same cumulative probabilities (equal area) in the density functions.

As in the case of the crack growth curves, the solution of the compatibility condition states that only hyperbolas or straight lines are the only solution to define a valid $K_c^* - T^*$ field. Nevertheless, only the first option is in accordance with the physical properties of the brittle-to-ductile transition curve in the lower and intermediate zones, as previously indicated.

Once the valid $K_c - T$ field is defined, as a result of the application of the compatibility condition, the equivalent notch fracture toughness K_c can be transformed by means of the TCD method to any other notch radius condition K_c^N according to Eq. (9.33). As previously show with the models derived from the scale-effect property, the original $K_c - T$ may be converted into the $K_c^N - T$ one. On the one side, the quantile function F^{-1} allows the equivalent fracture

toughness to be explicitly derived, as

$$K_c(\rho_0; T) = F^{-1}(p; T) = \frac{\delta(-\log(1-p))^{1/\beta} + \lambda}{B-T} + C, \quad (9.47)$$

$$K_c(\rho_0; T) = F^{-1}(p; T) = \frac{\delta(\log(-\log(1-p))) + \lambda}{B-T} + C, \quad (9.48)$$

which are alternative definitions to Eqs. (9.34) and (9.35), respectively. On the other side, the notch fracture toughness K_c^N is obtained by substituting Eqs. (9.47) and (9.48) into Eq. (9.33):

$$K_c^N(\rho; T) = \left[\frac{\delta(-\log(1-p))^{1/\beta} + \lambda}{B-T} + C \right] \sqrt{1 + \frac{\rho}{4L(T)}}, \quad (9.49)$$

$$K_c^N(\rho; T) = \left[\frac{\delta(\log(-\log(1-p))) + \lambda}{B-T} + C \right] \sqrt{1 + \frac{\rho}{4L(T)}}. \quad (9.50)$$

In Figure 9.11, the resulting parametric family of failure percentile in the $K_c^N - T$ field is depicted for two different notch radii. As can be seen, the statistical distribution for a given temperature is transformed from one notch radius into another one according to the TCD method, while the statistical distribution over a given notch radius evolves for the different temperatures according to the compatibility condition.

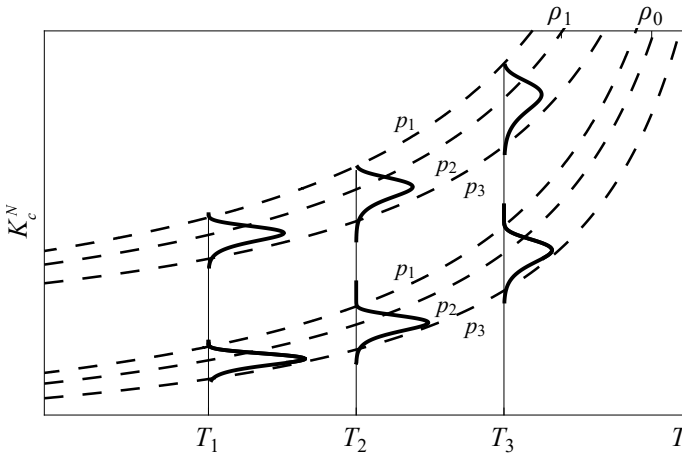


Figure 9.11: Schematic illustration of the $K_c^N - T$ field for two different notch radii, depicting the density functions of the notch fracture toughness for different temperatures.

In summary, the proposed models based on the compatibility condition evidence that the analytical definition of the $K_c - T$ field must not be performed by considering only the distribution of the fracture toughness for a given tem-

perature, as the master curve method suggests in Eq. (9.7). In fact, the complementary distribution of the notch radius for a given temperature must also be defined by fulfilment of the compatibility condition, both being dependent each other. As a more satisfactory solution, the Weibull-Weibull and Gumbel-Gumbel models allow the brittle-to-ductile transition curve to be defined by considering the extremal character of both variables the fracture toughness and temperature, related to the minimal and maximal family of distributions, respectively. Additionally, the temperature and the notch radius effects might be jointly considered.

Parameter estimation

The parameter estimation of the proposed models based on the compatibility condition is equivalently to that already applied in the analogous case of the $T^* - t^*$ field in subsection 6.5.3, as will be shown in the practical example of subsection 9.5.2. The experimental data considered as input in this estimation is the equivalent fracture toughness for each temperature from the Chapter 9 represented in the $K_c - T$ field, based on the TCD method. Then, the rest of the steps required are directly adopted from those originally proposed by Castillo and Fernández-Canteli (2009) for modelling the crack growth field, namely: a) estimation of the B and C asymptotes from the experimental data for the equivalent fracture toughness K_c vs. temperature T , b) estimation of the parameters of the Weibull and Gumbel distributions and c) derivation of the final expressions for both Weibull-Weibull and Gumbel-Gumbel models. For the sake of brevity, the reader is referred to the original work due to Castillo and Fernández-Canteli (2009).

9.4.4 Proposed Bayesian Models

Though the models proposed and those currently used in literature represent certainly probabilistic approaches, use of Bayesian techniques offer further improvement in the reliability context allowing the confidence intervals of the model parameters and of the percentile curves to be determined by means of the use of OpenBUGS software.

Based on the scheme already described for the viscoelastic case, the prior distributions of the parameters from the original Weibull-Weibull and Gumbel-Gumbel models are defined assuming them to follow a uniform distribution, which for the former case are established as:

$$\begin{aligned} \lambda &\sim U(\lambda_{\min}, \lambda_{\max}), & \delta &\sim U(\delta_{\min}, \delta_{\max}), & C &\sim U(C_{\min}, C_{\max}), \\ \beta &\sim U(\beta_{\min}, \beta_{\max}), & B &\sim U(B_{\min}, B_{\max}), \end{aligned} \quad (9.51)$$

where the limits for each of the parameters are selected by the user. The corresponding code programming to be implemented in the Weibull-Weibull model, as an example, will be shown in the practical example of subsection 9.5.2). The application to the Gumbel case is straightforward.

9.5 Examples of Practical Application

In order to illustrate the practical use of the proposed model, the experimental data from an experimental campaign on two ferritic steels S275J5, carried out by Madrazo et al. (2014), is analyzed. The experimental programme consists of 95 and 102 compact test (CT) specimens for S275JR and S355J2 steels, respectively, with notch radius values: 0,0.15,0.25,0.50,1.00 and 2.00 mm, tested at different temperatures. For further details about the experimental campaign, regarding materials, geometries, testing temperatures, load-bearing capacity results, and tensile properties of the two materials at the different temperatures (yield stress, ultimate tensile strength, and Young modulus), see Madrazo et al. (2014).

9.5.1 Proposed methodology for the notch effect

Figure 9.12 depicts the results from the proposed Weibull model when applied to the S275JR experimental data. On the left, the cdf of the equivalent notch fracture toughness K_c is plotted according to Eq. (9.20). The points, representing failures for different notch radii and given temperatures, are pooled together into one single curve, showing an acceptable agreement between theoretical and experimental data. On the right, the probabilistic $K_c^N - \rho$ fields for different temperatures are plotted as percentile curves. The estimates for the proposed model are listed in Table 9.1. Similarly, Figure 9.13 shows the corresponding results for the S355J2 steel.

Table 9.1: Dimensional Weibull parameters model from the assessment of the experimental data for the S275JR and S355J2 ferritic steels from Madrazo et al. (2014).

	T [° C]	Parameters				
		λ [MPa·mm ^{0.5}]	δ [MPa·mm ^{0.5}]	β [-]	L [mm]	\overline{K}_{IC} [MPa·mm ^{0.5}]
S275JR	-120	25.518	27.614	2.013	0.0192	46.841
	-90	12.230	50.141	2.955	0.0059	62.729
	-50	24.628	54.807	2.594	0.0038	78.179
	-30	64.872	65.573	2.922	0.0085	117.715
S355J2	-196	63.447	247.586	2.904	0.028	32.276
	-150	37.866	100.776	3.516	0.0096	61.452
	-120	12.383	54.952	2.445	0.014	132.629
	-100	11.193	22.103	61.094	0.078	296.546

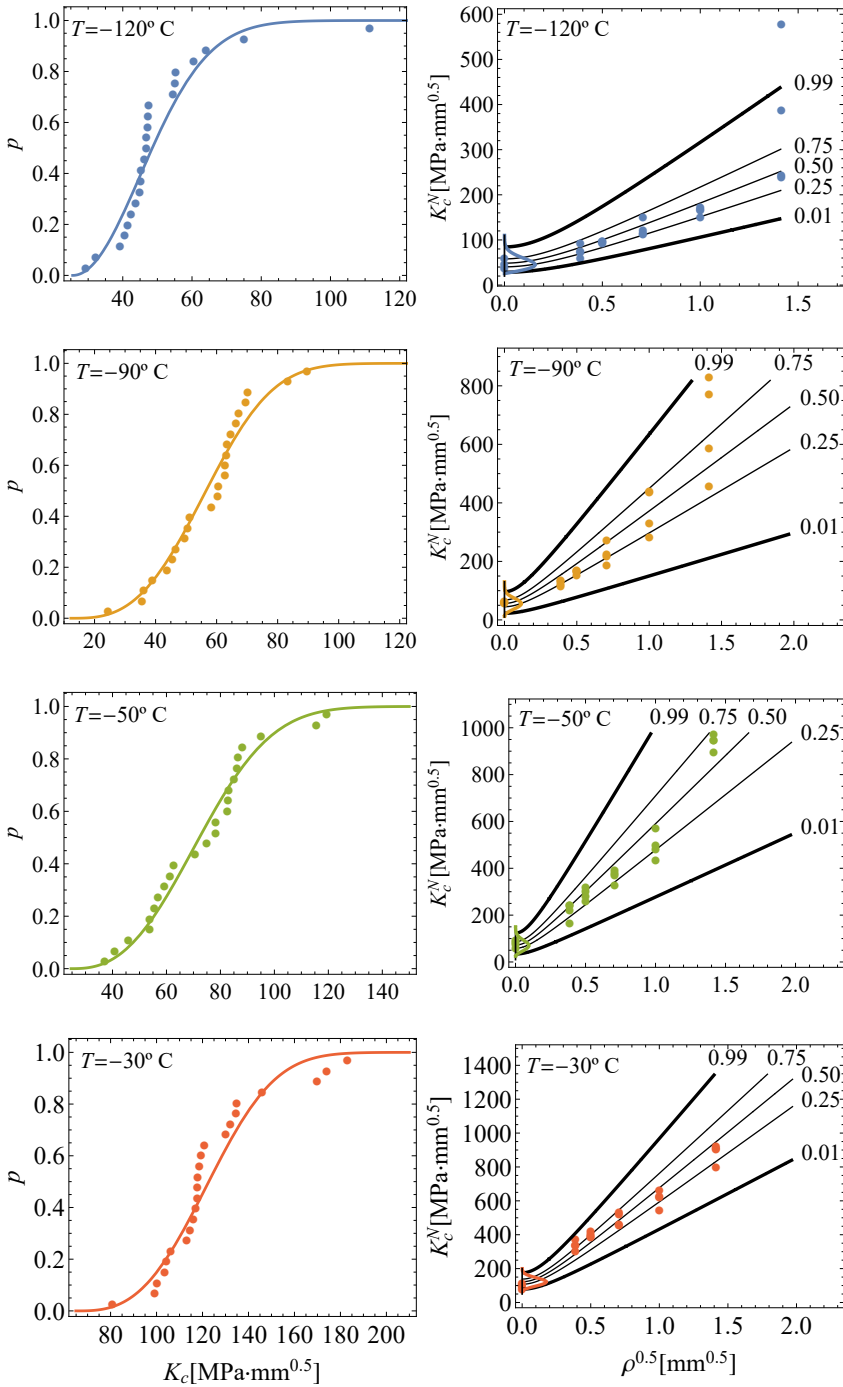


Figure 9.12: Plots $p - K_c$ and $K_c^N - \rho^{0.5}$ for ferritic steel S275JR data from Madrazo et al. (2014).

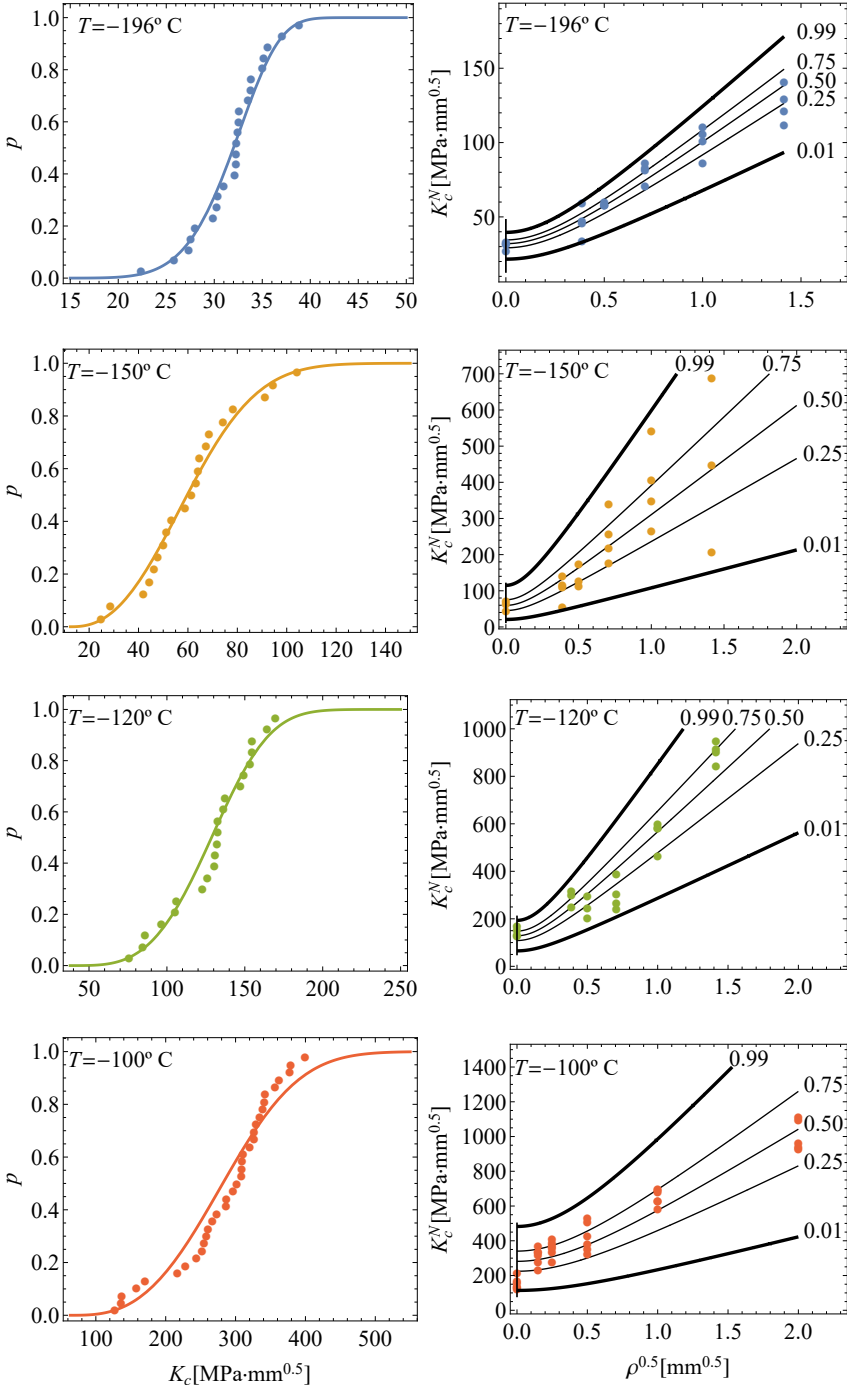


Figure 9.13: Plots $p - K_c$ and $K_c^N - \rho^{0.5}$ for ferritic steel S355J2 data from Madrazo et al. (2014).

9.5.2 Proposed methodology for notch and temperature effects

In this section, the proposed models, either based on the scale-effect property or on the compatibility condition, are applied to the experimental fracture results from the external campaign reported by Madrazo et al. (2014), involving different notch radius and temperature conditions.

Proposed models based on the scale-effect property

The proposed models provide the equivalent fracture toughness for different temperatures, using a unique mathematical model to evaluate both effects jointly. They are based on the scale-effect property applied to the experimental statistical distributions resulting from the TCD method. The experimental distributions for both metallic materials are shown in Figure 9.14, which summarizes the information from Figure 9.12 and Figure 9.13. Next, the estimates of the model parameters are obtained directly for the two materials considered by minimizing the function of Eq. (9.39) for the Weibull model, based on the paper probability concept. The estimates are collected in Table 9.2.

As an additional result, the Q_T factors are also obtained, one per each temperature, by fitting them according to the solution of the functional equation (3.35). As occurs in the viscoelastic proposed models, the experimental Q_T factors show an exponential decreasing trend. In this way, a linear function is obtained from Eq. (9.40) if $\log Q_T$ is plotted as a function of the temperature for both materials, as shown in Figure 9.14. As a result, the scale-effect property allows to evaluate jointly each of these experimental curves to be assessed providing an acceptable agreement between the theoretical and experimental cdf's.

Table 9.2: Parameter estimates for the scale-effect derived Weibull model when analyzing data from Madrazo et al. (2014).

Material	Parameters				
	λ	δ	β	θ_0	θ_1
S275JR	5.37	223.24	3.90	1.29	-0.036
S355J2	11.86	145.11	3.23	-10.34	-0.086

Additionally, the proposed models, based on the scale-effect, allow the alternative field $K_c - T$, i.e. the lower and intermediate zones of the brittle-to-ductile transition curve, to be derived directly. In fact, Eqs. (9.34) and (9.35) can be contemplated as regression models of the equivalent fracture toughness as a function of the temperature, taking into account the definition of the Q_T factors according to Eq. (9.40).

Figure 9.15 shows the $K_c - T$ field for the Weibull model with the family of percentile curves for both materials. The experimental density distributions of the equivalent notch fracture toughness obtained from the TCD model are also plotted for the different temperatures. In this way, the proposed model allows the

temperature effect to be predicted according to the scale-effect property. Note that each of the experimental points for different temperatures represents one fracture result for a particular notch radii, so that the TCD method allows all of them to be pooled into one single cdf.

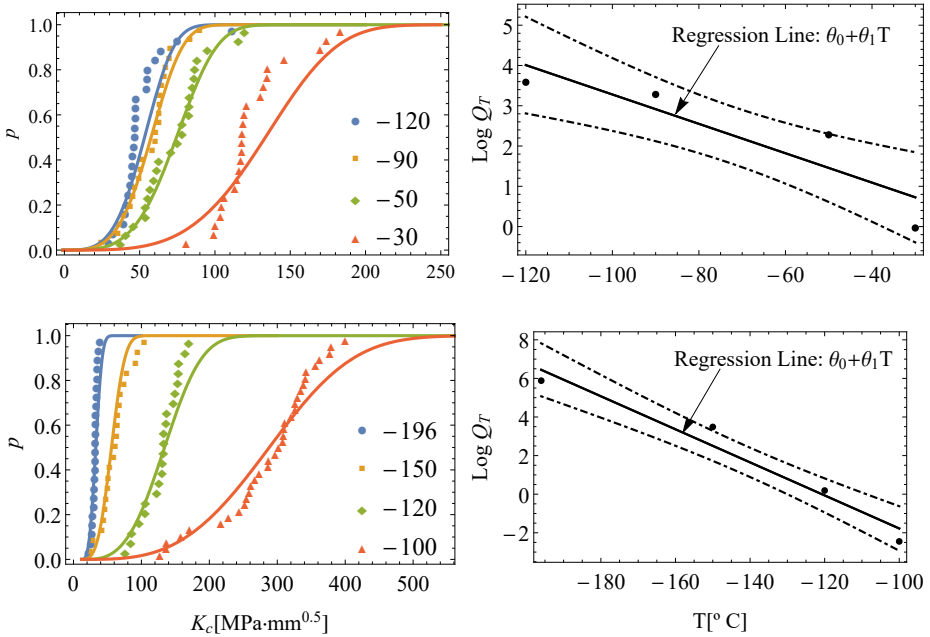


Figure 9.14: Theoretical predictions and experimental data, from Madrazo et al. (2014), of the fracture toughness for S275JR (top) and S355J2 (bottom) steels for different notch radii and Celsius temperatures (left) and Q_T functions with 95% confidence intervals (right).

Proposed models based on the compatibility condition

As an alternative to the scale-effect based models, the Weibull-Weibull model, arising from the compatibility condition, are now applied to a practical example in this subsection. As mentioned in the description of the parameter estimation, the experimental data used as the input in the proposed model is the resulting $K_c - T$ field for the equivalent fracture toughness as defined by the TCD method. This corresponds to the experimental data plotted in Figure 9.16, which are the same than those represented in Figure 9.15. For the sake of brevity, the Weibull-Weibull model is only applied to the S355J2 experimental data.

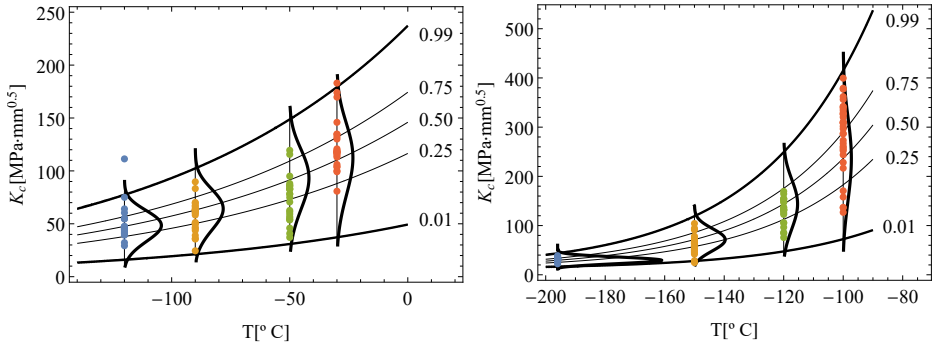


Figure 9.15: Theoretical predictions for the $K_c - T$ field according to the scale-effect on the Weibull model and experimental data for the S275JR (left) and S355J2 (right) steels from Madrazo et al. (2014).

The first step in the estimation of the Weibull-Weibull model parameters consists in assessing the B and C parameters, representing the model asymptotes, whose values are:

$$C = 2.2 \times 10^{-14}; \quad B = 7.047, \quad (9.52)$$

from which the experimental values of the normalizing variable can be directly computed. As a result, the experimental data, obtained from different notch radius and temperature conditions, are pooled together into one single cdf pertaining to the Weibull distribution, whose parameters can be estimated as,

$$\lambda = 6.85; \quad \delta = 2.76; \quad \beta = 7.55, \quad (9.53)$$

as shown in Figure 9.16, together with the resulting percentile curves in the lower and intermediate zones of the brittle-to-ductile transition curve in a log-log plot, which is also usually in literature. As mentioned above, the Weibull-Weibull model allows all the experimental data obtained from heterogeneous notch radius and temperature conditions to be pooled into one single cdf, which acts as a general master curve. In this way, the material may be properly characterized. It is recalled that the general master curve arises from the compatibility condition which includes both extremal events by relating the equivalent fracture toughness to the temperature.

Finally, once the $K_c - T$ field for the equivalent fracture toughness is estimated, the corresponding $K_c^N - \rho^{0.5}$ field for each temperature can also be directly derived from Eq. (9.49) for the Weibull-Weibull model and Eq. (9.50) for the Gumbel-Gumbel model, respectively. The resulting fields are shown in Figure 9.17 for the experimental data of the S355J2 steel using the Weibull model for different temperatures along with the corresponding theoretical curves based on the TCD method by substitution of the parameters K_c and L from Table 9.1 into Eq. (9.5).

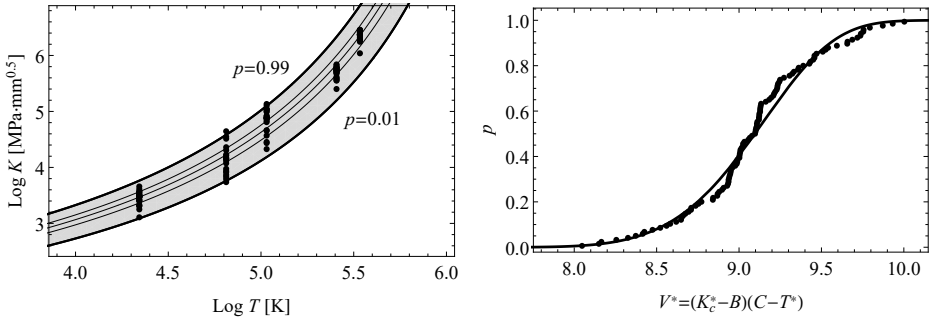


Figure 9.16: Theoretical predictions for the $K_c - T$ according to the compatibility model and experimental data for the S355J2 steel from Madrazo et al. (2014).

As can be seen, additionally to the contributions in the $K_c - T$ field, the proposed models, based on the compatibility condition, also allows the distribution of the notch fracture toughness for any combination of notch radius and temperature to be univocally recovered. This succeeds from the application of strong statistical conditions implying extremal events, i.e. minimal and maximal ones, for both involved variables. Note also that the deterministic TCD method is only focused on the median value of the notch fracture toughness for different temperatures, while the proposed method provides the whole family of percentile curves. Both approaches almost coincide at the median percentile curve for all temperatures, whereas only the proposed model is able to consider reliably the inherent variability of the fracture results.

Proposed Bayesian models

Finally, the Bayesian technique is applied to the experimental data for the S355J2 steel using the Weibull-Weibull model. As in the viscoelastic case, the required code to implement this model in the OpenBUGS software is listed in Code 9.1 in flat format based on an analogous one as that proposed to assess the S-N Field (see Castillo et al. (2019)), where the prior distributions proposed in Eq. (6.50) are included and the original values of the model are taken from Eq. (9.52) and (9.53).

It is worth mentioning that the generalized extreme value for maxima is the only extreme value distribution implemented in OpenBUGS, so that the proposed Weibull-Weibull model, based on both maxima and minima cases, must be implemented according to the distribution for maxima.

Once the experimental data is loaded onto OpenBUGS and the previous code implemented, the number of simulations is defined for the initial process (burn-in process) and for the final sample. Then, the model is executed. In this case, taking into account the computational time of OpenBUGS and the expected variability associated with the fracture problems, 1,000 and 20,000 simulations

are recommended for the initial and final samples, respectively. Then, once the code is executed, the program furnishes both the convergence analysis and the parameters of the posterior distributions, which are introduced into Eq. (5.17) to derive the posterior predictive distribution. As a result, the percentiles of the fracture failure percentiles, i.e. the confidence intervals of each percentile, are obtained for the original version of the proposed Weibull-Weibull model.

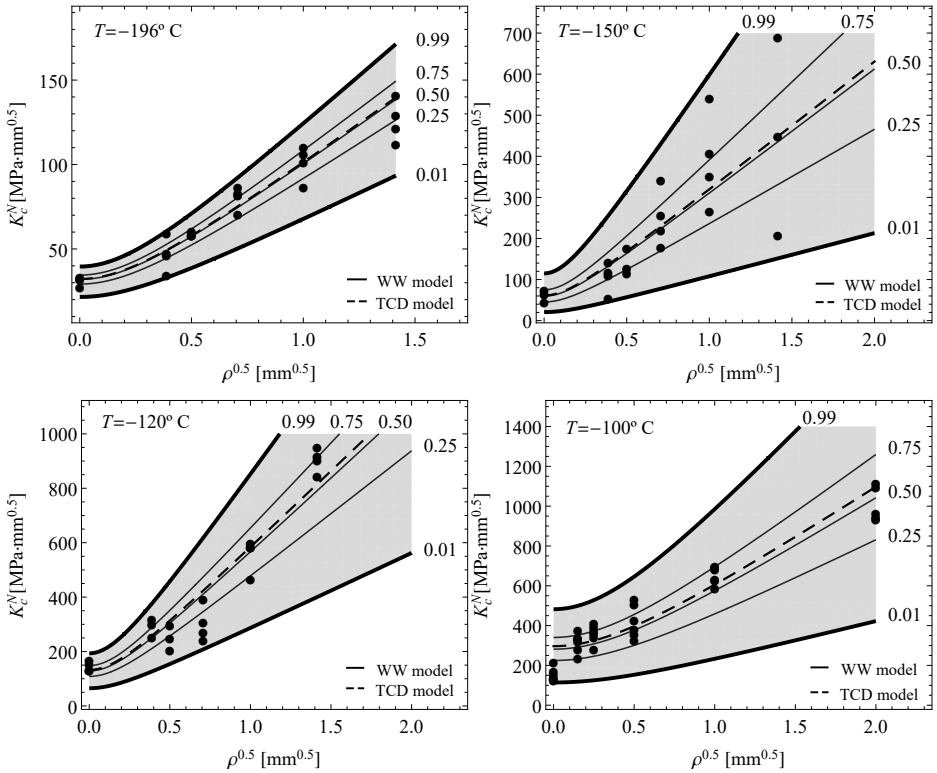


Figure 9.17: $K_c^N - \rho^{0.5}$ field depicting the theoretical failure predictions for both Weibull-Weibull (WW) and the theory of critical distances (TCD) models, respectively, for the experimental data of the S355J2 steel from Madrazo et al. (2014).

Figure 9.18 shows the resulting $K_c - T$ field with the family of percentile curves from the original Weibull-Weibull model as calculated in the previous subsection along with their associated family of percentile curves derived from posterior predictive distributions provided by the OpenBUGS software.

As can be seen, the Bayesian version of the proposed Weibull-Weibull model, apart of considering the temperature effect, extends the probabilistic definition of the $K_c - T$ field by providing the confidence intervals of the original percentiles

as determined from the experimental data. As a result, the engineering design of notched components becomes more reliable than before.

Code 9.1: OpenBUGS code to implement the Weibull-Weibull model.

```

1: model {
2:   for(i in 1:M) {
3:     aux1[i] <- Delta[i] - Delta0
4:     aux2[i] <- N0 - (lambda + delta) / aux1[i]
5:     V[i] <- -aux1[i] * (N0 - N[i])
6:     aux3[i] <- delta / (beta * aux1[i])
7:     aux4[i] <- -(-1/beta)
8:     logN[i] <- -(N[i])
9:     logN[i] ~ dgev(aux2[i], aux3[i], aux4[i])
10:    H[i] <- -N[i]
11:    for(s in 1:ns){
12:      Deltasigma[s] <- minDelta + (s-1) * (maxDelta - minDelta) / (ns-1)
13:      for(p in 1:np){
14:        N01[s, p] <- N0 - ((lambda + delta) / (Deltasigma[s] - Delta0) + delta /
15:        Deltasigma[s] - Delta0) * (1 - pow(-log(percentiles[p]), 1/beta))
16:        N0 ~ dunif(minN0, maxN0)
17:        Delta0 ~ dunif(minDelta, maxDelta)
18:        beta ~ dunif(minbeta, maxbeta)
19:        lambda ~ dunif(minlambda, maxlambda)
20:        delta ~ dunif(mindelta, maxdelta)
21:      }

```

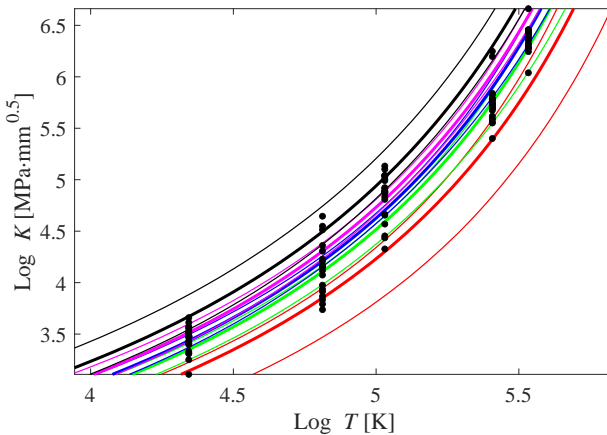


Figure 9.18: $K_c - T$ field for the experimental data of the S355J2 steel with theoretical percentile curves for $p = 0.01, 0.10, 0.50, 0.90, 0.99$ from the Weibull-Weibull model, and confidence intervals 0.01–0.99 from the Bayesian approach.

Finally, the posterior predictive density distributions of the Weibull-Weibull model parameters for the experimental data of the S355J2 steel from Madrazo et al. (2014), as supplied by OpenBUGS software, are illustrated in Figure 9.19.

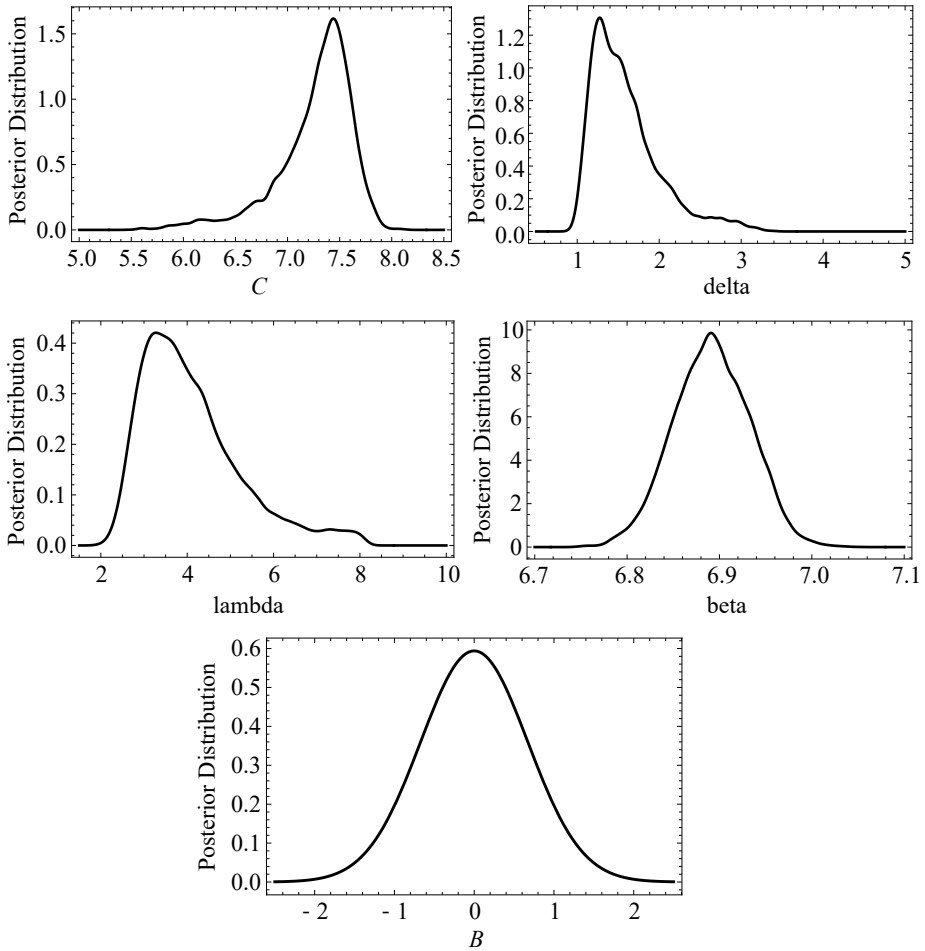


Figure 9.19: Posterior predictive distributions for the Weibull-Weibull model parameters as supplied by OpenBUGS for the experimental ata of S355J2 steel from Madrazo et al. (2014).

9.6 Concluding Remarks

An extension of the methodology currently used to model the notch effect on the fracture toughness is presented in this chapter. The intrinsic random nature of the fracture toughness must be considered in the fracture characterization of materials, an issue usually ignored by the current deterministic methodologies, such as the theory of critical distances on which the proposed methodology is based. To this aim, some minimum necessary conditions to achieve building valid models to analyze the notch effect are formally established at the beginning of this chapter. Under these assumptions, the proposed methodology transforms

the results of the notch fracture toughness values for different notch radii into the equivalent values for a reference radius. This allows the so-called equivalent notch fracture toughness to be defined, assuming a minimal Weibull distribution. Once its cdf is estimated, the transformation can be undone from the reference notch radius into any other radius by virtue of the TCD. In other words, the $K_c^N - \rho$ can be completely defined in a probabilistic sense, allowing to predict the cdf of the fracture toughness of the material for any notch radius.

In addition, two different models are proposed for describing the simultaneous effect of the notch root radius and the temperature on the probability of failure of notched components. Once the experimental data at different notch radius K_c^N are transformed into the equivalent fracture toughness K_c for the smooth specimen condition, the scale-effect and the compatibility are proposed as possible approaches to describe the temperature effect. As a result, the lower and intermediate zones of the brittle-to-ductile transition curve can be properly assessed in a probabilistic manner. The resulting field can be transformed univocally to recover the notch fracture toughness, both effects being predicted as $K_c^N - T$ and $K_c^N - \rho$ fields.

An external experimental campaign performed for different notch radius and temperature conditions is used to demonstrate the applicability of the proposed methodologies in this chapter, either focused on the notch effect or combined with the temperature one.

V

Conclusions, Original
Contributions and Future Work

10

Conclusions

10.1 Conclusions

The principal conclusions drawn from this thesis are grouped with relation to three different concepts:

Phenomenological model building

- a) Phenomenological-mathematical models, like the ones developed in this thesis, must be based on a minimum set of physical and statistical requirements in order for the models to be valid. In this way, fundamental errors and model limitations due to arbitrary assumptions are avoided.
- b) A general methodology is proposed for the systematic building of phenomenological models that integrates the mandatory conditions, properly identified in the model from the experimental analysis of the phenomenon under study.

Viscoelastic characterization models

- a) The normalization of the viscoelastic variable under study (relaxation modulus) with respect to its inherent twofold bounding limits represented by

elastic and relaxed moduli, as well as the observation of its monotonically decreasing character, suggest it be represented, by definition, as a survival function. This evidences the statistical basis underlying the viscoelastic phenomena in their different manifestations.

- b) The selection of the cdf of the normal distribution to describe the time evolution of the normalized relaxation module is justified by using the central limit theorem when the total elongation of a viscoelastic sample in a creep test is supposed to be the sum of the random elongations of a large set of primary elements in which the specimen is virtually divided.
- c) The long-term characteristics of the relaxation phenomenon requires the extrapolation of available data from the short term curves recorded in the tests for different temperatures towards the limiting cases, $t \rightarrow 0$ and $t \rightarrow \infty$. Thus, the use of distributions from the generalized extreme value family represents the natural solution for the viscoelastic characterization. In particular, the Gumbel distribution, as the domain attraction of the normal and log-normal ones, appears as the optimal candidate to completely describe the relaxation modulus over time.
- d) Temperature effect is the most influential external effect on the evolution of viscoelastic properties, contributing positively towards viscoelastic characterization. The temperature effect is handled with the normal and Gumbel approaches proposed, based on the stability condition. To this end, two different model solutions are developed in this thesis:
 - Firstly, the temperature effect is supposed to act as a change of the scale parameter on the cumulative distribution function of both normal and Gumbel distributions. The estimation of a master curve for a reference temperature succeeds from the short-term curves recorded in the experimental campaign at different temperatures in an experimental window interval between two fixed times due to practical limitations of the tests.
 - Secondly, the statistical compatibility condition between the value of the relaxation modulus over time for a given temperature $E^*(t^*; T^*)$ and that along temperature for a given time $E^*(T^*; t^*)$ is applied allowing the $T^* - t^*$ field to be analytically defined. As a result, all experimental data from the short-time relaxation curves at different temperature are pooled together into one sole unique Gumbel cumulative distribution function representing the most suitable equation to fit the master curve. Once this field is estimated, the master curves in both $E^*(t^*; T^*)$ and $E^*(T^*; t^*)$ fields can be derived directly.
- e) The viscoelastic phenomena prove to be stochastic processes, in which time and temperature are the main influencing variables besides the limiting values, i.e. elastic and relaxed moduli. The Bayesian technique allows the probabilistic definition of the main viscoelastic variables, i.e. relaxation modulus and creep compliance, to be achieved for both types of deterministic viscoelastic approaches, currently-used and statistics-based ones,

respectively. This is achieved through the definition of the statistical distributions of the intervening parameters.

- f) An experimental campaign of relaxation tests on PVB, a widely used viscoelastic material, is performed at eight different temperatures to corroborate the applicability of the proposed models to the viscoelastic characterization.
- g) Additional viscoelasticity-related phenomena, such as the moisture effect, physical ageing and the curing effect, are successfully handled using the same viscoelastic models, proving the general applicability of the approaches and methodology proposed.
- h) Interconversion between the different procedures to define the viscoelastic functions (relaxation and creep tests, as static tests, and varying frequency test, as dynamic test) is performed according to the classical procedure using the Fourier and Laplace transforms. This methodology is equally applicable to the interconversion among the viscoelastic master curves with the models proposed in this thesis. Once the relaxation modulus is estimated, the master curve for the rest of the viscoelastic functions can be univocally obtained for any other reference temperature.

Fracture characterization models

- a) The valuable experience gained with the development of the models applied to the definition of the viscoelastic strain and stress evolution over time contributes to the future design of viscoelastic materials against static and fatigue failures. In this way, current deterministic methodologies to describe the notch effect on fracture resistance properties based on the theory of the critical distances are extended to a probabilistic version. The same models as those developed for the viscoelastic characterization, are used for this task, allowing prediction of the notch fracture toughness to be used as reference for percentile values.
- b) The temperature effect is included in the aforementioned probabilistic model to account for its recurrent presence in the service conditions of real components, leading to the proposal of the following two models:
 - The temperature effect is supposed to act as a change of the scale parameter on the cumulative distribution function of the notch fracture toughness, allowing both $K_c^N - \rho$ and $K_c^N - T$ fields to be derived analytically.
 - The compatibility condition between the cumulative distribution function of the fracture toughness for a given temperature and the distribution of the temperature for a given fracture toughness is accounted for. This allows the lower and intermediate zones of the brittle-to-ductile transition curve for any condition of notch and temperature to be probabilistically defined.

- c) The applicability of the proposed probabilistic models for fracture characterization is corroborated using an extensive experimental campaign on two ferritic steels, S255JR and S355J2, involving different notch and temperature conditions.

10.2 Conclusiones

Las principales conclusiones de esta tesis doctoral pueden ser agrupadas con relación a tres grandes líneas:

Derivación de modelos fenomenológicos

- a) Un modelo fenomenológico-matemático, como los desarrollados en esta tesis, debe de estar basado en un conjunto de requisitos físicos y estadísticos para que pueda ser considerado válido. De esta forma, se consiguen evitar limitaciones y errores fundamentales debido a la asunción de hipótesis arbitrarias.
- b) Se propone una metodología general para la construcción sistemática de modelos fenomenológico-matemáticos que permite integrar las condiciones necesarias para su validez, debidamente identificadas en el modelo del análisis experimental del fenómeno bajo estudio.

Modelos de caracterización viscoelástica

- a) La normalización de la variable viscoelástica bajo estudio (módulo de relajación) con respecto a su inherente acotación doble por los módulos elástico y relajado, así como por su carácter estrictamente decreciente, sugieren su representación por medio de una función de supervivencia, por definición. Con ello se evidencia la base estadística que subyace bajo el fenómeno viscoelástico en sus diferentes manifestaciones.
- b) La selección de la función de distribución acumulada de la normal para describir la evolución en el tiempo del módulo normalizado de relajación se justifica a través del teorema central del límite, al considerar la elongación total de una probeta viscoelástica en un ensayo típico de fluencia como la debida a la suma de las elongaciones aleatorias de un conjunto de elementos primarios en las que puede ser dividida dicha probeta.
- c) Las características a largo plazo del fenómeno de relajación deben de ser extrapoladas a partir de los datos disponibles de las curvas cortas a distintas temperaturas para los casos límite $t \rightarrow 0$ y $t \rightarrow \infty$. Por ello, el uso de la familia de distribuciones de valores extremos surge como una solución natural al problema de caracterización viscoelástica. Particularmente, la distribución de Gumbel, al ser el dominio de atracción de las distribuciones

normal y log-normal, constituye un candidato óptimo para describir el módulo de relajación con el tiempo de forma completa.

- d) El efecto de la temperatura constituye el efecto externo más influyente en las propiedades viscoelásticas, contribuyendo positivamente en la caracterización de este tipo de materiales. Este efecto se aborda en esta tesis a través de las distribuciones normal y de Gumbel, de acuerdo a la condición de estabilidad de las mismas. Con ello, se proponen dos modelos distintos:
- En el primer caso, el efecto de la temperatura se considera que actúa modificando el parámetro de escala de las funciones de distribución acumuladas normal y de Gumbel. Así, la estimación de la curva maestra se obtiene a partir de las curvas cortas experimentales a diferentes temperaturas, comprendidas en una ventana temporal debido a limitaciones prácticas en estos ensayos.
 - En segundo lugar, la condición de compatibilidad estadística se aplica entre la distribución del módulo de relajación para una temperatura dada $E^*(t^*; T^*)$ y la distribución del módulo para un tiempo dado $E^*(T^*; t^*)$, permitiendo así la definición analítica del campo $T^* - t^*$. Como resultado, todos los datos experimentales a distintas temperaturas pueden ser resumidos en una única curva perteneciente a la distribución acumulada de Gumbel, actuando así como la curva maestra más general posible. Una vez obtenida la estimación de este campo, entonces todas las curvas maestras en ambos campos $E^*(t^*; T^*)$ y $E^*(T^*; t^*)$ pueden ser directamente obtenidas.
- e) Los fenómenos viscoelásticos representan procesos estocásticos, siendo el tiempo y la temperatura las variables más influyentes en su comportamiento, junto con los valores límite, es decir, el módulo elástico y el módulo relajado. Por ello, las técnicas Bayesianas permiten definir de una forma probabilística las funciones viscoelásticas, particularmente los módulos de relajación y de fluencia, a partir tanto de los modelos actualmente en uso como de los propuestos en este trabajo, lo que se consigue mediante la definición de las distribuciones estadísticas de los parámetros que intervienen.
- f) Se realizó una campaña experimental de ensayos de relajación a un material viscoelástico conocido como PVB, para ocho temperaturas distintas con el objetivo de corroborar la aplicabilidad de los modelos propuestos en la caracterización viscoelástica.
- g) Otros fenómenos relacionados con la viscoelasticidad, tales como el efecto de la humedad, el envejecimiento o el grado de curado, son también analizados a partir de los modelos propuestos, demostrándose así la aplicabilidad general de los mismos.
- h) La interconversión entre las distintas funciones viscoelásticas (ensayos de relajación y fluencia, como ensayos estáticos, y los ensayos dinámicos) se

realiza de acuerdo a los métodos clásicos basados en las transformadas de Fourier y de Laplace. Esta metodología también puede ser aplicada a partir de los modelos propuestos en esta tesis. Así, una vez que el módulo de relajación es estimado, el resto de curvas maestras para las distintas funciones viscoelásticas pueden obtenerse unívocamente para cualquier temperatura de referencia.

Modelos de caracterización a fractura

- a) El desarrollo de los modelos propuestos para la definición del estado de deformaciones o de tensiones en materiales viscoelásticos permite una caracterización viscoelástica ante fallos estáticos o dinámicos en fatiga. En este sentido, se propone una extensión de las metodologías actuales determinísticas para la descripción del efecto de entalla en las propiedades a fractura basadas en la teoría de las distancias críticas a una versión probabilística. Así, los modelos desarrollados para la caracterización viscoelástica son también propuestos para la predicción de la tenacidad a fractura en componentes entallados.
- b) El efecto de la temperatura se incluye en estos modelos probabilísticos debido a su presencia concurrente con el efecto de entalla en condiciones reales de servicio, dando lugar a dos modelos distintos:
 - En primer lugar, el efecto de la temperatura se asimila como un cambio en el parámetro de escala de la distribución de la tenacidad a fractura de componentes entallados, permitiendo así la derivación analítica de los campos $K_c^N - T$ y $K_c^N - \rho$.
 - En segundo lugar, la condición de compatibilidad entre la distribución de la tenacidad a fractura para una temperatura dada y la distribución de la temperatura para un valor de la tenacidad a fractura dada se aplica para obtener la definición probabilística de las zonas intermedia e inferior de la curva de transición frágil a dúctil para cualquier condición de temperatura y radio de entalla.
- c) La aplicabilidad de los modelos probabilísticos propuestos se corrobora mediante la consideración de una extensa campaña experimental externa sobre dos aceros ferríticos, S255J2 y S355JR, para varias condiciones de temperatura y de radio de entalla.

Original Contributions

11.1 Original Contributions

The original contributions are presented with the same three concepts used in the conclusions chapter.

Phenomenological model building

- a) A general methodology to build phenomenological-mathematical models applicable to viscoelastic characterization is proposed. The models are based on physical properties of the phenomenon studied, and satisfy a minimum set of mandatory conditions to be considered a valid model.
- b) The parameters and influencing variables acting on the viscoelastic model are consistently recognized and the main variable normalized before being identified as the suitable statistical function. The physical meanings of the model parameters are acknowledged.

Viscoelastic characterization models

- a) Two novel approaches for viscoelastic characterization based on statistical functions are developed to define the field of the relaxation modulus, $E(t, T)$, as the paradigm of viscoelastic characterization.

- The first approach, derived from scale effect considerations and the uniqueness principle, admits two variants denoted, respectively, the normal model, founded on the central limit theorem when referred to the creep deformation; and the Gumbel model, based on extreme value considerations for the limiting cases, $t \rightarrow 0$ and $t \rightarrow \infty$.
- The second approach allows the $T^* - t^*$ field to be analytically defined. The field is derived from the compatibility condition between the values of the relaxation modulus over time for a given temperature $E^*(t^*; T^*)$, and along temperature for a given time $E^*(T^*; t^*)$.

Both models involve advantageous assessments of the short-time relaxation curves recorded in the experimental campaign, proving to overcome the limitations evidenced by the TTS models currently used. In this way, new advances in modeling fracture and fatigue models in viscoelastic materials are promoted.

- b) The Bayesian technique is applied to deterministic models to provide a probabilistic version of the real stochastic evolution of the relaxation modulus from the statistical distributions of the intervening parameters using OpenBUGS software. As a result, the value of the relaxation modulus, including its limiting values, are predicted as percentile values for any time and temperature.
- c) ProVisco, a friendly software for viscoelastic characterization of materials is developed. This software automatically applies the novel models to the experimental data from relaxation campaigns including tests at different temperatures. It also derives the master curves at any reference temperature of interest along with the analytical definition of the particular selected model. Different potential applications are also identified, such as its implement in finite element packages for creating material model libraries.

Fracture characterization models

- a) A probabilistic methodology to model the notch effect on fracture toughness, based on the theory of critical distances, is derived. This represents a contribution for towards future developments in the probabilistic prediction of viscoelastic fracture and fatigue. As a result, the $K_c^N - \rho$ field is defined probabilistically for any notch condition and experimental results from different notch conditions can be jointly assessed for the material characterization.
- b) The precedent methodology is extended by including the temperature and notch effect, using the scale-effect and the compatibility condition. In this way, the lower and intermediate zones of the brittle-to-ductile transition curve are probabilistically defined allowing both $K_c^N - T$ and $K_c^N - \rho$ fields to be derived directly.

11.2 Contribuciones Originales

Las contribuciones originales de esta tesis doctoral se presentan agrupadas en los mismos tres conceptos de las conclusiones.

Contribuciones con respecto a la derivación de modelos matemáticos

- a) Se ha propuesto una metodología general para la derivación sistemática de modelos fenomenológico-matemáticos, aplicable en la caracterización viscoelástica. Estos modelos están basados en las propiedades del fenómeno bajo estudio, debiendo de satisfacer un conjunto de condiciones necesarias de validez.
- b) Se han identificado las variables, propiedades y condiciones necesarios para la derivación de modelos viscoelásticos, permitiendo así una correcta identificación de las distribuciones estadísticas más adecuadas. También se ha recogido el significado físico de los parámetros de los modelos propuestos.

Contribuciones con respecto a los modelos de caracterización viscoelástica

- a) Se han desarrollado dos aproximaciones a la caracterización viscoelástica basadas en el uso de funciones estadísticas para la definición de la evolución del módulo de relajación en el tiempo, es decir, el campo $E(t; T)$, siendo éste el paradigma de la caracterización viscoelástica.
 - La primera aproximación se basa en la consideración del efecto de escala y en la condición de unicidad, presentando dos variantes posibles, denominadas modelo normal, basado en el teorema central del límite cuando se considera un ensayo de fluencia; y el modelo de Gumbel, basado en consideraciones de la teoría de valores extremos, especialmente enfocado para los casos límite $t \rightarrow 0$ y $t \rightarrow \infty$.
 - La segunda aproximación permite la definición analítica del campo $T^* - t^*$, la cual se obtiene a partir de la aplicación de la condición de compatibilidad entre la distribución que representa la evolución temporal del módulo de relajación para una temperatura dada, $E^*(t^*; T^*)$, y la evolución con la temperatura para un tiempo dado $E^*(T^*; t^*)$.

Ambas aproximaciones permiten la estimación de las curvas cortas de relajación a distintas temperaturas obtenidas en campañas, además de evitar las inconsistencias y desventajas de los modelos TTS actuales. En este sentido, se consideran unas bases teóricas adecuadas para la posible construcción de modelos para la predicción de fractura y fatiga de materiales viscoelásticos.

- b) Se han aplicado las técnicas Bayesianas a modelos determinísticos para proporcionar una versión probabilística de la evolución estocástica del módulo de relajación a partir de las distribuciones estadísticas seleccionadas, por medio del software OpenBUGS. De esta forma, los valores del módulo de relajación pueden ser obtenidos en forma de curvas percentiles para cualquier temperatura o tiempo de interés.
- c) Se ha desarrollado un software para la aplicación de la metodología de caracterización viscoelástica propuesta, denominado ProVisco. Este software permite evaluar los datos experimentales relativos a curvas cortas obtenidas a distintas temperaturas de forma automática para obtener las curvas maestras del material a cualquier temperatura. También se han identificado posibles aplicaciones del software desarrollado, tales como su implementación o conexión con paquetes de cálculo por elementos finitos para la creación de librerías de modelos de materiales viscoelásticos.

Contribuciones con respecto a los modelos de caracterización a fractura

- a) Se ha desarrollado una metodología probabilística para la modelización del efecto de entalla en las propiedades a fractura, basada en la teoría de las distancias críticas, la cual permite sentar las bases para un posible desarrollo posterior de modelos de predicción de fatiga y fractura en materiales viscoelásticos. A partir de esta metodología propuesta, el campo $K_c^N - \rho$ puede ser definido probabilísticamente para cualquier condición de entalla, permitiendo así una evaluación conjunta de diferentes campañas experimentales bajo distintos radios de entalla en la caracterización del material.
- b) La metodología propuesta para la modelización del efecto de entalla se extiende para considerar el efecto combinado con la temperatura, basado en la propiedad de efecto de escala y en la condición de compatibilidad, permitiendo también así la definición probabilística de las zonas inferior e intermedia de la curva de transición frágil-dúctil, de donde obtener directa e unívocamente los campos $K_c^N - T$ y $K_c^N - \rho$.

12

Future Work

12.1 Future Work

In this chapter some possible activities of research are recommended for continuing the advances achieved in this thesis as future research on both viscoelastic and fracture characterization of materials.

Future work in viscoelastic characterization

- a) To check the applicability of the proposed phenomenological models when applied to a varied spectrum of linear viscoelastic materials other than PVB.
- b) To extend the phenomenological models developed in the thesis to the possibly more real case in which both limiting cases, i.e. the initial and relaxed modulus are dependent on the temperature.
- c) To apply the Bayesian technique to evaluate the influence of the time interval length, selected in the experimental program, on the assessment of the parameters and viscoelastic variable prediction in an attempt of optimizing the ratio reliability/cost and relaxing the experimental procedures.
- d) To apply Bayesian techniques to accomplish the probabilistic definition of the viscoelastic functions (relaxation and compliance modulus) resulting

from the interconversion methods including the time-frequency relation.

- e) To implement the software ProVisco to include additionally the viscoelastic model based on compatibility, besides that based on scale effect already presently handled. Ditto with the Bayesian assessment of the aforementioned models.
- f) To develop the interconversion among viscoelastic functions, i.e. relaxation modulus, creep compliance and dynamic tests, using the viscoelastic models proposed and its implementation in the software ProVisco.
- g) To develop friendly interfaces allowing the interconnection with FEM packages, such as Abaqus or Ansys, to be easily performed taking advantage of the contributions achieved with proposed models in this thesis.
- h) To search an optimal computational interconversion, in terms of numerical algorithms and coding, among viscoelastic functions using the Laplace or Fourier transforms in order to reduce the required CPU time. Note that the proposed viscoelastic models involve transformations of normal and Gumbel cdfs, instead of those of simple exponential functions, as currently used.

Future work in fracture characterization models

- a) To take advantage of the experience already gained in the development of phenomenological models in viscoelasticity and fracture of metals to build fracture and fatigue models to reliable hazard prediction in the practical design of viscoelastic materials, as further extension of the approaches developed in this thesis
- b) To extend the proposed methodology focused on fracture of notches to describe both lower and intermediate zones in the brittle-to-ductile transition curve of other metallic materials
- c) To explore the suitability of the proposed phenomenological models to include the scale-effect due to the specimen geometry. In such a case, different geometry conditions maintaining homothetic ratio but also different notch and temperature conditions involved in the experimental campaign could be jointly evaluated in the fracture characterization of materials.
- d) To develop a software program, based on the proposed models, for the automatic assessment of the experimental results from fracture characterization campaigns as an input. Includes implementing Bayesian assessment to define model parameters in a probabilistic manner.
- e) To develop a software interface to implement the proposed models in finite element packages to define the brittle-to-ductile transition as a percentile curves.

12.2 Trabajo Futuro

En este capítulo se recomiendan algunas propuestas de investigación para continuar con los avances logrados en esta tesis a modo de trabajo futuro tanto para la caracterización viscoelástica como a fractura.

Trabajo futuro en la caracterización viscoelástica

- a) Aplicación de los modelos propuestos a una mayor variedad de materiales viscoelásticos lineales, demostrando así su generalidad y robustez en la caracterización viscoelástica.
- b) Aplicación de los modelos desarrollados en esta tesis para casos posiblemente más reales en los que los valores límite, es decir, los módulos inicial y relajado, sean dependientes de la temperatura.
- c) Aplicación de las técnicas Bayesianas para la evaluación de la influencia del tamaño de la ventana temporal seleccionada en la campaña experimental, permitiendo así optimizar la ratio entre fiabilidad y coste con la consecuente relajación de dichas campañas experimentales.
- d) Aplicación de las técnicas Bayesianas en la interconversión entre funciones viscoelásticas, permitiendo así una definición probabilística de estas funciones a partir de la estimación del módulo de relajación.
- e) Extensión del programa ProVisco para incluir la estimación del modelo basado en la condición de compatibilidad, aparte de aquellos basados en la propiedad de escala, así como la aplicación de las técnicas Bayesianas de OpenBUGS.
- f) Extensión del programa ProVisco con la inclusión de la interconversión entre funciones viscoelásticas de relajación y fluencia, ambos en estático y dinámico, a partir de los modelos propuestos.
- g) Desarrollo de aplicaciones o interfaces que permitan la interconexión del programa ProVisco con otros paquetes de cálculo por elementos finitos para poder crear nuevas librerías de modelos de material viscoelástico a partir de la evaluación realizada en base a una campaña experimental con su correspondiente definición analítica.
- h) Optimización del coste computacional del cálculo de las interconversiones entre funciones viscoelásticas basadas en los modelos propuestos mediante el uso de algoritmos numéricos para el cálculo rápido de las transformadas de Fourier o Laplace, dado que los modelos propuestos implican aproximaciones numéricas para las transformadas de distribuciones como la normal o Gumbel, frente a simples funciones exponenciales actualmente en uso.

Trabajo futuro en la caracterización a fractura

- a) Desarrollo de modelos fenomenológicos para la predicción de fallo a fractura y fatiga en el diseño de componentes viscoelásticos como extensión de los modelos propuestos en esta tesis en viscoelasticidad y en fractura de materiales metálicos.
- b) Extensión de la metodología propuesta para la definición de las zonas inferior e intermedia en la curva de transición frágil a dúctil a otros materiales metálicos.
- c) Extensión de los modelos fenomenológicos propuestos para incluir el efecto de escala debido a la geometría de la probeta, manteniéndose la condición de homotéticas, de tal forma que pueda ser tenido en cuenta este efecto junto con el debido al radio de entalla y la temperatura.
- d) Desarrollo de un software basado en los modelos propuestos para la evaluación automática de resultados experimentales a fractura, con la inclusión de las técnicas Bayesianas para definir los parámetros de los modelos de forma probabilística.
- e) Desarrollo de interfaces software que permitan la conexión con paquetes de elementos finitos para la creación de modelos de material que incluyan la curva de transición frágil a dúctil en su concepción probabilística.

VI

Appendixes

Appendix A

Appendix A. Solution of the Weibull-Gumbel Model

The functional equation (3.82) resulting from the application of the compatibility condition between the Weibull and Gumbel distributions can be written as follows:

$$[a(x) + b(x)y]^{c(x)} = \exp [d(y) + e(y)x], \quad (\text{A.1})$$

from where by setting $x = 0$ in (A.1), it results:

$$[a(0) + b(0)y]^{c(0)} = \exp [d(y)], \quad (\text{A.2})$$

such that the unknown function $d(y)$ can now be determined, that is,

$$d(y) = \log(A + By)^\beta, \quad (\text{A.3})$$

where

$$A = a(0), B = b(0) \text{ and } \beta = c(0). \quad (\text{A.4})$$

On the other hand, by setting $x = 1$ in (A.1), it results:

$$[a(1) + b(1)y]^{c(1)} = \exp [d(y) + e(y)], \quad (\text{A.5})$$

that is,

$$e(y) = \log \left\{ [a(1) + b(1)y]^{c(1)} \right\} - \log(A + By)^\beta, \quad (\text{A.6})$$

from where the unknown function $e(y)$ can be derived as follows

$$e(y) = \log \frac{(C + Dy)^\alpha}{(A + By)^\beta}, \quad (\text{A.7})$$

with some arbitrary constants defined as

$$C = a(1), D = b(1) \text{ and } \alpha = c(1). \quad (\text{A.8})$$

Then, by making $y = 0$ in (A.1) and considering (A.3) and (A.7), it leads to:

$$a(x) = \exp \left[\frac{d(0) + e(0)x}{c(x)} \right] = \left\{ A^\beta \left(\frac{C^\alpha}{A^\beta} \right)^x \right\}^{1/c(x)}. \quad (\text{A.9})$$

such that by setting $y = 1$ and $y = 2$ in (A.1) and considering (A.3) and (A.7), it follows respectively:

$$a(x) + b(x) = \exp \left[\frac{d(1) + e(1)x}{c(x)} \right] = \left\{ (A + B)^\beta \left[\frac{(C + D)^\alpha}{(A + B)^\beta} \right]^x \right\}^{1/c(x)}, \quad (\text{A.10})$$

$$a(x) + 2b(x) = \exp \left[\frac{d(2) + e(2)x}{c(x)} \right] = \left\{ (A + 2B)^\beta \left[\frac{(C + 2D)^\alpha}{(A + 2B)^\beta} \right]^x \right\}^{1/c(x)}, \quad (\text{A.11})$$

and from (A.9), (A.10) and (A.11) it follows

$$b(x) = \left\{ (A + B)^\beta \left[\frac{(C + D)^\alpha}{(A + B)^\beta} \right]^x \right\}^{1/c(x)} - \left\{ A^\beta \left(\frac{C^\alpha}{A^\beta} \right)^x \right\}^{1/c(x)} \quad (\text{A.12})$$

$$b(x) = \left\{ (A + 2B)^\beta \left[\frac{(C + 2D)^\alpha}{(A + 2B)^\beta} \right]^x \right\}^{1/c(x)} - \left\{ (A + B)^\beta \left[\frac{(C + D)^\alpha}{(A + B)^\beta} \right]^x \right\}^{1/c(x)} \quad (\text{A.13})$$

which imposes (A.12) and (A.13) to be equal, from where two different possibilities must be distinguished:

- a) *Case 1: Non-constant $c(x)$.* The arbitrary constants must be consistent, such that,

$$A + 2B = A + B = A \text{ and } C + 2D = C + D = C, \quad (\text{A.14})$$

that is, $B = D = 0$, or

$$c(x) = \beta \text{ and } \frac{C + 2D}{A + 2B} = \frac{C + D}{A + B} = \frac{C}{A} = k, \quad (\text{A.15})$$

where k is another constant. Hence, the condition (A.14) leads to constant $d(y)$ and $e(y)$ functions, which is a not valid model. Therefore, the only possible model is obtained for (A.15), that is, for $C = kA$ and $D = kB$.

b) *Case 2: Constant $c(x)$.* From (A.9), (A.12), (A.3) and (A.7), it results

$$a(x) = Ak^x, \quad (\text{A.16})$$

$$b(x) = Bk^x, \quad (\text{A.17})$$

$$c(x) = \beta, \quad (\text{A.18})$$

$$d(y) = \beta \log(A + By), \quad (\text{A.19})$$

$$e(y) = \beta \log(k), \quad (\text{A.20})$$

from where (A.1) holds identically, that is,

$$[a(x) + b(x)y]^{c(x)} = \exp [d(y) + e(y)x] = [(A + By)k^x]^\beta, \quad (\text{A.21})$$

which leads to

$$\begin{aligned} F(x|y) &= 1 - \exp \{- \exp (\beta \log [(A + By)k^x])\} \\ &= 1 - \exp \left\{ - \exp \left[\frac{\log(k^x(y - G)) - \lambda}{\delta} \right] \right\}; \quad x \geq 0; \quad y \geq G \end{aligned} \quad (\text{A.22})$$

and

$$F(y|x) = 1 - \exp \left\{ - \left[\frac{k^x(y - G)}{\delta} \right]^\beta \right\}; \quad x \geq 0; \quad y \geq G, \quad (\text{A.23})$$

where

$$G = -A/B, \lambda = -\log B \text{ and } \delta = 1/\beta, \quad (\text{A.24})$$

being both (A.22) and (A.23) the most general solution of the Weibull-Gumbel model.

Bibliography

- Abe, A., Albertsson, A. C., Dusek, K., Genzer, J., Kobayashi, S., Lee, K. S., Leibler, L., Long, T. E., Manners, I., Möller, M., Terentjev, E. M., Vicent, M. J., Voit, B., and Wiesner, U. (2000). *Viscoelasticity Atomistic Models Statistical Chemistry*, volume 152 of *Advances in Polymer Science*. Springer-Verlag Berlin Heidelberg.
- Aczel, J. and Dhombres, J. (1989). *Functional Equations in Several Variables*. Encyclopedia of Mathematics and its Applications. Cambridge University Press, Cambridge.
- Aczél, J. (1966). *Lectures on Functional Equations and their Applications*. Academic Press, 1 edition.
- Aczél, J. (1986). On scientific laws without dimensional constants. *Journal of Mathematical Analysis and Applications*, 119:389–416.
- Aczél, J. (1987). *A Short Course on Functional Equations Based Upon Recent Applications to the Social and Behavioral Sciences*. Springer Netherlands, 1 (pag. 35) edition.
- Adam, G. and Gibbs, J. H. (1965). On the temperature dependence of cooperative relaxation properties in glass-forming liquids. *The Journal of Chemical Physics*, 43(1):139–146.
- Advani, S. G. and Sozer, E. M. (2010). *Process Modeling in Composites Manufacturing*. CRC Press, 2 edition.
- Alfrey, T. and Doty, P. (1945). The methods of specifying the properties of viscoelastic materials. *Journal of Applied Physics*, 16(11):700–713.

- Álvarez-Vázquez, A., Fernández-Canteli, A., Castillo, E., Pelayo, F., Muñiz-Calvente, M., and Lamela-Rey, M. J. (2020a). A novel approach to describe the time-temperature conversion among relaxation curves of viscoelastic materials. *Materials*, 18:1809–1824.
- Álvarez-Vázquez, A., Fernández-Canteli, A., Castillo, E., Pelayo, F., Muñiz-Calvente, M., and Lamela-Rey, M. J. (2020b). A time- and temperature-dependent viscoelastic model based on the statistical compatibility condition. *Materials & Design*, 193:108828.
- Álvarez-Vázquez, A., Muñiz-Calvente, M., Fernández-Canteli, A., Lamela, M. J., and Castillo, E. (2020c). A geometry and temperature dependent regression model for statistical analysis of fracture toughness in notched components. *Engineering Fracture Mechanics (Under review)*.
- Anderson, T. L. (2017). *Fracture Mechanics. Fundamentals and Applications*. CRC Press, 4 edition.
- Anderssen, R. S., Husain, S., and Loy, R. J. (2004). The kohlrusch function: properties and applications. *Australian & New Zealand Industrial and Applied Mathematics Journal*, 45:c800–c816.
- Arnold, B. C. (2004). *Castillo-Galambos Functional Equation*. American Cancer Society.
- Arnold, B. C., Balakrishnan, N., and Nagaraja, H. N. (2008). *A First Course in Order Statistics*. Textbooks in Probability and Statistics. Society for Industrial and Applied Mathematics (SIAM), 1 edition.
- Arnold, B. C., Castillo, E., and Sarabia, J. M. (1993). Multivariate distributions with generalized pareto conditionals. *Statistics & Probability Letters*, 17:361–368.
- Arnold, B. C., Castillo, E., and Sarabia, J. M. (1994). A conditional characterization of the multivariate normal distribution. *Statistics & Probability Letters*, 19:313–315.
- Arnold, B. C., Castillo, E., and Sarabia, J. M. (1998). Some alternative bivariate gumbel models. *Environmetrics*, 9:599–616.
- Arnold, B. C., Castillo, E., and Sarabia, J. M. (1999). *Conditional Specification of Statistical Models*. Springer Verlag New York, 1 edition.
- ASTM 1820–11 (2011). Standard test method for measurement of fracture toughness. Standard, American Society for Testing and Materials, Philadelphia.
- ASTM 1921–97 (2005). Standard test method for determination of reference temperature T_0 , for ferritic steels in the transition range. Standard, American Society for Testing and Materials, Philadelphia.
- Astrom, B. T. (1997). *Manufacturing of Polymer Composites*. CRC Press, 1 edition.

- Aulova, A., Govekar, E., and Emri, I. (2016). Determination of relaxation modulus of time-dependent materials using neural networks. *Mechanics of Time-Dependent Materials*, 21:331–349.
- Bae, J. E., Cho, K. S., Seo, K. H., and Kang, D. G. (2011). Application of geometric algorithm of time-temperature superposition to linear viscoelasticity of rubber compounds. *Korea-Australia Rheology Journal*, 23:81—87.
- Balakrishnan, N. and Nevzorov, V. B. (2003). *A Primer on Statistical Distributions*. John Wiley & Sons, 1 edition.
- Balakrishnan, N. and Rao, C. R. (1998a). *Order Statistics: Applications*, volume 17 of *Handbook of Statistics*. Elsevier Science, 1 edition.
- Balakrishnan, N. and Rao, C. R. (1998b). *Order Statistics: Theory and Methods*, volume 16 of *Handbook of Statistics*. Elsevier Science, 1 edition.
- Bao, Y. and Jin, Z. (1993). Size effects and a mean-strength criterion for ceramics. *Fatigue & Fracture of Engineering Materials & Structures*, 8:829—35.
- Barenblatt, G. I. (1996). *Scaling, Self-similarity, and Intermediate Asymptotics*. Cambridge Texts in Applied Mathematics, 1 edition.
- Barenblatt, G. I. (2003). *Scaling*. Cambridge Texts in Applied Mathematics, 1 edition.
- Bavaud, F. (1987). Statistical mechanics of viscoelasticity. *Journal of Statistical Physics*, 46:753–775.
- Berry, J., Burghes, D., Huntley, I., James, D., and A.O.Moscardini, editors (1984). *Teaching and Applying Mathematical Modelling*. John Wiley.
- Bestul, A. and Chang, S. (1964). Excess entropy at glass transformation. *Journal of Chemical Physics*, 40:3731—3733.
- Bogdanoff, J. L. and Kozin, F. (1987). Effect of length on fatigue life of cables. *Journal of Engineering Mechanics*, 113:925–940.
- Boltzmann, L. (1878). Zur theorie der elastischen nachwirkung. *Annalen der Physik*, 241(11):430–432.
- Bradshaw, R. D. and Brinson, L. C. (1997). Physical aging in polymers and polymer composites: An analysis and method for time-aging time superposition. *Polymer Engineering & Science*, 37(1):31–44.
- Bridgman, P. (1922). *Dimensional Analysis*. Yale University Press, New Heaven, CT.
- Brinson, Hal F., B. L. C. (2015). *Polymer Engineering Science and Viscoelasticity. An Introduction*. Springer US, 1 edition.

- Brinson, L. C. and Gates, T. S. (1995). Effects of physical aging on long term creep of polymers and polymer matrix composites. *International Journal of Solids and Structures*, 32(6):827 – 846. Time Dependent Problems in Mechanics.
- Brooke, A., Kendrick, D., Meeraus, A., Raman, R., and Rosenthal, R. E. (1998). *GAMS. A User's Guide*. GAMS Development Corporation, Washington, DC.
- Buckingham, E. (1915). The principle of similitude. *Nature*, 96:396–397.
- Bueche, F. (1962). Rate and pressure effects in polymers and other glass-forming substances. *Journal of the American Chemical Society*, 36:2940–2946.
- Buttlar W.G., Roque R., R. B. (1998). Automated procedure for generation of creep compliance master curve for asphalt mixtures. *Journal of the Transportation Research Board*, 1630:28—36.
- Carpinteri, A. and Mainardi, F. (1997). *Fractals and Fractional Calculus in Continuum Mechanics*. CISM International Centre for Mechanical Sciences. Springer-Verlag Wien, 1 edition.
- Castillo, E. (1988). *Extreme Value Theory in Engineering*. Academic Press, 1 edition.
- Castillo, E., Calviño, A., Nogal, M., and Lo, H. K. (2014a). On the probabilistic and physical consistency of traffic random variables and models. *Computer-Aided Civil and Infrastructure Engineering*, 29:496–517.
- Castillo, E. and Fernández-Canteli, A. (2001). A general regression model for lifetime evaluation and prediction. *International Journal of Fracture*, 107(2):117–137.
- Castillo, E., Fernández-Canteli, A., and Siegele, D. (2014b). Obtaining S–N curves from crack growth curves: an alternative to self-similarity. *International Journal of Fracture*, 187:159–172.
- Castillo, E. and Fernández-Canteli, A. (1986). A statistical model for lifetime analysis. *Electric*, 84:5–21.
- Castillo, E. and Fernández-Canteli, A. (2009). *A Unified Statistical Methodology for Modeling Fatigue Damage*. Springer Netherlands, 1 edition.
- Castillo, E., Fernández-Canteli, A., Castillo, C., and Mozos, C. (2010). A new probabilistic model for crack propagation under fatigue loads and its connection with wöhler fields. *International Journal of Fatigue*, 32(4):744 – 753.
- Castillo, E., Fernández-Canteli, A., Esslinger, V., and Thürliman (1985). Statistical models for fatigue analysis of wires, strands and cables. In *IABSE Proceedings*, volume 82, pages 1–140.
- Castillo, E., Fernández-Canteli, A., and Hadi, A. S. (1999). On fitting a fatigue model to data. *International Journal of Fatigue*, 21(1):97–106.

- Castillo, E., Fernández-Canteli, A., Ruiz-Tolosa, J. R., and Sarabia, J. M. (1988). Statistical models for analysis of fatigue life of long elements. *Journal of Engineering Mechanics*, 116:1036–1049.
- Castillo, E. and Galambos, J. (1987a). Bivariate distributions with normal conditionals. In *Proceedings of the IASTED International Symposium on Simulation, Modeling and Development SMD-87*, pages 59–62.
- Castillo, E. and Galambos, J. (1987b). Lifetime regression models based on a functional equation of physical nature. *Journal of Applied Probability*, 24(1):160–169.
- Castillo, E. and Galambos, J. (1989). Conditional distributions and the bivariate normal distribution. *Metrika*, 36:209–214.
- Castillo, E. and Galambos, J. (1990). Bivariate distributions with weibull conditionals. *Analysis Mathematica*, 16:3–9.
- Castillo, E. and Hadi, A. S. (1994). Parameter and quantile estimation for the generalized extreme-value distribution. *Environmetrics*, 5(4):417–432.
- Castillo, E. and Hadi, A. S. (1995). Modeling lifetime data with application to fatigue models. *Journal of the American Statistical Association*, 90(431):1041–1054.
- Castillo, E., Hadi, A. S., Balakrishnan, N., and Sarabia, J. M. (2004a). *Extreme Value and Related Models with Applications in Engineering and Science*. Wiley Series in Probability and Statistics, 1 edition.
- Castillo, E., Iglesias, A., and Ruiz-Cobo, R. (2004b). *Functional Equations in Applied Sciences*. Elsevier Science, 1 edition.
- Castillo, E., Muniz-Calvente, M., Fernández-Canteli, A., and Blasón, S. (2019). Fatigue assessment strategy using bayesian techniques. *Materials*, 12(19).
- Castillo, E., O'Connor, J., and Nogal, M. (2014c). On the physical and probabilistic consistency of some engineering random models. *Structural Safety*, 51:1–12.
- Castillo, E. and Pruneda, E. (2001). *Estadística Aplicada*. Moralea, 1 edition.
- Castillo, E. and Ruiz-Cobo, M. R. (1992). *Functional Equations and Modelling in Science and Engineering*, volume 161 of *Monographs and Textbooks in Pure and Applied Mathematics*. Marcel Dekker Inc., New York.
- Cauchy, A. L. (1821). *Cours d'Analyse d l'Ecole Polytechnique*, volume 1 of *Analyse Algébrique*. Debure, Paris.
- Chen, T. (2000). Determining the Prony series for a viscoelastic material from time-varying strain data. Technical Report NASA/NTM-2000-210123, NAS 1.15:210123, ARL-TR-2206, L-17978, NASA.

- Cho, K. S. (2009). Geometric interpretation of time-temperature superposition. *Korea-Aust Rheol J*, 21:13—16.
- Cho, K. S. (2016). *Viscoelasticity of Polymers. Theory and Numerical Algorithms*. Springer Series in Materials Science. Springer Netherlands, 1 edition.
- Christensen, R. M. (1982). *Theory of Viscoelasticity*. Dover Publications, 2 edition.
- Cicero, S., Gutiérrez-Solana, F., and Álvarez, J. (2008). Structural integrity assessment of components subjected to low constraint conditions. *Engineering Fracture Mechanics*, 10:3038—59.
- Cicero, S., Madrazo, V., Carrascal, I. A., and Cicero, R. (2011a). Assessment of notched structural components using failure assessment diagrams and the theory of critical distances. *Engineering Fracture Mechanics*, 16:2809—25.
- Cicero, S., Madrazo, V., and García, T. (2011b). The notch master curve: a proposal of master curve for ferritic-pearlitic steels in notched conditions. *Engineering Fracture Mechanics*, 16:2809—25.
- Coles, S. (2001). *An Introduction to Statistical Modeling of Extreme Values*. Springer Series in Statistics. Springer-Verlag London.
- Cowie, J., Ferguson, R., Harris, S., and McEwen, I. (1998). Physical ageing in poly(vinyl acetate)—3. structural relaxation and its effect on the stress relaxation modulus. *Polymer*, 39(18):4393 – 4397.
- Creager, M. and Paris, P. C. (1967). Elastic field equations for blunt cracks with reference to stress corrosion cracking. *International Journal of Fracture*, 4:247—52.
- David, H. A. and Nagaraja, H. N. (2010). *Order Statistics*. John Wiley & Sons, third edition.
- de Haan, L. and Ferreira, A. (2010). *Extreme Value Theory: An Introduction*. (Springer Series in Operations Research and Financial Engineering) Springer, 1st edition edition.
- de Oliveria, J. T. (1984). *Statistical Extremes and Applications*. NATO ASI Series. D. reidel Publishing Company, Lisbon, 1 edition.
- DeVault, G. P. and McLennan, J. A. (1965). Statistical mechanics of viscoelasticity. *Physical Review*, 137:A724—A730.
- Doolittle, A. and Doolittle, D. (1957). Studies in newtonian flow v. further verification of the free space viscosity equation. *Journal of Applied Physics*, 28:901—905.
- Drozdov, A. (1998). *Viscoelastic Structures*. Academic Press, 1 edition.

- Emri, I. and Pavsek, V. (1992). On the influence of moisture on the mechanical properties of polymers. *Materials Forum*, 16:123–131.
- Emri, I. and Tschoegl, N. (1993). Generating line spectra from experimental responses. Part I: Relaxation modulus and creep compliance. *Rheologica Acta*, 32:311–321.
- Emri, I. and Tschoegl, N. (1994). Generating line spectra from experimental responses. Part IV: Application to experimental data. *Rheologica Acta*, 33:60–70.
- Emri, I. and Tschoegl, N. (1995). Determination of mechanical spectra from experimental responses. *International Journal of Solids and Structures*, 32(2):817–826.
- Emri, I., von Bernstorff, B., Cvelbar, R., and Nikonov, A. (2005). Re-examination of the approximate methods for interconversion between frequency- and time-dependent material functions. *Journal of Non-Newtonian Fluid Mechanics*, 129(2):75–84.
- Eyring, H. (1936). Viscosity, plasticity, and diffusion as examples of absolute reaction rates. *The Journal of Chemical Physics*, 4(4):283–291.
- Fabrizio, M. and Morro, A. (1992). *Mathematical Problems in Linear Viscoelasticity*. Studies in Applied and Numerical Mathematics (SIAM), 1 edition.
- Falmagne, J. C. and Narens, L. (1983). Scales and meaningfulness of quantitative laws. *Synthese*, 55:287–325.
- Fernández, P., Lamela, M., and Fernández-Canteli, A. (2011). Study of the interconversion between viscoelastic behaviour functions of PMMA. *Mechanics of Time-Dependent Materials*, 15(2):169—180.
- Ferry, J. D. (1950). Mechanical properties of substances of high molecular weight. vi. dispersion in concentrated polymer solutions and its dependence on temperature and concentration. *Journal of the American Chemical Society*, 72(8):3746–3752.
- Ferry, J. D. (1980). *Viscoelastic Properties of Polymers*. John Wiley and Sons, 3 edition.
- Findley, W. N., Lai, J. S., and Onaran, K. (1976). *Creep and Relaxation of Non-linear Viscoelastic Materials. With and Introduction to Linear Viscoelasticity*. Dover Publications.
- Frank, K. H., George, D. A., Schluter, C. A., Gealy, S., and Horos, D. R. (1993). Notch toughness variability in bridge steel plates. Technical Report 335, National Cooperative Highway Research Program, Washington, D.C.
- Freudenthal, A. and Gumbel, E. (1956). Physical and statistical aspects of fatigue. volume 4 of *Advances in Applied Mechanics*, pages 117 – 158. Elsevier.

- Frigg, R. and Hartmann, S. (2017). Models in science. In Zalta, E. N., editor, *The Stanford Encyclopedia of Philosophy*. Metaphysics Research Lab, Stanford University, spring 2017 edition.
- Galambos, J. (1978). *The Asymptotic Theory of Extreme Order Statistics*. John Wiley & Sons.
- Galambos, J. (1982). The role of functional equations in stochastic model building. *Aequationes Mathematicae*, 25:21–41.
- Galambos, J. (1984). *Introductory Probability Theory*. Probability: Pure and Applied. CRC Press.
- Galambos, J. (1995). *Advanced Probability Theory*. Probability: Pure and Applied. CRC Press.
- Galambos, J. and Kotz, S. (1978). *Characterizations of Probability Distributions. A Unified Approach with an Emphasis on Exponential and Related Models*, volume 675 of *Lectures Notes in Mathematics*. Springer-Verlag Berlin Heidelberg.
- Gergesova, M., Zupančič, B., Saprunov, I., and Emri, I. (2011). The closed form t-T-P shifting (CFS) algorithm. *Journal of Rheology*, 55:1–16.
- Glinka, G. and Newport, A. (1987). Universal features of elastic notch-tip stress fields. *International Journal of Fatigue*, 9(3):143 – 150.
- Gnedenko, B. (1943). Sur la distribution limite du terme maximum d’une serie aleatoire. *Annals of Mathematics*, 44(3):423–453.
- Goldstein, M. (1963). Some thermodynamic aspects of the glass transition: Free volume, entropy, and enthalpy theories. *Journal of Chemical Physics*, 39:3369—3374.
- Gross, B. (1953). *Mathematical Structure of the Theories of Viscoelasticity*. Hermann & C., Paris.
- Gross, B. (1969). Time-temperature superposition principle in relaxation theory. *Journal of Applied Physics*, 40:3397.
- Gumbel, E. J. (1958). *Statistics of extremes*. Columbia University Press, New York.
- Gutierrez-Lemini, D. (2014). *Engineering Viscoelasticity*. Springer US.
- Haario, H., von Hertzen, R., Karttunen, A. T., and Jorkama, M. (2014). Identification of the viscoelastic parameters of a polymer model by the aid of a MCMC method. *Mechanics Research Communications*, 61:1–6.
- Hermida, . and Povolo, F. (1994). Analytical-numerical procedure to determine if a set of experimental curves can be superimposed to form a master curve. *Polym Journal*, 26:981 — 992.

- Hernández, W., Castello, D., Roitman, N., and Magluta, C. (2017). Thermorheologically simple materials: A bayesian framework for model calibration and validation. *Journal of Sound and Vibration*, 402:14 – 30.
- Holmström, K. and Petersson, J. (2002). A review of the parameter estimation problem of fitting positive exponential sums to empirical data. *Applied Mathematics and Computation*, 126(1):31–61.
- Honerkamp, J. and Weese, J. (1993). A note on estimating mastercurves. *Rheologica Acta*, 32(1):57–64.
- Hou, T. and Chen, H. (2012). Isothermal physical aging of peek and pps investigated by fractional maxwell model. *Polymer*, 53(12):2509 – 2518.
- Hutchinson, J. and Cortés, P. (2018). Physical aging of shape memory polymers based upon epoxy-thiol “click” systems. *Polymer Testing*, 65:480 – 490.
- Hutchinson, J. M. (1995). Physical aging of polymers. *Progress in Polymer Science*, 20(4):703 – 760.
- ISO 18437-6:2017 (2017). Mechanical vibration and shock — Characterization of the dynamic mechanical properties of visco-elastic materials — Part 6: Time-temperature superposition. Standard, International Organization for Standardization, Geneva, CH.
- Janas, V. and McCullough, R. (1987). The effects of physical aging on the viscoelastic behavior of a thermoset polyester. *Composites Science and Technology*, 30(2):99 – 118.
- Jones, D. I. G. (2001). *Handbook of Viscoelastic Vibration Damping*. John Wiley & Sons.
- Jonscher, A. K. (1977). The ‘universal’ dielectric response. *Nature*, 267:673–679.
- Justo, J., Castro, J., Cicero, S., Sánchez-Carro, M., and Husillos, R. (2017). Notch effect on the fracture of several rocks: Application of the theory of critical distances. *Theoretical and Applied Fracture Mechanics*, 90:251 – 258.
- Kapur, J. N. (1988). *Mathematical Modelling*. New Age International Ltd.
- Kawakatsu, T. (2004). *Statistical Physics of Polymers. An Introduction*. Advanced Texts in Physics. Springer-Verlag Berlin Heidelberg.
- Kim, Y. K. and White, S. R. (1996). Stress relaxation behavior of 3501-6 epoxy resin during cure. *Polymer Engineering & Science*, 36(23):2852–2862.
- Knauss, W. and Emri, I. (1981). Non-linear viscoelasticity based on free volume consideration. *Computers & Structures*, 13(1):123 – 128.
- Knauss, W. G. (2008). The sensitivity of the time-temperature shift process to thermal variations—a note. *Mechanics of Time-Dependent Materials*, 12:179–188.

- Knauss, W. G. and Emri, I. (1987). Volume change and the nonlinearly thermo-viscoelastic constitution of polymers. *Polymer Engineering & Science*, 27(1):86–100.
- Knauss, W. G. and Kenner, V. H. (1980). On the hygrothermomechanical characterization of polyvinyl acetate. *Journal of Applied Physics*, 51(10):5131–5136.
- Koeller, R. C. (1984). Applications of fractional calculus to the theory of viscoelasticity. *Journal of Applied Mechanics*, 51(2):299–307.
- Kohlrausch, R. (1854). Theorie des elektrischen rückstandes in der leidener flasche. *Annalen der Physik*, 167(1):56–82.
- Kotz, S., Read, C. B., Balakrishnan, N., and Vidakovic, B. (2005). *Encyclopedia of Statistical Sciences*. John Wiley Sons, 2 edition.
- Lakes, R. (2009). *Viscoelastic Materials*. Cambridge University Press, Cambridge, 1 edition.
- Leadbetter, M. R., Lindgren, G., and Rootzen, H. (1983). *Extremes and Related Properties of Random Sequences and Processes*. Springer Series in Statistics. Springer-Verlag New York.
- Leaderman, H. (1942). *Elastic and Creep Properties of Filamentous Materials*. PhD thesis, Massachusetts Institute of Technology, California, EE.UU.
- Leaderman, H., Smith, R. G., and Jones, R. W. (1954). Rheology of polyisobutylene. ii. low molecular weight polymers. *Journal of Polymer Science*, 14(73):47–80.
- Legendre, A. M. (1971). *Elements de geometrie. Note II*. Didot, Paris.
- Li, H. and Zhang, B. (2016). Improved models of viscosity and relaxation modulus for epoxy resin during cure. *Polymer Engineering & Science*, 56(6):617–621.
- Lin, Y., Hwang, S., Lee, H., and Huang, D. (2011). Modeling of viscoelastic behavior of an epoxy molding compound during and after curing. *IEEE Transactions on Components, Packaging and Manufacturing Technology*, 1(11):1755–1760.
- Lin, Y.-H. (2010). *Polymer Viscoelasticity: Basics, Molecular Theories, Experiments and Simulations*. World Scientific, 2nd edition.
- Loeve, M. (1977). *Probability Theory I*, volume 45 of *Graduate Texts in Mathematics*. Springer-Verlag New York, 4 edition.
- Luce, R. (1964). A generalization of a theorem of dimensional analysis. *Journal of Mathematical Psychology*, 1(2):278 – 284.
- Lunn, D., Thomas, A., Best, N., and Spiegelhalter, D. (2000). Winbugs — a bayesian modelling framework: concepts, structure, and extensibility. *Statistics and Computing*, 10:325—337.

- Madrazo, V., Cicero, S., and García, T. (2014). Assessment of notched structural steel components using failure assessment diagrams and the theory of critical distances. *Engineering Failure Analysis*, 36:104–120.
- Mainardi, F. (2010). *Fractional Calculus and Waves in Linear Viscoelasticity. An Introduction to Mathematical Models*. Imperial College Press, 1 edition.
- Mainardi, F. (2018). *Fractional Calculus: Theory and Applications*. MDPI: Mathematics, 1 edition.
- Mainardi, F., Masina, E., and Spada, G. (2019). A generalization of the Becker model in linear viscoelasticity: creep, relaxation and internal friction. *Mechanics of Time-Dependent Materials*, 23:283–294.
- Maiti, A. (2019). Second-order statistical bootstrap for the uncertainty quantification of time-temperature-superposition analysis. *Rheologica Acta*, 58:261–271.
- Marques, S. P. C. and Creus, G. J. (2012). *Computational Viscoelasticity*. SpringerBriefs in Computational Mechanics. Springer-Verlag Berlin Heidelberg, 1 edition.
- Martin, R. (2012). *Ageing of Composites*. Woodhead Publishing in Materials, Cambridge, 1 edition.
- Matvienko, Y. G. (2004). Local fracture criterion to describe failure assessment diagrams for a body with a crack/notch. *International journal of Fracture*, 124:107–112.
- McCrum, N. G. and Morris, E. L. (1964). On the measurement of the activation energies for creep and stress relaxation. *Proceedings of the Royal Society of London*, 281:258–273.
- Meyer, W. J. (1984). *Concepts of Mathematical Modeling*. Dover Publications.
- Münstedt, H. and Schwarzl, F. R. (2014). *Deformation and Flow of Polymeric Materials*. Springer-Verlag Berlin Heidelberg.
- Morland, L. W. and Lee, E. H. (1960). Stress analysis for linear viscoelastic materials with temperature variation. *Transactions of the Society of Rheology*.
- Moskovic, R. (1993). Statistical analysis of censored fracture toughness data in the ductile to brittle transition temperature region. *Engineering Fracture Mechanics*, 44(1):21 – 41.
- Muñiz-Calvente, M. (2017). *The generalized local approach. A methodology for probabilistic assessment of fracture under different failure criteria*. PhD Thesis in Industrial Engineering, University of Oviedo, Gijón, Asturias, Spain.

- Muñiz-Calvente, M., Álvarez Vázquez, A., Cicero, S., Correia, J., de Jesus, A. M. P., Blasón, S., Fernández-Canteli, A., and Berto, F. (2019). Study of the influence of notch radii and temperature on the probability of failure: a methodology to perform a combined assessment. *Fatigue Fracture of Engineering Materials and Structures*, X(X):1–11.
- Murthy, D. N. P., Xie, M., and Jiang, R. (2004). *Weibull Models*. Wiley Series in Probability and Statistics. John Wiley & Sons.
- Naya, S., Meneses, A., Tarrío-Saavedra, J., Artiaga, R., Lopez-Beceiro, J., and Gracia-Fernandez, C. (2013). New method for estimating shift factors in time–temperature superposition models. *Journal of Thermal Analysis and Calorimetry*, 113:453–460.
- Neuber, H. (1958). *Kerbspannungslehre*. Springer Verlag Berlin Heidelberg.
- Neuber, H. (1961). *Theory of notch stresses: principles for exact calculation of strength with reference to structural form and material*, volume 4547. USAEC Office of Technical Information.
- Nowick, A. (1972). *Anelastic Relaxation in Crystalline Solids*. Materials Science Series [v. 1]. New York, Academic Press.
- Nutting, P. G. (1921). A new general law of deformation. *Journal of the Franklin Institute*, 191(5):679–685.
- Onogi, S., Sasaguri, K., Adachi, T., and Ogihara, S. (1962). Time–humidity superposition in some crystalline polymers. *Journal of Polymer Science*, 58(166):1–17.
- Orchestrator, T. A. (2008). *User Manual*. TA Instruments – Waters LLC, New Castle, (v7.2.0.4) edition.
- Oseli, A., Aulova, A., Gergesova, M., and Emri, I. (2016). Time-temperature superposition in linear and non-linear domain. *Materials Today: Proceedings*, 3(4):1118 – 1123. 32nd DANUBIA ADRIA SYMPOSIUM on Advanced in Experimental Mechanics.
- Palmer, R., Stein, D., Abrahams, E., and Anderson, P. (1984). Models of hierarchically constrained dynamics for glassy relaxation. *Physical Review Letters*, 53(10):958–961.
- Park, S. W. and Schapery, R. A. (1999a). Methods of interconversion between linear viscoelastic material functions[part i – a numerical method based on prony series. *International Journal of Solids and Structures*, 36:1653–1675.
- Park, S. W. and Schapery, R. A. (1999b). Methods of interconversion between linear viscoelastic material functions. part ii – an approximate analytical method. *International Journal of Solids and Structures*, 36:1677–1699.

- Pelayo, F., Lamela-Rey, M., Muniz-Calvente, M., López-Aenlle, M., Álvarez Vázquez, A., and Fernández-Canteli, A. (2017). Study of the time-temperature-dependent behaviour of PVB: Application to laminated glass elements. *Thin-Walled Structures*, 119:324–331.
- Peterson, R. (1953). *Stress Concentration Design Factor*. John Wiley & Sons, New York.
- Peterson, R. E. (1959). Notch sensitivity. In Sines, G. and Waisman, J. L., editors, *Metal Fatigue*, pages 293–306. McGraw-Hill, New York.
- Piccio, R. (1970). *Tensile fatigue characteristics of sized polyester/viscose yarn and their effect on weaving performance*. Master's Thesis in Engineering, North Carolina State Univ.
- Pilkey, W. D. and Pilkey, D. F. (2008). *Peterson's Stress Concentration Factor*. John Wiley & Sons, 3 edition.
- Pineau, A. (1981). Review of fracture micromechanisms and a local approach to predicting crack resistance in low strength steels. In Francois, D., editor, *Advances in Fracture Research, 5th International Conference on Fracture*, volume 2, pages 553–577.
- Pineau, A. (1992). Global and local approaches of fracture — transferability of laboratory test results to components. In Argon, A., editor, *Topics in Fracture and Fatigue*, chapter 6. Springer, New York.
- Pluvinage, G. (1998). Fatigue and fracture emanating from notch; the use of the notch stress intensity factor. *Nuclear Engineering and Design*, 185:173–84.
- Povolo, F. and Hermida, . B. (1993). *Recent Theoretical Developments in the Analysis of the Viscoelastic Behaviour of Materials*, volume 8 of *Condensed Matter Theories*, pages 573–587. Springer, Boston, MA.
- Rabotnov, Y. N. (1980). *Elements of Hereditary Solid Mechanics*. Mir Publishers, Moscow, 1 edition.
- Radaj, D. (2014). State-of-the-art review on extended stress intensity factor concepts. *Fatigue & Fracture of Engineering Materials & Structures*, 37(1):1–28.
- Rappel, H., Beex, L., and Bordas, S. (2018). Bayesian inference to identify parameters in viscoelasticity. *Mechanics of Time-Dependent Materials*, 22:221–258.
- Rappel, H., Hale, L. B. J., Noels, L., and Bordas, S. (2019). A tutorial on bayesian inference to identify material parameters in solid mechanics. *Archives of Computational Methods in Engineering*, pages 1–25.
- Renardy, M., Hrusa, W. J., and Nohel, J. A. (1987). *Mathematical problems in viscoelasticity*, volume 35 of *Pitman Monographs and Surveys in Pure and Applied Mathematics*. John Wiley and Sons, New York, 1 edition.

- Riande, E., Diaz-Calleja, R., Prolongo, M., Masegosa, R., and Salom, C. (1999). *Polymer Viscoelasticity: Stress and Strain in Practice*, volume 35 of *Pitman Monographs and Surveys in Pure and Applied Mathematics*. Marcel Dekker Inc., New York, 1 edition.
- Ritchie, R. O., Knott, J. F., and Rice, J. R. (1973). On the relationship between critical tensile stress and fracture toughness in mild steel. *Journal of the Mechanics and Physics of Solids*, 21:395–410.
- Rivin, E. I. (2010). *Handbook on Stiffness & Damping in Mechanical Design*. ASME Press.
- Rouse, P. E. (1953). A theory of the linear viscoelastic properties of dilute solutions of coiling polymers. *The Journal of Chemical Physics*, 21(7):1272–1280.
- Saaty, T. L. and Joyce, M. A. (1981). *Thinking with models: mathematical models in the physical, biological, and social sciences*. Oxford: Pergamon Press.
- Sadeghinia, M., Jansen, K., and Ernst, L. (2012). Characterization of the viscoelastic properties of an epoxy molding compound during cure. *Microelectronics Reliability*, 52(8):1711 – 1718. ICMAT 2011 - Reliability and variability of semiconductor devices and ICs.
- Saseendran, S. (2017). *Effect of Degree of Cure on Viscoelastic Behavior of Polymers and their Composites*. PhD thesis, Luleå University of Technology, Luleå, Sweden.
- Schwarzl, F. and Staverman, A. J. (1952). Time-temperature dependence of linear viscoelastic behavior. *Journal of Applied Physics*, 23:838–843.
- Schwarzl, F. R. (1990). *Polymer Mechanics: Structure and Mechanical Behavior of Polymers (in German)*. Springer-Verlag Berlin Heidelberg.
- Schwarzl, F. R. and Struik, L. C. E. (1967). Analysis of relaxation measurements. *Advances in Molecular Relaxation Processes*, 1:201–255.
- Sedov, L. I. (1993). *Similarity and Dimensional Methods in Mechanics*. CRC Press, 10 edition.
- Shaw, M. T. and MacKnight, W. J. (2018). *Introduction to Polymer Viscoelasticity*. John Wiley & Sons, 4 edition.
- Simon, V., Weigand, B., and Goma, H. (2017). *Dimensional Analysis for Engineers*. Mathematical Engineering. Springer International Publishing.
- Sonin, A. A. (2001). *The Physical Basis of Dimensional Analysis*. Department of Mechanical Engineering, MIT, Cambridge, 2 edition.
- Stouffer, D. C. and Wineman, A. S. (1971). Linear viscoelastic materials with environmental dependent properties. *The Indian Journal of Statistics*, 9:193–212.

- Struik, L. (1977). *Physical aging in amorphous polymers and other materials*. PhD thesis, TU Delft, Faculty of Applied of Sciences, Netherlands.
- Sullivan, J. (1990). Creep and physical aging of composites. *Composites Science and Technology*, 39(3):207 – 232.
- Szirtes, T. and Rózsa, P., editors (2006). *Applied Dimensional Analysis and Modeling*. Mathematical Engineering. Butterworth-Heinemann.
- Tan, Q.-M. (2011). *Dimensional Analysis. With Case Studies in Mechanics*. Springer-Verlag Berlin Heidelberg, 1 edition.
- Taylor, D. (2007). *The Theory of Critical Distances. A New Perspective in Fracture Mechanics*. Elsevier Science, London, 1 edition.
- Tissaoui, J. (1996). *Effects of Long-Term Creep on the Integrity of Modern Wood Structure*. PhD thesis, Faculty of the Virginia Polytechnic Institute, Blacksburg, Virginia.
- Tobolsky, A. V. and Andrews, R. D. (1945). Systems manifesting superposed elastic and viscous behavior. *The Journal of Chemical Physics*, 13(1):3–27.
- Tobolsky, A. V. and McLoughlin, J. R. (1952). Elastoviscous properties of polyisobutylene. v. the transition region. *Journal of Polymer Science*, 8(5):543–553.
- Towers, D., Edwards, D., and Hamson, M. (2001). *Guide to Mathematical Modelling*. Mathematical Guides. Red Globe Press, 2 edition.
- Tschoegl, N. (1989). *The Phenomenological Theory of Linear Viscoelastic Behavior. An Introduction*. Springer-Verlag Berlin Heidelberg, 1 edition.
- Tschoegl, N. (1997). Time dependence in material properties: An overview. *Mechanics of Time-Dependent Materials*, 1:3–31.
- Tschoegl, N. and Emri, I. (1993). Generating line spectra from experimental responses. Part II: Storage and loss functions. *Rheologica Acta*, 32:322–327.
- Tschoegl, N., Knauss, W. G., and Emri, I. (2002). The effect of temperature and pressure on the mechanical properties of thermo- and/or piezorheologically simple polymeric materials in thermodynamic equilibrium – a critical review. *Mechanics of Time-Dependent Materials*, 6:53–99.
- Uchaikin, V. V. (2013). *Fractional Derivatives for Physicists and Engineers*, volume I, II of *Nonlinear Physical Science*. Springer-Verlag Berlin Heidelberg.
- Volterra, V. (1959). *Theory of functionals*. Dover, New York.
- Wallin, K. (1984a). The scatter in K_{IC} results. *Engineering Fracture Mechanics*, 19:1085–1093.
- Wallin, K. (1984b). The size effect in K_{IC} results. *Engineering Fracture Mechanics*, 19:1085–1093.

- Wallin, K. (1984c). Statistical modelling of fracture in the ductile-to-brittle transition region. In Blauel, J. G. and Schwalbe, K. H., editors, *Defect Assessment in Components – Fundamentals and Applications.ESIS/EGF9*, pages 415–445. Mechanical Engineering Publications, London.
- Wallin, K. (1991). Fracture toughness transition curve shape for ferritic structural steels. In Teoh, S. and Lee, K., editors, *Fracture of Engineering Materials and Structures*. Springer, Dordrecht.
- Wallin, K. (1999a). The master curve method: a new concept for brittle fracture. *International Journal of Materials and Product Technology*, 14:342 – 354.
- Wallin, K. (1999b). Statistical re-evaluation of the asme kic and kir fracture toughness reference curves. *Nuclear Engineering and Design*, 193(3):317 – 326.
- Wallin, K. (2002). Master curve analysis of the “euro” fracture toughness dataset. *Engineering Fracture Mechanics*, 69(4):451 – 481.
- Ward, I. M. and Sweeney, J. (2012). *Mechanical Properties of Solid Polymers*. John Wiley & Sons, 3 edition.
- Williams, G. and Watts, D. C. (1969). Non-symmetrical dielectric relaxation behaviour arising from a simple empirical decay function. *Transactions on the Faraday Society*, 66:80–85.
- Williams, M., Landel, R., and Ferry, J. (1955). The temperature dependence of relaxation mechanisms in amorphous polymers and other glass-forming liquids. *Journal of the American Chemical Society*, 77:3701–3707.
- Wineman, A. (2009). Nonlinear viscoelastic solids—a review. *Transactions on the Faraday Society*, 14:300–366.
- Wiscombe, W. and Evans, J. (1977). Exponential-sum fitting of radiative transmission functions. *Journal of Computational Physics*, 24(4):416–444.
- Yen, C. S. and Dolan, T. J. (1952). A critical review of the criteria for notch-sensitivity in fatigue of metals. In *Univeristy of Illinois Bulletin*, number 398. University of Ollinois Engineering Experiment Station, Illinois, rbana.
- Zhao, J., Knauss, W. G., and Ravichandran, G. (2007). Applicability of the time–temperature superposition principle in modeling dynamic response of a polyurea. *Mechanics of Time-Dependent Materials*, 11(3):289–308.
- Zimm, B. H. (1956). Dynamics of polymer molecules in dilute solution: Viscoelasticity, flow birefringence and dielectric loss. *The Journal of Chemical Physics*, 24(2):269–278.
- Zohuri, B. (2015). *Dimensional Analysis and Self-Similarity Methods for Engineers and Scientists*. Springer International Publishing, 1 edition.
- Zohuri, B. (2017). *Dimensional Analysis Beyond the Pi Theorem*. Springer International Publishing, 1 edition.

Publications

The Ph.D. candidate has disseminated the research developed during the last years through the following journal articles and oral or poster presentations:

Journal Publications

- Authors:* F. Pelayo, M. J. Lamela-Rey, M. Muñiz-Calvente, M. López-Anelle, A. Álvarez-Vázquez and A. Fernández-Canteli
Title: Study of the time-temperature-dependent behaviour of PVB: Application to laminated glass elements
Journal: Thin-Walled Structures, 119:324–331 (2017)
DOI: 10.1016/j.tws.2017.06.030
Impact Factor: 2.81 – Q1 (JCR)
- Authors:* S. Vantadori, M. Muñiz-Calvente, D. Scorza, A. Fernández-Canteli, A. Álvarez-Vázquez, A. Carpinteri
Title: The generalised local model applied to Fibreglass
Journal: Composite Structures, 202:1353–1360 (2018)
DOI: 10.1016/j.compstruct.2018.06.073
Impact Factor: 4.101 – Q1 (JCR)

3. *Authors:* M. Muniz-Calvente, A. Ramos, F. Pelayo, A. Álvarez, M.J. Lamela and A. Fernández-Canteli
Title: Probabilistic failure analysis for real glass components under general loading conditions
Journal: Fatigue & Fracture Engineering Materials & Structures, 42(6):1283–1291 (2019)
DOI: 10.1111/ffe.13011
Impact Factor: 2.533 – Q1 (JCR)
4. *Authors:* M. Muñoz-Calvente, A. Álvarez-Vázquez, S. Cicero, S. Blasón, J. Correia, A. M. P. de Jesus, A. Fernández-Canteli and F. Berto
Title: Study of the influence of notch radii and temperature on the probability of failure: a methodology to perform a combined assessment
Journal: Fatigue & Fracture Engineering Materials & Structures, 42(12):2663–2673 (2019)
DOI: 10.1111/ffe.13082
Impact Factor: 2.533 – Q1 (JCR)
5. *Authors:* M. Muñoz-Calvente, L. Venta-Viñuela, A. Álvarez-Vázquez, F. Pelayo, M. J. Lamela and A. Fernández-Canteli
Title: A probabilistic approach for assessing and predicting failure of notched components
Journal: Materials, 12(24):4053 (2019)
DOI: 10.3390/ma12244053
Impact Factor: 2.972 – Q2 (JCR)
6. *Authors:* M. Casasola, M. J. Lamela, A. Fernández-Canteli, M. Muñoz-Calvente, F. Pelayo, A. Álvarez-Vázquez, A. Salazar and J. M. Pintado
Title: Fracture characterization of epoxy adhesives using pre-cracked CT samples
Journal: Materials, Methods & Technologies 13:25–37 (2019)
Impact Factor: 0.72 – Q1 (SJR)
7. *Authors:* A. Álvarez-Vázquez, A. Fernández-Canteli, E. Castillo, F. Pelayo, M. Muñoz-Calvente and M. J. Lamela
Title: A novel approach to describe the time-temperature conversion among relaxation curves of viscoelastic materials
Journal: Materials, 13(8):1809–1824 (2020)
DOI: 10.3390/ma13081809
Impact Factor: 2.972 – Q2 (JCR)

8. *Authors:* A. Álvarez-Vázquez, A. Fernández-Canteli, E. Castillo, F. Pelayo, M. Muñiz-Calvente and M. J. Lamela
Title: A time- and temperature-dependent viscoelastic model based on the statistical compatibility condition
Journal: *Materials & Design*, 193:108828–108835 (2020)
DOI: 10.1016/j.matdes.2020.108828
Impact Factor: 5.770 – Q1 (JCR)
9. *Authors:* A. Álvarez-Vázquez, M. Muñiz-Calvente, A. Fernández-Canteli, M. J. Lamela and E. Castillo
Title: A geometry and temperature dependent regression model for statistical analysis of fracture toughness in notched components
Journal: *Engineering Fracture Mechanics* (2020) (*Under Review*)

International and National Conferences

1. *Authors:* Álvarez Vázquez A., F. Pelayo., Blasón S., Muñiz Calvente M., Lamela M.J., Fernández Canteli A. and Castillo E.
Title: Aplicación de un modelo de Weibull de fatiga al comportamiento viscoelástico de materiales
Conference: XXXV Encuentro del Grupo Español de Fractura (GEF)
Publication: *Anales de Mecánica de la Fractura Volumen XXXV* (ISSN-0213-3727) (Pages: 433–438)
Place and date: Málaga (Spain) 14–16 March 2018
Contribution: Oral Presentation
2. *Authors:* M. Muñiz Calvente, F. Pelayo, Álvarez Vázquez A., A. Martinho, J. McKenna, M. J. Lamela, A. Salazar, J. M. Pintado and A. Fernández Canteli
Title: Metodología para la caracterización probabilística de polímeros
Conference: XXXV Encuentro del Grupo Español de Fractura (GEF)
Publication: *Anales de Mecánica de la Fractura Volumen XXXV* (ISSN-0213-3727) (Pages: 237–242)
Place and date: Málaga (Spain) 14–16 March 2018
Contribution: Oral Presentation
3. *Authors:* M. Muñiz Calvente, P. Fernández Fernández, A. Álvarez Vázquez and M. J. Lamela Rey
Title: Aprendizaje colaborativo en Teoría de Estructuras
Conference: XXVI Congreso Universitario de Innovación Educativa en las Enseñanzas Técnicas (CUIEET)
Publication: *Proceedings of CUIEET* (ISBN: 978-84-17445-02-7) (Pages: 559-566)
Place and date: Gijón (Spain) 25–27 June 2018
Contribution: Oral Presentation

4. *Authors:* Álvarez-Vázquez A., M. Muñiz-Calvente, S. Cicero, S. Blasón, J. Correia, A. M. P. de Jesus and A. Fernández-Canteli
Title: Derivation of cdf of failure from specimens with different notch radii and temperatures
Conference: XVIII International Conference on New Trends in Fatigue and Fracture (NT2F)
Publication: Proceedings (ISBN: 978-989-20-8548-7)
Place and date: Lisboa (Portugal) 18–21 July 2018
Contribution: Oral Presentation

5. *Authors:* Álvarez-Vázquez A., F. Pelayo., Blasón S., Muñiz-Calvente M., Lamela M.J., Fernández-Canteli A. and Castillo E.
Title: A compatible model for analyzing the temperature effect on the relaxation modulus
Conference: XI International Conference on the Mechanics of Time-Dependent Materials (MTDM)
Place and date: Milan (Italy) 4–7 September 2018
Contribution: Oral Presentation

6. *Authors:* F. Pelayo, Álvarez-Vázquez A., Barrientos E., Muñiz-Calvente M., Lamela M.J. and Fernández-Canteli A.
Title: A novel device for testing soft materials under shear and compression loading conditions
Conference: XI International Conference on the Mechanics of Time-Dependent Materials (MTDM)
Place and date: Milan (Italy) 4–7 September 2018
Contribution: Oral Presentation

7. *Authors:* Álvarez Vázquez A., Muñiz Calvente M., Pelayo F., Lamela Rey M. J., Fernández-Canteli A. and Castillo E
Title: Predicción probabilística de fractura en componentes metálicos entallados mediante la obtención de la curva maestra del material
Conference: XXXVI Encuentro del Grupo Español de Fractura
Publication: Anales de Mecánica de la Fractura Volumen XXXVI (ISSN-0213-3725) (Pág.: 101-106)
Place and date: Sevilla (Spain) 3–5 April 2019
Contribution: Oral Presentation

8. *Authors:* Casasola Paesa M., Lamela Rey M. J., Fernández Canteli A., Muñiz Calvente M., Pelayo F. and Álvarez Vázquez A.
Title: Caracterización a fractura de la resina epoxi EPOLAM 2025 mediante probetas CT preagrietadas
Conference: XXXVI Encuentro del Grupo Español de Fractura
Publication: Anales de Mecánica de la Fractura Volumen XXXVI (ISSN-0213-3725) (Pág.: 207-212)
Place and date: Sevilla (Spain) 3–5 April 2019
Contribution: Oral Presentation
9. *Authors:* Muniz Calvente M., Castillo E., Fernández-Canteli A., Blasón S. and Álvarez-Vázquez A.
Title: Los percentiles de los percentiles: Un paso más allá en fatiga
Conference: XXXVI Encuentro del Grupo Español de Fractura
Publication: Anales de Mecánica de la Fractura Volumen XXXVI (ISSN-0213-3725) (Pág.: 444-449)
Place and date: Sevilla (Spain) 3–5 April 2019
Contribution: Oral Presentation
10. *Authors:* Álvarez Vázquez A., Muñiz Calvente M., Pelayo F., Lamela Rey M. J., Fernández-Canteli A. and Castillo E
Title: Statistical approach to mechanics of viscoelastic solids. A novel paradigm for modelling time-temperature superposition principle
Conference: I Colloquium of the Spanish Theoretical and Applied Mechanics Society (STAMS 2019)
Place and date: Madrid (Spain) 28–29 March 2019
Contribution: Poster Presentation
11. *Authors:* M. Casasola, M.J. Lamela, A. Fernández-Canteli, M. Muñiz-Calvente, F. Pelayo, A. Álvarez-Vázquez, A. Salazar and J. M. Pintado
Title: Fracture characterization of epoxy adhesives using pre-cracked CT samples
Conference: I Colloquium of the Spanish Theoretical and Applied Mechanics Society (STAMS 2019)
Place and date: Madrid (Spain) 28–29 March 2019
Contribution: Poster Presentation
12. *Authors:* M. Muñiz-Calvente, S. Blasón, A. Álvarez and A. Fernández-Canteli
Title: The Generalized Local Model (GLM): a probabilistic approach to ensure transferability in the practical design
Conference: I International Symposium on Risk Analysis and Safety of Complex Structures and Components (IRAS 2019)
Place and date: Porto (Portugal) 1–2 July 2019
Contribution: Oral Presentation

13. *Authors:* M. Muñiz-Calvente, A. Álvarez-Vázquez and F. Pelayo
Title: Aprendizaje colaborativo a través de Youtube
Conference: XXVII Congreso Universitario de Innovación Educativa en las Enseñanzas Técnicas (CUIEET)
Place and date: Alcoy (Spain) 17–19 June 2019
Contribution: Oral Presentation
14. *Authors:* A. Álvarez-Vázquez, M. Muñiz-Calvente, F. Pelayo, M. J. Lamela-Rey and E. Castillo
Title: Evaluación de resultados de proyectos docentes mediante el uso de estadísticos de orden
Conference: XXVII Congreso Universitario de Innovación Educativa en las Enseñanzas Técnicas (CUIEET)
Place and date: Alcoy (Spain) 17–19 June 2019
Contribution: Oral Presentation
15. *Authors:* M. Casasola, M.J. Lamela, A. Fernández-Canteli, M. Muñiz-Calvente, F. Pelayo, A. Álvarez-Vázquez, A. Salazar and J. M. Pintado
Title: Fracture characterization of epoxy adhesives using pre-cracked CT samples
Conference: Materials, Methods & Technologies
Place and date: Burgas (Bulgary) 23–27 June 2019
Contribution: Oral Presentation
16. *Authors:* M. Casasola, L. Viñuela, M.J. Lamela, M. Muñiz-Calvente, F. Pelayo, A. Álvarez-Vázquez, A. Fernández-Canteli, A. Salazar and J. M. Pintado
Title: Caracterización de la resina epoxi epolam 2025
Conference: Congreso Iberoamericano de Ingeniería Mecánica
Place and date: Cartagena de Indias (Colombia) 207–215 November 2019
Contribution: Oral Presentation
17. *Authors:* M. Muñiz-Calvente, L. Venta-Viñuela, A. Álvarez-Vázquez, F. Pelayo, M. J. Lamela and A. Fernández-Canteli
Title: Predicción de fallo de componentes poliméricos entallados usando un modelo probabilístico
Conference: V Iberian Conference on Structural Integrity (IbCSI)
Place and date: Coimbra (Portugal) 25–27 March 2020
Contribution: Virtual Presentation
18. *Authors:* M. Muñiz-Calvente, A. Álvarez-Vázquez, L. Venta-Viñuela, F. Pelayo, M. J. Lamela and A. Fernández-Canteli
Title: Influence of the scale effect on the reduction of fatigue strength of notched components
Conference: XXIII European Fracture Conference (ECF)
Place and date: Funchal (Portugal) 27–28 June 2020 (Postponed)